Indian J Chem
FEBRUARY 1991
CODEN : IJOCAP 30A(2) 105-202 (1991)
ISSN : 0019-5103

Indian Journal of

CHEMISTRY

SECTION A

Inorganic, Bio-inorganic, Physical, Theoretical & Analytical Chemistry

Published by
PUBLICATIONS & INFORMATION DIRECTORATE, CSIR, NEW DELHI
in association with
THE INDIAN NATIONAL SCIENCE ACADEMY, NEW DELHI

THE WEALTH OF INDIA

An Encyclopaedia of Indian Raw Materials and Industrial Products, published in two series :

(i) Raw Materials, and **(ii) Industrial Products.**

RAW MATERIALS

The articles deal with Animal Products, Dyes & Tans, Essential Oils, Fats & Oils, Fibres & Pulps, Foods & Fodders, Drugs, Minerals, Spices & Flavourings, and Timbers and other Forest products. Names in Indian languages, and trade names are provided.

For important crops, their origin, distribution, evolution of cultivated types and methods of cultivation, harvesting and storage are mentioned in detail. Data regarding area and yield and import and export are provided. Regarding minerals, their occurrence and distribution in the country and modes of exploitation and utilization are given. The articles are well illustrated. Adequate literature references are provided.

Eleven volumes of the series covering letters A – Z have been published.

Vol. I: A (Revised) Rs. 300.00; Vol. 2B (Revised) Rs.220.00. Vol. I (A-B) Rs.120.00; Vol. II (C) Rs.200.00; Vol. III (D-E) with index to Vols. I-III Rs.158.00; Vol. IV (F-G) Rs.150.00; Vol. IV Suppl. Fish & Fisheries Rs.84.00; Vol. V (H-K) Rs.171.00; Vol. VI (L-M) Rs.220.00; Vol. VI: Suppl. on Livestock including poultry Rs.153.00; Vol. VII (N-Pe) Rs.150.00; Vol. VIII (Ph-Re) Rs.129.00; Vol. IX (Rh-Sc) Rs.200.00; Vol. X (Sp-W) Rs.338.00; Vol. XI (X-Z) with Cumulative Index to Vols. I-XI Rs.223.00.

INDUSTRIAL PRODUCTS

Includes articles giving a comprehensive account of various large, medium and small scale industries. Some of the major industries included are : Acids, Carriages, Diesel Engines, Fertilizers, Insecticides & Pesticides, Iron & Steel, Paints & Varnishes, Petroleum Refining, Pharmaceuticals, Plastics, Ship & Boatbuilding, Rubber, Silk, etc.

The articles include an account of the raw materials and their availability, manufacturing processes, and uses of products, and industrial potentialities. Specifications of raw materials as well as finished products and statistical data regarding production, demand, exports, imports, prices, etc. are provided. The articles are suitably illustrated. References to the sources of information are provided.

Nine volumes of the series covering letters A – Z have been published.

Part I (A-B) Rs.87.00; Part II (C) Rs.111.00; Part III (D-E) with Index to Parts I-III Rs.150.00; Part IV (F-H) Rs.189.00; Part V (I-L) Rs.135.00; Part VI (M-Pi) Rs.42.00; Part VII (Pl-Sh) Rs.220.00; Part VIII (Sl-Tl) Rs.99.00; Part IX (To-Z) with index to Parts I-IX Rs.120.00

HINDI EDITION : BHARAT KI SAMPADA—PRAKRITIK PADARTH

Vols. I to VII and two supplements of Wealth of India—Raw Materials series in Hindi already published.

Published Volumes :

Vol. I (अ-औ) Rs. 57.00; Vol. II (क) Rs. 54.00; Vol. III (ख-न) Rs. 54.00; Vol. IV (प) Rs. 125.00; Vol. V (फ-मेरे) Rs. 90.00; Vol. VI (मेल-रू) Rs. 120.00; Vol. VII (रे-वाटा) Rs. 203.00; Vol. VIII (वाय-सीसे) Rs. 300.00.

Supplements :

Fish & Fisheries (Matsya & Matsyaki) Rs. 74.00;

Livestock (Pashudhan aur Kukkut Palan) Rs. 51.00

Vols. IX to XI under publication.

Please contact :

SENIOR SALES AND DISTRIBUTION OFFICER

PUBLICATIONS & INFORMATION DIRECTORATE, CSIR

Hillside Road, New Delhi 110 012

INDIAN JOURNAL OF CHEMISTRY

Section A: Inorganic, Bio-inorganic, Physical, Theoretical & Analytical Chemistry

Published by the Publications & Information Directorate (CSIR), Hillside Road, New Delhi 110 012

Director: Dr G P Phondke

The Indian Journal of Chemistry is issued monthly in two sections: A and B. Communications regarding contributions for publication in the journal should be addressed to the Editor, Indian Journal of Chemistry, Publications & Information Directorate, Hillside Road, New Delhi 110 012.

Correspondence regarding subscriptions and advertisements should be addressed to the Sales & Distribution Officer, Publications & Information Directorate, Hillside Road, New Delhi 110 012.

The Publications & Information Directorate (CSIR) assumes no responsibility for the statements and opinions advanced by contributors. The Editorial Board in its work of examining papers received for publication is assisted, in an honorary capacity by a large number of distinguished scientists, working in various parts of India.

Annual Subscription: Rs. 400.00 £ 100.00 $ 150.00; 50% discount admissible to research workers and students and 25% discount to non-research individuals on annual subscription.

Single Copy: Rs. 40.00 £ 10.0 $ 15.00

Payments in respect of subscriptions and advertisements may be sent by cheque, bank draft, money order or postal order marked payable to Publications & Information Directorate, Hillside Road, New Delhi 110 012.

Claims for missing numbers of the journal will be allowed only if received within 3 months of the date of issue of the journal plus the time normally required for postal delivery of the journals and the claim.

AUTHOR INDEX

Indian Journal of Chemistry

Sect. A: Inorganic, Bio-inorganic, Physical, Theoretical & Analytical

VOL. 30A NUMBER 2 FEBRUARY 1991

CONTENTS

Authors for correspondence are indicated by (*)

Indian Journal of Chemistry
Vol. 30A, February 1991, pp 105-108

MNDO calculations on hydrogen bonding complexes of cyanides and isocyanides, and of acetylene and diacetylene: Use of modified core-repulsion potential

A K Chandra & M Banerjee*
Department of Chemistry, University of Burdwan, Burdwan 713 104

Received 21 June 1990; accepted 10 September 1990

Some H-bonded complexes are studied with the MNDO/H method, proposed originally by Burstein and Issaev(BI). The advantage of using BI potential is that, with the same general form of the core-potential function one can calculate the H-bonding energy of all pairs X . . . H (X = N, O, F, C) by changing only the values of the parameters in different situations. The sets of parameters chosen for carbon are seen to perform well for the isocyanides as well as for the unsaturated π-systems (acetylene and diacetylene), but generality in this aspect needs to be established after further application to various types of compounds. As carbon exhibits different types of bonding in different environments, it is unlikely that the same set of parameters would perform equally well in all situations. A bond order dependent parameter may provide a more general solution to this problem.

It is now well known that the usual MNDO[1] method overestimates the core-repulsion energy in the case of H-bonded systems. Recently several authors[2-4] have modified the MNDO method to take care of this extra repulsion. Burstein and Issaev[2] have proposed a method, designated as BI method, for systems in which N, O and F participate in H-bonding. The present work is aimed in studying the H-bonds between cyanides, isocyanides and the simple proton donors. This is further supplemented with the interesting complexation of acetylene and diacetylene with HF. Following the microwave and infrared analysis of acetylene-HF[5,6] and diacetylene-HF[7] complexes in solid argon matrix, enough experimental data are available for testing our MNDO based model. We propose sets of parameters for different classes of compounds in our context of modifying the BI-type of potential. This practice of empirical fitting is in common use in MNDO based studies[3,4].

Method

In the MNDO method[1], the function of the form(1) is used for core-core repulsion energy between atoms A and B:

$$E_{AB} = Z_A Z_B \Gamma_{AB}[1 + f(R_{AB})] \quad \ldots(1)$$

where Z_A, Z_B are core charges, Γ_{AB} is the two center two-electron repulsion integral, R_{AB} is the interatomic distance and $f(R_{AB})$ is an empirical function of the form (2)

$$f(R_{AB}) = \exp(-\alpha_A R_{AB}) + \exp(-\alpha_B R_{AB}) \quad \ldots(2)$$

where α_A and α_B are atomic parameters.
Burstein and Issaev proposed a new expression (see Eq. 3) of $f(R_{AB})$ for atom pairs (X, H) taking part in the H-bonding of the type X . . . H − Y[Y = N, O, F].

$$f(R_{XH}) = \alpha_1 \exp(-\alpha_2 R_{XH}^2) \quad \ldots(3)$$

They proposed $\alpha_1 = 1.0$ and $\alpha_2 = 2.0$ for all X . . .H pairs (where X = N, O, F). In our present work, we have used $\alpha_2 = 1.9$, instead of 2.0 for the N . . . H bond which distinctly produces better results for the cyanide complexes.

For the C . . . H − O/F bonds, as are involved in the isocyanide complexes, $\alpha_1 = 1.2$ and $\alpha_2 = 1.8$ are used. To our knowledge no attempt has been made to modify the core potential in MNDO theory for studying H-bonds in which carbon atom is involved.

For studying the H-bond of the type C . . H − F, as is involved in acetylene and diacetylene complexes, $\alpha_1 = 1.2$ and $\alpha_2 = 2.0$ are used. Although attempts are made to fit empirically both the energetic and structural aspects of H-bonding, major emphasis is given for the energetics, making considerable allowance for the structural parameters.

Results and Discussion

Complexes of cyanide and isocyanide

In Table 1, H-bonding energies and X . . H − Y distances, calculated presently for the complexes of RCN an RNC (R = H, CH_3) with HF, H_2O, CH_3OH are presented along with the corresponding *ab initio* results, where available. It is seen that the isocyanide

Table 1—H-bonding energies (kcal/mol) and Y–H . . X distances (Å)

Proton acceptor	Proton donor (Y–H)	Energy MNDO/H	*ab initio*	Distance MNDO/H	Distance *ab initio*
CH_3CN	HF	9.42		2.58	
	H_2O	4.85		2.67	
	$HOCH_3$	3.78	5.39	2.91	3.10
CH_3NC	HF	9.86		2.65	
	H_2O	5.50		2.71	
	$HOCH_3$	5.84	5.88	2.71	
HCN	HF	9.47	8.90	2.60	2.90
	H_2O	4.81	4.90	2.65	
HNC	HF	9.71	9.30	2.65	2.99
	H_2O	5.33	5.10	2.70	
	$HOCH_3$	5.77		2.69	

Table 2—H-bonding energies and structures of acetylene-HF 1:1 complex

Structure	Calc. quantities	MNDO/H	MNDO	*ab initio*
	ΔE (kcal/mol)	1.52	0.19	1.70
σ-complex	$R_{c..F}$(Å)	2.86	4.66	2.32
	< F..C–H(deg.)	0	2.5	9
π-complex	ΔE(kcal/mol)	2.47	0.08	2.60
	$R_{*..H}$ (Å)	1.77	4.54	2.34

*Denotes the C ≡ C bond centre.

Table 3—H-bonding energies (kcal/mol) of diacetylene-HF 1:1 complex

Structure	MNDO/H	*ab initio*[a]
σ-complex	1.95	3.10
Trans. state	0.40	—
non-symm. π-complex	2.16	0.96
symm. π-complex	2.14	1.60

[a]Ref. 12

complexes are stabler than the cyanide counterparts. Similar observations have been made in *ab initio* calculations[8,9] employing a 4-31G basis set. The extra stability of the isocyanide complexes can be explained in the line of electron redistribution[8,9] obtained through a Mulliken population analysis. In the CH_3NC . . $HOCH_3$ complex, an amount of 0.037 (0.046)† elecronic charge is transferred to CH_3OH whereas in CH_3CN . . $HOCH_3$ only 0.028 (0.025) electronic charge is transferred. For HNC . . HF and HCN . . HF the electronic charge values are 0.043(0.044) and 0.032(0.025) respectively. This extra charge transfer in the former supports the greater stability of the iscyanide complexes.

Contrary to observations (see Ref. 2) the BI parameters are not general for calculating H-bonding enegies for all types of compounds containing N, O, F donar atoms. The parameters $\alpha_1 = 1.2$, $\alpha_2 = 1.8$ chosen for carbon perform well for the isocyanides to produce a better fit for the hydrogen bonding energy.

Thus, judging from the viewpoint of simplicity and, economy gained through an order of magnitude in our approach over the very accurate MP2 perturbative *ab initio* calculations[10] employing a double zeta basis set with polarization functions, our results appear to be encouraging for extension to large organic molecules.

Complexes of acetylene and diacetylene

Microwave spectrum at very low temperature[5,6] of acetylene-HF confirmed T-shaped structure with the HF submolecule attached to the π-bond. The reverse σ-type complex HF . . HC ≡ CH was not obtained experimentally and *ab initio* calculations[11] showed that the reverse σ-complex was less stable by about 0.9 kcal/mol than the observed π-complex. Infrared spectrum of the diacetylene-HF in matrix isolation[7] characterises two 1:1 complexes: a weak π-complex and a weak reverse σ-complex. Two model structures (**I** and **I′**) were given for the π-complex and an almost linear structure(**II**) for the σ-complex. From vibrational data it was not possible to discriminate between the localised model **I** and the oscillating model **I′** for the π-complex

†Quantities within parentheses are the *ab initio* charge transfer values as calculated by Mulliken population analysis at 4-31G level[8].

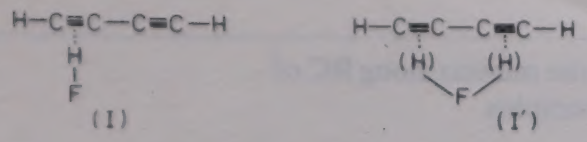

(I) (I′)

and it was inferred that the former was a consequence of high barrier to exchange of HF submolecule between the triple bonds and the latter was of a relatively low barrier. In any case, the symmetric π-complex with HF hydrogen lying below the C – C single bond was not considered to represent a stable species and was identified with the barrier to exchange. Matrix experiments established that **II** is closer in stability to **I** than the corresponding acetylene species, but the experiments could not determine the stabler one of **I** and **II**.

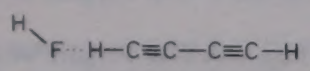

(II)

Our MNDO/H investigation on this problem has been carried out with the carbon parameters $\alpha_1 = 1.2$ and $\alpha_2 = 2.0$. Using the same α_2 here, as in isocyanide complexes, resulted in slight betterment of H-bonding distances at the expense of energy and was consequently not considered. The results for acetylene-HF calculations together with *ab initio* data[11] are presented in Table 2. It is found that the unmodified MNDO calculations produce unrealistic values which predict too weak stabilisation.

The search for stable forms of the complex has been carried out through structural optimisation along a chosen reaction coordinate which connects the symmetric π-complex at one end and the reverse σ-complex at the other end with an intermediate transition state where the HF submolecule turns around. The potential energy profile for the acetylene-HF system is shown in Fig. 1. It is observed that our calculations predict the π-complex to be stabler than the σ-complex by 0.95 kcal/mol whereas *ab initio* calculations predict the same by 0.9 kcal/mol.

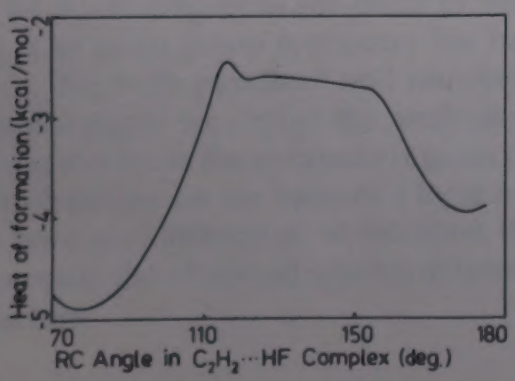

Fig. 1—Plot of MNDO heat of formation versus reaction coordinate angle in the acetylene-HF complex.

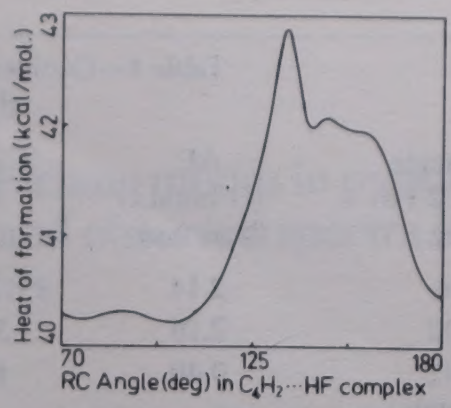

Fig. 2—Plot of MNDO heat of formation versus reaction coordinate angle in the diacetylene-HF complex.

A similar study with diacetylene-HF is presented in Table 3. Here *ab initio* data[12] based on STO-3G basis calculations produce results which exhibit remarkable stability of the reverse σ-complex by an energy magnitude which overwhelms the relative π-, σ- stability in acetylene-HF complex. Moreover, in literature[12] there might be a minor error in Table 1 in the possible interchange of H-bond energy values in the π-complex columns, making consideration for which brings the data of relative stability in line with those of H-bonding. However, it has been admitted[12] that the symmetrical π-structure is stabler of the two possible π-structures.

In our opinion the results of STO—3G calculations are not compatible with the experimental findings of Patten and Andrews[7]. It is known[2-4] that MNDO/H reproduces 4-31G quality of calculations and we observe that our calculations of the diacetylene-HF system reveals features supported by experimental work. From Fig. 2 and Table 4 it is apparent that the potential energy surface bears minima at three locations given by the reaction coordinate angle (*1-C2-F8) values 76°, 102° and 180°. The first point characterises a symmetric π-complex with HF submolecule vertically below the C2-C5 bond centre (structure **III**). The second point corresponds to a non-symmetric π-complex with the HF submolecule below the C2 ≡ C3 bond centre and the third point to a reverse σ-complex. From Table 3 it is also evident that, though the π-complex structure **I** is slightly more favoured, the energy difference between the symmetrical and non-symmetrical. π-structures indicates a very low barrier to oscillations of the HF unit. The energy of reverse σ-structure is higher than those of the π-

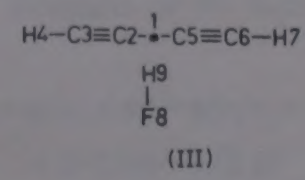

(III)

Table 4—Geometrical parameters at the minima along RC of diacetylene-HF 1:1 complex

RC angle ⟨*1-C2-F8 (deg.)	ΔE (H-bond.) (kcal/mol)	⟨C2-F8-H9 (deg.)	R_{*1-H9}	R_{C2-H9}	R_{C3-H9} (Å)	R_{C2-F8}	R_{C3-F8}
76	2.14	14.22	1.76	1.89	2.58	2.82	3.32
102	2.16	352.20	2.15	1.85	1.91	2.82	2.82
142	0.40	106.60	5.67	5.19	4.48	4.83	3.96
(Tr. state)							
180	1.95	⟨H−F..H = 183.1		$R_{H..F}$ = 1.77			

ones, but still we find that they are energetically more close (energy difference 0.2 kcal/mol) and even closer than the corresponding structures in acetylene-HF.

References

1 Dewar M J S & Thiel W, *J Am chem Soc*, 99 (1977) 4899.
2 Burstein Y A & Issaev A N, *Theor Chim Acta*, 64 (1984) 397.
3 Voityuk A A & Bliznyuk A A, *Theor Chim Acta*, 71 (1987) 327.
4 Voityuk A A & Bliznyuk A A, *Theor Chim Acta*, 72 (1987) 223.
5 Legon A C, Aldrich P O & Flygare W H, *J chem Phys*, 75 (1981) 625.
6 Aldrich P O, Legon A C & Flygare W H, *J chem Phys*, 75 (1981) 2126.
7 Patten K O & Andrews L, *J phys Chem*, 90 (1986) 3910.
8 Tang T H & Fu X Y, *Int J Quant Chem*, 24 (1983) 317.
9 Kollman P, McKelvey J, Johansson A & Rothenberg S, *J Am chem Soc*, 97 (1975) 955.
10 Amos R D, Gaw J F, Handy N C, Simandiras E D & Somasundram K, *Theor Chim Acta*, 71 (1987) 41.
11 Frisch M, Pople J A & Delbene J, *J chem Phys*, 78 (1983) 4063.
12 Medhi C & Bhattacharyya S P, *Proc Indian Acad Sci* (Chem Sci), 100 (1988) 293.

Indian Journal of Chemistry
Vol. 30A, February 1991, pp 109-112

Vibrational overtone manifold of the CH stretching modes in pyridine and nitrobenzene: An analysis of the theoretical and observed spectra in terms of structural factors

Dipak K Mandal
Department of Chemistry, Presidency College, 86/1, College Street, Calcutta 700 073, (India)
and
A K Ray*†
Department of Chemistry, Maulana Azad College, 8, Rafi Ahmed Kidwai Road, Calcutta 700 013, (India)

Received 20 February 1990; revised and accepted 25 July 1990

A local mode model has been used for the calculation of the first overtone CH stretching spectra of pyridine and nitrobenzene; the theoretical spectra have been compared with the recorded spectra in the overtone regions. The observed spectra for pyridine and nitrobenzene show a striking difference which has been interpreted in terms of structural factors.

The normal mode picture is applicable to small-amplitude vibrations where the potential energy can be approximated by a harmonic function. The problem of normal mode vibration can be exactly solved in terms of normal coordinates of the system. But the normal mode picture becomes unsuitable when the vibrational states become highly excited because the couplings between different normal modes become quite large.

The local mode picture is useful for the discussion of highly excited vibrational states[1]. However, the local mode model has been successfully used for the description of lower excited states also, in a number of polyatomic molecules[2-5].

Recently, a local mode analysis for the CH stretching overtone spectra of toluene has been reported[5]. A study of the vibrational overtone manifold of the CH stretching modes in the presence of electron-attracting nitrogen as a ring atom (pyridine) and as a group outside the ring (nitrobenzene) would be interesting from the point of view of local mixing. The point group symmetry has been shown to be C_{2v} for both pyridine[6] and nitrobenzene[7]. In the present paper we report the analysis of the CH stretching modes in the overtone regions of pyridine and nitrobenzene on the basis of a local mode model. We have also attempted to interpret the striking differences in the observed spectra in terms of structural factors.

†Present address: Department of Chemistry, Krishnanagar Government College, Dist-Nadia, West Bengal, India

Materials and Methods

Pyridine and nitrobenzene samples were BDH reagents; the liquid samples were used after double distillation. The spectra were recorded on a Cary 17D spectrophotometer using a path length of 1 cm. The record was made in the first overtone region (1550-1800 nm) by using a spec-pure grade carbon tetrachloride solution (1:10) of both pyridine and nitrobenzene. For the second (1050-1200 nm) and third (800-900 nm) overtone regions the spectra of pure pyridine and nitrobenzene were recorded. The spectra observed for the first and second overtone regions of the CH stretching modes are reproduced in Figs 1 and 2.

Theory

To analyze the overtone spectra we employed the model Hamiltonian[5] for a moleclar system of C_{2v} point group, having five coupled CH oscillators, using nearest-neighbour ring CH bond interactions.

$$H = \sum_{i=1}^{5} \left(\frac{p_i^2}{2\mu} + V(r_i) \right) + H' \qquad \ldots (1)$$

$$H' = \sum_{i=1}^{4} (\xi_i p_i p_{i+1} + \eta_i r_i r_{i+1}) \qquad \ldots (1a)$$

The matrix elements of the hamiltonian are given by,

$$\langle v_i v_j | H | v_i v_j \rangle = \omega(v_i + v_j) - x[v_i(v_i + 1) + v_j(v_j + 1)] + 5/2\,(\omega - 1/2\,x) \qquad \ldots (2)$$

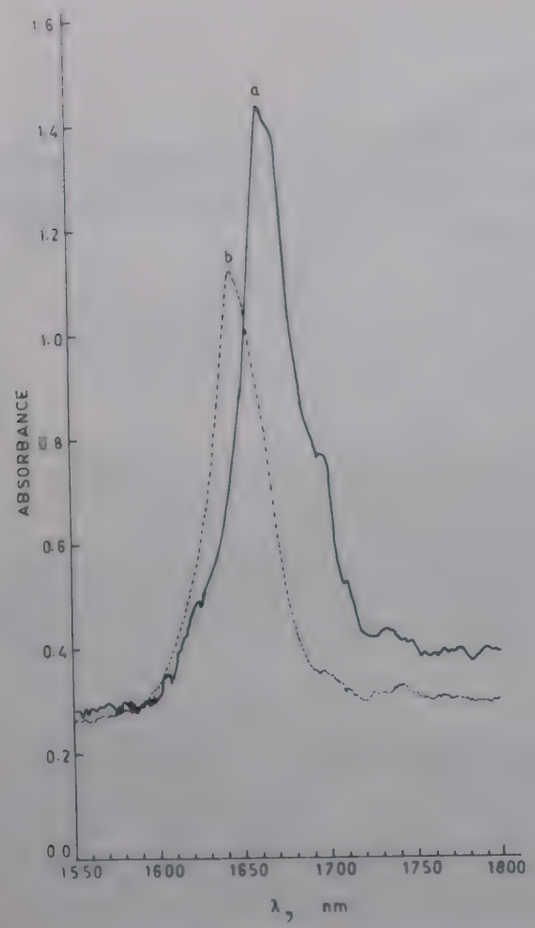

Fig.1—The observed first overtone CH stretching spectra of (a) pyridine and (b) nitrobenzene in the range 1550-1800 nm

$$\langle v_i + 1\, v_{i+1} - 1 | H | v_i v_{i+1} \rangle = \tfrac{1}{2} K_i [(v_i + 1) v_{i+1}]^{1/2} \quad \ldots (2a)$$

$$\langle v_i - 1\, v_{i+1} + 1 | H | v_i v_{i+1} \rangle = \tfrac{1}{2} K_i [v_i (v_{i+1} + 1)]^{1/2} \quad \ldots (2b)$$

$$\text{where } K_i = \omega [\xi_i \mu + \eta_i / f], \quad \ldots (2c)$$

ξ_i and η_i are kinetic and potential energy interaction terms, μ the reduced mass, f the harmonic force constant; $4\pi^2 c^2 \omega^2 = f/\mu$ and x is the anharmonicity constant $V(r_i)$ is the anharmonic potential function for the diatomic oscillators, all of which are defined by identical parameters.

The excited state $|v_i\rangle$ indicates the state where only the ith oscillator is excited to v_i, $|I,J\rangle$ is a state where both the ith and jth oscillators are excited to $v = 1$ state.

For the first excited state ($v = 1$), the Hamiltonian has been diagonalised by using symmetrized basis kets[3] and one immediate outcome of this formulation is that the coupling parameters K_1 (*ortho-meta* interaction) and K_2 (*meta-para* interaction) are readily evaluated from the knowledge of the fundamental frequencies by the relations.

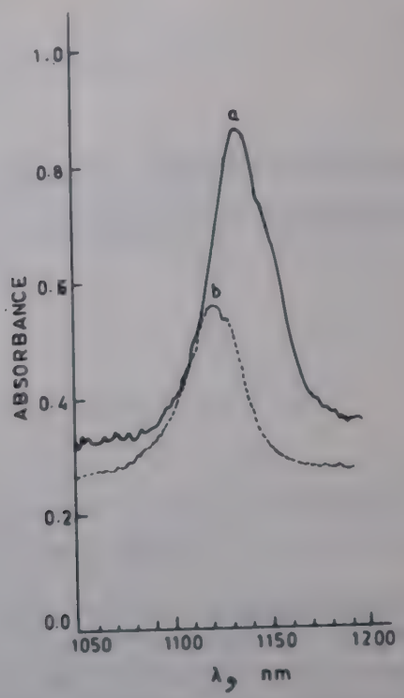

Fig.2—The observed second overtone CH stretching spectra of (a) pyridine and (b) nitrobenzene in the range 1050-1200 nm

$$\omega_{1,3}(a_1) = \omega - 2x \pm \tfrac{1}{2}(K_1^2 + 2K_2^2)^{1/2}$$

$$\omega_2(a_1) = \omega - 2x$$

$$\omega_{4,5}(b_2) = \omega - 2x \pm \tfrac{1}{2} K_1 \quad \ldots (3)$$

For the second excited state, the symmetrized ket vectors for a_1 and b_2 symmetry species and the vibrational Hamiltonian matrix are given in the Appendix[1]. The first overtone frequencies were obtained by solving numerically the 9×9 a_1 and 6×6 b_2 matrices given in the Appendix 1.

Calculation and Discussion

The calculations of the CH stretching modes for both pyridine and nitrobenzene were performed following the procedure of Ghosh *et al.*[5] with the help of four parameters ω, x, K_1 and K_2. The parameters K_1 and K_2 were obtained from the observed splitting of fundamental frequencies according to Eq. (3) and the constants ω and x were obtained from the best fit of the observed data for the fundamental and the overtones ($v = 2,3,4$). The observed and calculated frequencies for pyridine and nitrobenzene are listed in Tables 1 and 2 respectively.

A comparison of the overtone frequencies of pyridine and nitrobenzene shows a striking difference. In the case of pyridine, for the first overtone region (Table 1), the observed splitting of bands agrees fairly well with the calculated frequencies. The bands at 6231 and 6154 cm^{-1} are closer to the combination modes and are weaker. The calculated local mode frequencies for the first overtone region are mostly

Table 1—CH stretching fundamental and overtone frequencies of pyridine

v	Obs., cm^{-1} (nm)	Calc., cm^{-1}[a]	
		a_1	b_2
1	3094.2[b]	3092.6	
	3072.8[b]	3065	
	3030.1[b]	3037.4	
	3086.9[b]		3087.2
	3042.4[b]		3042.8
2	6231 (1605)	6191	
	6154	6154	6170
		6151	6146
		6122	6124
		6108	6102
	6013 (1663)	6084	
	5988 (1670)	6019	6017
	5910 (1695)	6011	6001
		5999	
3	8842 (1131)	8865[c]	
4	11628 (860)[d]	11600[c]	

(a) $\omega = 3175$, $x = 55$, $K_1 = 44.5$, $K_2 = 33$ (all in cm^{-1})
(b) Fundamental frequencies are taken from ref. 6
(c) $\omega v - xv(v+1)$
(d) spectrum not shown

Table 2—CH stretching fundamental and overtone frequencies of nitrobenzene

v	Obs., cm^{-1} (nm)	Calc. (cm^{-1})[a]	
		a_1	b_2
1	3111[b]	3101	
	3082[b]	3070	
	3049[b]	3039	
	3093[b]		3101
	3031[b]		3039
2		6202	
		6171	6171
		6170	6170
		6140	6140
		6109	6109
	6080 (1645)	6078	
		6040	6040
		6040	
		6010	6010
3	8928 (1120)	8910[c]	
4	11710 (854)[d]	11680[c]	

(a) $\omega = 3170$, $x = 50$, $K_1 = 62$, $K_2 = 0$ (all in cm^{-1})
(b) Fundamental frequencies are taken from ref. 7
(c) $\omega v - xv(v+1)$
(d) spectrum not shown

clustered around two values $2\omega - 6x$ and $2\omega - 4x$ which correspond to the overtone $|2_i\rangle$ and combination $|1_i 1_j\rangle$ modes. For nitrobenzene, the value of K_2 is zero. A very strong absorption at 6080 cm^{-1} corresponds to the overtone $|2_i\rangle$ mode. Combination modes are not observed. The calculation for the first overtone region (Table 2) shows that several modes are degenerate and the calculated splitting of the bands is not resolved in the observed spectra. For the higher overtones ($v = 3,4$) of both pyridine and nitrobenzene the roles of K_1 and K_2 become insignificant and the calculation is done with the formula $\omega v - xv(v+1)$ which shows that anharmonicity dominates in the higher overtones and the vibrational energy is almost completely localized.

The observed first overtone spectra of nitrobenzene show no splitting of bands though the splitting should have been expected in the planar nitrobenzene due to van der Waals interaction between nitro group and the adjacent hydrogen atoms as the van der Waals interaction has been shown to be mainly responsible for the splitting of modes in other cases[8,9]. It appears then that the van der Waals interaction is less significant as the planar C_{2v} version of nitrobenzene would be a poor representation of the molecule in the liquid state and the result is perhaps representative of nitrobenzene where the nitro group is twisted out of the plane of the ring[10] still possessing C_{2v} symmetry. Pyridine is planar and has a C_{2v} symmetry[6]. The presence of electron-attracting ring nitrogen causes flow of charge from all positions—the *ortho* carbons (C_2 and C_5) being affected the most. This may lead to slightly stronger *ortho-meta* coupling than *meta-para* coupling, giving rise to a small difference in the values of K_1 and K_2. For pyridine, the van der Waals interaction is not important. Here the unshared electron pair in the hybrid orbital of the nitrogen atom lies in the plane of C – H bonds and may, therefore, exert a strong field effect. Thus, the different adjacent hydrogen atoms in pyridine are in different electrical fields and this factor may, to a large extent, account for the splitting of the modes.

Acknowledgement

We are thankful to Prof. N.K. Sinha, Head of the Department of Chemistry, Bose Institute for his permission for the use of Cary 17D Spectrophotometer at RSIC, Calcutta. We also thank Dr. G K Kar and Mr P K Mandal for helpful discussions.

APPENDIX

Symmetrized ket vectors for $v=2$, a_1 symmetry species and the vibrational Hamiltonian matrix

$|S\ 2_1\rangle = |2_3\rangle$

$|S\ 2_2\rangle = (1/\sqrt{2})[|1_1\ 1_3\rangle + |1_3\ 1_5\rangle]$

$|S\ 2_3\rangle = (1/\sqrt{2})[|1_2\ 1_3\rangle + |1_3\ 1_4\rangle]$

$|S\ 2_4\rangle = (1/\sqrt{2})[|2_1\rangle + |2_5\rangle]$

$|S\ 2_5\rangle = (1/\sqrt{2})[|1_1\ 1_2\rangle + |1_4\ 1_5\rangle]$

$|S\ 2_6\rangle = (1/\sqrt{2})[|1_1\ 1_4\rangle + |1_2\ 1_5\rangle]$

$|S\ 2_7\rangle = (1/\sqrt{2})[|2_2\rangle + |2_4\rangle]$

$|S\ 2_8\rangle = |1_1\ 1_5\rangle$

$|S\ 2_9\rangle = |1_2\ 1_4\rangle$

$$\begin{bmatrix}
2\omega-6x & 0 & K_2 & 0 & 0 & 0 & 0 & 0 & 0 \\
0 & 2\omega-4x & 1/2\ K_1 & 0 & 1/2\ K_2 & 1/2\ K_2 & 0 & 0 & 0 \\
K_2 & 1/2\ K_1 & 2\omega-4x & 0 & 0 & 0 & K_2/\sqrt{2} & 0 & K_2/\sqrt{2} \\
0 & 0 & 0 & 2\omega-6x & K_1/\sqrt{2} & 0 & 0 & 0 & 0 \\
0 & 1/2\ K_2 & 0 & K_1/\sqrt{2} & 2\omega-4x & 0 & K_1/\sqrt{2} & 0 & 0 \\
0 & 1/2\ K_2 & 0 & 0 & 0 & 2\omega-4x & 0 & K_1/\sqrt{2} & K_1/\sqrt{2} \\
0 & 0 & K_2/\sqrt{2} & 0 & K_1/\sqrt{2} & 0 & 2\omega-6x & 0 & 0 \\
0 & 0 & 0 & 0 & 0 & K_1/\sqrt{2} & 0 & 2\omega-4x & 0 \\
0 & 0 & K_2/\sqrt{2} & 0 & 0 & K_1/\sqrt{2} & 0 & 0 & 2\omega-4x
\end{bmatrix}$$

Symmetrized ket vectors for $v=2$, b_2 symmetry species and the vibrational Hamiltonian matrix

$|S\ 2_2\rangle = (1/\sqrt{2})[|1_1\ 1_3\rangle - |1_3\ 1_5\rangle]$

$|S\ 2_3\rangle = (1/\sqrt{2})[|1_2\ 1_3\rangle - |1_3\ 1_4\rangle]$

$|S\ 2_4\rangle = (1/\sqrt{2})[|2_1\rangle - |2_5\rangle]$

$|S\ 2_5\rangle = (1/\sqrt{2})[|1_1\ 1_2\rangle - |1_4\ 1_5\rangle]$

$|S\ 2_6\rangle = (1/\sqrt{2})[|1_1\ 1_4\rangle - |1_2\ 1_5\rangle]$

$|S\ 2_7\rangle = (1/\sqrt{2})[|2_2\rangle - |2_4\rangle]$

$$\begin{bmatrix}
2\omega-4x & 1/2\ K_1 & 0 & 1/2\ K_2 & 1/2\ K_2 & 0 \\
1/2\ K_1 & 2\omega-4x & 0 & 0 & 0 & K_2/\sqrt{2} \\
0 & 0 & 2\omega-4x & K_1/\sqrt{2} & 0 & 0 \\
1/2\ K_2 & 0 & K_1/\sqrt{2} & 2\omega-4x & 0 & K_1/\sqrt{2} \\
1/2\ K_2 & 0 & 0 & 0 & 2\omega-4x & 0 \\
0 & K_2/\sqrt{2} & 0 & K_1/\sqrt{2} & 0 & 2\omega-4x
\end{bmatrix}$$

References

1 Wallace R & Wu A A, *Chem Phys*, 39 (1979) 221.

2 Mortensen O, Henry B R & Mohammadi M A, *J chem Phys*, 75 (1981) 4800.

3 Halonen L & Child M S, *Molec Phys*, 46 (1982) 239.

4 Halonen L & Child M S, *J chem Phys*, 79 (1983) 559.

5 Ghosh P N, Panja P K & Pal C M, *Chem Phys Lett*, 148 (1988) 337.

6 Wong K & Coulson S D, *J molec Spectros*, 104 (1984) 126.

7 Laposa J D, *Spectrochim Acta, Part A*, 35 (1979) 65.

8 Nakagaki R & Hanazaki I, *Chem Phys Lett*, 83 (1981) 512.

9 Moss D B, Parmenter C S & Ewing G E, *J chem Phys*, 86 (1987) 51.

10 Stewart J J P, Bosco S R & Carper W R, *Spectrochim Acta, Part A*, 42 (1986) 13.

Indian Journal of Chemistry
Vol. 30A, February 1991, pp 113-116

Molecular complexes of TCNE with acetanilides: Part 1

G Venkateshwarlu, M Shantha & B Subrahmanyam*
Department of Chemistry, Osmania University, Hyderabad 500 007, India

Received 1 February 1990; revised 21 June 1990; accepted 17 July 1990

Molecular complexes of TCNE with some acetanilides have been studied using electronic spectroscopy. Each complex exhibits two charge transfer bands which are attributed to the formation of two isomeric complexes R_x and R_y differing in the orientation of the donor and acceptor molecules. The ionization potentials of highest occupied and penultimate molecular orbitals of the donors have been calculated from the positions of the CT bands. The stabilities of the complexes with R_x configuration are found to be greater than those with R_y configuration. The stabilities of both the complexes increase with increase in electron releasing ability of the substituents. In general, the stabilities of the acetanilide-TCNE complexes are found to be greater than those of the TCNE complexes with correspondingly substituted benzenes. This is attributed to the stronger dipole-dipole interactions in acetanilide-TCNE complexes than the dipole-induced dipole interactions in the benzene-TCNE complexes.

Extensive studies have been made on the molecular complexes of TCNE with a variety of aromatic compounds and substituted benzenes as donors[1-10]. The π-complexes (I) of TCNE with aniline and N-alkylanilines were found to be very much unstable and decomposed soon into stable σ-complexes (II)[11,12].

The greater stability of the σ-complex than that of the π-complex was attributed to the zwitterionic structure of the former, due to the interaction of the non-bonded electrons of the N atom with benzene ring[11,12].

If this is the case, the suppression of the formation of zwitter ion is expected to stabilise the π-complex. For this purpose, acetylated anilines

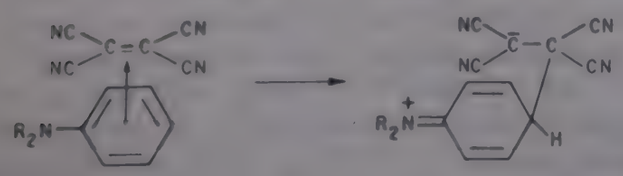

I II

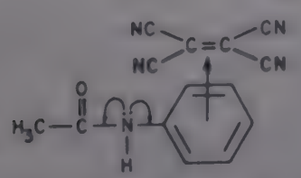

III

were chosen in the present study because the amide resonance (III) retards the zwitter ion formation.

Materials and Methods

The acetanilides were prepared by acetylation of substituted anilines. The solids obtained were recrystallised twice from methanol and were TLC-pure. Spectrograde chloroform was used as solvent. A sample of TCNE (Fluka A G) was twice recrystallised from chlorobenzene and was vacuum-sublimed.

The electronic spectra were recorded at 25°C on a Specord UV-VIS double beam spectrophotometer using a matched pair of quartz cells of 1 cm path length. Freshly prepared solutions of TCNE (4.33×10^{-4} *M*) and acetanilides (0.01 to 0.30 *M*) were mixed just before recording the spectra. Colour changes observed on mixing the donor and acceptor indicated complex formation. The complexes were stable for several hours unlike those of N-alkylanilines.

The formation constants of the complexes were determined by Benesi-Hildebrand method[13]. The linearity of the Benesi-Hildebrand plots indicated the formation of 1:1 complexes which was also verified by Job's continuous variation method.

Results and Discussion

The complex of acetanilide and TCNE was pale yellow in colour and exhibited two CT bands at 390 nm and 420 nm. Complexes with substi-

Table 1 – Charge transfer bands and formation constants of acetanilide-TCNE complexes

Substituent	$\lambda_{1\,max}$ (nm)	$\varepsilon_{1\,max}$ (lit. mol^{-1} cm^{-1})	IP_1 (eV)	K_1 (lit. mol^{-1})	$\lambda_{2\,max}$ (nm)	$\varepsilon_{2\,max}$ (lit. mol^{-1} cm^{-1})	IP_2 (eV)	K_2 (lit. mol^{-1})
$(H_3C)_2N$	650	450	7.62	5.00	394	480	9.12	24.2
H_3CO	600	530	7.82	1.70	392	560	9.13	4.42
H_3C	540	1425	8.20	0.91	391	1440	9.14	1.68
H	420	1720	8.80	0.63	390	1750	9.15	0.88
Br	400	2450	9.08	0.52	—	—	—	—

IV V

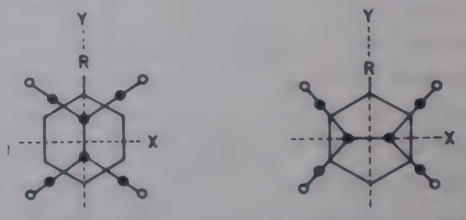

Y–Configuration X–Configuration

VI VII

tuted acetanilides also exhibited two bands (except that of *p*-bromoacetanilide). The position of the first band (390 nm) was almost the same in all the complexes. The position of the second band (420 nm), however, varied with the substituent (Table 1). The ratio of the intensities of the two bands remained constant on dilution indicating the presence of complexes of only one composition.

The two CT bands of acetanilide may be due to the excitation of electrons of the donor from two different orbitals (of small energy difference) to a single lowest unoccupied molecular orbital (LUMO) of the acceptor[1-3,6] or excitation of electrons from the same energy level of the donor to two different energy levels of the acceptor[14]. In the former type of charge transfer, for a common acceptor and different donors, it was shown that the difference between the λ_{max} of two CT bands is dependent on the nature of donor used. In the latter type of charge transfer, the difference remains constant for any donor. As the difference in λ_{max} of the two bands of the acetanilides-TCNE complexes varied from donor to donor, the complexes were inferred to be of the former type (Table 1). The bands are, therefore, due to the excitation of the two electrons from the highest filled orbitals, ψ_s and ψ_{as} of the acetanilides, to the lowest empty orbital of the TCNE.

This type of complexes differ in the relative orientation of the donor and acceptor molecules. The ψ_s and ψ_{as} orbitals of the donor differ in their nodal planes. The symmetrical orbital ψ_s has a transverse nodal plane (IV) whereas the antisymmetrical orbital ψ_{as} has a longitudinal plane (V).

If Mulliken's[15] maximum overlap principle is applied, two isomeric complexes with the following orientations are expected (VI, VII).

For mono- and di-substituted benzenes having electron releasing groups, theory predicts that the longer wavelength (lower energy) band arises from the R_x configuration (VI) and the shorter wavelength (higher energy) band from R_z configuration (VII), of the complex[1].

Effect of substituents on CT bands

The shorter wavelength CT band (390 nm) of acetanilide-TCNE complex is little affected by the change in substituents (Table 1). This is because it arises due to donation of electron from the ψ_{as} orbital which does not encompass the substituent.

Significant changes, however, were noticed in the long wavelength CT band (420 nm). It was shifted to longer wavelengths by the electron donating groups, viz., $N(CH_3)_2$, OCH_3 and CH_3, and the shifts were in the order: $N(CH_3)_2 > OCH_3 > CH_3 > H$.

The shifts of the bands can be explained in terms of mesomeric and inductive interactions of the substituents. The $+M$ effect of $N(CH_3)_2$ and OCH_3 and the $+I$ interaction of CH_3 boost up the energy of the ψ_s orbital and bring it closer to the LUMO of the TCNE and, therefore, shift the CT band to longer wavelengths.

The 400 nm band of the *p*-bromoacetanilide complex is broad. It may be due to the overlap of

two CT bands with a small difference in the λ_{max}. The 420 nm band of acetanilide complex must have suffered a hypsochromic shift due to the bromo substituent which, by its inductive influence, stabilises (lowers the energy) the donor level. This results in merging of the two bands and appearance of a broad band.

The $h\nu_{CT}$ was found to bear a linear relationship with Hammett σ_p^+ constants (Fig. 1).

Ionization potentials

The ionization potentials of the substituted acetanilides were calculated using Briegleb's equation[16] and are shown in Table 1.

$$h\nu_{CT} = 0.83\, I^D - 4.42 \text{ eV}$$

The ionization potentials of acetanilides obtained from the shorter wavelength CT bands were found to be nearly constant and ranged between 9.12 and 9.15 eV. These are very close to the ionization potential of benzene (9.24 eV). The ionization potentials obtained from the longer wavelength bands differed widely. Acetanilides with electron releasing groups have lower ionization potentials (7.62 eV to 8.80 eV). The IP of *p*-bromoacetanilide (9.08) is a little higher than that of acetanilide.

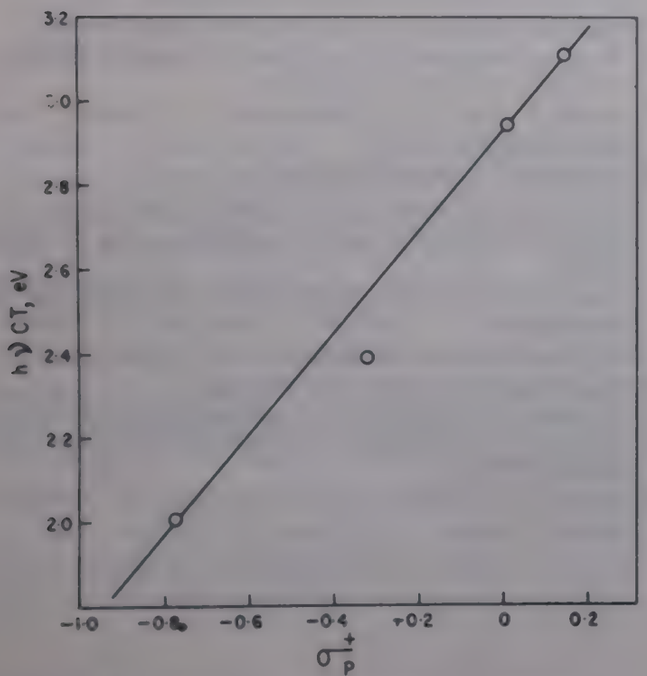

Fig. 1 – Plot of $h\nu_{CT}$ vs Hammett σ_p^+ constants

Formation constants of the complexes

As the two CT bands observed for complexes of each of the acetanilides were considered to be due to two isomeric configurational complexes, the formation constants were determined for both the complexes individually and are presented in Table 1.

The formation constants of the complexes with R_x configuration are greater than those of R_y configuration. This may be due to the steric hindrance offered by $NHCOCH_3$ and the *p*-substituent to the approach of TCNE onto the benzene ring in R_y configuration. The approach of the acceptor is, however, unhindered in the R_x configuration and, hence, this complex is more stable.

The association constants of the complexes increase with electron releasing ability of the substi-

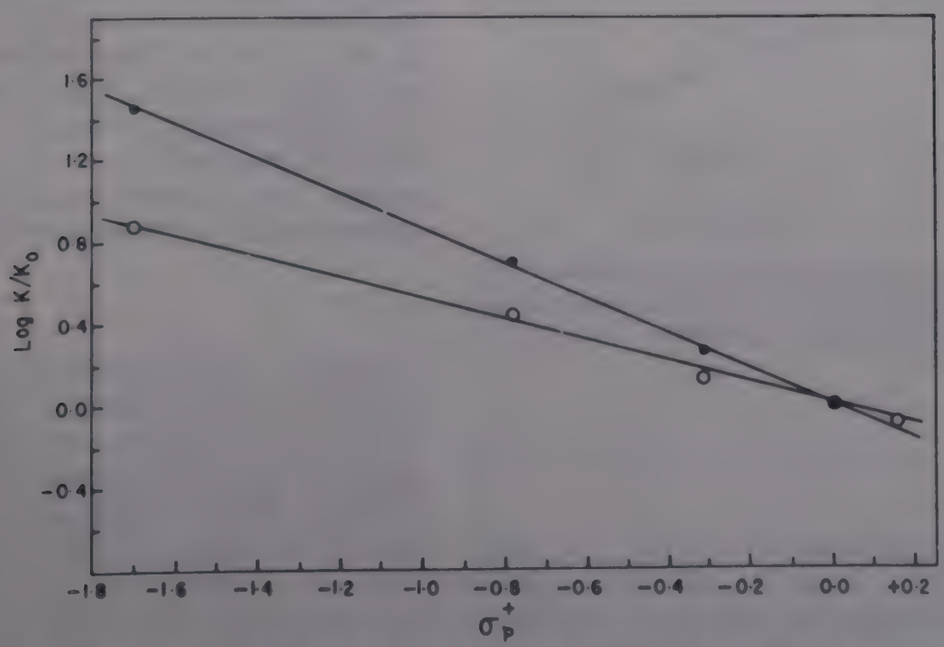

Fig. 2 – Plot of $\log K/K_0$ of R_x (●) and R_y (○) isomeric complexes vs Hammett σ_p^+ constants

tuents in the benzene ring and are in the order: $N(CH_3)_2 > OCH_3 > CH_3 > H > Br$.

The logarithmic functions of the formation constants of both the isomeric complexes were found to bear linear relationship with the Hammett σ_p^+ constants (Fig. 2).

It is interesting to note that the stabilities of the complexes of substituted acetanilides with TCNE are greater than those of the correspondingly substituted benzenes-TCNE complexes.

The stability of the complex, besides the ionization potentials of the donor, depends on the polarisability[17], dipole moment of the donor[18] and the polarising power of the acceptor[19]. In a series of complexes with the same acceptor, stability depends upon the polarisability and dipole moment of the donor. The attractive forces in benzene-TCNE complex are the dipole-induced dipole. In acetanilide they are dipole-dipole interaction. The non-bonded electrons of the N-atom interact with benzene ring and enable acetanilide to acquire greater polarity (zwitter ion structure) and form a strong complex with TCNE. Hence, the stabilities of these complexes are higher than those of benzene-TCNE complexes.

Acknowledgement

The authors are thankful to Prof. T. Navaneeth Rao, Vice-Chancellor, Osmania University for his kind help and constant encouragement and Head of the Department of Chemistry, Osmania University, Hyderabad for providing facilities.

References

1 Zweig A, *J phys Chem*, 67 (1963) 506.
2 Voigt E M, *J Am chem Soc*, 86 (1964) 3611.
3 Voigt E M & Reid C, *J Am chem Soc*, 86 (1964) 3930.
4 Kuznetsov V A, Egorochkin A N & Razuvaev G A, *Zh prikl Spektrok*, 22 (1975) 952.
5 Cornish A J & Eaborn C, *J chem Soc Perkin Trans II*, 8 (1975) 874.
6 Reichenbach G, Sanitini S & Aloisi G G, *J chem Soc Faraday Trans I*, 73 (1977) 95.
7 Frey J E, *Appl Spectrosc Rev*, 23 (1987) 247.
8 Mourad A F E, *Spectrochim Acta*, 44A (1988) 55.
9 Sanchez Martinez E, Diaz Calleja R, Berges P, Kudnig J & Klar G, *Synth Met*, 32 (1989) 79.
10 Ghosh R, Dutta K K & Mukherjee A K, *Indian J Chem*, 28A (1989) 95.
11 Rappoport Z, *J chem Soc*, (1963) 4498.
12 Rappoport Z & Horowitz A, *J chem Soc*, (1964) 1348.
13 Benesi H A & Hildebrand J H, *J Am chem Soc*, 71 (1949) 2703.
14 Iwata S, Tanaka J & Nagakura S, *J Am chem Soc*, 88 (1966) 894.
15 Mulliken R S, *J chem Phys chim Biol*, 51 (1954) 341.
16 Briegleb, *Z Electrochem*, 59 (1955) 184.
17 Anderson H D & Littamnick D, *J chem Soc*, (1950) 1089.
18 Ferguson F N & Garner A Y, *J Am chem Soc*, 76 (1954) 1167.
19 Brown H C & Brady J D, *J Am chem Soc*, 74 (1952) 3570.

Indian Journal of Chemistry
Vol. 30A, February 1991, pp 117-118

Quenching of excited uranyl ion during its photochemical reduction by triphenylphosphine: Part 1—Effect of monosubstituted benzene derivatives

M S Sidhu*, (Miss) A Chopra & S S Sandhu
Department of Chemistry, Guru Nanak Dev University, Amritsar 143 005, India

Received 13 March 1990; revised 24 August 1990; accepted 1 October 1990

The relative rates of quenching of excited uranyl ion by benzonitrile, acetophenone, bromobenzene, chlorobenzene, biphenyl and aniline have been measured during photochemical reduction of uranyl ion by triphenylphosphine. The quenching of excited uranyl ion increases in proportion to the inductive effect of the substituent group on benzene ring.

Aromatic hydrocarbons[1], substituted arylaldehydes and acetophenones[2] and benzoic acids[3] efficiently quench uranyl ion luminescence and substituents on the aromatic ring show a linear relationship between the relative rates of quenching and Hammett substituent constants. Luminescence quenching studies have so far been made using fluorescence spectrometer[4-6]. However, the Stern-Volmer type quenching constants have been measured using a UV-visible spectrophotometer by quenching the photochemical reaction, where the quenchers, simply quench the excited species through physical deactivation. The title investigation is an extension of earlier work from our laboratory[7].

Materials and Methods

Uranyl acetate, triphenylphosphine, sulphuric acid, acetone, aniline, biphenyl, chlorobenzene, bromobenzene, acetophenone and benzonitrile (all AR reagent) were used as such. Electronic absorption spectra of all the solutions irradiated in sunlight for 10 min, were recorded on a UV-visible Shimadzu 240 recording spectrophotometer. Other experimental details are described in the earlier publication[7].

Results

Like simple aromatic hydrocarbons[1], these monosubstituted benzene derivatives do not interact with ground state uranyl ion in aqueous acetone solution. However, the presence of these aromatic compounds reduces the quantum yield of photochemical reduction of uranyl ion (see Fig. 1). Decrease in the absorbance at 650 nm (the λ_{max} of U(IV) formation) is used to evaluate Stern-Volmer quenching constants K_{sv} from the slope of the linear relationship (1).

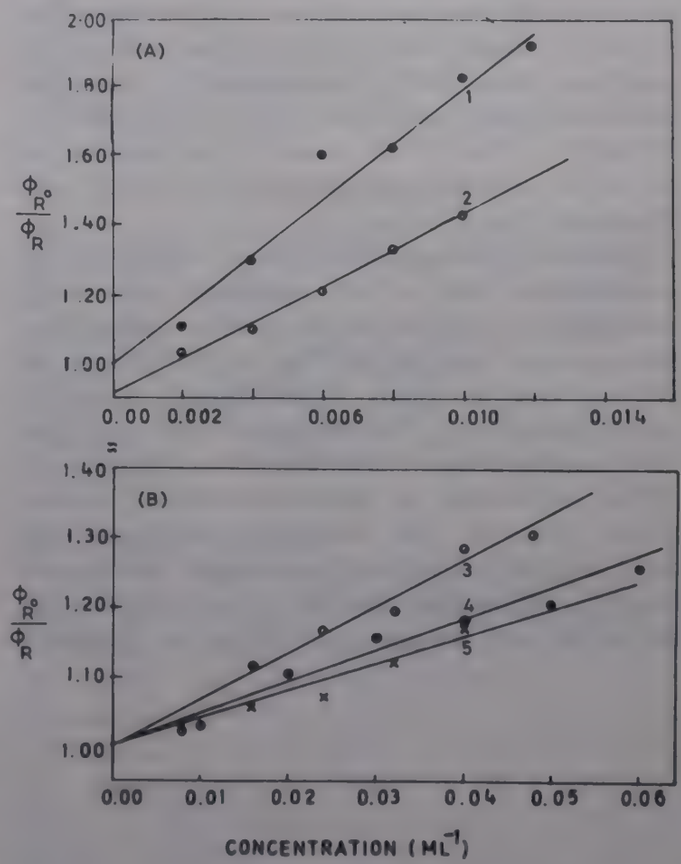

Fig. 1—Stern-Volmer plots for quenching of excited uranyl ion. [(A): 1; aniline, 2; biphenyl, (B): 3; chlorobenzene, 4; bromobenzene, and 5; acetophenone]

$$\frac{\phi_{R^0}}{\phi_R} = 1 + K_{sv}[Q] \qquad \ldots(1)$$

Where ϕ_{R0} and ϕ_R are quantum yields of photochemical reduction of uranyl ion with triphenylphosphine in the absence and presence of the quencher (Q) respectively. The values are given in Table 1.

Table 1—Stern-Volmer type quenching constants of excited uranyl ion with monosubstituted benzene derivatives $[UO_2^{2+}]=[PPh_3]=0.01$ mol.dm^{-3}, $[H^+]=0.10$ moldm^{-3} at 30 ± 2°C

Derivative	K_{sv} (dm^{3}mol^{-1})
Aniline	80.0
Biphenyl	50.0
Chlorobenzene	6.66
Bromobenzene	4.44
Acetophenone	3.90
Benzonitrile	4.10

Discussion

The positive charge of uranyl ion localized on the uranium atom, is well protected and is not involved in the interaction with benzene derivatives in the ground state. However, exposure to light delocalizes the positive charge on the axial oxygen atoms of the uranyl ion, as a result of which excited uranyl ion forms donor-acceptor type complex with benzene derivatives. This in turn reduces the efficiency of photochemical reduction of uranyl ion by triphenylphosphine (Fig. 1).

Monosubstitution on the benzene ring of aromatic quenchers plays a very significant role in the quenching of the electronically excited uranyl ions. Due to negative inductive effect of substituents on the ring, and resonance stabilization of acetophenone, benzonitrile, chlorobenzene and bromobenzene, positive charge is delocalized over the ring, resulting in decrease in π-electron density. Consequently there is poor interaction with positively charged excited uranyl ion. Like anisole[7], the high value of K_{sv} with aniline may be due to positive inductive effect and resonance stabilization of aniline. The delocalization of negative charge over the ring helps in faster donor-acceptor complex formation with electronically excited uranyl ion leading to enhanced physical deactivation.

Biphenyl slightly deviates from linear Stern-Volmer plot (intercept = 0.93, less than unity). If the two phenyl groups were coplanar, the extension of the aromatic π-electron cloud would have quenched electronically excited uranyl ion very strongly. However, non-coplanarity due to free rotation of the phenyl groups may be responsible for its milder quenching action in comparison to that of aniline, but much stronger quenching action in comparison to that of other quenchers. Physical deactivation of excited uranyl ion due to aromatic π-electron cloud competes with its photochemical reduction with triphenylphosphine.

Acknowledgement

Financial assistance by the CSIR, New Delhi is gratefully acknowledged.

References

1 Matsushima R & Sakuraba S, *J Am chem Soc*, 93 (1971) 7143; Matsushima R, *J Am chem Soc*, 94 (1972) 6010.
2 Matsushima R, Mori K & Suzuki M, *Bull chem Soc Japan*, 49 (1976) 38.
3 Ahmad M, Cox A, Kemp T J & Sultana Q, *J chem Soc Perkin(II)*, (1975) 1867.
4 Kemp T J & Burrows H D, *Chem Soc Rev*, 3 (1974) 139.
5 Matsushima R, Fujimori H & Sakuraba S, *J chem Soc Faraday Trans I*, (1974) 1702; Sakuraba S & Matsushima R, *Bull chem Soc Japan*, 44 (1971) 2915; 44 (1971) 1278.
6 Sandhu S S, Sidhu M S & Singh R J, *J Photochem*, 39 (1987) 229; *J Photochem Photobiol (A:) Chem*, 42 (1988) 251.
7 Sidhu M S, Singh R J, Sakaria P & Sandhu S S, *J Photochem Photobiol (A:) Chem*, 46 (1989) 221; *J chem Educ*, 7 (1990) 622.

Indian Journal of Chemistry
Vol. 30A, February 1991, pp 119-124

Voltammetric behaviour of some substituted acetophenone oximes and semicarbazones

B Bhaskar Reddy, N Y Sreedhar & S Jayarama Reddy*
Department of Chemistry, Sri Venkateswara University, Tirupati 517 502

Received 2 January 1990; revised 4 May 1990; accepted 11 September 1990

The electrochemical reduction behaviour of some substituted acetophenone oximes and semicarbazones has been studied by employing advanced electrochemical techniques in different supporting electrolytes. Based on the kinetic parameters evaluated, electrode mechanism is proposed.

Though the reduction mechanism of substituted oximes[1-4] and semicarbazones[5-9] has been investigated polarographically by several workers reduction of substituted acetophenone oximes and semicarbazones such as *o*-methoxyacetophenone oxime (*o*MAO), 3,4-dimethoxyacetophenone oxime (DMAO), *o*-methoxyacetophenone semicarbazone (*o*MAS) and 3,4-dimethoxyacetophenone semicarbazone (DMAS) has not been taken up for study. Hence, we undertook the title investigation using electrochemical techniques such as DC polarography, cyclic voltammetry, AC polarography, differential pulse polarography, rotating ring disk voltammetry, millicoulometry and controlled potential electrolysis

Materials and Methods

The compounds used were prepared by the method described by Vogel and their purity checked by thin layer chromatography and melting point determination. The chemicals used were of AR grade. Polarographic assays were performed using a polarographic analyser model 364 supplied by PARC, USA coupled with BD 8 Kipp & Zonen x-t recorder. A dropping mercury electrode (flow rate, 2.73 mgs^{-1}) was used as the working electrode and a saturated calomel electrode (SCE) as reference. AC and differential pulse polarograms were recorded with Metrohm unit coupled with E 506 polarecord and E 612 VA-Scanner. Cyclic voltammograms were obtained by digital electronics 2000 x-y/t recorder in conjunction with the above unit. A hanging mercury drop electrode of area 0.04438 cm^2 and dropping mercury electrode of area 0.0223 cm^2 were employed as working electrodes and the Ag/AgCl(s), Cl^- electrode was used as reference electrode. Platinum wire was used as the auxiliary electrode. A glassy carbon ring disk electrode was used as the working electrode.

The *p*H measurements were carried out with an Elico digital *p*H meter. All experiments were carried out at 28 ± 1°C.

An appropriate amount of oxime or semicarbazone was dissolved in required quantity of methanol or DMF and the solution diluted with the supporting electrolyte to 10 ml. The solution was deoxygenated by passage of nitrogen gas for five minutes and then the polarogram was recorded. Universal buffers of *p*H ranging from 2.0 to 12.0 including 1 *M* $HClO_4$ were used as supporting electrolytes.

Results and Discussion

From the experimental results obtained, it is found that the aromatic acetophenones presently investigated undergo reduction in acidic media (*p*H ≤ 6.0). The azomethine group ($\geq C=N-$) present in all these compounds is reduced to the corresponding amino group ($\geq CH-NH_2$) in a four electron process as found by millicoulometric technique. No reduction is noticed in neutral and alkaline media (*p*H ≥ 6.5). This kind of reduction behaviour was also observed in parent compounds such as acetophenone oxime[10] and acetophenone semicarbazone[11].

Representative data for 'n' values:

Millicoulometry[12] was carried out in 1 *M* $HClO_4$

	Cell A	Cell B
Diffusion current before electrolysis	i_1 (μA) = 7.5	1.05
Diffusion current after electrolysis	i_2 (μA) = 3.85	2.70

	Cell A	Cell B
Drop time before electrolysis	t_1 (sec) = 2.0	2.00
Drop time after electrolysis	t_2 (sec) = 3.2	3.20

In acidic media, the single wave/peak obtained is ascribed to the reduction of the protonated azomethine group. When compared to the protonated form, the reduction of the neutral form is found to be difficult. Besides this, the electron donating (+*I*) methyl group which is directly linked to the azomethine group hinders the reduction in neutral and alkaline media. This may also be due to the formation of electroinactive anion (RNO^-). By comparing the half-wave potentials of these substituted acetophenone oximes and semicarbazones, the ease of reduction is seen to follow the order: *o*-methoxyacetophenone oxime > 3,4-dimethoxyacetophenone oxime > *o*-methoxyacetophenone semicarbazone < 3,4-dimethoxyacetophenone semicarbazone.

Final product formed in the controlled potential electrolysis was identified as the corresponding amine by IR (vNH:3300 cm^{-1}, δ NH_2:1600 cm^{-1}).

In all the compounds studied the electrochemical reduction processes are found to be irreversible as evidenced from the disobedience of Tomes' criterion, log-plot analysis, shift in reduction potentials towards more negative values with increase in *p*H of the supporting electrolyte and also from the absence of anodic peak in the reverse scan. Typical cyclic voltammogram of 3,4 DMAO is shown in Fig. 1. The nature of the waves was found to be diffusion controlled in all the buffer systems studied as shown by the linear plots of i_d versus $h^{1/2}$ and i_p versus $V^{1/2}$ passing through the origin. This indicates the adsorption free nature of the electroactive species. A typical AC polarogram of 3,4 DMAS is shown in Fig. 2. The collection efficiency (N) calculated from the rotating ring disk voltammetry (0.177 for *o*MAO) is observed to be in good agreement with the theoretical value (0.179) for all the compounds indicating the absence of kinetic complications in the electrode processes. Typical rotating ring disk voltammogram of *o*MAO is shown in Fig. 3.

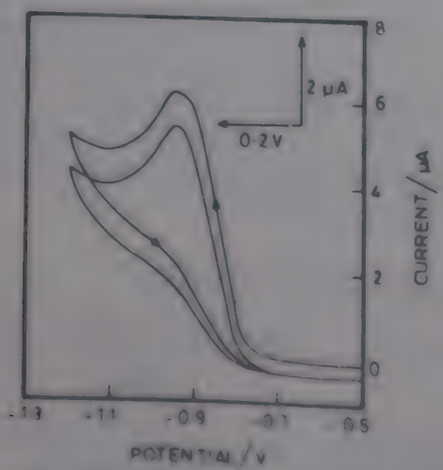

Fig. 1 – Typical cyclic voltammogram of 3,4-dimethoxyacetophenone oxime in *p*H 4.0, concentration: 0.5 m*M*, solvent: 20% MeOH, sweep rate: 40 mVs^{-1}.

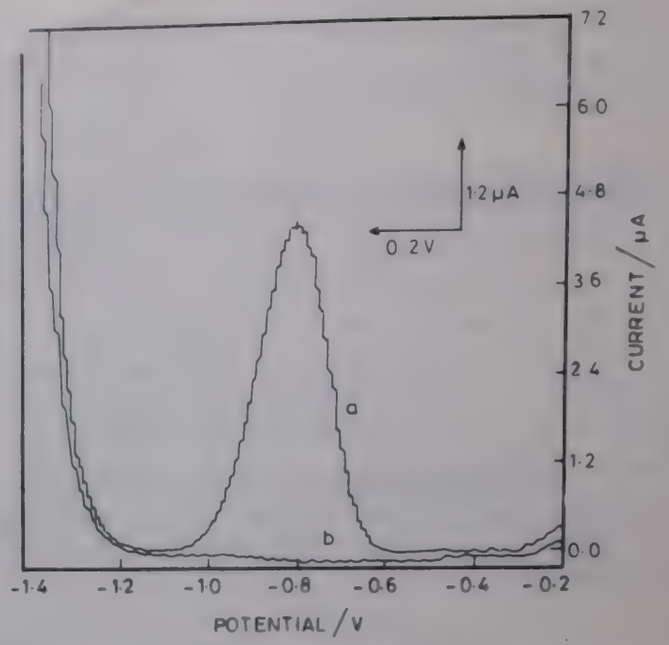

Fig. 2 – Typical A.C. polarogram of 3,4-dimethoxyacetophenone semicarbazone in 1*M* $HClO_4$, concentration: 0.5 m*M*, solvent: 20% DMF, drop time: 3.0 sec, a = A.C. peak, b = base line.

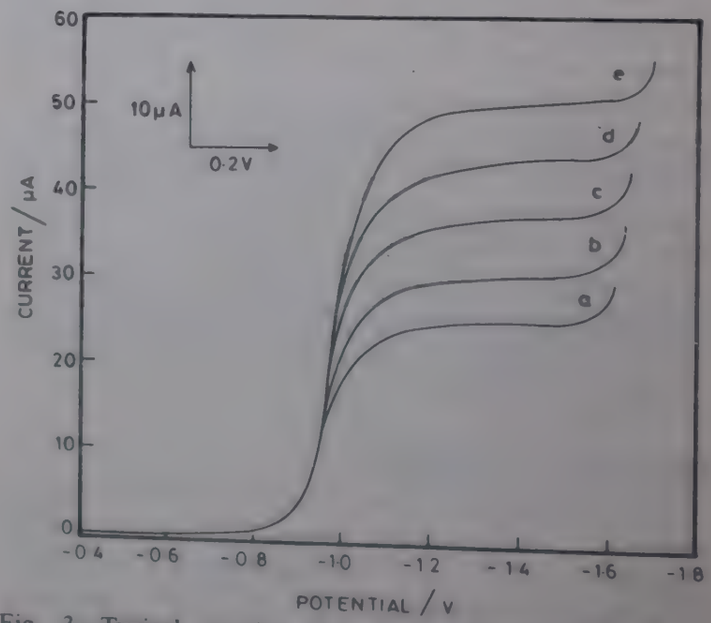

Fig. 3 – Typical rotating ring disk voltammogram of *o*-methoxyacetophenone oxime in *p*H 2.0, concentration: 0.5 m*M*, solvent: 20% MeOH, sweep rate: 50 mVs^{-1}, a = 500 RPM, b = 1000 RPM, c = 1500 RPM, d = 2000 RPM, e = 2500 RPM.

Table 1 – Typical D.C. polarographic data of some substituted acetophenone oximes and semicarbazones

[Concentration: 0.5 m*M*, Drop time: 3.0 sec]

Supporting electrolyte	Solvent: 20% MeOH (20% DMF)				αn_a				$D \times 10^6/cm^2 s^{-1}$				$k^0_{f,h}/cm\ s^{-1}$			
	OMAO		3,4 DMAO		OMAO	3,4 DMAO	OMAS	3,4 DMAS	OMAO	3,4 DMAO	OMAS	3,4 DMAS	OMAO	3,4 DMAO	OMAS	3,4 DMAS
	$-E_{1/2}$ V	i_d μA	$-E_{1/2}$ V	i_d μA												
1*M* $HClO_4$	0.70 (0.89)	9.2 (9.8)	0.78 (0.81)	9.6 (10.4)	1.02	1.12	0.96	0.94	6.68	6.82	5.94	6.01	1.58×10	1.62×10	2.92×10	1.98×10
Universal buffer of *p*H 2.0	0.78 (0.86)	8.3 (9.3)	0.83 (0.83)	8.4 (9.9)	0.98	0.96	0.83	0.89	6.36	6.73	5.04	5.21	2.31×10	2.28×10	2.01×10	1.72×10
*p*H 4.0	0.94 (1.01)	7.4 (8.1)	0.96 (1.04)	7.6 (8.4)	0.91	0.83	0.78	0.85	5.79	5.89	4.62	4.72	5.09×10	5.10×10	3.02×10	3.49×10
*p*H 6.0	1.05 (1.09)	5.8 (6.7)	1.06 (1.12)	5.8 (6.8)	0.80	0.76	0.59	0.79	4.96	4.98	4.23	4.37	3.14×10	1.46×10	2.18×10	4.21×10

OMAO – *o*-methoxy acetophenone oxime 3,4 DMAO – 3,4 dimethoxy acetophenone oxime

OMAS – *o*-methoxy acetophenone semicarbazone 3,4 DMAS – 3,4-dimethoxy acetophenone semicarbazone

Table 2 – Typical cyclic voltammetric data of some substituted acetophenone oximes and semicarbazones

[Concentration: 0.5 m*M*, Sweep rate: 40 mVs^{-1}]

Supporting electrolyte	Solvent: 20% MeOH (20% DMF)				αn_a				$D \times 10^6/cm^2 s^{-1}$				$k^0_{f,h}/cm\ s^{-1}$			
	OMAO		3,4 DMAO		OMAO	3,4 DMAO	OMAS	3,4 DMAS	OMAO	3,4 DMAO	OMAS	3,4 DMAS	OMAO	3,4 DMAO	OMAS	3,4 DMAS
	$-E_p$ V	i_p μA	$-E_p$ V	i_p μA												
1*M* $HClO_4$	0.67 (0.89)	8.61 (9.8)	0.72 (0.81)	6.73 (10.4)	0.68	0.71	0.82	0.84	6.54	6.62	7.99	7.84	1.52×10	1.58×10	5.71×10	4.96×10
Universal buffer of *p*H 2.0	0.76 (0.86)	8.34 (9.3)	0.81 (0.88)	6.52 (9.90)	0.62	0.68	0.75	0.72	6.21	6.24	7.32	7.10	2.14×10	1.18×10	5.17×10	4.41×10
*p*H 4.0	0.89 (1.01)	7.96 (8.1)	0.95 (1.04)	6.31 (8.4)	0.71	0.64	0.67	0.69	5.46	5.58	6.74	5.21	4.98×10	1.60×10	4.36×10	3.43×10
*p*H 6.0	1.01 (1.09)	7.68 (6.7)	1.04 (1.12)	5.48 (6.8)	0.59	0.61	0.58	0.61	4.90	4.49	4.28	4.69	3.04×10	1.48×10	3.91×10	2.60×10

Table 3 – Typical A.C. polarographic data of some substituted acetophenone oximes and semicarbazones

[Concentration: 0.5 m*M*, Drop time: 3.0sec]

Supporting electrolyte	Solvent: 20% MeOH (20% DMF) OMAO		3,4 DMAO		αn_a				$D \times 10^6/cm^2\ s^{-1}$				$k^0_{f,h}/cm\ s^{-1}$			
					OMAO	3,4 DMAO	OMAS	3,4 DMAS	OMAO	3,4 DMAO	OMAS	3,4 DMAS	OMAO	3,4 DMAO	OMAS	3,4 DMAS
	$-E_s$ V	i_s μA	$-E_s$ V	i_s μA												
1*M* $HClO_4$	0.70 (0.89)	3.1 (2.8)	0.78 (0.81)	2.7 (4.5)	0.46	0.49	0.87	0.92	6.28	6.36	8.02	8.06	1.62×10	1.71×10	6.07×10	6.96×10
Universal buffer of *p*H 2.0	0.79 (0.86)	2.8 (2.7)	0.84 (0.88)	2.5 (4.25)	0.41	0.46	0.70	0.81	6.02	6.14	7.36	7.81	5.28×10	6.41×10	5.81×10	6.14×10
*p*H 4.0	0.95 (1.00)	2.7 (2.4)	0.97 (1.03)	2.1 (3.9)	0.36	0.42	0.68	0.87	5.80	5.81	6.81	7.24	4.08×10	4.16×10	4.24×10	5.79×10
*p*H 6.0	1.05 (1.10)	2.5 (2.2)	1.13 (1.12)	1.9 (3.55)	0.39	0.39	0.42	0.79	4.96	4.99	5.43	6.89	4.16×10	5.14×10	2.58×10	4.31×10

Table 4 – Typical differential pulse polarographic data of some substituted acetophenone oximes and semicarbazones

[Concentration: 0.5 m*M*, Drop time: 2.0 sec]

Supporting electrolyte	Solvent: 20% MeOH (20% DMF) OMAO		3,4 DMAO		αn_a				$D \times 10^6/cm^2\ s^{-1}$				$k^0_{f,h}/cm\ s^{-1}$			
					OMAO	3,4 DMAO	OMAS	3,4 DMAS	OMAO	3,4 DMAO	OMAS	3,4 DMAS	OMAO	3,4 DMAO	OMAS	3,4 DMAS
	$-E_m$ V	i_m μA	$-E_m$ V	i_m μA												
1*M* $HClO_4$	0.66 (0.90)	10.9 (10.8)	0.76 (0.79)	11.9 (10.6)	0.48	0.51	0.79	0.68	5.42	5.76	7.09	5.98	2.16×10	3.26×10	5.96×10	5.93×10
Universal buffer of *p*H 2.0	0.75 (0.88)	10.41 (10.65)	0.83 (0.86)	11.32 (10.45)	0.52	0.48	0.51	0.51	5.29	5.49	6.91	5.36	5.44×10	6.67×10	5.46×10	5.38×10
*p*H 4.0	0.86 (0.98)	9.65 (10.50)	0.94 (1.01)	10.95 (10.20)	0.59	0.44	0.59	0.59	5.04	5.33	6.26	4.28	6.26×10	4.96×10	4.94×10	4.18×10
*p*H 6.0	0.98 (1.08)	8.42 (10.35)	1.11 (1.10)	9.46 (9.85)	0.57	0.49	0.48	0.47	4.91	4.99	5.41	3.71	8.41×10	6.43×10	2.53×10	2.51×10

Table 5 – Typical rotating ring disk voltammetric data of some substituted acetophenone oximes and semicarbazones [Concentration: 0.5 m*M*, Sweep rate: 50 mVs^{-1}]

Supporting electrolyte	$D \times 10^6$/cm^2 s^{-1}				$k^0_{f,h}$/cm s^{-1}				Collection efficiency			
	OMAO	3,4 DMAO	OMAS	3,4 DMAS	OMAO	3,4 DMAO	OMAS	3,4 DMAS	OMAO	3,4 DMAO	OMAS	3,4 DMAS
Universal buffer of												
*p*H 2.0	5.94	6.16	6.31	6.71	1.54×10	1.69×10	1.94×10	2.12×10	0.177	0.176	0.178	0.178
*p*H 4.0	4.28	4.21	5.74	5.97	6.21×10	5.24×10	5.86×10	6.42×10	0.175	0.174	0.175	0.172

$E_{1/2}$ and E_p values obtained for all the compounds are found to be *p*H dependent and shift cathodically indicating the involvement of proton in the electrode process. The consequent increase in the *p*H value increases the dissociation constant of the protonated species and these factors affect the protonation rate and consequently the $E_{1/2}/E_p$ values of the reduction wave/peak get shifted to more negative values.

An increase in the [solvent] in the polarographic test solution shifts the half-wave potentials towards more negative potentials with the decrease in diffusion current. The reason for this may be partly an increase in the viscosity of the medium and adsorption of the solvent molecules on the surface of electrode[13].

From the experimental results, it is found that the maximum suppressor, triton X-100 (0.002%) was used to suppress the maxima observed in all the compounds in DC polarography.

The variation of diffusion current and peak current with the *p*H of the supporting electrolyte influences the diffusion coefficient values also which vary in the same manner. The reason for slight decrease in diffusion coefficient values with increase in *p*H may be the decrease in the availability of protons. The diffusion coefficient values obtained for all the compounds are found to be of the order of 10^{-6} cm^2 s^{-1}. The D values evaluated from all the techniques are observed to be in good agreement for all the compounds. This is evidenced from the adsorption free nature of the electrode reaction. But, the diffusion coefficient values obtained from rotating ring disk voltammetry are found to be higher than those observed from other techniques. In the latter techniques, unstirred solutions were used and convection was eliminated as far as possible. But, in rotating ring disk voltammetric method, the convection transport of the depolariser to the electrode plays an important role. As much more material can be brought to the electrode by convection than pure diffusion, the current becomes larger than that in pure diffusion. This may be the reason for the higher diffusion coefficient[14,15] values obtained in this technique.

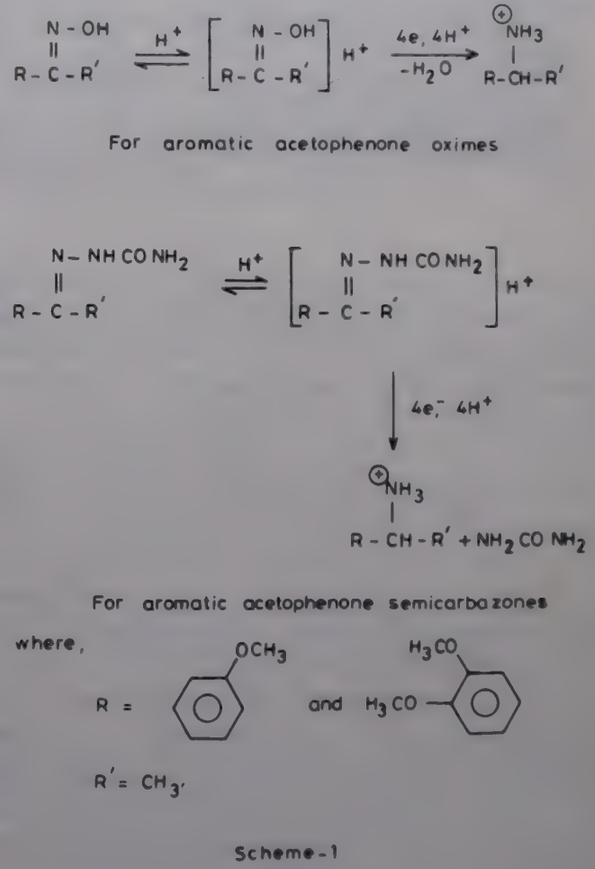

Scheme-1

The rate constant values obtained for the reduction of all the compounds decrease with increase in *p*H of the supporting electrolyte showing that the electrode reaction tends to become more and more irreversible. The heterogeneous forward rate constant values are observed to be high in acidic medium indicating that the rate of reaction is fast in this medium as the protonated

form is getting reduced. On comparing the rate constant values obtained for *o*MAO and 3,4 DMAS, oxime group ($\succ C=N-OH$) is seen to be reduced more easily than semicarbazone group ($\succ C=N-NHCONH_2$). The values obtained for transfer coefficient (α), diffusion coefficient (D) and heterogeneous forward rate constant ($k^0_{f,h}$) for all the compounds are given in Tables 1 to 5.

On the basis of the above results of the present investigation as well as on the basis of the literature data, the reduction mechanism shown in Scheme 1 may be proposed for different compounds.

References

1 Mollin J, Grambal F, Kasparok F, Kucerova T & Lasovsky J, *Chem Zvesti*, 33(4) (1979) 458.

2 Damle M V, Tiwari M, Malshe P T & Kaushal R, *Bull Soc chim Belg*, 89(12) (1980) 1015.

3 Koricanac, Zagorka, Stankovic & Branislava, *Acta Pharm Jugosl*, 33 (3-4) (1983) 215.

4 Bezuglyi V D, Zhukova T V & Shapovalov V A, *Vestn-khark Univ*, 242 (1983) 77.

5 Malik W U & Dua P N, *Indian J Chem*, 21 (1982) 1083.

6 Arvind K, Mishra & Gode K D, *Analyst*, 110 (1985) 1373.

7 Goyal R N & Minoda A, *J Indian chem Soc*, 62 (1985) 202.

8 Morales A, Richter P & Toral M I, *Analyst*, 112 (1987) 965.

9 Kitaev Yu P, Kitaeva M Yu, Latypova V Z, Zaripova R M, Vafina A A & Ilyasov A V, *IZV Akad Nauk SSSR Ser Khim*, 707 (1988).

10 Souchay P & Ser S, *J chim Phys*, 49 (1952) C 172.

11 Kitaev Yu P, Budnikov G K & Arbuzkov A E, *IZV Akad Nauk SSSR Otd Chim Nauk*, 5 (1961) 824.

12 Devries T & Kroon J L, *J Am chem Soc*, 75 (1953) 2484.

13 Meites L, *Polarographic techniques*, 2nd Ed. (Wiley-Interscience, New York) (1965) 141.

14 Levich V G, *Physicochemical hydrodynamics*, (Prentice Hall Englewood Cliffs, NJ) (1962).

15 Adams R N, *Electrochemistry at solid electrodes*, (Dekker, New York) (1969) 214.

Indian Journal of Chemistry
Vol. 30A, February 1991, pp 125-129

Kinetics and mechanism of formation of binuclear complexes of iron(III) with malonatopentaaminecobalt(III) and *trans*-bis(Hmalonato)bis-(ethylenediamine)cobalt(III) ions in aqueous solution

Nigamananda Das & Rabindra K Nanda*
Department of Chemistry, Utkal University, Bhubaneswar 751 004

Received 20 July 1990; accepted 1 October 1990

The kinetics of formation of binuclear complexes between iron(III) and malonatopentaaminecobalt(III) and *trans*-bis(Hmalonato)bis(ethylenediamine)cobalt(III) have been studied using stopped-flow technique in the concentration ranges $[H^+] = 0.050\text{-}0.30$, $[Fe(III)] = 0.005\text{-}0.03$, and $I = 0.5$ mol dm^{-3} and over the temperature range 15.0 to 30.0°C. A general mechanism is proposed which accounts for the available data on the formation of binuclear species involving mainly the reactions of Fe^{3+} and $FeOH^{2+}$ with the undissociated form of the cobalt(III) substrates. The rate data for the various paths for *trans*-bis(Hmalonato)bis(ethylenediamine)cobalt(III) are slightly higher than those for the corresponding pentaamine analogues. The activation parameters for the various paths are also reported.

The kinetic studies on metal ion catalysed aquation at the cobalt(III) centre of binuclear precursor complexes formed between iron(III) and several carboxylatoaminecobalt(III) complexes[1-9] have revealed that a rapid and reversible equilibrium is established between the added aquo metal ion and the cobalt(III) complexes. However, kinetics of rapid formation of binuclear species of Fe(III) and Al(III) with unused donor function of bound dicarboxylate ligands in different cobalt(III) substrates have been very sparingly studied[10-12]. Dash and Harris[10-11] have reported the kinetics of reversible complexation of iron(III) with oxalatopentaaminecobalt(III) and some salicylatopentaaminecobalt(III) substrates. Our objectives in undertaking the title study are to study the effect of the basicity of bound carboxylate ligand, size of chelate ring in the binuclear complex and the overall charge of the cobalt(III) substrate on the kinetics of its complexation with Fe(III).

Materials and Methods

Malonatopentaaminecobalt (III) and *trans*-bis-(Hmalonato)bis(ethylenediamine)cobalt (III) perchlorates were prepared and characterised as described earlier[3,8]. Stock solution of iron(III) perchlorate was prepared and the iron(III) and free acid contents of the stock solution were estimated as described previously[8]. All other chemicals used were reagent grade. All the solutions were prepared in doubly distilled water.

Kinetic measurements

The kinetics of formation of the binuclear species was followed at 350 nm (absorbance increases with time) using a HITECH SF 51 stopped-flow spectrophotometer with Apple IIGS computer interface. The rate measurements were made under pseudo-first order conditions at 15-30°C [for $Co(en)_2(malH)_2^+$] and at 25°C [for $Co(NH_3)_5(malH)^{2+}$] (where $malH = O_2CCH_2COOH^{-1}$) employing $[Fe(III)]_T = 5.0 \times 10^{-3}$ to 30.0×10^{-3} mol dm^{-3} and $[H^+] = 0.05\text{-}0.30$ mol dm^{-3}. Ionic strength was adjusted to 0.5 mol dm^{-3} with $NaClO_4$. Other kinetic details were similar to those described earlier[10]. The pseudo-first order rate constants were obtained by fitting the exponential trace displayed on the monitor to a first order equation using appropriate computer program supplied by M/S Hitech Scientific Ltd (UK). The observed rate constants reported are average of at least five kinetic runs and the errors quoted are standard deviations. All other calculations were made using appropriate least squares programs adopted to Apple IIGS PC.

Results and Discussion

Rate data for the formation of the binuclear species are collected in Tables 1 and 2. It is evident that the pseudo-first order constants increase linearly with $[Fe^{3+}]_T$ at a fixed acidity resulting in a constant finite intercept for k_{obs} versus $[Fe^{3+}]_T$ plots at $[H^+]_T = 0.05\text{-}0.30$ mol dm^{-3} (see Fig. 1). It is, therefore, reasonable to assume that the acid dependence of the reaction results only from the $Fe(OH_2)^{3+}/Fe(OH_2)_5OH^{2+}$ equilibrium. The slopes of such plots, however, very inversely with $[H^+]_T$. The observed first order dependence of k_{obs} with $[Fe^{3+}]_T$ is

Table 1—Rate data for complexation of *trans*-$[Co(en)_2(malH)_2]^+$ with Fe(III) at $I = 0.5$ mol dm^{-3}

$[HClO_4]_T$ (mol dm^{-3})	$10^3[Fe^{3+}]_T$ (mol dm^{-3})	k_{obs} (s^{-1})			
		15.0 ± 0.1°C	20.0 ± 0.1°C	25.0 ± 1°C	30.0 ± 0.1°C
0.05	4.793	2.89 ± 0.09	5.28 ± 0.28	9.87 ± 0.28	16.35 ± 0.25
	7.67	3.30 ± 0.11	6.50 ± 0.19	11.92 ± 0.30	20.09 ± 0.29
	10.54	3.67 ± 0.10	7.26 ± 0.18	13.30 ± 0.33	23.06 ± 0.41
0.075	4.793	2.88 ± 0.08	4.79 ± 0.27	8.33 ± 0.14	14.88 ± 0.26
	7.67	3.17 ± 0.06	5.38 ± 0.16	9.54 ± 0.19	17.01 ± 0.38
	10.54	3.50 ± 0.08	6.14 ± 0.14	10.62 ± 0.37	19.63 ± 0.28
	15.33	3.98 ± 0.10	7.05 ± 0.13	12.80 ± 0.22	23.31 ± 0.09
0.10	4.793	2.74 ± 0.05	4.54 ± 0.28	8.16 ± 0.24	13.43 ± 0.25
	7.67	2.98 ± 0.09	5.27 ± 0.19	9.37 ± 0.36	15.42 ± 0.16
	10.54	3.22 ± 0.08	5.71 ± 0.17	10.11 ± 0.44	17.41 ± 0.36
	14.85	3.55 ± 0.10	6.53 ± 0.14	11.65 ± 0.20	19.85 ± 0.53
	20.13	3.92 ± 0.11	7.16 ± 0.20	13.36 ± 0.20	23.55 ± 0.14
0.2	4.793	—	4.15 ± 0.23	7.26 ± 0.21	12.79 ± 0.69
	7.67	2.76 ± 0.11	4.53 ± 0.31	7.79 ± 0.23	14.36 ± 0.40
	10.54	2.87 ± 0.12	4.87 ± 0.19	8.60 ± 0.19	16.30 ± 0.62
	15.33	3.14 ± 0.06	5.36 ± 0.15	9.64 ± 0.24	17.80 ± 0.41
	20.13	3.30 ± 0.06	6.02 ± 0.20	10.61 ± 0.24	19.60 ± 0.57
0.3	10.54	–	4.49 ± 0.26	8.17 ± 0.47	14.23 ± 0.48
	15.33	–	5.06 ± 0.23	9.20 ± 0.25	15.67 ± 0.41
	20.13	–	5.20 ± 0.25	10.04 ± 0.29	16.89 ± 0.79
	30.67	–	6.08 ± 0.12	11.19 ± 0.25	19.90 ± 1.09

Table 2—Rate data for complexation of $(NH_3)_5ComalH^{2+}$ with Fe(III) at $I = 0.5$ mol dm^{-3}, 25.0 ± 0.1°C

$[HClO_4]_T$ (mol dm^{-3})	10^3 [Fe(III)]$_T$ (mol dm^{-3})	k_{obs} (s^{-1})	k_f (dm^3 mol^{-1} s^{-1})	k_r (s^{-1})
0.05	4.793	8.02 ± 0.18	541.8 ± 15.8	5.43 ± 0.12
	7.67	9.67 ± 0.29		
	10.54	11.12 ± 0.25		
0.075	4.793	7.04 ± 0.21	377.0 ± 30.0	5.16 ± 0.31
	7.67	8.23 ± 0.27		
	10.54	8.99 ± 0.14		
	15.33	11.12 ± 0.23		
0.10	4.793	6.59 ± 0.30	315.3 ± 15.9	5.09 ± 0.20
	7.67	7.45 ± 0.23		
	14.85	9.97 ± 0.27		
	20.13	11.28 ± 0.31		
0.20	7.67	6.57 ± 0.33	207.3 ± 6.3	4.92 ± 0.10
	10.54	7.09 ± 0.32		
	15.33	8.06 ± 0.21		
	20.13	9.13 ± 0.23		
0.30	10.54	6.36 ± 0.17	136.6 ± 5.6	4.96 ± 0.11
	15.33	7.05 ± 0.27		
	20.13	7.77 ± 0.14		
	30.67	9.08 ± 0.23		

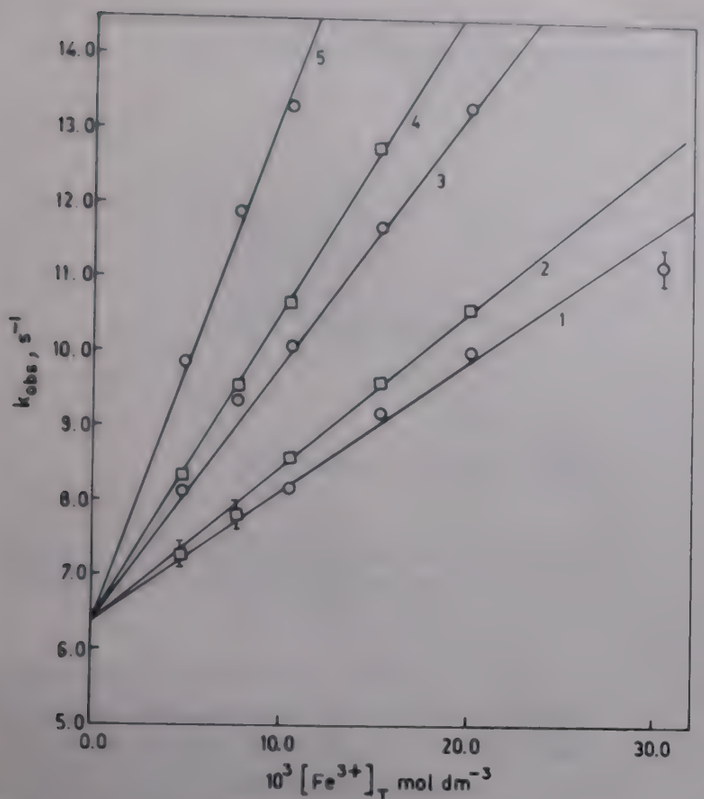

Fig. 1—k_{obs} versus $10^3\,[Fe^{3+}]_T$ plot at 25°C (1, 2, 3, 4 and 5 for $[H^+] = 0.3, 0.2, 0.1, 0.075$ and 0.05 mol dm^{-3}, respectively)

indicative of the fact that only (1 : 1) binuclear complex is formed between Fe(III) and either of the substrates.

The possible reaction mechanism consistent with observed facts can be deleneated as in Scheme 1.

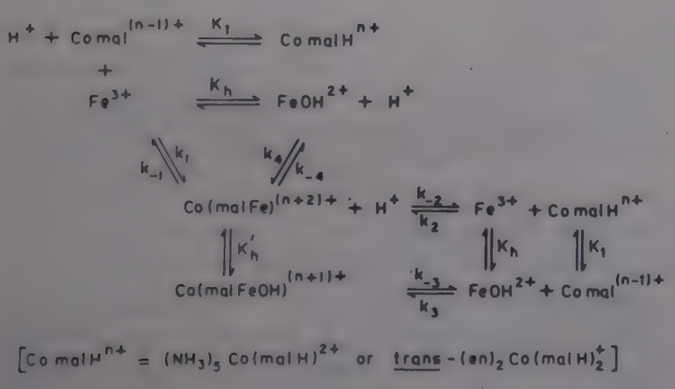

Scheme 1

where,

$$k_{obs} = k_f f_1 f_2 [Fe^{3+}]_T + k_r f_3 \quad \ldots (1)$$

$$k_f = (k_1 K_1 + k_4 K_h)[H^+]^{-1} + k_2 + k_3 K_1 K_h [H^+]^{-2} \quad \ldots (2)$$

$$k_r = (k_{-1} + k_{-4}) + k_{-2}[H^+] + k_{-3} K_h'[H^+]^{-1} \quad \ldots (3)$$

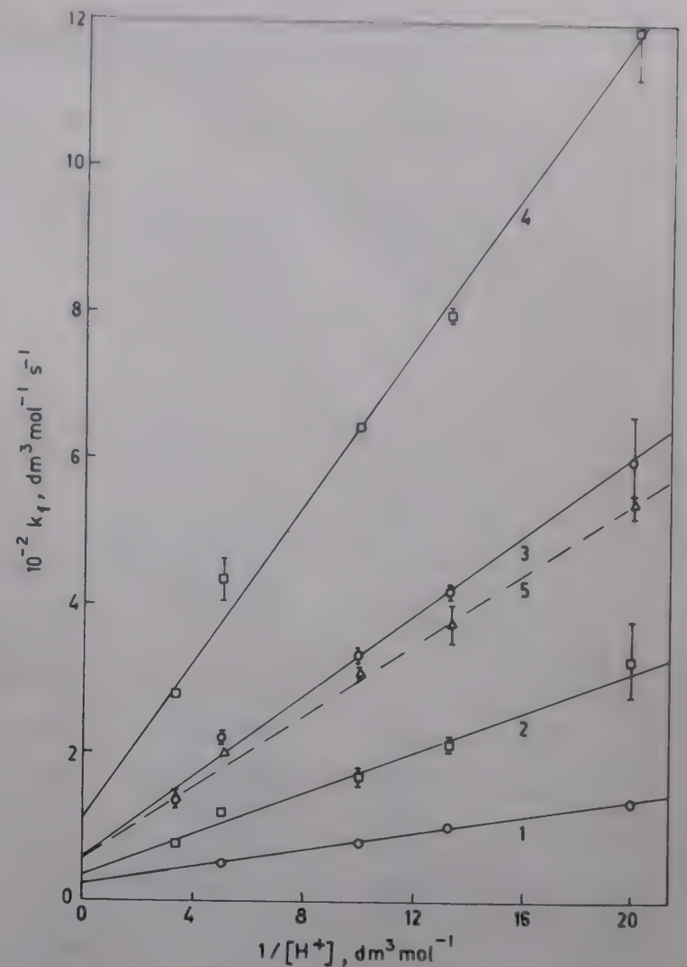

Fig. 2—$10^{-2}\,k_f$ versus $1/[H^+]$ plot (1, 2, 3 and 4 for *trans*-$[Co(en)_2(malH)_2]^+$; 5 for $[(NH_3)_5Co(malH)]^{2+}$)

$$f_1 = [H^+]/([H^+] + k_h) \quad \ldots (4)$$

$$f_2 = [H^+]/([H^+] + K_1) \quad \ldots (5)$$

$$f_3 = [H^+]/([H^+] + K_h') \quad \ldots (6)$$

Values of K_h were obtained from literature[13†]. The values $10^4\ K_1$ for $(NH_3)_5Co(malH)^{2+}$ and $(en)_2Co(malH)_2^+$ at 30°C are 2.88 and 5.01, respectively. Values of K_h' are not known, nor they can be derived from our data. However, it can be assumed to be somewhat smaller than K_h (ref. 10). With the use of these values if follows that f_1, f_2, f_3 are reduced to unity in the acidity range used. k_f and k_r calculated from least squares slopes and intercepts of k_{obs} versus $[Fe^{3+}]_T$ plots are given in Tables 2 and 3. The inverse acidity dependence of k_f and no deviation from the linearity of the plots in Fig. 2 suggest

†The values of the hydrolysis constant of $Fe(OH_2)_6^{3+}$ (K_h) (1.48×10^{-3} and 2.44×10^{-3} dm^3 mol^{-1} at 20 and 30°C and $I = 0.5$ mol dm^{-3} respectively) were obtained by intrapolation of literature data. K_h is 1.18×10^{-3}, 1.90×10^{-3} and 3.2×10^{-3} at 15, 25 and 35°C respectively, ($I = 0.5$ mol dm^{-3})[13]. With use of these values it can readily be shown that $[H^+]$ of the reaction medium as adjusted by added $HClO_4$ is changed only negligibly by the hydrolysis of $Fe(OH_2)_6^{3+}$.

Table 3—Rate parameters for the formation of *trans*-$[Co(en)_2(malH)malFe]^{3+}$ species

$[HClO_4]_T$ (mol dm^{-3})	k_f (dm^3 mol^{-1} s^{-1})	k_2 (dm^3 mol^{-1} s^{-1})	$10^{-3}\,k_4$ (dm^3 mol^{-1} s^{-1})	k_r (s^{-1})
		15.0 ± 0.1°C		
0.05	136.0 ± 3.5	21.4 ± 4.2	5.00 ± 0.35	2.24 ± 0.03
0.075	105.5 ± 2.3	–	–	2.37 ± 0.02
0.10	78.3 ± 1.8	–	–	2.37 ± 0.02
0.20	50.7 ± 1.5	–	–	2.36 ± 0.02
		20.0 ± 0.1°C		
0.05	330.0 ± 50.0	43.5 ± 12.7	8.97 ± 1.38	3.84 ± 0.44
0.075	215.0 ± 12.0	–	–	3.79 ± 0.14
0.10	167.0 ± 13.0	–	–	3.95 ± 0.18
0.20	119.0 ± 4.0	–	–	3.60 ± 0.06
0.30	75.0 ± 6.0	–	–	3.78 ± 0.15
		25.0 ± 0.1°C		
0.05	603.0 ± 67.0	86.3 ± 17.2	13.22 ± 1.02	7.07 ± 0.52
0.075	421.1 ± 10.5	–	–	6.29 ± 0.09
0.10	334.0 ± 8.0	–	–	6.60 ± 0.12
0.20	222.2 ± 7.0	–	–	6.19 ± 0.09
0.30	136.0 ± 15.0	–	–	7.08 ± 0.34
		30.0 ± 0.1°C		
0.05	119.2 ± 80.0	109.0 ± 15.0	21.77 ± 0.72	10.71 ± 0.58
0.075	800.6 ± 11.5	–	–	11.00 ± 0.16
0.10	645.8 ± 5.8	–	–	10.36 ± 0.08
0.20	435.0 ± 32.0	–	–	11.08 ± 0.42
0.30	281.0 ± 7.0	–	–	11.31 ± 0.11

that the last term in Eq. (2) is insignificant and can be neglected. The values of k_2 were derived from the intercepts of least squares plots of k_f versus $[H^+]^{-1}$ (Eq. 2). The slopes of such plots are equal to $(k_1K_1 + k_4K_h)$. However, in the acidity range used in this study both the cobalt(III) substrates will exist practically (> 99.8%) in their undissociated acid forms ($pK = 3.54$ for $(NH_3)_5CoO_2CCH_2CO_2H^{2+}$ at $I = 0.3$ mol dm^{-3}, temp. = 25°C; and $pK_1 = 3.30 \pm 0.01$, $pK_2 = 4.0 \pm 0.02$ for *trans*-$(en)_2Co(O_2CCH_2CO_2H)_2^+$ at $I = 0.1$ mol dm^{-3} and temp = 30°C). Hence k_2-path is likely to be insignificant. Neglecting this path the slope of k_f versus $[H^+]^{-1}$ plot equals k_1K_1 from which k_1 is calculated. Since k_f is independent of $[H^+]$ or $[H^+]^{-1}$, it is reasonable to assume that acid dependent paths (k_3 and k_4) do not contribute significantly to the overall dissociation rate (see Eq. 3). Thus k_r is identified with k_1. The associated activation parameters for various paths are collected in Table 4.

It is interesting to note (see Tables 2 and 3) that the rates of formation of $Co(malFe)^{n+2+}$ for pentaamine and bis(en)$_2$ complexes are comparable and these are also comparable with analogous data for the reaction of Fe^{3+} with $(NH_3)_5CoC_2O_4H^{2+}$ reported by Dash and Harris[10] when due allowance is made for the basicities of malonate and oxalate bound to cobalt(III). Further the electrostatic repulsion between the interacting like-charge cations (Co^{III} and Fe^{III}) is likely to be less for the Hmalonato complex than that for corresponding oxalato complex. This is compatible with observed rate of anation of $Fe(OH_2)_5OH^{2+}$ by Hmal ($k = 13 \times 10^4$ dm^3 mol^{-1} s^{-1} at 25°C; see ref. 14). Presumably this is one of the reasons why reaction path k_2 was observed for the malonato complex the analogous path for the reaction of $(NH_3)_5CoC_2O_4H^{2+}$ with $Fe(OH_2)_6^{3+}$ was, however, not observed. The present view on the ligand substitution reactions at Fe(III) centres is that I_d and I_a mechanisms operate

Table 4—Rates and activation parameters for binuclear complexation reactions $(NH_3)_5Co(malH)^{2+}$ and *trans*-$[Co(en)_2(malH)_2]^+$ with Fe^{3+}, $I = 0.5$ mol dm^{-3}

		$\Delta H^{\ddagger}$ (kJ mol^{-1})	$\Delta S^{\ddagger}$ (JK^{-1} mol^{-1})
k_2, s^{-1} dm^3 mol^{-1}	86.2 ± 17.2	75.8 ± 10.4	44.4 ± 39.94
	(71.1 ± 13.9)		
	small*		
10^{-4} k_4, s^{-1} dm^3 mol^{-1}	1.32 ± 0.21	68.5 ± 1.53	31.2 ± 5.1
	(1.26 ± 0.10)		
	0.46*		
k_{-4}, s^{-1}[a]	6.64 ± 0.42	72.2 ± 1.73	12.8 ± 5.9
	(5.11 ± 0.20)		
	0.5*		

[a]At 25.0 ± 1°C, Values in parentheses are for $(NH_3)Co(malH)^{2+}$ and all others are for *trans*-$[Co(en)_2(malH)_2]^+$
*Analogous data for the oxalatopentaammine ion at 25°C, $I = 1.0$ mol dm^{-3}

for $Fe(OH_2)_6^{3+}$ and $Fe(OH_2)_5OH^{2+}$ respectively[10,15]. The values of outersphere association constant, K_{os}, for the substrates under consideration cannot be greater than unity considering the electrostatic effect[16]. In this context, it is worth noting that the values of k_2* and k_4* for both the substrates (k_2* ≃ 80 ± 20 s^{-1} and k_4* ≃ (1.3 ± 0.50) × 10^4 s^{-1})[†] at 25°C are lower then the values of water exchange rate constant of iron(III) species ($k_{ex}^{25°C} = 1.6 \times 10^2$ s^{-1} and 1.4×10^5 s^{-1} for $Fe(OH_2)_6^{3+}$ and $Fe(OH_2)_5OH^{2+}$ respectively[14]). Hence water dissociation from Fe(III) centre is more likely to be rate-controlling for the formation of binuclear complex at least for $Fe(OH_2)_5OH^{2+}$. However, compared to $Fe(OH_2)_5OH^{2+}$, the mechanism of substitution reaction at $Fe(OH_2)_6^{3+}$ centre is more likely to be I_a as also suggested in the case of formation of binuclear complex of iron(III) with several salicylatopentaamine cobalt(III) complexes[11].

The rate constants for the spontaneous dissociation path (k_{-4}) for both the cobalt(III) substrates are comparable and are ~ 10 times higher than that for $(NH_3)_5CoC_2O_4Fe^{4+}$. However, in comparison to Fe(III)-monochloroacetate[10,18] ($k_{-4} \simeq 20$ s^{-1}) the Fe(III)-malonato species under consideration dissociates nearly four-times slower. These differences are not large enough considering the complexity of the reactions. It, however, might indicate that the binuclear species of the malonato complexes, are more prone to exist in the non-chelated form (A)

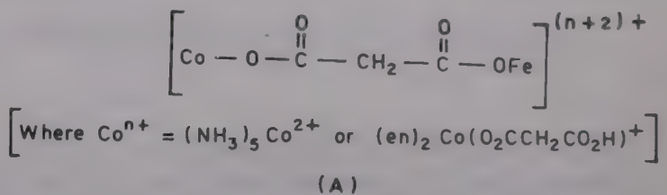

(A)

The activation enthalpies and entropies (see Table 4) for the formation and dissociation of the binuclear species are almost alike and fall in the range expected for similar other substitution reactions of Fe(III) using conventional ligands.

Acknowledgement

We are thankful to Prof A C Dash for many helpful discussions. ND thanks the CSIR, New Delhi for the award of a senior research fellowship.

References

1 Dash A C & Nanda R K, *Inorg Chem*, 13 (1974) 655.
2 Dash A C & Nanda R K, *J Indian chem Soc*, 52 (1975) 289.
3 Dash A C & Nanda R K, *J inorg nucl chem*, 37 (1975) 2139.
4 Dash A C, *J inorg nucl Chem*, 40 (1978) 132.
5 Dash A C & Nanda R K, *Inorg Chem*, 12 (1975) 2024.
6 Nanda R K & Dash A C, *J inorg nucl Chem*, 36 (1974) 1595.
7 Dash A C, Khatoon S & Nanda R K, *Indian J Chem*, 23A (1984) 997.
8 Das N N & Nanda R K, *Indian J Chem*, 28A (1989) 26.
9 Das N N & Nanda R K, *Transition Met Chem*, 15 (1990) 293.
10 Dash A C & Harris G M, *Inorg Chem*, 21 (1982) 1265.
11 Dash A C & Harris G M, *Inorg Chem*, 21 (1982) 2336.
12 Dash A C, *Inorg Chem*, 22 (1983) 837.
13 Connick R E, Hepler L G, Huges Z Z, Kury Jr. J W, Latimar W M & Taso M S, *J Am chem Soc*, 78 (1956) 1827.
14 Cavasino F P & Di Dio E, *J chem Soc (A)*, (1971) 3176.
15 Grant M & Jordan R B, *Inorg Chem*, 20 (1981) 55.
16 Hammes G G & Steinfeld J I, *J Am chem Soc*, 84 (1962) 4639.
17 Gouger S & Stuehr J, *Inorg Chem*, 13 (1974) 379.
18 Perlmutter Hayman B & Tapuhi E, *J coord Chem*, 6 (1976) 31.

[†]It is generally accepted[15,17] that the derived second-order rate constants, k in substitutions of this type are a combination of rapid outer sphere precursor complex formation with equilibrium constant K_{os} and a rate constant for dissociative water elimination such that $k = k^* K_{os}$ for small values of K_{os}.

Indian Journal of Chemistry
Vol. 30A, February 1991, pp 130-135

Chain initiation in persulphate initiated aqueous polymerization of methacrylonitrile under inert atmosphere and mechanism of persulphate decomposition

Sukumar Guchhait, Monoranjan Banerjee & Ranajit Singha Konar*

Chemistry Department, R.E. College, Durgapur 713 209

Received 11 December 1989; revised 7 May 1990; accepted 11 May 1990

It has been found that the initial rate of persulphate decomposition in the persulphate concentration range of 0.40×10^{-2} to 3.00×10^{-2} mol dm^{-3} and the monomer, methacrylonitrile (MAN), concentration range of 0.16 to 0.40 mol dm^{-3} may be given by the following expression,

$$\frac{-d(S_2O_8^{2-})}{dt} \propto [MAN]^{1.38 \pm 0.05} \times [S_2O_8^{2-}]^{1.17 \pm 0.05}$$

A reaction scheme has been suggested to explain the kinetic data.

In the persulphate initiated aqueous and emulsion polymerization of vinyl monomers, the chain initiation is suggested to occur by a mechanism shown in Scheme 1 (see refs. 1-5).

(A) $S_2O_8^{2-} \xrightarrow{k_1} 2S\dot{O}_4^-$

(B) $S\dot{O}_4^- + H_2O \rightarrow HSO_4^- + \dot{O}H$

(C) $2\dot{O}H \rightarrow H_2O_2$ (or $H_2O + \frac{1}{2}O_2$)

(D) $S\dot{O}_4^- + M \rightarrow \dot{M}_1$ $(=O_3-S-O-\dot{M})$

(E) $\dot{M}_j + M \xrightarrow{k_p} \dot{M}_{j+1}$

(F) $2\dot{M}_j \rightarrow$ Polymer

Scheme 1

Such a mechanism predicts that the rate of persulphate decomposition would be independent of [monomer] and also on the nature of the monomer. However, this contention is not found valid. Dunn[6] has suggested that induced decomposition of persulphate may occur by steps (G) and (H).

(G) $S\dot{O}_4^- + M\,(=RH) \rightarrow HSO_4^- + \dot{R}$

(H) $\dot{R} + S_2O_8^{2-} \rightarrow R-O-SO_3^- + SO_4^-$

Dunn's mechanism predicts that *p*H of aqueous solution will decrease with increase in [monomer] but this was not supported by experimental facts[7,8]. While studying the emulsion polymerization of vinyl acetate initiated by persulphate, Chang[9] suggested that the R radicals are produced from the chain transfer reactions taking place in the latex particles. Being very small in size, R radicals would diffuse into the aqueous phase to cause further induced decomposition. If all the R radicals thus are oxidised by persulphate ions in the aqueous phase, then there would be no polymerization at higher [persulphate]. Sarkar *et al.*[10] studied the aqueous polymerization of vinyl acetate and found that at higher [persulphate] ($> 10^{-2}$ mol dm^{-3}) the polymerization does occur but the polymers so obtained are partly insoluble in common solvents namely benzene, acetone, etc. This of course indicates that at higher [persulphate] the polymerization reaction mechanism is very complex and probably cross-linked polymer would form. Since very little work[1,2] has been done on the aqueous and emulsion polymerization of methacrylonitrile (MAN), initiated by potassium persulphate, we report herein the mode of chain initiation of aqueous polymerization of MAN and the mode of persulphate decomposition.

Materials and Methods

Purification and processing of reagents have been described elsewhere in detail[7,8]. Potassium persulphate (GR, E Merck) was recrystallised three times from doubly distilled water. Methacrylonitrile (MAN) (AG, Fluka; stabilised by hydroquinone) was washed with 1% NaOH, followed by distilled water till free of alkali and dried over anhydrous calcium chloride. It was distilled under reduced pressure and vacuum fractionated, and the middle fraction (refractive index = 1.401 at 25°C) was collected and stored at −5°C. Before use the monomer was tested for the presence of peroxide. If peroxide was

detected, the monomer was refluxed under nitrogen atmosphere and distilled before use. The reaction was carried out in a hermetically sealed pyrex flask fitted with a Hg-seal stirrer and connectors for passing nitrogen and for extracting solutions[7,8]. It was noted that the aqueous solution of MAN did not alter the *p*H of the distilled water (6.9-7.0 at 25°C). During the reaction at 50°C samples were collected at different times and quenched immediately in ice. The *p*H of the solution was measured at room temperature (25 ± 3°C). Persulphate was estimated by the method of Kolthoff and Carr[11]. Percentage conversion of monomer to polymer was estimated gravimetrically. Polymer molecular weight ($\bar{M}_v$) was measured viscometrically in DMF solvent at 30°C using Mark-Houwnik's equation[12], $[\eta] = 0.36 (\bar{M}_v)^{0.503}$ where $[\eta]$ is in ml/gm and $\eta_{sp}/C = [\eta] + K_h[\eta]^2C$, the Huggin's constant K_h was found to be 0.366, C is the concentration of polymer in DMF in g/100 ml.

Results

The results of persulphate decomposition in the presence of MAN are shown in Figs 1 to 4 and Table 1. It is found that the rates of persulphate decomposition increase with increase in [monomer]. Initial rates of persulphate decomposition were estimated at various [monomer] and at a given [persulphate], by plotting the time average rates of persulphate decomposition as a function of time and extrapolating the resulting linear plot to zero time (Fig. 1) to get the initial rate at zero time. It is also found that in the absence of monomer, the rate of persulphate decomposition is independent of time (Fig. 1, curve, E) in the early stages of the reaction, whereas in the presence of monomer the rates of decomposition were decreased with time and with the conversion of monomer to polymer (Fig. 1). Initial rates of persulphate decomposition were also determined by the tangent method of Hinshelwood and

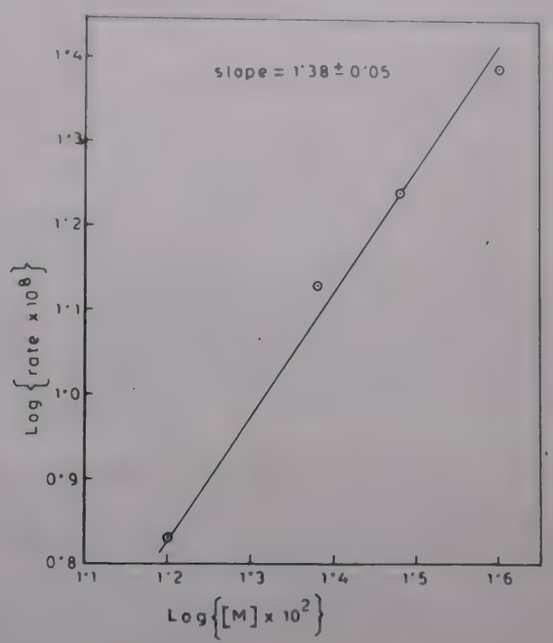

Fig. 2—Order plot for the monomer with respect to the persulphate decomposition log (initial rate of persulphate decomposition, in mol dm^{-3}s^{-1}) versus log (initial monomer concentration, in mol dm^{-3}) has been plotted. The slope of the line 1.38 ± 0.05, gives the order of the monomer.

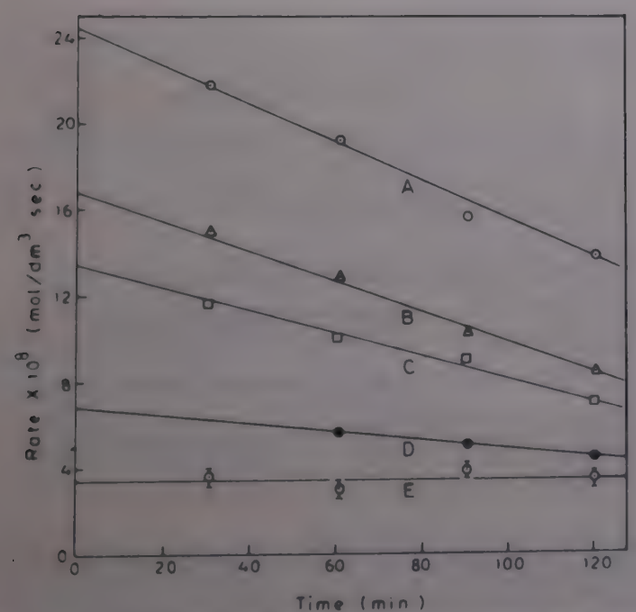

Fig. 1—Average rates of persulphate decomposition at various concentrations of the monomer (MAN) and at a given concentration of persulphate (2.0×10^{-2} mol dm^{-3}), (A) 0.40, (B) 0.30, (C) 0.24, (D) 0.16, (E) 0.00 (mol dm^{-3}) of the monomer (MAN). It is assumed that the extrapolated rates at zero time are the initial rates at various concentration of the monomer (MAN).

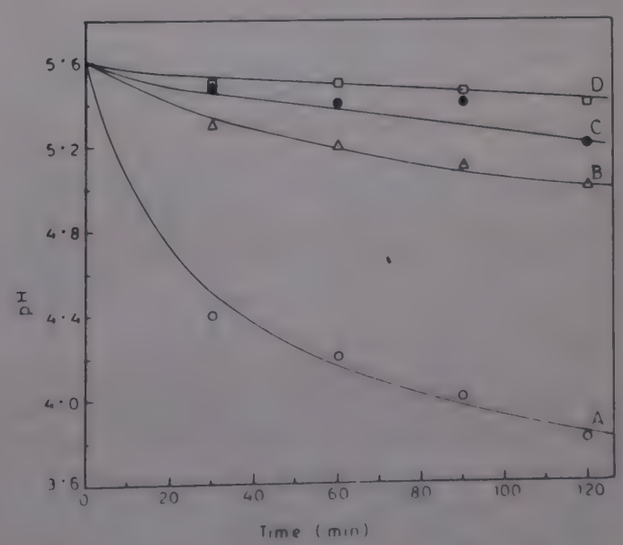

Fig. 3—Effect of [monomer] on the *p*H change of the aqueous solutions of persulphate (0.50×10^{-2} mol dm^{-3}) during its decomposition at 50°C. *p*H was measured at 25°C: (A) persulphate alone, (B) persulphate and monomer (0.12 mol dm^{-3}), (C) persulphate and monomer (0.24 mol dm^{-3}), (D) persulphate and monomer (0.48 mol dm^{-3}).

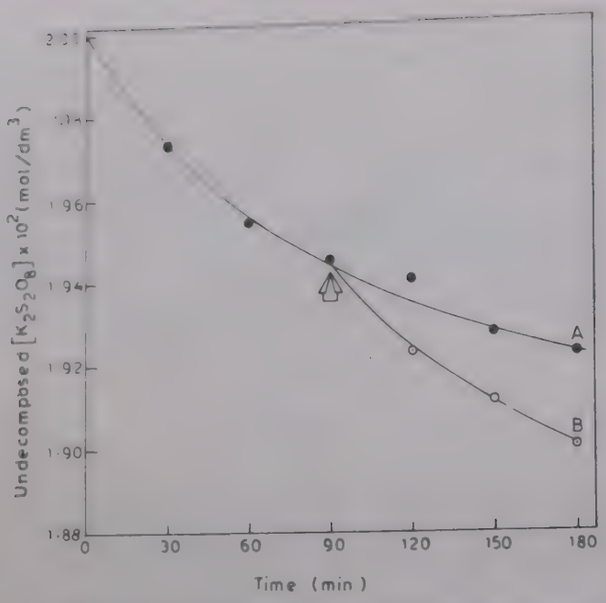

Fig. 4—Effect of monomer when injected late in run on the decomposition of persulphate (KPS) Curve A: (receipe MAN = 0.30 mol dm^{-3}), KPS = 2.0×10^{-2} mol dm^{-3}) (●), curve B where extra (0.10 mol dm^{-3}) MAN was injected after 90 minutes. Arrow in the figure indicates the point at injection. The injected monomer accelerates the rate of decomposition (○).

the rates obtained by the two different methods agree within ± 10.0%. The order in [monomer] was found to be 1.38 ± 0.05. Fig. 2 shows the time average rates of persulphate decomposition at various [persulphate] and at a given [monomer]. From the initial rates the order in [persulphate] was found to be about 1.17.

Fig. 3 shows the *p*H variations with time during the reaction in the presence and absence of monomer. The *p*H of the persulphate solution decreased rapidly initially, and then slowly with time. Increase in [MAN] in the solution reduced the rate at which *p*H decreased, but the *p*H change (i.e. Δ*p*H) was not zero in this system even when the solution was saturated with monomer (4.0% v/v, at 50°C), whereas Δ*p*H was almost zero in the persulphate-acrylonitrile system[5] containing 8.5% acrylonitrile (w/v). It is found that the monomer injected late in a run accelerated the rates of persulphate decomposition Fig. 4), indicating that the monomer in the aqueous phase is interacting with the $S_2O_8^{2-}$ ions.

Data in Table 1 show the conversion of monomer to polymer with time in the aqueous polymerization of MAN. The viscosity average molecular weight ($\bar{M}_v$) of the polymer was of the order of 10^5. The Huggin's constant (K_H) in DMF was 0.366 at 30°C. The latex particles were found unstable in the presence of higher persulphate (1.0×10^{-2} mol dm^{-3}). We did not investigate here the polymer end groups, because it is well known that in the persulphate initiated polymerization of vinyl monomers, end groups are hydroxyl and sulphate[11].

Table 1—Molecular weights and colloidal stability of polymers in the latex solution

[MAN] = 0.24×10^{-2} mol dm^{-3}, [$K_2S_2O_8$] = 0.50×10^{-2} mol dm^{-3}, [K_2SO_4] = 0.25×10^{-2} mol dm^{-3}

Reaction time (min.)	Conversion (%) of monomer to polymer	Colloidal stability m.mol $MgSO_4$/dm^3	$[\eta] \times 10^{-2}$ ml/gm	$\bar{M}_v \times 10^{-5}$
60	6.65	62.0	—	—
90	10.53	—	1.59	2.49
120	13.36	60.24	1.66	2.73
135	15.65	57.80	1.63	2.62
165	18.28	53.20	1.56	2.42

Discussion

The simple mechanism (see Scheme 1) of persulphate decomposition in the presence of a vinyl monomer predicts that the rate of persulphate decomposition should be independent of [monomer]. This is in contrast to the result obtained presently. We propose Scheme 2 to account for the results obtained in this investigation.

$$S_2O_8^{2-} \rightarrow 2S\dot{O}_4^- \quad \text{in the aqueous phase} \quad \ldots(1)$$

$$S\dot{O}_4^- + H_2O \rightarrow HSO_4^- + \dot{O}H \text{ in the aqueous phase} \quad \ldots(2)$$

$$2\dot{O}H \rightarrow H_2O_2 \text{ (or } H_2O + \tfrac{1}{2}O_2\text{) in the aqueous phase} \quad \ldots(3)$$

$$S\dot{O}_4^- + M \rightarrow \dot{M}_1\,[= \bar{O}_3 - S - O - CH_2 - \dot{C}(CH_3)CN]$$
in the aqueous phase $\ldots(4)$

$$S\dot{O}_4^- + M \rightarrow (\dot{M}_1),\,[= \dot{C}H_2 - C(CH_3)(CN) - OSO_3^-]$$
in the aqueous phase $\ldots(4a)$

$$S\dot{O}_4^- + M \rightarrow HSO_4^- + CH = C(CH_3) - CN$$
$$\text{or } CH_2 = C(\dot{C}H_2) - CN$$
in the aqueous phase $\ldots(4b)$

$$S_2O_8^{2-} + M \rightarrow \dot{M}_1 + S\dot{O}_4^- \quad \text{in the aqueous phase} \quad \ldots(5)$$

$$\dot{M} + M' = RH \rightarrow MH + \dot{R} \quad \text{in water, in the particle and also at the particle water interface} \quad \ldots(6)$$

$$\dot{M} + M \xrightarrow{k_j} \dot{M}_{j+1} \quad \ldots(7)$$

$$\dot{M}_{j_s} \rightleftharpoons \dot{M}_{j_r} \quad \text{in the particle-water interface and where } j = 1 \text{ to } 10 \quad \ldots(8)$$

$(\dot{M}_j)_w + P$ (dead particle) $\rightleftharpoons P^*$ (active particle) ...(9)

$(\dot{M}_j)_w + S_2O_8^{2-} \rightarrow (M_j - O - SO_3^-)_w + S\dot{O}_4^-$ in water, ...(10)

$(M)_w \rightleftharpoons (M)_p$ at the particle water interface ...(11)

$2(\dot{M}_j)_w \xrightarrow{k_{tw}}$ Polymer in water ...(12)

$2(\dot{M}_i)_p \xrightarrow{k_p}$ Polymer in a latex particle or between two active particles if they coagulate together; i = 1 to any value, say 1000 or more ...(13)

Scheme 2

In the absence of monomer, SO_4^- primary free radicals are produced only in reaction (1) and would disappear via reaction (2), and so the solution would be acidic. *p*H of the solution would decrease with time which is consistent with the results shown in Fig. 3. In the presence of monomer, $S\dot{O}_4^-$ radicals are also produced via the reactions (5) and (10), and disappear via steps (2), (4) and (4a). If the monomer is highly reactive towards $S\dot{O}_4^-$ radicals, and where $S\dot{O}_4^-$ addition to the olefinic double bond of the monomer is not hindered due to the steric effect of the adjacent alkyl groups viz. CH_3, C_2H_5, C_6H_5 etc., then almost all $S\dot{O}_4^-$ radicals would disappear via step (4), as was found in the persulphate-acrylonitrile system[8]. In the latter system, the *p*H of the medium did not alter when the aqueous solution was saturated with the monomer[8]. In the MAN-persulphate system however, slight change in *p*H even when the aqueous solution was saturated with MAN (Fig. 3) indicates that either reaction (2) or (4b) or both are occurring. It seems to us that because of the steric effect of the CH_3 group in MAN, reaction (4a) is unlikely to occur. Reaction (4b) requires higher activation energy[14] and hence may not be important here at low temperature[1] (50°C). It appears that even when the solution was saturated with MAN, reaction (2) was not totally suppressed, since $S\dot{O}_4^-$ radicals do not react with MAN vigorously[15].

From the data shown in Fig. 1, the first order rate constant (k_1) of the reaction (1), viz. $S_2O_8^{2-} \rightarrow 2S\dot{O}_4^-$, was found to be 1.71×10^{-6} s^{-1}, which agrees with the literature values[4], viz. $(1.3$ to $2.61) \times 10^{-6}$s^{-1} at 50°C. In our measurement we found that k_1 was independent of *p*H in the *p*H range of 4 to 7, while Kolthoff *et al.*[1,16] and Wilmarth *et al.*[5] reported that k_1 was almost independent of *p*H in the *p*H range of 3 to 13. Below *p*H = 3 and above 13, k_1 was found to increase rapidly at a given temperature[4,5,18]. Only Breuer and Jenkins[18] reported that k_1 was *p*H dependent, and the maximum value of k_1 ($= 2.8 \times 10^{-6}$s^{-1}) was observed at *p*H 7 and 50°C. Such a high value of k_1 was not reported by any other worker[3-5]. Since the order in [monomer] is not zero, it seems that there are other reactions which would account for the higher rates of persulphate decomposition in the presence of the monomer.

The most plausible reactions which seem to reflect the effect of varying [monomer] are reactions (5) and (10), in which $S_2O_8^{2-}$ ions interact with the monomer directly and also with the water soluble monomeric free radicals, viz. $\dot{M}_1$ $[= \bar{O}_3 - S - O - CH_2 - \dot{C}(CH_3) - CN]$ and $\dot{R}[= CH_2 = C(\dot{C}H_2) - CN$ or $\dot{C}H_2 - C(= CH_2) - CN]$ which are resonating structures. For simple kinetic treatment, it is assumed that $\dot{M}_1$ and $\dot{R}$ are indistinguishable. It follows from the Scheme 2 that

$$\frac{-d[S_2O_8^{2-}]}{dt} = k_1[S_2O_8^{2-}] + k_5[S_2O_8^{2-}][M] + k_{10}(M_j)_w[S_2O_8^{2-}] \quad ...(14)$$

Rate of initiation in the aqueous phase $(R_i)_w$, is given by

$$(R_i)_w = \{2k_1[S_2O_8^{2-}] + 2k_5[M][S_2O_8^{2-}] + k_{10}(\dot{M}_j)_w[S_2O_8^{2-}]\}V_w \quad ...(15)$$

where V_w is the volume fraction of water, V_p is the volume fraction of polymer, so that $V_w + V_p = 1.0$. Assuming (1) and (5) are major chain initiating reactions, and neglecting (10), we get,

$$(R_i)_w = \{2k_1 + 2k_5[M]\}[S_2O_8^{2-}]V_w \quad ...(16)$$

Under our experimental conditions, $V_w \gg V_p$ and so here $V_w \cong 1.0$.

Rate of termination in the aqueous phase, $(R_t)_w$, is given by

$$(R_t)_w = 2k_{tw}(\dot{M}_j)_w^2 V_w \quad ...(17)$$

In the steady state, $(R_i)_w = (R_t)_w$, and hence

$$(\dot{M}_j)_w = k_{tw}^{-0.5}\{k_1 + k_5[M]\}^{0.5}[S_2O_8^{2-}]^{0.5} \quad ...(18)$$

Combining (14) and (18), we get

$$\frac{1}{[S_2O_8^{2-}]}\left\{\frac{-d[S_2O_8^{2-}]}{dt}\right\} = \{k_1 + k_5[M]\} + k_{10}k_{tw}^{-0.5} \times \{k_1 + k_5[M]\}^{0.5}[S_2O_8^{2-}]^{0.5} \quad ...(19)$$

Hence a plot of left hand side of Eq. (19) versus $[S_2O_8^{2-}]^{0.5}$ should be linear at a given [monomer] (Fig. 5). From the slope and the intercept of such a plot, k_5 and k_{10} have been estimated, taking $k_1 = 1.71 \times 10^{-6}$ s^{-1} and $k_{tw} = 7.32 \times 10^9$ ($dm^3.mol^{-1}s^{-1}$) from Dainton *et al.*[19] for the aqueous polymerization of acrylonitrile since k_{tw} for the aqueous polymerization of MAN is not known. The [monomer] was 0.36 ($mol\,dm^{-3}$) and k_5 was found as 1.12×10^{-5} ($dm^3mol^{-1}s^{-1}$) and k_{10} as 1.46×10^3 ($dm^3mol^{-1}s^{-1}$). It may be pointed out here that Dainton's k_p and k_t for the aqueous polymerization of acrylonitrile have been questioned by McCarthy *et al.*[20] who believe that Dainton's k_p and k_t values were very high.

Fig. 4 shows that the monomer injected late in a run increased the rate of persulphate decomposition pointing to a crucial role of monomer in persulphate decomposition in the aqueous phase. Since in a given run, the rate of persulphate decomposition was found to decrease continuously with time (Fig. 1) or with the conversion of monomer to polymer, it is clear that the polymer in the latex particles was not responsible for the induced decomposition of persulphate in this system. Further, the polymer was found to be soluble in DMF indicating that no cross-linked polymer was formed during the reaction. In the vinyl acetate-persulphate and methyl acrylate-persulphate systems, it was observed[21] that the monomer injected late in a run had no measurable effect on the rates of persulphate decomposition. it is believed that these monomers are good solvents for their respective polymers, and so they are quickly absorbed by the existing latex particles in the system, and very little of the injected monomer remains in the aqueous phase. For MAN, the distribution coefficient (i.e. concentration of monomer in the polymer phase/concentration of monomer in the aqueous phase at 50°C) is very low (about 1.80), whereas that of vinyl acetate or methyl acrylate is very high[21], viz. about 22.0 ± 2.0.

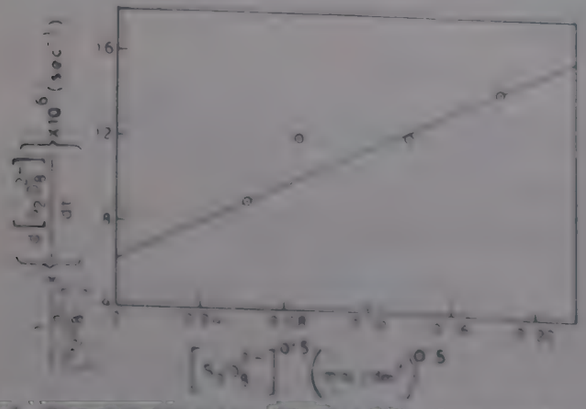

Fig. 5 — Plot of $\left\{-\frac{d[S_2O_8^{2-}]}{dt}\right\} \times 10^6$ (sec^{-1}) versus $[S_2O_8^{2-}]^{0.5}$ at a given monomer [as shown in Eq. (19)]

The data in Table 1 show that the rate of polymerization is very slow and the total conversion in 165 mins is also very small, viz. only about 18%. It seems that the locus of polymerization was shifted overwhelmingly from the aqueous phase to the surface of the latex particles, where polymerization occurred at slow rate due to the relatively low [monomer] at the reaction site, even though the polymerization occurred at an accelerated rate. The colloidal stability of the latex particles was found to decrease with time, which indicates that incipient coagulation of the latex particles was taking place during the reactions. Molecular weight of polymer was found to increase with time in the early stages of the reaction, attain a maximum and then decrease with time. This observation is probably associated with the change of polymerization rates with time. Similar observation were noted in the emulsion polymerization of styrene[22] and also in the aqueous and emulsion polymerizations of methyl acrylate[23] and of ethyl acrylate.

Conclusion

The data presented here show clearly that the major initiation reactions in the persulphate-water-MAN system are reactions (1) and (5). In fact, at a [monomer] of 0.30 mol dm^{-3}, $k_1 = 1.71 \times 10^{-6}s^{-1}$, $k_5 = 1.12 \times 10^{-5}$ $dm^3mol^{-1}s^{-1}$ and at $[K_2S_2O_8] = 10^{-3}mol\,dm^{-3}$, we find that

$$\frac{(R_i)_5}{(R_i)_1} = \frac{2k_5[M][S_2O_8^{2-}]}{2k_1[S_2O_8^{2-}]}$$

$$= \frac{1.12 \times 10^{-5} \times 0.3}{1.71 \times 10^{-6}} \simeq 2.0$$

i.e. the rate of initiation (R_i) due to step (5) is twice that due to step (1). Kinetic analysis also suggests that a part of the water soluble radicals are oxidised by the persulphate ions in the aqueous phase.

Acknowledgement

One of us (RSK) thanks the CSIR, New Delhi for a research grant and SG also thanks the CSIR for a junior research fellowship.

References

1 Bovey F A, Kolthoff I M, Medalia A I & Meehan E J, *Emulsion polymerization* (Interscience, N. Y.) 1955.
2 Blackley D C, *Emulsion polymerization* (Applied Science Publ. London) 1975.
3 House D A, *Chem Rev*, 62 (1962) 185; *Coord chem Rev*, 23 (1977) 223.
4 Behrman E J & Edwards J O, *Rev Inorga Chem*, 2 (1980) 179

5 Wilmarth W K, Schwartz N & Giuliano C R, *Coord chem Rev*, 51 (1983) 243.
6 Dunn A S, *Emulsion polymerization*, edited by I Piirma (Academic Press, New York) 1982, p 221.
7 Adhikari M S, Sarkar S, Banerjee M & Konar R S, *J appl polym Sci*, 34 (1987) 109.
8 Sarkar S, Adhikari M S, Banerjee M & Konar R S, *J appl polym Sci*, 35 (1988) 1441.
9 Litt M H & Chang K H S, *Emulsion polymerization of vinyl acetate*, edited by M S El-Aasser & J W Vander Hoff, Sci Publ, (London), p. 137.
10 Sarkar S, Adhikari M S, Banerjee M & Konar R S, *J appl polym Sci*, (in press).
11 Kolthoff I M & Carr E M, *Anal Chem*, 25 (1953) 298.
12 Brandrup J & Immergut E H edited, *Polymer hand book*, (Wiley Interscience, N. Y.) 1975.
13 Saha M K, Ghosh P & Palit S R, *J polym Sci*, A2 (1964) 1365; Mandal B M & Palit S R, *J polym Sci*, Part A-1 (1971) 3301; Banthia A K, Mandal B M & Palit S R, *Makromol chem*, 175 (1974) 413.
14 Benson S W, *Foundation of chemical kinetics*, (McGraw Hill, New York) 1960.
15 Mc Ginniss V D & Kah A F, *J coatings Tech*, 49 (1977) 61.
16 Kolthoff I M, Meehan E J & Carr E M, *J Am chem Soc*, 75 (1953) 1439; Kolthoff I M & Miller I K, *J Am chem Soc*, 73 (1951) 3055.
17 Singh U C & Venkatarao K, *J inorg nucl chem*, 38 (1976) 541.
18 Breuer M M & Jenkins A D, *Trans Faraday Soc*, 59 (1963) 1310.
19 Dainton F S & Seaman P H, *J polym Sci*, 39 (1959) 279; Dainton F S, Seaman P H, James D G L & Eaton R S, *J polym Sci*, 34 (1959) 209.
20 Mc Carthy S J, Elbing E E, Wilson I R, Gilbert R G, Napper D H & Sangster D F, *Macromolecules*, 19 (1986) 2440.
21 Guchhait S, Sarkar S, Banerjee M & Konar R S, (To be published).
22 Chatterjee S, Banerjee M & Konar R S, *J polym Sci, Polym chem*, 16 (1978) 1517.
23 Banerjee M & Konar R S, *Polymer (London)* 27 (1986) 147.

Indian Journal of Chemistry
Vol. 30A, February 1991, pp 136-139

Kinetics and mechanism of oxidation of tris(2,2′-bipyridyl)-cobalt(II) by *p*-benzoquinone—Micellar effect of sodium dodecyl sulphate

P V Subba Rao*, G S R Krishna Rao & K Ramakrishna

School of Chemistry, Andhra University, Visakhapatnam 530 003

Received 1 December 1989; revised 7 August 1990; accepted 18 September 1990

Oxidation of tris(2,2′-bipyridyl)-cobalt(II) by *p*-benzoquinone is first order in each of the reactants. The energy and entropy of activation are 42 ± 8 kJ mol^{-1} and -105 ± 25 JK^{-1}mol^{-1}. The second order rate constant is not influenced by change in [bipyridyl] when present in excess. The kinetic results are compatible with outer sphere electron transfer mechanism. The micellar effect of sodium dodecyl sulphate(SDS) on this reaction has been investigated. The binding constant of *p*-benzoquinone has been determined spectrophotometrically.

The kinetics of redox reactions of *p*-benzoquinone(PBQ) with many organic and inorganic substrates except those of polypyridyl complexes of Co(II) have been reported[1-5]. The interest in such an investigation led us to carry out the title work.

Materials and Methods

All solutions were prepared in conductivity water. Cobalt(II) was standardised by titration against EDTA solution using xylenol orange as indicator and PBQ solution by iodometric method. The *p*H of the reaction mixture was always maintained constant at 3.6 using 0.1 moldm^{-3} acetic acid-acetate buffer. The *p*H of the medium (20% (v/v) aqueous methanol) has been calculated using the method of Deligny and Rehback[6]. A 0.1 moldm^{-3} solution of the complex, Co(bipy)$_3^{2+}$ was prepared by mixing Co(II) and 2,2′-bipyridyl in the stoichiometric ratio. SDS (Fluka) was purified using the literature method and the purity was further checked by determining its critical micelle concentration(cmc).

Oxidation products—A solution of Co(bipy)$_3^{2+}$ (0.05 mol dm^{-3}) was mixed with excess of PBQ at *p*H 3.6 and the reaction allowed to go to completion. The organic components were removed by extraction with ether and the absorption spectrum was found to overlap with that of Co(bipy)$_3^{3+}$ obtained by electrolytic oxidation of Co(bipy)$_3^{2+}$ under identical conditions. Such a spectral coincidence was not observed at *p*H different from 3.6. This is in conformity with the earlier findings[7]. The oxidation product in the ether extract was identified as hydroquinone(H$_2$Q).

Stoichiometry—To determine the stoichiometry of the reaction, a known concentration of Co(bipy)$_3^{2+}$ was mixed with different concentrations of PBQ in 20% (v/v) methanol at *p*H 3.6. The absorbance of each of these reaction mixtures was measured at various times, till the constancy in absorbance (determined at 420 nm) was observed. The plot of the limiting absorbance versus [PBQ] has shown an inflexion at the ratio of [Co(bipy)$_3^{2+}$]:[PBQ] = 2:1. Therefore, the stoichiometry of the reaction can be represented by the following equation:

$$2\text{Co(bipy)}_3^{2+} + \text{PBQ} \xrightarrow{2\text{H}^+} 2\text{Co(bipy)}_3^{3+} + \text{H}_2\text{Q}$$

Reaction kinetics—The course of the reaction was followed spectrophotometrically by measuring the change in absorbance of the reaction mixture at 420 nm. The cells used to magnify the absorbance were 4 cm long. The absorbance, A_t of the reaction mixture at time t is given by

$$A_t = \varepsilon_1[\text{Co(bipy)}_3^{2+}]_t + \varepsilon_2[\text{Co(bipy)}_3^{3+}]_t + \varepsilon_3[\text{PBQ}]_t \quad \ldots 1$$

and the absorbance, A_∞ at the completion of the reaction is given by

$$A_\infty = \varepsilon_2[\text{Co(bipy)}_3^{3+}]_0 \quad \ldots 2$$

when PBQ and Co(bipy)$_3^{2+}$ are taken in the stoichiometric ratio

But, when PBQ is in excess,

$$A_\infty = \varepsilon_2[\text{Co(bipy)}_3^{3+}]_0 + \varepsilon_3[\text{PBQ}] \quad \ldots 3$$

From Eqs (1-3), it can be shown that under both the conditions

$$A_t - A_\infty = (\varepsilon_1 - \varepsilon_2 + \varepsilon_3/2)[Co(bipy)_3^{2+}]_t \quad \ldots(4)$$

Results

When PBQ and $Co(bipy)_3^{2+}$ were taken initially in stoichiometric ratio, the plot of $1/(A_t - A_\infty)$ versus time was found to be linear, showing that the reaction obeyed total second order kinetics. The second order rate constants (k or k_{exp}) were reproducible within 5%. Keeping $[PBQ]_0$ fixed and varying $[Co(bipy)_3^{2+}]_0$, initial rates were determined and the plot of initial rate versus $[Co(bipy)_3^{2+}]_0$ was linear passing through the origin, showing first order dependence in $[Co(bipy)_3^{2+}]$. Similarly the plot of initial rate versus $[PBQ]_0$ at fixed $[Co(bipy)_3^{2+}]$ was linear passing through the origin, showing first order dependence in [PBQ] also.

The rates are not influenced by variation in [bipyridyl] in excess over the stoichiometric concentration. For example, under the conditions $[PBQ] = 1.0 \times 10^{-3}$ mol dm^{-3}, $[Co(bipy)_3^{2+}] = 2.0 \times 10^{-3}$ mol dm^{-3}, solvent = MeOH (20% v/v), pH = 3.6, $\mu = 5.0 \times 10^{-2}$ mol dm^{-3} and temp = 25 ± 0.1°C when 10^3[bipyridyl] was changed from 8 to 14 mol dm^{-3}, k remained constant at 2.39 ± 0.03 mol^{-1}dm^{3}s^{-1}. Further, the rates are insensitive to change in ionic strength (μ = 0.01-0.1). The second order rate constants were also determined at different temperatures. The energy of activation and entropy of activation have been found to be 42 ± 8 kJ mol^{-1} and −105 ± 25 JK^{-1}mol^{-1} respectively. The negative entropy of activation is typical of a bimolecular rate-determining step.

Determination of binding constant from spectral data

The binding constant of PBQ in the presence of different [SDS] in excess and in 20% (v/v) methanol medium was determined using Eq. (5).

$$\frac{1}{A_s - A_W^o} = \frac{1}{A_M^o - A_W^o}\left(1 + \frac{1}{K_B C}\right) \quad \ldots(5)$$

where A_W^o and A_M^o are the absorbances in the absence of surfactant and limiting absorbance upon complete incorporation into the micellar phase respectively. A_s is absorbance in the presence of SDS and K_B is the binding constant of PBQ, C is equal to [SDS] − cmc (cmc = 8.4×10^{-3} mol dm^{-3}). A plot of $1/(A_s - A_W^o)$ versus 1/C (Fig. 1) was linear, from which the value of K_B was calculated to be 1.36×10^2 mol^{-1}dm^3 from the ratio of intercept/slope.

Discussion

It has been reported that Co(II) and Co(III) form 1:3 complexes with 2,2'-bipyridyl. The stability constant of Co(II) complex is quite high (log β = 16.02). Hence all Co(II) will be present in the form of $Co(bipy)_3^{2+}$ under the conditions, [bipy]/[cobalt(II)] ≥ 3. Since the reaction obeys first order kinetics in $[Co(bipy)_3^{2+}]$ and [PBQ], it is evident that both $Co(bipy)_3^{2+}$ and PBQ are present in the rate-limiting step and the reaction involves direct one-electron transfer between the two reactants forming $Co(bipy)_3^{3+}$ and a free radical intermediate PBQ$^-$. The latter is believed to oxidize $Co(bipy)_3^{2+}$ in a subsequent fast step. The formation of free radical intermediate is supported by the polymerisation of acrylonitrile by the reaction mixture in the absence of air. PBQ or $Co(bipy)_3^{2+}$ alone does not initiate polymerization. The authors believe that the reaction proceeds through an outer sphere (Scheme 2) rather than an inner sphere mechanism (Scheme 1).

$$Co(bipy)_3^{2+} + H^+ \rightleftharpoons Co(bipy)_2H_2O^{2+} + Hbipy^+$$

$$Co(bipy)_2H_2O^{2+} + PBQ \rightleftharpoons Co(bipy)_2PBQ^{2+} + H_2O$$

$$\downarrow \text{slow}$$

$$Co(bipy)_3^{3+} + PBQ^-$$

$$PBQ^- + Co(bipy)_3^{2+} \xrightarrow[\text{fast}]{2H^+} Co(bipy)_3^{3+} + H_2Q$$

Scheme 1

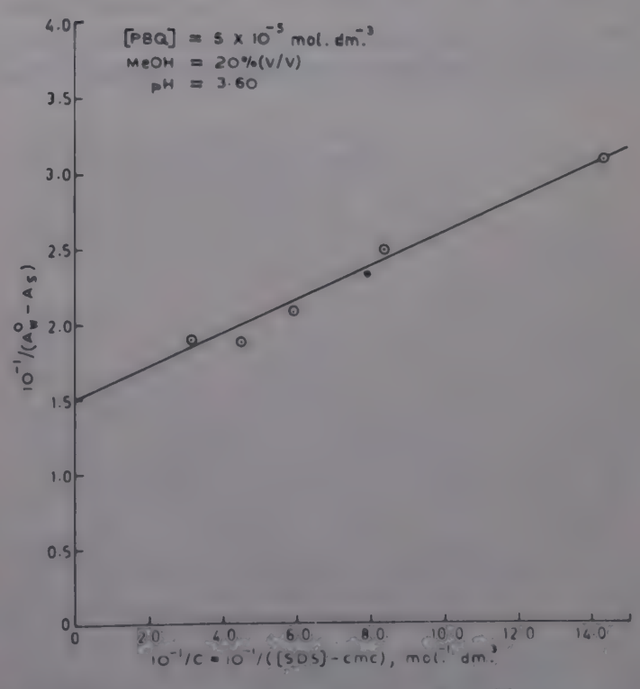

Fig. 1 — Plot of $1/(A_s^o - A_s)$ versus 1/C ([PBQ] = 5×10^{-5} mol dm^{-3}, solvent = MeOH (20%, v/v), pH = 3.60)

$$Co(bipy)_3^{2+} + PBQ \xrightarrow{slow} Co(bipy)_3^{3+} + PBQ^{\cdot-}$$

$$PBQ^{\cdot-} + Co(bipy)_3^{2+} \xrightarrow[fast]{2H^+} Co(bipy)_3^{3+} + H_2Q$$

Scheme 2

The inner sphere mechanism (Scheme 1) is ruled out by the fact that the rate of the reaction is not affected by change in [bipyridyl] (as required by the inner sphere mechanism). Further, PBQ is not as good a ligand as bipyridyl to substitute it from the $Co(bipy)_3^{2+}$.

Micellar effect of sodium dodecyl sulphate (SDS)

SDS, above its cmc accelerates oxidation of $Co(bipy)_3^{2+}$ by PBQ. The rate-[surfactant] profile exhibits a maximum (Fig. 2) typical of micellar-catalysed bimolecular processes[8]. The micellar catalysis shows that electron transfer is more rapid in the micellar phase. This is in sharp contrast to the behaviour observed with more hydrophobic quinones. Thus in the oxidation of benzyl viologen radical cation by duroquinone, vitamin K_1, 2,3-dimethyl naphthaquinone and menadione, SDS has been reported to have inhibitory effect[9]. The more rapid electron transfer in the micellar region may be due to the concentration and environmental effects. The presence of a maximum[10] signifies that the increase in the volume of the micellar phase is accompanied both by increase in the quantity of the substance passing into it from water and by decrease in the concentration of the substance in the micellar phase. The first process tends to accelerate the reaction by increasing the relative proportion of the more rapid micellar reaction which predominates at low [surfactant], while the quantity of substance passing into micelles is small. The second process viz. dilution of the reactants in the micellar phase, slows down the reaction and predominates at high [surfactant]. These two factors are responsible for the observed maximum in the rate-[surfactant] profile.

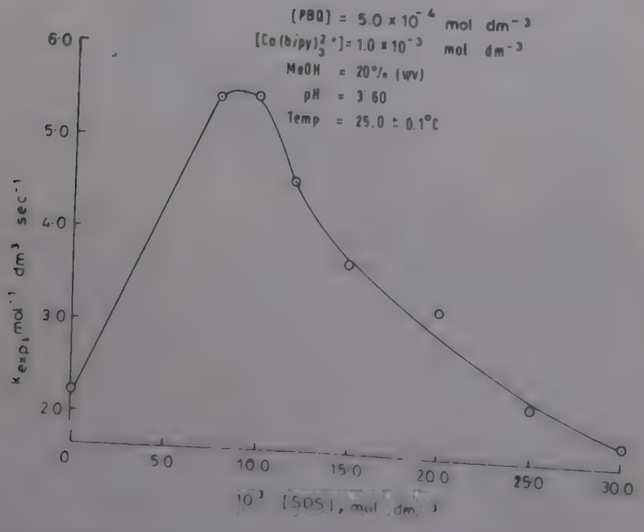

Fig. 2—Plot of k_{exp} versus [SDS] ([PBQ] = 5.0×10^{-4} mol dm^{-3}, [$Co(bipy)_3^{2+}$] = 1.0×10^{-3}, solvent = MeOH (20%, v/v), pH = 3.60, temp = 25.0 ± 0.1°C)

The micellar effect can be described by using the pseudo-phase model of Berezin *et al.*[10] who derived rate law[6] for a general biomolecular micellar-catalysed reaction.

$$k_{exp} = \frac{(k_M P_A P_B + k'_M P_A + k''_M P_B)C\bar{V} + k_W(1 - C\bar{V})}{(1 + K_A C)(1 + K_B C)} \quad \ldots(6)$$

In Eq. (6), P's and K's are the partition coefficients and binding constants, M, W, A and B represent quantities related to the micellar phase, aqueous phase, $Co(bipy)_3^{2+}$ and PBQ respectively. k_M and k_W represent the second order rate constants in micellar and aqueous phases, k'_M refers to the rate constant of the reaction between reactant A in the micellar phase and reactant B in aqueous phase, k''_M represents the reverse situation, C represents [surfactant]-cmc. The cmc value of SDS in 20%(v/v) methanol-water mixture was taken as 8.4×10^{-3} mol dm^{-3} from literature[11].

The partition coefficient of the ionic species $Co(bipy)_3^{2+}$, viz. P_A, between aqueous and micellar phase is given by Eq. (7)

$$P_A = e^{-Z\psi/25.7} \text{ at } 25°C \quad \ldots(7)$$

where Z is the ionic charge (+2). ψ is the surface potential of the micelle. Assuming a value of ψ = 110-120 mv, P_A has a value 5.0×10^3-1.0×10^4. Since $K = P\bar{V}$, where $\bar{V}$ = molar volume (0.246 mol^{-1}dm^3), the binding constant of $Co(bipy)_3^{2+}$ (K_A) should range between 1.2×10^3 to 2.5×10^3 mol^{-1}dm^3.

In the light of Eq. (6) it is evident that at [SDS] > 12.0×10^{-3} mol dm^{-3}, $(1 + K_A C) \simeq K_A C$. The complex is almost completely present in the micellar phase and hence the terms including k_W and k''_M can be neglected in comparison with other terms. Therefore Eq. (6) modifies to Eq. (8)

$$k_{exp} = \frac{\bar{k}_M K_B + k'_M}{1 + K_B C}, \text{ where } \bar{k}_M = \frac{k_M}{\bar{V}} \quad \ldots(8)$$

which can be rearranged to Eq. (9),

$$\frac{1}{k_{exp}} = \frac{1}{\bar{k}_M K_B + k'_M} + \frac{K_B C}{\bar{k}_M K_B + k'_M} \quad \ldots(9)$$

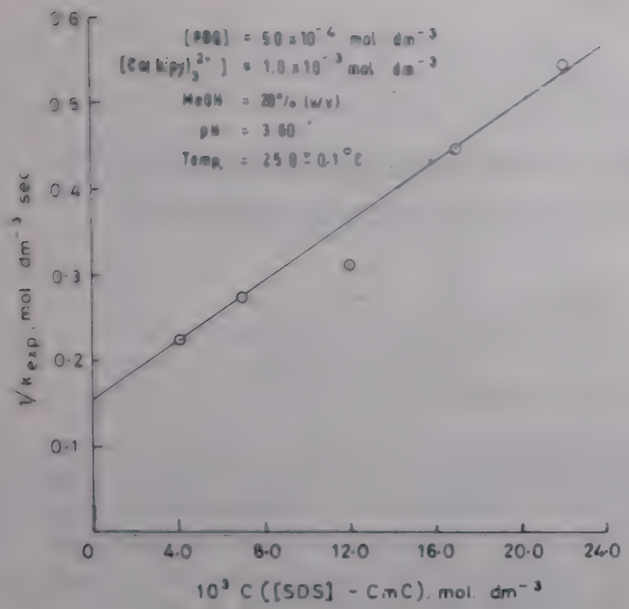

Fig. 3—Plot of $1/k_{exp}$ versus C ($[PBQ] = 5.0 \times 10^{-4}$ mol dm^{-3}, $[Co(bipy)_3^{2+}] = 1.0 \times 10^{-3}$ mol dm^{-3}, solvent = MeOH (20%, v/v), pH = 3.60, temp = 25.0 ± 0.1°C)

According to Eq. (9) the plot of $1/k_{exp}$ versus C should be linear. This is found to be true from the rate data determined at $[SDS] > 12 \times 10^{-3}$ mol dm^{-3} (Fig. 3). The ratio of slope/intercept yields the value of $K_B = 1.19 \times 10^2$ mol^{-1}dm^3, which is in reasonable agreement with the value obtained from spectral data, i.e. 1.36×10^2 mol^{-1}dm^3. From the value of the reciprocal of the intercept, $(\bar{k}_M K_B + k'_M)$ has been found to be 6.7 mol^{-1}dm^{3}s^{-1}.

Acknowledgement

One of us (KRK) thanks the CSIR, New Delhi for financial assistance.

References

1 Ogata Y, Sawaki Y & Gotoh S, *J Am chem Soc*, 90 (1968) 3469.
2 Amonkar K S & Ghosh B N, *Curr Sci*, 42 (1973) 719.
3 Muralikrishna U & Krishnamurthy M, *Indian J Chem*, 22A (1983) 858.
4 Levison S A & Marcus R A, *J phys Chem*, 72 (1968) 358.
5 Inagaki Y J, Osugi J & Sasaki M, *J chem Soc, Perkin Trans II* (1985) 115.
6 Deligny C L & Rehback M, *Rec Trans Chim*, 79 (1960) 727.
7 Ohashi K, Natsuzawa M, Hamano E & Yamamoto K, *Bull chem Soc Jpn*, 49 (1976) 2440.
8 Pelizzetti E & Pramauro K, *Inorg Chem*, 19 (1980) 1408.
9 Hulig S M, Dionne B C & Redgus M A J, *J phys Chem*, 90 (1986) 5873.
10 Berezin I V, Martinek K & Yatsimirkii A K, *Russ chem Rev* (Engl. Transl), 42 (1973) 787.
11 Panda L & Behera G B, *J Indian chem Soc*, LXII (1985) 44.

Indian Journal of Chemistry
Vol. 30A, February 1991, pp 140-143

Kinetics and mechanism of oxidation of 2-mercaptobenzathiazole by 2,6-dichlorophenolindophenol in aqueous acetone medium

R K Tiwari & K K Mishra*
Department of Postgraduate Studies & Research in Chemistry, R.D. University, Jabalpur 482 001

Received 1 January 1990; revised 3 September 1990; accepted 5 October 1990

Kinetics of the title reaction have been investigated in the presence of hydroxyl ions in acetone-water medium (60%, v/v). Two moles of the substrate are oxidised by one mole of In. The reaction follows a pseudo-first order kinetics in [indophenol] at lower concentration of 2-mercaptobenzathiazole (MBT) while at higher [MBT], the order in [In] becomes 1/2. The order in [MBT] is nearly two. The rate shows a fractional dependence in $[OH^-]$. The variation in ionic strength does not influence the rate but the rate increases with increase in the dielectric constant of the medium. Addition of disulphide causes a change in order in [In] without affecting the rate constant while addition of the leuco base accelerates the reaction rate. Activation parameters have been evaluated and a reaction scheme showing a disproportionation of the intermediate charge transfer complex as the rate determining step has been proposed.

In earlier communications from our laboratory the kinetics and mechanism of oxidation of a variety of sulphydryl compounds including thiols, thiol acids and thioureas by 2,6-dichlorophenolindophenol (indophenol, In), a model for coenzyme-Q, in acidic and alkaline media were reported[1-10]. As an extension we report herein the kinetics of oxidation of an organic substrate having sulphur atom in a cyclic frame-work by indophenol.

Materials and Methods

Solution of indophenol (In, BDH) was prepared in doubly distilled water. Solution of 2-mercaptobenzathiazole (MBT, RSH; Fluka, Switzerland) was prepared in acetone (E. Merck, GR). The solutions were prepared afresh for each run and were stored under N_2. The oxidation product 2,2′-dithio-bis-benzathiazole was prepared by oxidising MBT with iodine[11] and recrystallized from ether. Dihydroindophenol (leuco dye) was prepared by reducing indophenol with purified SO_2 gas as described earlier[12]. The reaction was carried out in aq. acetone (60% v/v) in the presence of OH^- ions in vessels coated black outside.

The progress of the reaction was followed by measuring the decrease in [In] colorimetrically employing Klett-Summerson photoelectric colorimeter fitted with a light filter no. 62 (590-660 nm) since indophenol shows maximum absorbance at 644 nm ($\varepsilon_{max} = 8.0 \times 10^3$ dm^3 mol^{-1} cm^{-1}).

Results

The stoichiometric investigations revealed that two moles of the substrate were oxidised by one mole of In to form the corresponding disulphide.

$$2\ RSH + In \rightarrow RSSR + H_2In$$

The formation of the corresponding disulphide was confirmed by recording the UV spectra of the reaction mixture after completion of the reaction (excess acetone in the reaction mixture was evaporated and the residue was dissolved in ethanol). The spectrum exhibited a peak at 271 nm which is in good agreement with the reported value of λ_{max} for 2,2′-dithio-bis-benzathiazole in ethanol[13].

The reaction followed a first order kinetics in [oxidant] in the presence of a large excess of [MBT]. The order in [oxidant], however, changed from 1 to 1/2 with increase in [MBT] beyond 8.0×10^{-4} mol dm^{-3} (Table 1). These conclusions were verified graphically as well as by van't Hoff's differential methods.

The order in [substrate] was nearly 2 as revealed by the initial rate measurement method. The pseudo-first order rate constant remained practically unaffected on varying the initial [indophenol] beyond 3.0×10^{-5} mol dm^{-3}. For example under the conditions as in Table 1 and $[MBT] = 8.0 \times 10^{-4}$ mol dm^{-3}, $k_1 \times 10^4$ remained constant at 5.74 ± 0.14 s^{-1} when $[In] \times 10^5$ was varied from 3.0 to 5.0 mol dm^{-3}.

Table 1 – Effect of variation in [MBT] on rate constant

$[In] = 4.0 \times 10^{-5}$ mol dm^{-3}, $[NaOH] = 3.0 \times 10^{-4}$ mol dm^{-3}, Acetone = 60% (v/v), $I = 3.0 \times 10^{-4}$ mol dm^{-3}, temp = 35°C

$[MBT] \times 10^4$ mol dm^{-3}	$k_1 \times 10^4$ s^{-1}	$k_{1/2} \times 10^6$ mol$^{1/2}$ dm$^{-3/2}$ s^{-1}
8.0	5.45	—
10.0	—	4.17
12.0	—	6.08
14.0	—	7.77
16.0	—	9.82

The rate decreased linearly with increase in $[OH^-]$. At $[OH^-]$ higher than 7.4×10^{-3} mol dm^{-3}, a deviation towards a second order in indophenol has been noticed but this aspect could not be investigated due to non-reproducible nature of the kinetic runs under these conditions. The ionic strength of the system was not maintained constant in these investigations because a variation in ionic strength did not influence the rate.

The rate increased with increase in the dielectric constant of the medium indicating the participation of polar molecules in the rate determining step. For example under identical conditions as in Table 1 and $[MBT] = 8.0 \times 10^{-4}$ mol dm^{-3} when dielectric constant of the medium was increased from 33 to 56 (% v/v of acetone was changed from 75 to 40), $k_1 \times 10^4$ increased from 2.99 to 11.8 s^{-1}.

The rate of the reaction was not influenced by the external addition of the reaction product i.e. the corresponding disulphide to the reaction system but it increased on addition of the leuco dye. Here again, the reaction adhered to a half order kinetics in [indophenol] when the runs were made in the presence of the disulphide while the addition of leuco base registered a first order behaviour in [oxidant].

The enthalpy of activation was determined using the Arrhenius plots and was found to be 37.0 kJ mol^{-1}. The entropy ($\Delta S^{\neq}$) and the free energy of activation ($\Delta G^{\neq}$) were evaluated in the usual manner and were found to be -190 J deg^{-1} mol^{-1} and 95.7 kJ mol^{-1} respectively.

Discussion

The kinetic results are best explained by assuming the participation of an intermediate of the type InOH$^-$ formed by the action of OH$^-$ ions on indophenol molecule (Eq. 1).

$$In + OH^- \overset{K_1}{\rightleftharpoons} InOH^- \quad \ldots (1)$$

The formation of such an intermediate has already been reported by Bishop and Tong in the case of quinones[14]. Further, second order kinetics in 2-mercaptobenzathiazole is observed in spite of a transition in order in [indophenol]. It seems that dimeric species of the substrate is the principal reactant. Such associations of sulphydryl compounds interalia through intermolecular H-bonding has been reported earlier[15]. In the presence of OH^- ion 2-MBT will be partly dissociated to give thiolate anion which is presumed to form the dimer represented as C_1 (see Eq. 2). Thus,

$$RSH + RS^- \overset{K_2}{\rightleftharpoons} C_1 \quad \ldots (2)$$

The species C_1 is shown to react with $InOH^-$ to form an intermediate, presumably a charge transfer complex, represented as C_2 (Eq. 3).

$$C_1 + InOH^- \overset{K_3}{\rightleftharpoons} C_2 + OH^- \quad \ldots (3)$$

The CT complex (C_2) may undergo a homolytic cleavage to produce the thiyl ($RS^{\cdot}$) and the semi-reduced indophenol ($HIn^{\cdot}$) radicals in the rate-determining step (Eq. 4).

$$C_2 \overset{k_1}{\underset{k_{-1}}{\rightleftharpoons}} RS^{\cdot} + HIn^{\cdot} + RS^- \quad \ldots (4)$$

It may be mentioned here that the formation of $RS^{\cdot}$ radical[16] and semi-reduced indophenol radical[17] have been reported in literature. Incidentally, the participation of free radicals in this system is evidenced by the polymerisation of acrylonitrile when added to the reaction system. The radicals may subsequently lead to the formation of the end products as shown in Eqs (5 and 6).

$$HIn + RSH \overset{k_2}{\rightarrow} RS^{\cdot} + H_2In \quad \ldots (5)$$

$$RS^{\cdot} \overset{k_3}{\rightarrow} 1/2\ RSSR \quad \ldots (6)$$

The rate of reaction would be given by Eq. (7).

$$-\frac{d[In]}{dt} = k_1[C_2] - k_{-1}[RS^{\cdot}][HIn^{\cdot}][RS^-] \quad \ldots (7)$$

Assuming steady state for $RS^{\cdot}$ and $HIn^{\cdot}$ radicals,

$$[RS^{\cdot}] = \frac{2k_1[C_2]}{2k_{-1}[HIn^{\cdot}][RS^-] + k_3} \quad \ldots (8)$$

and

$$[HIn^{\cdot}] = \frac{(k_2^2k_3^2[RSH]^2 + 8k_{-1}k_2k_1k_3[RSH][RS^-][C_2])^{1/2}}{4k_{-1}k_2[RSH][RS^-]} - \frac{k_3}{4k_{-1}[RS^-]} \quad \ldots (9)$$

From Eqs (1-3),

$$[C_2] = K_1K_2K_3[RSH][RS^-][In] \quad \ldots (10)$$

Thus,

$$[HIn^{\cdot}] = \frac{(k_2^2k_3^2 + 8k_{-1}k_2k_1k_3K_1K_2K_3[RS^-]^2[In])^{1/2}}{4k_{-1}k_2[RS^-]} - \frac{k_3}{4k_{-1}[RS^-]} \quad \ldots (11)$$

On substituting the value of $[RS^{\cdot}]$ and $[HIn^{\cdot}]$ in Eq. (7), the rate expression is given by Eq. (12).

$$-\frac{d[In]}{dt} = k_1[C_2] - k_{-1}[RS^-][HIn^{\cdot}] \quad \frac{2k_1[C_2]}{2k_{-1}[HIn^{\cdot}][RS^-] + k_3} \quad \ldots (12)$$

or,

$$-\frac{d[In]}{dt} = b[RSH][RS^-][In] \cdot \frac{2k_2k_3}{(k_2^2k_3^2 + a[RS^-]^2[In])^{1/2} + k_2k_3} \quad \ldots (13)$$

where $a = 8k_{-1}k_2k_1k_3K_1K_2K_3$ ... (14)

$$b = k_1K_1K_2K_3 \quad \ldots (15)$$

From Eq. (13), it is obvious that if k_2k_3 is sufficiently large, then the rate expression would predict a second order kinetics in [2-MBT] and a first order dependence in [In] as observed at low [2-MBT] (Eq. 16).

$$-\frac{d[In]}{dt} = b[RSH][RS^-][In] \quad \ldots (16)$$

However, if [RSH] is larger, then the rate expression (13) will be valid and under these conditions, the reaction will adhere to near second order kinetics in [2-MBT] while the order in [indophenol] will gradually show a transition from one to 1/2 as has been observed. It may be mentioned here that at sufficiently large [2-MBT], k_2k_3 should become negligibly small in the denominator of Eq. (13) and this will lead to Eq. (17).

$$-\frac{d[In]}{dt} = \frac{2bk_2k_3}{a}[RSH][In]^{1/2} \quad \ldots (17)$$

Thus, under these circumstances, one would also notice a change in order in [substrate] but poor solubility of 2-MBT and its oxidation product in the solvent matrix employed in these investigations did not permit us to check this possibility.

The proposed reaction scheme explains the salient kinetic features of the reaction but does not give an explanation for slight increase in rate on the addition of dihydroindophenol in the reaction system. It is reported[18] that semiquinone radicals (HD) dimerise to give leuco base and the parent dye as shown in Eq. (18).

$$HD + HD \rightarrow H_2D + D \quad \ldots (18)$$

It seems likely that the formation of leuco base renders the reaction givn in Eq. (18) reversible to some extent and thus, its addition slightly increases the rate.

The complex dependence of rate on $[OH^-]$ is in harmony with earlier observations on these systems[19] and it appears that the formation and disproportionation of the CT complex are highly *p*H dependent. It may also be added here that 2-MBT, like thiol acids, may exhibit thiol-thione tautomerism[20].

The increase in $[OH^-]$ will tend to increase the concentration of relatively less reactive thione form and will cause a retardation in rate.

Acknowledgement

One of us (RKT) is thankful to the UGC, New Delhi for the award of a research fellowship.

References

1 Mishra K K & Sinha B P, *Proceedings symp non-aq. media and molten salts* (*Atomic Energy Commission India*), 1978; Chem Abs, 96 (1982) 84892 K.

2 Shrivastava A K, Mishra K K & Sinha B P, *Indian J Chem*, 17B (1979) 48.

3 Mishra K K, Shrivastava A K & Sinha B P, *Phosphorus & Sulfur*, 10 (1981) 99.

4 Rastogi M, Mishra K K & Sinha B P, *Indian J Chem*, 20B (1981) 726.
5 Pandey N K, Mishra K K & Kashyap M, *Phosphorus & Sulfur*, 12, (1982) 179.
6 Kashyap M, Mishra K K & Pandey N K, *Can J Chem*, 60 (1982) 1928.
7 Pandey N K & Mishra K K, *Bull Soc Chim France*, I (5-6) (1982) 179.
8 Shrivastava M, Mishra K K & Sinha B P, *Int J chem Kin*, 14 (1982) 451.
9 Kashyap M & Mishra K K, *Oxid Commun*, (1982) 461.
10 Kalla K G & Mishra K K, *Phosphorus & Sulfur*, 35 (1988) 183.
11 Kolthoff I M, Anastasi A & Tan B H, *J Am chem Soc*, 80 (1958) 3235.
12 Mishra K K & Sinha B P, *Indian J Chem*, 15A (1977) 1079.
13 *Organic spectral data*, edited by J K Mortimer, Vol. I (Interscience, New York) (1964) 544.
14 Bishop C A & Tong L K J, *J Am chem Soc*, 87 (1965) 501.
15 S Patai, *The chemistry of the thiol group* (Wiley Interscience, London) Part I (1974) 141.
16 S Patai, *The chemistry of the thiol group* (Wiley Interscience, London) Part I (1974) 313.
17 Leach S J, Baxendale J H & Evans M G, *Austr J Chem*, 6 (1953) 409.
18 Rohatgi-Mukherjee K K, *Fundamentals of photochemistry* (Wiley Eastern, India) (1978) 242.
19 Kharasch N, *Organic sulfur compounds* (Pergamon, New York) (1961) Vol. I, 99.
20 Karchmer J H, *The analytical chemistry of sulphur and its compounds*, Part II (Wiley-Interscience, New York) (1972) 504.

Indian Journal of Chemistry
Vol. 30A, February 1991, pp 144-147

Kinetics and mechanism of alkaline hydrolysis of malonamide and dicyandiamide

M Arif Niaz & A Aziz Khan*
Department of Chemistry, Aligarh Muslim University, Aligarh 202 002

Received 18 March 1990; revised and accepted 31 August 1990

Kinetics of hydrolysis of malonamide and dicyandiamide have been studied in 0.1 to 1.5 mol dm^{-3} and 0.25 to 2.0 mol dm^{-3} sodium hydroxide respectively. Malonamide hydrolysis follows irreversible first order consecutive path:

$$\text{Malonamide} \xrightarrow[-NH_3]{k_1} \text{malonamic acid} \xrightarrow[-NH_3]{k_2} \text{malonic acid}$$

The variation of k_1 and k_2 with [NaOH] is in good agreement with equations, $1/k_1 = B_1 + B_2/[OH^-]$ and $1/k_2 = C_1 + C_2/[OH^-]$, where B_1, B_2, C_1, and C_2 are empirical constants. The mechanism proposed involves monoanionic tetrahedral intermediate. Dicyandiamide hydrolysis follows the path:

$$\text{Dicyandiamide} \xrightarrow{\text{fast}} \text{guanylurea} \xrightarrow{\text{slow}} \text{guanidine} + \text{ammonia} + \text{carbondioxide}$$

The variation of observed rate constants with [NaOH] is in good agreement with equation $k_{obs} = B_1 + B_2[OH^-]$. Mechanism of hydrolysis involves both mono and dianionic tetrahedral intermediates and their breakdown to the products is the rate-determining step.

The formation of unstable tetrahedral intermediate has been propsed while discussing the mechanism of alkaline hydrolysis of amides[1-3], anilides[4-6], and imides[7,8]. In case of alkaline hydrolysis of diamides, formation of amic acid as stable intermediate was also reported[9,10]. The studies on the alkaline hydrolysis of diamides are found to be limited. The reason is that the reaction has a consecutive nature and ammonia is evolved in both the steps. The transcendental rate expressions obtained are not solved easily for rate constants. In continuation of our work on consecutive reactions[7,8] and hydrolysis of amides[11] under alkaline medium, we report herein the results of hydrolysis of malonamide and dicyandiamide.

Materials and Methods

Malonamide (Fluka), dicyandiamide (AR, BDH) and KNO_3 (E. Merck) were used as such. Concentrated stock solution of sodium hydroxide (E. Merck) of about 17 mol dm^{-3} was prepared. It was filtered to remove undissolved carbonate and then diluted to prepare the required solution.

Purified nitrogen gas was bubbled through the reaction mixture for stirring and to sweep off ammonia during the course of reaction. The reactions were studied by estimating [ammonia] at regular time intervals spectrophotometrically by Nesslerization[7,8,11].

Results and Discussion

(1) *Malonamide hydrolysis*

The rate of reaction was significantly changed after the completion of 50% reaction which indicates that hydrolysis of malonamide occurs in two steps. Since an excess of $[OH^-]$ was used, the hydrolysis was found to follow an irreversible first order consecutive reaction path: $A \xrightarrow[-NH_3]{k_1} B \xrightarrow[-NH_3]{k_2} C$; where A, B, and C represent malonamide, malonamic acid, and malonic acid respectively. This reaction leads to Eq. (1) for $[NH_3]$ as a function of time, t, and rate constants, k_1 and k_2.

$$[NH_3] = A_0\left[2 - \left(\frac{k_1 - 2k_2}{k_1 - k_2}\right)e^{-k_1 t} - \left(\frac{k_1}{k_1 - k_2}\right)e^{-k_2 t}\right] \quad \ldots (1)$$

On making following substitution,

$\phi = [NH_3]/A_0 - 2$; $\theta = k_1 t$ and

$\rho = k_2/k_1$

Eq. (1) converts to Eq. (2).

$$\phi(\rho - 1) = e^{-\rho\theta} - (2\rho - 1)e^{-\theta} \quad \ldots (2)$$

Equation (2) can be solved[12], if θ is guessed as the value of θ and the error, ε, closely approximated from Eq. (4).

$$\theta = \theta_0 + \varepsilon \qquad \ldots (3)$$

$$\varepsilon \cong \frac{\phi(\rho-1)+(2\rho-1)e^{-\theta_0}-e^{-\rho\theta_0}}{(2\rho-1)e^{-\theta_0}-\rho e^{-\rho\theta_0}} \qquad \ldots (4)$$

We have determined values of θ using Eqs (3) and (4) in the ocmputer programme (FORTRAN IV) at a given ρ and at different time intervals from the value of $[NH_3]$ for a given set of reaction. The ratios of consecutive values of θ, i.e., θ_1/θ_2, θ_2/θ_3, θ_3/θ_4 ...., along with the corresponding ratios of time (t_1/t_2, t_2/t_3, t_3/t_4 ....) were calculated. Moreover, the various trial values of ρ were introduced and the best value of ρ was selected at which the difference between the sum of squares of ratios of θ and sum of squares of ratios of time was found to be minimum.

The rate constants were found insensitive to ionic strength. Studies were carried out at different temperatures, and activation parameters evaluated using Arrhenius and Eyring equations with linear least-squares technique. The values are: for A→B, $E_a = 36.73 \pm 1.33$ kJ mol^{-1}; $\Delta H^{\neq} = 33.88 \pm 1.33$ kJ mol^{-1}; $\Delta S^{\neq} = -208.62 \pm 3.85$ JK^{-1} mol^{-1}; for B→C, $E_a = 40.97 \pm 1.47$ kJ mol^{-1}; $\Delta H^{\neq} = 38.13 \pm 1.47$ kJ mol^{-1}; $\Delta S^{\neq} = -223.56 \pm 4.44$ JK^{-1} mol^{-1}.

The effect of [NaOH] was studied within a range of 0.1 to 1.5 mol dm^{-3} at 348K. The experimental data (Fig. 1) fit empirical Eqs (5 and 6).

$$1/k_1 = B_1 + B_2/[OH^-] \qquad \ldots (5)$$

$$1/k_2 = C_1 + C_2/[OH^-] \qquad \ldots (6)$$

In Eqs (5 and 6) B_1, B_2, C_1, and C_2 are empirical constants and their values are: 20.61 min, 6.12 mol min dm^{-3}, 3.63×10^2 min, and 1.90×10^2 mol min dm^{-3} respectively.

The mechanism consistent with the observed results for both the steps of hydrolysis of malonamide has been proposed and given in Scheme 1. In the Scheme, species like (2) and (5) are unreactive conjugate bases which have already been mentioned in detail[4]. On the basis of proposed mechanism rate Eqs (7) and (8) were derived by applying steady-state assumptions to the reactive tetrahedral intermediates.

$$k_1 = \frac{k_a k_b [OH^-]}{(k_{-a}+k_b)(1+K_1[OH^-])} \qquad \ldots (7)$$

$$k_2 = \frac{k'_a k'_b [OH^-]}{(k'_{-a}+k'_b)(1+K'_1[OH^-])} \qquad \ldots (8)$$

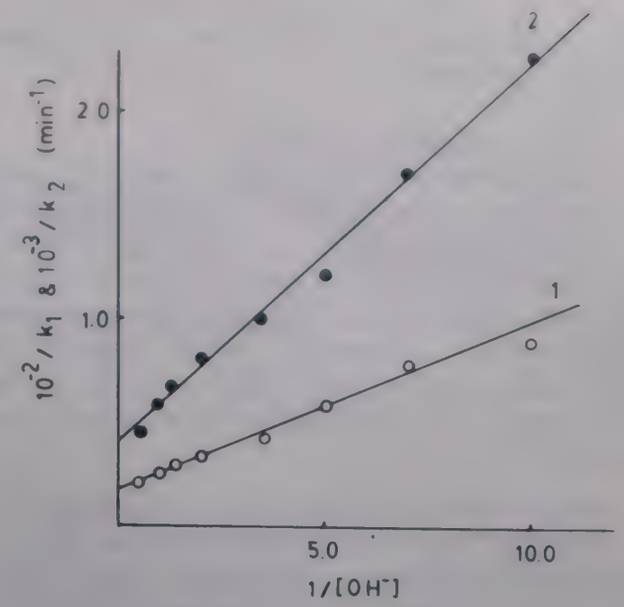

Fig. 1—Plots of the variation of $1/k_1$ (curve 1) and $1/k_2$ (curve 2) with $1/[OH^-]$ for hydrolysis of malonamide.

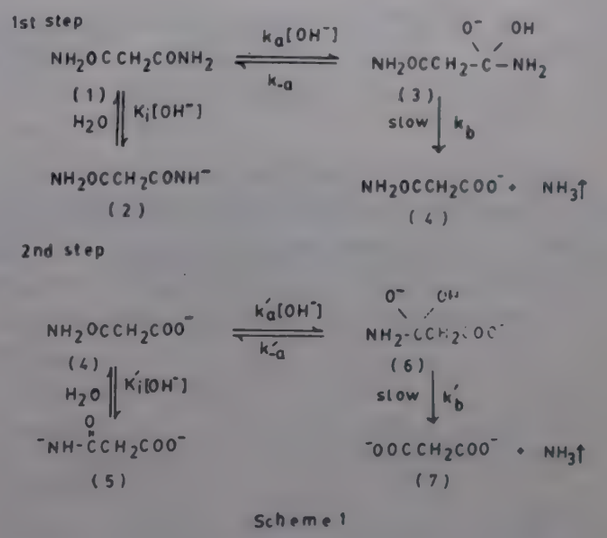

Scheme 1

Equations (7) and (8) are similar to the empirical equations (5) and (6) respectively with

$$B_1 = \frac{(k_{-a}+k_b)K_1}{k_a k_b};\ B_2 = \frac{(k_{-a}+k_b)}{k_a k_b};\ C_1 = \frac{(k'_{-a}+k'_b)K'_1}{k'_a k'_b}$$

and $C_2 = \dfrac{(k'_{-a}+k'_b)}{k'_a k'_b}$. It is evident that $K_1 = \dfrac{B_1}{B_2} = \dfrac{K_a}{K_w}$

and $K'_1 = \dfrac{C_1}{C_2} = \dfrac{K'_a}{K_w}$, where K_a and K'_a are ionization constants of malonamide and intermediate (4). Both are extremely weak acids and the approximate values of K_a and K'_a calculated in this way are 3.4×10^{-14} mol dm^{-3} and 1.9×10^{-14} mol dm^{-3} respectively. Such an order of acidity constants has al-

ready been reported by Bruylants and Kezdy[13] during the kinetic study of alkaline hydrolysis of substituted acetamides.

(2) *Dicyandiamide hydrolysis*

The pseudo-first order rate constants, k_{obs}, were insensitive to ionic strength. Effect of temperature on hydrolysis was studied over the range 343-371 K and various activation parameters were determined by using Arrhenius and Eyring equations with linear least-squares treatment. The values are: $E_a = 38.25 \pm 0.64$ kJ mol^{-1}; $\Delta S^{\neq} = -228.10 \pm 1.90$ JK^{-1} mol^{-1}; $\Delta H^{\neq} = 35.24 \pm 0.68$ kJ mol^{-1} and ln A = 3.21 ± 0.43 sec^{-1}.

Effect of [NaOH] on hydrolysis of dicyandiamide was studied ranging from 0.25 to 2.0 mol dm^{-3} at 368 K. The plots of k_{obs} versus [OH$^-$] are shown in Fig. (2). Experimental data fit the empirical Eq. (9).

$$k_{obs} = B_1 + B_2 [OH^-] \quad \ldots (9)$$

The linear unknown parameters B_1 and B_2 were determined using least-squares technique ($B_1 = 2.04 \times 10^{-3}$ min^{-1} and $B_2 = 3.51 \times 10^{-3}$ dm^3 mol^{-1} min^{-1}).

Hydrolysis of dicyandiamide in basic medium gives guanidine, carbondioxide and ammonia as products. In this reaction, guanylurea (I) is a stable intermediate product. The formation of (I) is much fast in comparison to its decomposition, therefore, overall reaction is pseudo-first order under highly alkaline medium and can be represented as:

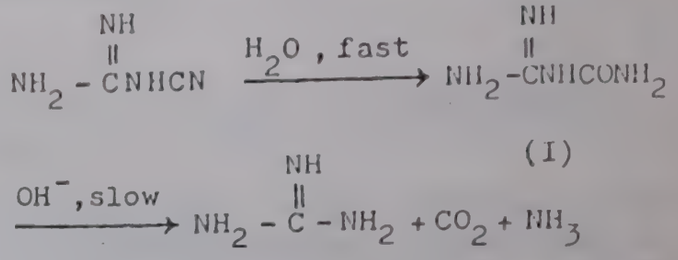

In alkaline medium, the primary reaction fo dicyandiamide leading to the formation of guanylurea was also described to occur rapidly, while the hydrolysis of guanylurea is a slow process[14].

During the alkaline hydrolysis of amides, the formation of monoanionic tetrahedral intermediate was suggested by Bender and coworkers[2,15] from the study of isotopic exchange and hydrolytic reactions of benzamide. In some cases, the reaction was found second order in OH$^-$ which explains removal of hydrolytic proton of monoanionic tetrahedral intermediate by OH$^-$ to form dianionic tetrahedral intermediate[4,13]. It was also described that the existence or nonexistence of dianionic tetrahedral intermediate in the rate-determining step depends upon [OH$^-$] and nature of acyl substrate. The rate-determining step of amide hydrolysis in the alkaline medium is base-catalyzed explulsion of $-NH_2$ group from the tetrahedral intermediate. It was supported by kinetic evidence[16] for a change in rate-determining step with increasing [OH$^-$]. Moreover, formation of tetrahedral intermediate from guanylurea cannot be considered rate-determining step because of sufficiently large negative value of entropy of activation ($\Delta S^{\neq} = -228.19$ JK^{-1} mol^{-1}). It explains proper orientation of several water molecules in the transition state which can be expected due to the existence of a high charged transition state[17].

The mechanism of hydrolysis of dicyandiamide consistent with observed results is given in Scheme 2. In the Scheme, species (II) is an unreactive conjugate base of guanylurea. Use of steady-state approximation for reactive tetrahedral intermediates lead to expression (10).

$$k_{obs} = \frac{k_1 k_2 K_h [OH^-] + k_1 k_3 K_1 K_h [OH^-]^2}{(1 + K_i [OH^-])(k_{-1} + k_2 + k_3 K_1 [OH^-])} \quad \ldots (10)$$

Conversion of (III) to products or back to reactants is more probable than its conversion to dianionic species[5], i.e., $(k_{-1} + k_2) \gg k_3 K_1 [OH^-]$. Therefore, Eq. (10) reduces to Eq. (11).

$$k_{obs} = \frac{k_1 k_2 K_h [OH^-] + k_1 k_3 K_1 K_h [OH^-]^2}{(1 + K_i [OH^-])(k_{-1} + k_2)} \quad \ldots (11)$$

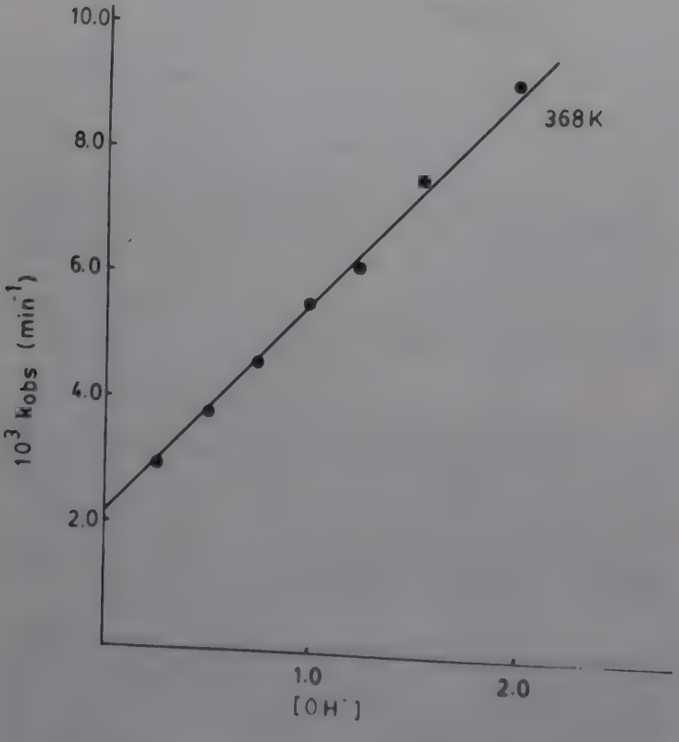

Fig. 2—Effect of [NaOH] on hydrolysis of dicyandiamide

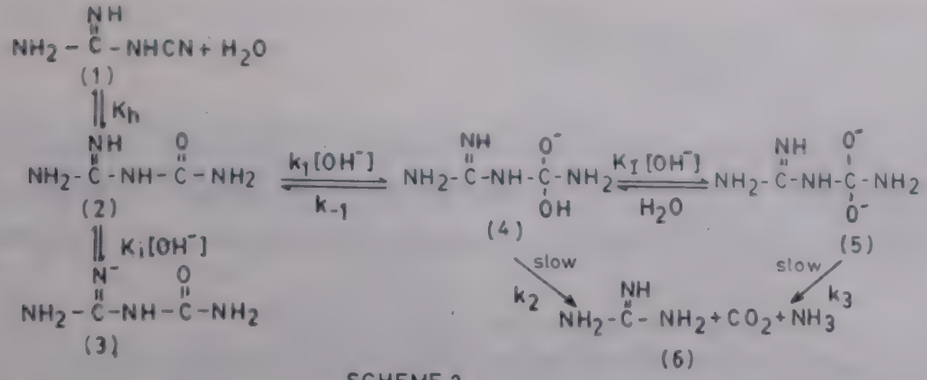

SCHEME 2

Being imino group of guanylurea potentially acidic in nature[18], the condition that $K_i[OH^-] \gg 1$ can be applied in highly alkaline medium. Then Eq. (11) simplifies to Eq. (12).

$$k_{obs} = \frac{k_1 k_2 K_h + k_1 k_3 K_I K_h [OH^-]}{(k_{-1} + k_2) K_i} \quad \ldots (12)$$

Equation (12) is similar to empirical Eq. (9) with

$$B_1 = \frac{k_1 k_2 K_h}{(k_{-1} + k_2) K_i}, \text{ and } B_2 = \frac{k_1 k_3 K_I K_h}{(k_{-1} + k_2) K_i}.$$

The species like (II) has been described as unreactive conjugate base by earlier workers[4,19]. But Mader[19] had suggested that the conjugate base is reactive towards the product formation. Brooke and Guttman[20] had also proposed that the ionized form of N-methylnicotinamide cation reacted with water to give tetrahedral intermediate. Although Scheme 2 is in accordance with kinetic data yet under high $[OH^-]$ following step (kinetically indistinguishable) cannot be ruled out.

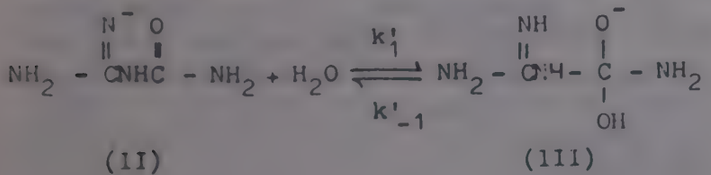

(II) (III)

Acknowledgement

We are thankful to CSIR, New Delhi for financial assistance to one of us (MAN) and computer centre, AMU.

References

1 Meloche I & Laidler K J, *J Am chem Soc*, 73 (1951) 1712.

2 Bender M L & Ginger R D, *J Am chem Soc*, 77 (1955) 348; Bender M L, Ginger R D & Unik J P, *J Am chem Soc*, 80 (1958) 1044.

3 Kezdy F & Bruylants A, *Bull Soc chim Belges*, 69 (1960) 602.

4 Biechler S S & Taft (Jr) R W, *J Am chem Soc*, 79 (1957) 4927.

5 Bender M L & Thomas R J, *J Am chem Soc*, 83 (1961) 4183.

6 Yamana T, Mizukami Y, Tsuji A, Yasuda Y & Masuda K, *Chem pharm Bull*, 20 (1972) 881.

7 Khan M N & Khan A A, *J org Chem*, 40 (1975) 1793.

8 Khan M N & Khan A A, *J Chem Soc, Perkin Trans II* (1979) 796.

9 Kezdy F & Bruylants A, *Bull Soc chim Belges*, 68 (1959) 225; Crooy P & Bruylants A, *Bull Soc chim Belges*, 73 (1964) 44.

10 Vigneron-Voortman B, Crooy P, Bruylants A & Baczynskyj L, *Bull Soc chim Belges*, 73 (1964) 753.

11 Khan M M & Khan A A, *Indian J Chem*, 14A (1976) 807; Niaz M A & Khan A A, *Int J chem Kinet* 22(5) (1990) 449.

12 Swain C G, *J Am chem Soc*, 66 (1944) 1696.

13 Bruylants A & Kezdy F, *Record chem Progr*, 21 (1960) 213.

14 Davis T L, *J Am chem Soc*, 43 (1921) 2230.

15 Bender M L, *Chem Rev*, 60 (1960) 53.

16 Schowen R L, Jayaraman H & Kershner L, *Tetrahedron Lett* (1966) 497.

17 Tillett J G & Wibbigs D E, *Tetrahedron Lett* (1971) 911.

18 Ray P, *Chem Rev*, 61 (1961) 322.

19 Mader P M, *J Am chem Soc*, 87 (1965) 3191.

20 Brooke D & Guttman D E, *J Am chem Soc*, 90 (1968) 4964.

Indian Journal of Chemistry
Vol. 30A, February 1991, pp 148-153

Kinetics and mechanism of oxidation of free and metal-bound thiocarbohydrazide by N-bromoacetamide and N-chloro- and N-bromo-benzamides in aquo-acidic and aquo-organic media

B Thimme Gowda* & P Jagan Mohana Rao
Department of Chemistry, Mangalore University, Mangalagangothri 574 199

Received 16 April 1990; revised 25 June 1990; accepted 9 August 1990

Kinetics of oxidation of free and Zn(II)-bound thiocarbohydrazide (TCH) by N-bromoacetamide (NBA), N-chlorobenzamide (NCB) and N-bromobenzamide (NBB) have been studied in aqueous, water-methanol and water-acetic acid (1:1, v/v) media in the presence of perchloric acid or buffer. The reactions show first order kinetics in [oxidant] and fractional order each in [substrate] and $[H^+]$. Addition of the reduced product of the oxidant decreases the rate of NBB oxidation, while it has no effect in NCB and NBA oxidations. Increase in either ionic strength or dielectric constant of the medium increases the rates of oxidation in all the cases. Both Michaelis-Menton type and two-pathway mechanisms have been considered to explain the results. The rate constants are also predicted from the deduced rate laws and the predicted values are in good agreement with the experimental constants providing support to the proposed mechanism. The metal complexation of thiocarbohydrazide has little effect either on the rate of oxidation or kinetic orders.

The title investigation is an extension of our previous work[1-7] on the kinetics and mechanism of oxidation of free and metal bound thiosemicarbazide and thiocarbohydrazide (TCH).

Materials and Methods

Preparation and purification of TCH etc. were reported elsewhere[5-7]. The stock solutions (0.10 mol dm^{-3}) of TCH and its zinc complex (0.05 mol dm^{-3}) were prepared in 0.10 mol dm^{-3} aqueous perchloric acid or hydrochloric acid.

N-Bromoacetamide (NBA), N-chlorobenzamide (NCB) and N-bromobenzamide (NBB) were prepared in the laboratory and their purities were checked by iodometric estimation of the amount of active halogen present in them.

Acetic acid was purified before use and all other reagents employed were of accepted grades of purity.

Kinetic measurements

Kinetic studies were made under pseudo-first order conditions ([substrate] ≫ [oxidant], 5 to 50 fold excess). The reactions were initiated by the rapid addition of requisite amounts of thermally equilibrated oxidant solution (0.0005-0.003 mol dm^{-3}), to solutions containing known amounts of preequilibrated substrate (0.005-0.05 mol dm^{-3}) and perchloric acid (0.01-0.30 mol dm^{-3}) or KCl – HCl buffer (and benzamide and mercuric acetate in NBB oxidations). The progress of the reaction was monitored for at least two half-lives by the iodometric determination of unreacted oxidant at regular intervals of time. The pseudo-first order rate constants (k_{obs}) were computed by the graphical methods and the values were reproducible within ± 4% error.

The aquo-organic solvents employed were water-methanol (1:1, v/v) and water-acetic acid (1:1, v/v).

Stoichiometry and product analysis

The stoichiometries of TCH – NBA, TCH – NCB and TCH – NBB reactions both of the free and metal-bound TCH were determined by allowing the reactions to go to completion at 303K and different $[HClO_4]$ (0.01-0.30 mol dm^{-3}) and [substrate]/[oxidant] ratios. The presence of sulphate and carbon dioxide in the reaction products were detected by standard tests. Further, sulphate was estimated gravimetrically and the yield was 90 ± 5%. Observed stoichiometries per mole of TCH in the free and Zn(II)-bound states may be represented by Eqs 1 and 2.

$$H_2NHNCSNHNH_2 + 8CH_3CONHBr + 6H_2O \rightarrow 8CH_3CONH_2 + 2N_2 + CO_2 + SO_4^{2-} + 8Br^- + 10H^+ \quad \ldots (1)$$

$$H_2NHNCSNHNH_2' + 8C_6H_5CONHX + 6H_2O \rightarrow 8C_6H_5CONH_2 + 2N_2 + CO_2 + SO_4^{2-} + 8X^- + 10H^+ \quad \ldots (2)$$

where X = Cl or Br.

Nitrogen evolved was also determined quantitatively.

Results

At fixed [substrate] (several fold excess over [oxidant]) and $[HClO_4]$, the plots of log [oxidant] versus time were linear at least for two half-lives for all oxidants. The pseudo-first order rate constants (k_{obs}) were unaffected by the changes in $[oxidant]_0$ (Table 1), establishing first order kinetics in [oxidant] in all the cases. At constant $[oxidant]_0$ and $[HClO_4]$, the rates increased with increase in [TCH] or [complex] with varying fractional order dependences in [substrate] (Table 2). The metal complexation of the ligand TCH had little effect either on the rate of oxidation or kinetic orders.

The rates of oxidations also increased with increase in $[HClO_4]$ (Table 1) with varying fractional order dependences in $[H^+]$ for all the oxidations (Table 2).

The variation in ionic strength of the medium with $NaClO_4$ had little effect on the rates of oxidations, while decrease in dielectric constant of the medium by increasing methanol or acetic acid content of the solvent decreased the rates (Table 3).

Addition of the reduced product of the oxidants had little effect in NBA and NCB oxidations, while the rate decreased in the case of NBB oxidation, with an inverse fractional order dependence in [benzamide]. The rates increased with increase in [mercuric acetate] in NBB oxidations (Table 3). Addition of sodium acetate and variation of ionic strength with it also had significant effect.

The [substrate] were varied at different temperatures and the coefficients of the rate controlling steps have been computed at each temperature. The latter constants were used to calculate the activation parameters from the Arrhenius and Eyring plots (Table 2).

Discussion

Mechanism of oxidations

(i) *N-Chlorobenzamide and N-bromoacetamide oxidations*

The kinetics of first order in [oxidant] and fractional order each in [substrate] and $[H^+]$, and non-influence of the reduced products of the oxidants may be explained by a Michaelis-Menton type mechanism (Scheme 1).

Table 1 – Pseudo-first order rate constants (k_{obs}) for the oxidation of thiocarbohydrazide (TCH) and its metal complex, $Zn(TCH)_2Cl_2$ by N-bromoacetamide (NBA) in aqueous medium at 283K, N-chlorobenzamide (NCB) in water-methanol (1:1, v/v) at 283 K and by N-bromobenzamide (NBB) in water-acetic acid (1:1, v/v) medium at 293 K in the presence of perchloric acid (ionic strength. $I = 0.30$ mol dm^{-3}) (values in parentheses are the *p*H values of reaction mixtures)

$10^3[oxidant]_0$ (mol dm^{-3})	$10^2[sub]_0$ (mol dm^{-3})	$[10^2[HClO_4]$ (mol dm^{-3})	$10^4 k_{obs}$ (s^{-1})						
			NBA		NCB		NBB[a]		
			TCH	Complex	TCH	Complex	TCH	Complex	TCH[b]
Effect of varying $[oxidant]_0$									
0.5	1.0	5.0	13.1	16.8	11.4	14.9	6.4	9.4	8.6
1.0	1.0	5.0	13.6	17.1	11.9	15.0	6.6	9.4	9.2
2.0	1.0	5.0	14.1	17.2	12.1	15.1	6.7	9.5	8.9
3.0	1.0	5.0	13.7	17.1	12.0	15.0	6.6	9.6	–
Effect of varying $[substrate]_0$									
1.0	0.5	5.0	9.6(1.56)	12.5	8.6(1.63)	10.4	5.6(0.83)	8.0	6.9(1.40)
1.0	1.0	5.0	13.6(1.65)	17.1	11.9(1.69)	15.0	6.6(0.87)	9.4	9.2(1.56)
1.0	2.0	5.0	17.6(1.89)	23.1	15.0(1.78)	19.7	8.2(0.95)	12.6	13.1(1.80)
1.0	3.0	5.0	21.7(2.24)	28.8	16.9(1.97)	21.7	9.8(1.09)	15.6	16.8(2.11)
1.0	5.0	5.0	28.4(2.73)	32.7	20.0(2.38)	23.2	13.0(1.51)	21.5	–
Effect of varying $[HClO_4]$									
1.0	1.0	1.0	–	–	8.2(2.75)	10.4	4.3(1.51)	6.0	5.5(2.19)
1.0	1.0	2.0	8.8(2.39)	17.1	9.7(2.16)	12.8	5.0(1.31)	6.8	7.0(2.07)
1.0	1.0	3.0	9.6(1.99)	13.7	11.0(1.98)	13.8	–	–	7.8(1.97)
1.0	1.0	5.0	13.6(1.65)	17.1	11.9(1.69)	15.0	6.6(0.87)	9.4	9.2(1.56)
1.0	1.0	10.0	17.2(1.32)	22.6	13.4(1.35)	15.9	9.4(0.57)	14.3	11.9(0.79)
1.0	1.0	20.0	24.4(0.97)	32.5	15.7(1.06)	17.1	15.7(0.28)	23.7	17.3(0.31)

[a]10^2[benzamide] = 200 $[Hg(OAc)_2]$ = 1.0 mol dm^{-3}; [b]Rate constants when $I = 0.30$ mol dm^{-3} with NaOAc.

$$RNHX + H^+ \overset{K_1}{\rightleftharpoons} (RNH_2X)^+ \quad \text{(fast)}$$

$$(RNH_2X)^+ + H_2NNC(SH)NHNH_2 \overset{K_2}{\rightleftharpoons} \text{Complex} \quad \text{(fast)}$$

$$\text{Complex} \overset{k_3}{\rightarrow} (RNH_2) + H_2NHNC(\overset{+}{S}X)NHNH_2 \quad \text{(slow)}$$

$$H_2NHNC(\overset{+}{S}X)NHNH_2 + H_2O \rightarrow H_2NHNC(SO)NHNH_2 + 2H^+ + X^- \quad \text{(fast)}$$

$$H_2NHNC(SO)NHNH_2 + 2(RNH_2X)^+ \rightarrow XHNHNC(SO)NHNHX + 2(RNH_3)^+ \quad \text{(fast)}$$

$$XHNHNC(SO)NHNHX + 5(RNH_2X)^+ + 5H_2O \rightarrow \text{Final products}$$

where R = CH_3CO(NBA), C_6H_5CO(NCB),
X = Cl(NCB), Br(NBA)

Scheme 1

Based on Scheme 1 rate laws (3-6) have been deduced.

$$-\frac{d[NCB]}{dt} = \frac{K_1K_2k_3[\text{oxidant}]_{tot}[S][H^+]}{1 + K_1[H^+] + K_1K_2[H^+][S]} \quad \ldots (3)$$

or

$$k_{obs} = \frac{K_1K_2k_3[S][H^+]}{1 + K_1[H^+] + K_1K_2[H^+][S]} \quad \ldots (4)$$

Eq. (4) may be rearranged as

$$\frac{1}{k_{obs}} = \frac{1 + K_1[H^+]}{K_1K_2k_3[H^+]}\frac{1}{[S]} + \frac{1}{k_3} \quad \ldots (5)$$

or

$$\frac{1}{k_{obs}} = \frac{1}{K_1K_2k_3[S]}\frac{1}{[H^+]} + \frac{1 + K_2[S]}{K_2k_3[S]} \quad \ldots (6)$$

Equations (5) and (6) predict linearities between $1/k_{obs}$ and $1/[S]$ or $1/[H^+]$. The plots of $1/k_{obs}$ versus $1/[S]$ and $1/k_{obs}$ versus $1/[H^+]$ were linear with finite intercepts on the ordinates in accordance with the predictions (see Fig. 1). Reciprocals of the former plots gave k_3; $10^3\ k_3\ (s^{-1})$ = NBA: 2.9 (TCH), 3.9 (complex); NCB: 2.2 (TCH), 2.6 (complex). Further, the substrate concentrations were varied at different temperatures (278-293 K) and the values of k_3 were computed at each temperature. Activation parameters were then calculated from the plots of log k_3 versus 1/T and log (k_3/T) versus 1/T (Table 2). The equilibrium constant K_2 was calculated from the intercept $(1 + K_2[S])/K_2k_3[S]$, of $1/k_{obs}$ versus $1/[H^+]$ plot by inserting k_3 and [S] value: K_2 ($dm^3\ mol^{-1}$) = NBA: 500 (TCH), 650 (complex); NCB: 312 (TCH), 303 (complex). Further, the constant K_1 was calculated from the slope of either of the two plots: K_1 ($dm^3\ mol^{-1}$) = NBA: 5.0 (TCH), 3.3 (complex); NCB: 16.3 (TCH), 28.7 (complex). The differences in equilibrium constants are due to the nature of solvents and the oxidants employed.

The computed constants K_1, K_2 and k_3 were employed to predict the rate constants as [S] and $[H^+]$ varied. The predicted values compared with the ex-

Table 2 – Kinetic data and activation parameters for the oxidation of TCH and its metal complex by NBA in aqueous, NCB in water-methanol medium (1:1, v/v) and by NBB in water-acetic acid medium (1:1, v/v)

Orders (n) observed in	Computed from												
	NBA				NCB				NBB, I with				
	k_{obs}		k_{eff}	k_{obs}	k_{obs}		k_{eff}	k_{obs}	$NaClO_4$			NaOAc	
	TCH	Complex	TCH	TCH (buffer)	TCH	Complex	TCH	TCH (buffer)	k_{obs} TCH	Complex	k_{eff} TCH	k_{obs} TCH	k_{eff} TCH
[Oxidant]	1.0	1.0	1.0	1.0	1.0	1.0	1.0	1.0	1.0	1.0	1.0	1.0	1.0
[Substrate]	0.46	0.44	0.84	0.53	0.32	0.35	0.46	0.38	0.33	0.48	0.46	0.47	0.64
[$HClO_4$]	0.45	0.44	0.40	0.57	0.24	0.22	0.17	0.49	0.65	0.66	0.36	0.35	0.25
Activation Parameters	Computed from												
	k_3		k_3		k_3	k_3	k_7		k_6	k_6			
log A	8.73		7.35		10.43	8.93	4.24		11.36	15.35			
E_a (kJ mol^{-1})	61.1		53.7		52.3	63.2	30.8		75.1	96.8			
$\Delta H^{\ddagger}$ (kJ mol^{-1})	63.2		49.7		51.2	58.1	30.6		74.2	96.9			
$\Delta S^{\ddagger}$ (JK^{-1})	−71.7		−117.5		−68.7	−36.2	−163.9		−72.4	−49.1			
$\Delta G^{\ddagger}$ (kJ mol^{-1})	83.4		83.0		72.7	78.6	77.0		83.1	97.3			

Table 3 – Effect of varying dielectric constant of the medium, addition of benzamide [RNH_2], mercuric acetate and sodium acetate on the rates of oxidation of TCH and its metal complex by NCB in 1:1 (v/v) water-methanol and by NBB in water-acetic acid (1:1, v/v) (Temp: 283 K (NCB), 293 K (NBB)

10^3 [RNH_2] (mol dm^{-3})	$10^4 k^a_{obs}$ (s^{-1})		% MeOH (or HOAc)	$10^4 k^a_{obs}$ (s^{-1})	
	TCH	Complex		TCH	Complex
		NCB oxidations			
0.5	12.0	15.2	40	14.2	17.6
1.0	11.9	15.0	50	11.9	15.0
2.0	11.7	14.8	60	9.5	12.9
3.0	11.5	14.6	70	7.8	11.2
		NBB oxidations			
50.0	8.7(11.1)[b]	12.3	40	9.3	14.1
100.0	6.6(9.2)	9.4	50	6.6	9.4
200.0	5.0(7.6)	6.6	60	4.8	5.9
300.0	4.2(6.8)	5.7	70	3.3	3.7
10^3[$Hg(OAc)_2$] (mol dm^{-3})			10^2[NaOAc] (mol dm^{-3})		
1.0	4.4	5.5	1.0	6.4	
2.0	5.1	6.8	2.0	7.3	
5.0	6.6	9.4	5.0	9.2	
10.0	7.6	11.5	10.0	10.4	
20.0	8.9	23.4	20.0	11.2	

[a] $10^3[\text{oxidant}]_0 = 10^2[\text{substrate}]_0 = 20[HClO_4] = 3.3$ $I = 1.0$ mol dm^{-3}.
[b] Rate constants when $I = 0.30$ mol dm^{-3} with NaOAc.

Table 4 – Comparison of predicted rate constants from the rate laws 5 or 6 and experimental values for the oxidation of thiocarbohydrazide and its metal complex by N-bromoacetamide in aqueous and by N-chlorobenzamide in 1:1 (v/v) water-methanol medium at 283 K as [substrate] and [$HClO_4$] varied

10^2[substrate]$_0$ (mol dm^{-3})	$10^4 k$ (s^{-1})							
	Pred.		Obs.		Pred.		Obs.	
	TCH	Complex	TCH	Complex	TCH	Complex	TCH	Complex
		NBA oxidations				NCB oxidations		
0.5	9.9	12.2	9.5	11.8	8.7	10.5	8.6	10.4
1.0	14.0	18.5	13.9	17.3	12.4	15.5	11.9	15.0
2.0	18.8	24.9	18.9	23.8	15.5	20.1	15.0	19.7
3.0	21.1	28.3	21.1	28.5	17.4	22.2	16.9	21.7
5.0	23.7	31.6	25.2	33.3	18.9	24.1	20.0	23.2
10^2[$HClO_4$] (mol dm^{-3})								
1.0	—	—	—	—	7.2	9.6	8.2	10.4
2.0	8.9	—	8.6	—	9.8	12.9	9.7	12.8
3.0	11.2	13.9	10.9	14.6	11.1	13.9	11.0	13.8
5.0	14.3	18.1	13.9	17.3	12.4	15.5	11.9	15.0
10.0	17.7	23.5	17.5	23.1	13.6	16.2	13.4	15.9
20.0	20.4	27.5	21.6	31.0	14.4	17.3	15.7	17.1

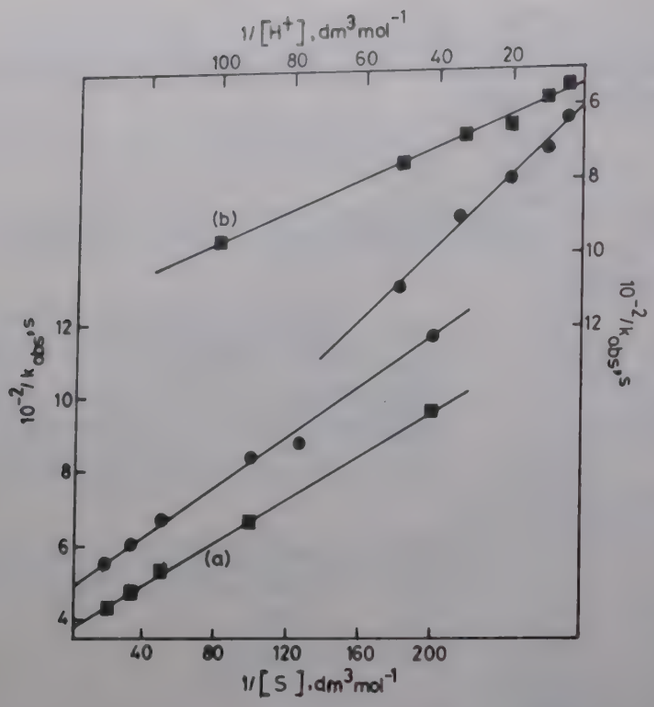

Fig. 1 – Plots of (a) $1/k_{obs}$ versus $1/[S]$ ($10^3[NCB]_0 = 20$ $[HClO_4] = 1.0$ mol dm^{-3}, medium: water-methanol (1:1, v/v), temp. 283 K, ● TCH, ■ complex)
(b) $1/k_{obs}$ versus $1/[H^+]$ ($10^3[NCB]_0 = 10^2[S]_0 = 1.0$ mol dm^{-3}, other conditions being the same ● TCH, ■ complex)

perimental constants are shown in Table 4. A good agreement between the two sets of values provides support to the suggested mechanism.

(ii) *N-Bromobenzamide oxidations*

The results can be explained by a two-pathway mechanism (Scheme 2) instead of a Michaelis-Menton type mechanism. The different behaviour may be due to change of solvent or medium.

$$C_6H_5CONHBr + S \overset{K_4}{\rightleftharpoons} C_6H_5CONH_2 + S' \quad \text{(fast)}$$

$$S' + H_2O \xrightarrow{k_5} S'' + H^+ + Br^- \quad \text{(slow)}$$

$$C_6H_5CONHBr + H^+ \xrightarrow{k_6} C_6H_5CONH_2 + Br^+ \quad \text{(slow)}$$

$$S'' + C_6H_5CONHBr \rightarrow \text{Products} \quad \text{(fast)}$$

$$Br^+ + S \rightarrow \text{Products} \quad \text{(fast)}$$

The other fast steps leading to stoichiometric products are similar to steps in Scheme 1.

Scheme 2

The combined rate laws (7-9) based on competitive steps have been deduced.

$$-\frac{d[NBB]}{dt} = \frac{K_4 k_5 [NBB][S][H_2O]}{[BA]} + k_6[NBB][H^+] \quad \ldots (7)$$

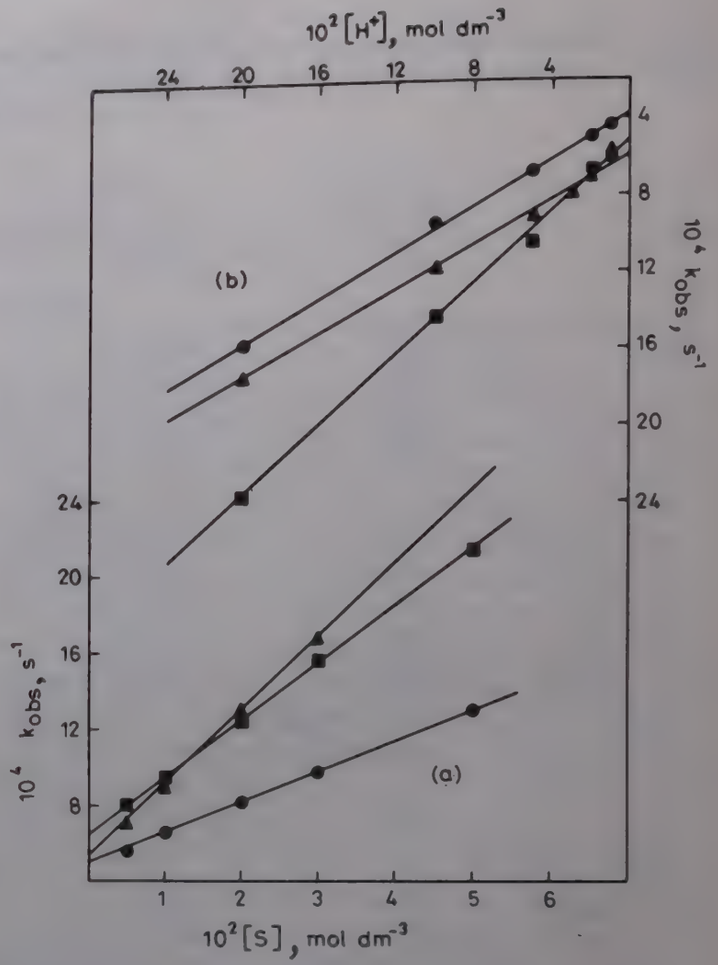

Fig. 2 – Plots of (a) k_{obs} versus [S] ($10^3[NBB]_0 = 20$ $[HClO_4] = 1.0$ mol dm^{-3}, medium: water-acetic acid (1:1, v/v), temp. 293 K)
(b) k_{obs} versus $[H^+]$ ($10^3[NBB]_0 = 10^2[S]_0 = 1.0$ mol dm^{-3}, other conditions being the same. ● TCH, ■ complex while $I = 0.30$ mol dm^{-3} with $NaClO_4$ and ▲ TCH while $I = 0.30$ mol dm^{-3} with NaOAc)

or

$$k_{obs} = \frac{K_4 k_5 [S][H_2O]}{[BA]} + k_6[H^+] \quad \ldots (8)$$

or

$$k_{obs} = \frac{K_4 k'_5 [S]}{[BA]} + k_6[H^+] \quad \ldots (9)$$

where $k'_5 = k_5[H_2O]$.

Rate law (9) is in conformity with the observed linearities of the plots between k_{obs} and [S], k_{obs} and $[H^+]$ (Fig. 2) and k_{obs} and $1/[BA]$ (figure not shown). Three sets of K_4k_5 and k_6 were calculated from the plots of k_{obs} versus [S], k_{obs} versus $1/[BA]$ and k_{obs} versus $[H^+]$. The constants computed from one of the plots were used to predict the rate constants as the other two concentrations were varied and vice-versa. The latter constants compared reasonably well with the experimental values testing the consistency of the rate law and hence the proposed mechanism. Further, the values of k_6 at different tem-

peratures and the corresponding activation parameters were calculated as described earlier.

The stoichiometric equations for the oxidation of TCH indicate that $[H^+]$ ions are generated in the course of the reaction, resulting in the variation of $[H^+]$, under conditions $[HClO_4] \leq$ [oxidant]. Hence it is natural to suspect that the kinetics observed may not give a true picture of oxidation process. To make sure that the kinetics determined are reliable, oxidation of TCH by NBA and NCB was also studied in KCl – HCl buffered aqueous and water-methanol (1:1, v/v) media. The results are shown in Table 5 and Fig. 1. In addition *p*H of the reaction mixtures as $[HClO_4]$ and [TCH] varied were measured (Table 1). The rate dependence in $[H^+]_{eff}$ was calculated from the measured *p*H values at varying $[HClO_4]$. The latter values were used to compensate the change in rate constant due to change in $[H^+]$ at different [TCH] ($k_{eff} = k_{obs}/[H^+]^n$). The effective rate constants (10^4 k_{eff}, s^{-1}) are NBA: 39.8, 58.4, 98.5, 167.1, 342.8; NCB: 16.0, 22.7, 29.2, 35.9, 49.7; NBB (*I* with $NaClO_4$): 11.2, 13.7, 17.9, 24.5, 46.1 and NBB (*I* with NaOAc): 15.4, 22.6, 36.9, 48.9, –, for 10^2 [TCH] = 0.5, 1.0, 2.0, 3.0 and 5.0, (mol dm^{-3}) respectively.

These values were used to calculate the rates at different [TCH] (see Table 2). The kinetic orders in [TCH] computed from the effective rate constants are relatively larger than the ones computed from the observed rate constants. This is as per our expectation.

The kinetic data calculated from the effective rate constants in acid medium and the results in buffered aqueous medium for NBA oxidations may also be explained by the mechanism shown in Scheme 1, and the related rate laws. Similar calculations and comparisons were made.

Oxidation of TCH by NCB in buffered water-methanol medium seems to occur by a competitive mechanism rather than a Michaelis-Menton type mechanism. This is also not unexpected as the behaviour of NCB as a source of Cl^+ would be different in the presence of Cl^-. The kinetic results under these conditions may be explained by the mechanism represented by the combined rate law (10). The plots of k_{obs} versus [TCH] and k_{obs} versus $[H^+]$ were linear.

$$-\frac{d[NCB]}{dt} = k_7[NCB][S] + k_8[NCB][H^+][Cl^-] \quad \ldots (10)$$

or

$$k_{obs} = k_7[S] + k'_8[H^+], \text{ where } k'_8 = k_8[Cl^-] \quad \ldots (11)$$

Table 5 – Pseudo-first order rate constants (k_{obs}) for the oxidation of TCH by NBA in buffered[a] aqueous and by NCB in buffered water-methanol (1:1, v/v) medium at 283 K

10^3[oxidant]$_0$ (mol dm^{-3})	10^2[TCH]$_0$ (mol dm^{-3})	*p*H	10^4 k_{obs} (s^{-1})	
			NBA	NCB
Effect of varying [oxidant]				
0.5	1.0	1.8	10.5	8.4
1.0	1.0	1.8	10.6	8.5
2.0	1.0	1.8	10.5	8.5
Effect of varying [substrate]				
1.0	0.5	1.8	8.6	6.8
1.0	0.75	1.8	8.6	—
1.0	1.0	1.8	10.6	8.5
1.0	2.0	1.8	14.8	11.8
1.0	3.0	1.8	18.2	14.4
Effect of varying *p*H				
1.0	1.0	1.2	21.3	17.2
1.0	1.0	1.5	15.3	10.9
1.0	1.0	1.8	10.6	8.5
1.0	1.0	2.1	6.8	6.5

[a]HCl – KCl buffer

The observed effects of variation in solvent composition on the rates of reactions may be explained by either Amis[8] or other concepts. The plots of log k_{obs} versus 1/D (or % MeOH or HOAc) were linear with negative slopes. Negative $\Delta S^{\ddagger}$ values may indicate that the transition states are more ordered than the reactants due to decrease in the number of degrees of freedom. Relatively high positive values for free energy of activation signals bond breaking in the formation of transition state.

The metal complexation of thiocarbohydrazide has very little effect either on the rates of oxidations or kinetic orders. It is also evident from the kinetic data and other results that NBB donates Br^+ species much more readily than NCB does Cl^+ species.

References

1 Gowda B T & Bhat J I, *Tetrahedron*, 43 (1987) 2119.

2 Gowda B T & Bhat J I, *Indian J Chem*, 27A (1988) 597, 974; 28A (1989) 211.

3 Gowda B T & Rao R V, *J chem Soc, Perkin Trans* 2, (1988) 355.

4 Gowda B T & Shengara B S, *Int J chem Kinet*, 21 (1989) 31.

5 Gowda B T & Shengara B S, *Proc Indian Acad Sci (Chem Sci)*, 101 (1989) 155.

6 Gowda B T & Ramachandra P, *J chem Soc, Perkin Trans* 2, (1989) 1067; *Indian J Chem*, 29A (1990) 680.

7 Gowda B T & Rao P J M, *Proc Indian Acad Sci (Chem Sci)*, 102 (1990) xxx; *Z phys Chem N.F.*, (1990) xxx.

8 Amis E S, *Solvent effects on reaction rates and mechanisms* (Academic, New York) 1966.

Indian Journal of Chemistry
Vol. 30A, February 1991, pp 154-157

Kinetics and mechanism of Pd(II) catalysed oxidation of mandelic and tartaric acids by chloramine-T in alkaline medium

Anju Shukla & Santosh K Upadhyay*
Department of Chemistry, H.B. Technological Institute, Kanpur 208 002

Received 22 June 1990; revised 21 August 1990; accepted 16 October 1990

The kinetics of Pd(II) catalysed oxidation of mandelic and tartaric acids by chloramine-T have been investigated in alkaline medium. A first order dependence of rate each in [substrate] and [catalyst] has been observed. The order of reaction in chloramine-T and alkali decreases at higher [chloramine-T] or [NaOH]. A suitable mechanism consistent with kinetic data is proposed and discussed.

The kinetics of redox reactions involving homogeneous catalysts such as platinum group metals particularly osmium(VIII)[1], ruthenium(III)[2,3], iridium(III)[4] have been extensively investigated from mechanistic point of view. However, the role of Pd(II) as homogeneous catalyst in such reaction has not been investigated so far, and hence the title reaction has been investigated.

Materials and Methods

DL-tartaric acid, mandelic acid, chloramine-T (CAT), and Pd(II) chloride and other reagents used were of AR grade. All the solutions were prepared in doubly distilled water.

The stock solution of Pd(II) chloride was prepared by dissolving the sample in dil. HCl, the final strength of Pd(II) chloride and HCl being kept at 22.5×10^{-3} mol dm^{-3} and 1.0×10^{-2} mol dm^{-3} respectively. Chloramine-T solution was standardised iodometrically. Stock solutions of CAT and Pd(II) chloride were stored in black coated bottles. The reaction vessels were also coated black from outside.

The reactions were initiated by the addition of preequilibrated CAT solution to other reagents solution, preequilibrated at the desired temperature, although the order of addition had no effect on the rate. The progress of the reaction was followed by determining [CAT] iodometrically in aliquots withdrawn after suitable time intervals. The iodine liberated by Pd(II) ion was taken into account. The temperature was maintained with an accuracy of ± 0.1°C.

The reaction mixture containing a known excess of [CAT] over [substrate] was kept in the presence of NaOH and Pd(II) chloride at 35°C for 72 hr. Estimation of unreacted CAT showed that one mole of mandelic and tartaric acids consumed one mole and two moles (more than two moles at lower [substrate]) of CAT respectively.

The presence of benzaldehyde as product in the case of mandelic acid was confirmed by forming its 2,4 DNP derivative and comparing its m.p. with that of an authentic sample. In case of tartaric acid, glyoxal, glyoxylic acid and formic acid were detected as the products.

The products were also determined under the kinetic conditions, i.e. at low [CAT]. Under these conditions the oxidation product of mandelic acid was benzaldehyde. However, in the case of tartaric acid the oxidation product was glyoxal.

Results

The reactions were studied at various initial [reactant]. The reactions do not proceed in the absence of Pd(II). However, in the presence of Pd(II), the log[CAT] versus time plots were linear upto 85% of the reactions and, therefore, pseudo-first order rate constants in CAT (k_{obs}) were evaluated from the slopes of these plots. The rate constants (k_{obs}) at different initial [reactant] are reported in Table 1. It is observed that an increase in initial [CAT] resulted in a decrease in the k_{obs} (Table 1). It was also observed that at high initial [CAT] the reactions were initially fast upto 10-20% of the reactions and log[CAT] versus time plots were showed curved initially upto 10-20% of the reactions and then showed a linear behaviour.

The plots of k_{obs} versus [substrate] or [Pd(II)] were linear passing through the origin suggesting first order dependence of rate each in [substrate] and [catalyst].

Table 1 – Dependence of rate constants at several initial [reactant] at 35°C

10^3 [CAT] (mol dm^{-3})	10^2 [S] (mol dm^{-3})	10^4 [Pd(II)]* (mol dm^{-3})	10^3 [OH$^-$] (mol dm^{-3})	$k_{obs} \times 10^4$ (s^{-1})	
				Tartaric acid	Mandelic acid
1.0	2.0	2.25	10.0	12.20	6.15
1.5	2.0	2.25	10.0	7.67	4.22
2.0	2.0	2.25	10.0	3.84	3.07
2.5	2.0	2.25	10.0	3.08	2.30
3.0	2.0	2.25	10.0	2.50	2.11
2.0	1.2	2.25	10.0	2.50	1.91
2.0	1.6	2.25	10.0	3.26	2.49
2.0	3.0	2.25	10.0	5.97	4.22
2.0	4.0	2.25	10.0	7.29	5.75
2.0	2.0	1.35	10.0	2.10	1.80
2.0	2.0	1.80	10.0	3.07	2.39
2.0	2.0	3.37	10.0	6.14	4.20
2.0	2.0	4.50	10.0	8.44	5.75

*In the case of tartaric acid, [Pd(II)] is half of the reported values in the table.

The effect of varying [OH$^-$] on the rate was studied at a fixed ionic strength ($\mu = 0.03$ mol dm^{-3}) maintained by the addition of sodium perchlorate. The amount of acid already present in the catalyst was taken into account. The plot of k_{obs} versus [OH$^-$] deviated from linearity (Fig. 1) suggesting that order in [OH$^-$] decreased from unity at higher [alkali]. Further at very high [alkali] ($> 20.0 \times 10^{-3}$ mol dm^{-3}) a retarding effect of OH$^-$ on the rate constant was also observed.

The effect of ionic strength on the rate of reaction was studied using sodium perchlorate. Addition of $NaClO_4$ (upto 0.04 mol dm^{-3}) in the reaction mixture showed an insignificant effect on the rate constant. Addition of *p*-toluene-sulphonamide (reaction product of CAT) in the reaction mixture had also no effect on the observed rate constants.

Successive addition of sodium chloride in reaction mixture decreased the observed rate constant in each case and a plot of $1/k_{obs}$ versus [Cl$^-$] was linear with an intercept.

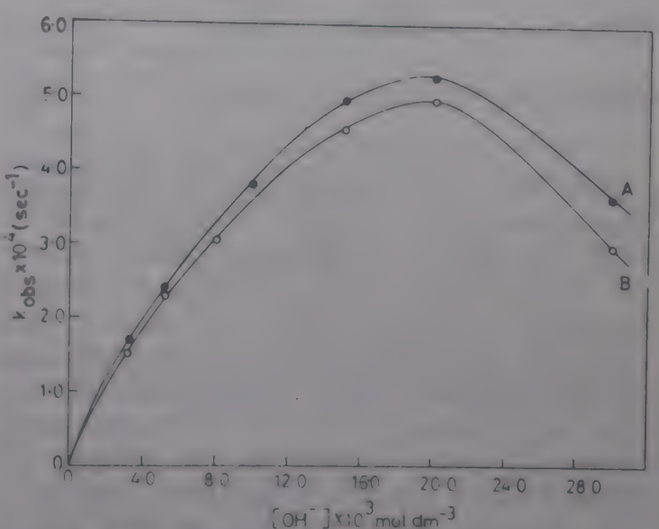

Fig. 1 – Plots of k_{obs} versus [OH$^-$] at 35°C. ([substrate] = 2.0×10^{-2} mol dm^{-3}, [chloramine-T] = 2.0×10^{-3} mol dm^{-3}, [Pd(II)] = 1.125×10^{-4} and 2.25×10^{-4} mol dm^{-3} for A and B respectively, $\mu = 0.03$ mol dm^{-3} maintained by the addition of sodium perchlorate. (A – tartaric acid and B – mandelic acid)

Discussion

Stock solution of Pd(II) chloride was prepared in dil. hydrochloric acid in which is is known to exist[5] as $[PdCl_4]^{2-}$. In order to understand the nature of Pd(II) ion in alkaline medium, in a separate set of experiment Pd(II) chloride solution was treated with sodium hydroxide. In a known excess of NaOH, the increasing amount of Pd(II) chloride was mixed and unreacted (free OH) amount of NaOH in the mixture was estimated volumetrically. The NaOH reacted with Pd(II) ion in nearly 1:2 stoichiometry when the concentration of Pd(II) ion in reaction mixture was low in comparison to that of OH$^-$ (or at high [alkali]). However, the 1:2 stoichiometry decreased on increasing [Pd(II)] and a 1:1 stoichiometry was observed at higher [Pd(II)] (or at low [OH$^-$]) in comparison to that of Pd(II).

On the basis of these observations, the equilibrium (1) and (2) can be suggested between $[PdCl_4]^{2-}$ and OH^-,

$$[PdCl_4]^{2-} + OH^- \rightleftharpoons [Pd(OH)Cl_3]^{2-} + Cl \quad \ldots (1)$$
$$(C_1) \qquad (C_2)$$

$$[Pd(OH)Cl_3]^{2-} + OH^- \rightleftharpoons [Pd(OH)_2Cl_2]^{2-} + Cl^- \quad \ldots (2)$$
$$(C_3)$$

CAT behaves like a strong electrolyte[6] and in aqueous solution ionises as,

$$RNNaCl \rightleftharpoons RNCl^- + Na^+$$

(where R represent $CH_3C_6H_4SO_2-$ group)

It has been observed that in aqueous alkaline solution, CAT is hydrolysed in accordance with Eqs (3) and (3a),

$$RNNaCl + H_2O \rightleftharpoons RNHCl + NaOH \quad \ldots (3)$$

$$RNHCl + NaOH \rightleftharpoons RNH_2 + NaOCl \quad \ldots (3a)$$

Thus in alkaline solution of CAT, RNHCl has been considered as the main oxidising species[7] of CAT. The absence of Michaelis-Menton reciprocal relationship[8] (a kinetic proof for the complex formation between substrate and catalyst) and strict first order dependence in [substrate] ruled out any complex formation between the substrate and catalyst. Based on the hydride ion abstracting capacity, a cyclic structure for the complex between RNHCl and OsO_4 has been suggested[9]. This structure shows that the electron density around the nitrogen atom (in RNHCl) is lowered, resulting in the weakening of N – Cl bond. Subsequently the hydride-ion abstracting capacity of N-chlorotoluene-*p*-sulphonamide (RNHCl) is increased after complexation, which, results in a interaction of complex with the appropriate form of the substrate. Since no oxidation of mandelic acid or tartaric acid occur with either palladous chloride or chloramine-T alone, it is reasonable to assume a similar complex between reactive species of palladous chloride and RNHCl.

Further, retarding effect of OH^- at high [alkali] (Fig. 1) indicates that species C_3 of the catalyst (step-2) which is formed at higher [alkali] is resistant towards CAT.

On the basis of the above facts and experimental results the mechanism as given in Scheme 1 can be proposed for the reaction under study. We have tried to confirm complex formation between Pd(II) chloride and CAT. The absorbance was measured (at 400 nm) for a series of solutions containing varying amounts of CAT with a constant amount of Pd(II) chloride (1.125×10^{-3} mol dm^{-3}) and NaOH (0.5×10^{-3} mol dm^{-3}). It is observed that addition of increasing amount of CAT gradually decreases the absorbance due to Pd(II) chloride until the [CAT]:[Pd(II)] ratio becomes 1:1. Thereafter, there is no further decrease in absorbance. However, a turbidity appears in the solutions after keeping for some time.

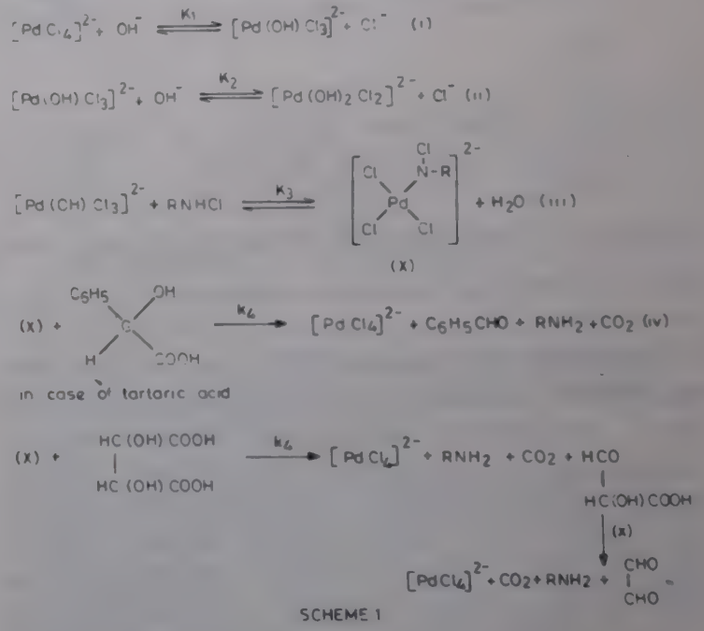

The formation of formic acid and glyoxalic acid as the end products in the presence of excess of oxidant may involve various unstable intermediates which are not easily identifiable.

According to the mechanism (Scheme 1), the rate of disappearance of CAT in terms of $[Pd(II)]_T$ may be given by Eq. (4)

$$\frac{-d[CAT]}{dt} = \frac{n k_4 K_1 K_3 [CAT][OH^-][Pd(II)]_T[S][Cl^-]}{[Cl^-]^2 + K_1[OH^-][Cl^-] + K_1K_3[CAT][OH^-][Cl^-] + K_1K_2[OH^-]^2} \quad \ldots (4)$$

(where n = 1 and 2 in case of mandelic acid and tartaric acid respectively, K_3 also includes water molecule). At lower [alkali], where species (C_3) does not exist and $K_2 = 0$, rate law (4) reduces to (5)

$$\frac{-d[CAT]}{dt} = \frac{n k_4 K_1 K_3 [CAT][OH^-][Pd(II)]_T[S]}{[Cl^-] + K_1[OH^-]\{1 + K_3[CAT]\}} \quad \ldots (5)$$

The experimental results, i.e. first order dependence each in [catalyst] and [substrate], a decrease in the observed rate constants at higher [alkali] and [CAT] and a retarding effect of Cl^- on the rate are in agreement with the rate law (5). At higher initial [CAT] the reactions are initially fast (upto 10-20% of reactions) suggesting a zero order dependence in [CAT]. This is also supported by rate law (5).

Further at higher [alkali] where the species (C_3) of the catalyst dominates, $K_1[OH^-]\{[Cl^-] + K_3[CAT][Cl^-] + K_2[OH^-]\} \gg [Cl^-]^2$ may be taken as a suitable approximation and therefore, rate law (4) reduces to (6)

$$\frac{-d[CAT]}{dt} = \frac{n k_4 K_3 [CAT][Pd(II)]_T[S][Cl^-]}{[Cl^-] + K_3[CAT][Cl^-] + K_2[OH^-]} \quad \ldots (6)$$

Rate law (6) explains the retarding effect of $[OH^-]$ on the rate at very high [alkali]. However, a negligible effect of Cl^- at high [alkali] is expected from Eq. (6).

The $[OH^-]$ producing the maximum rate can be obtained by differentiating Eq. (4) and applying the conditions for maxima, i.e. $d(V)/d[OH^-] = 0$ where V represents the rate of disappearance of CAT. The $[OH^-]$ producing the maximum rate is obtained by Eq. (7),

$$[OH^-] = [Cl^-]/(K_1 K_2)^{1/2} \quad \ldots (7)$$

which is independent of the [catalyst] or [substrate]. Figure 1 also shows that $[OH^-]$ showing the maximum rate is nearly independent of [substrate]. Further this has been verified experimentally. In separate set of experiments with the [catalyst] twice or thrice that of concentration used in Figure 1, the $[OH^-]$ producing the maximum rate remained unchanged.

Acknowledgement

The authors thank Prof. A K Vasishtha and Prof. R S Tewari, of our Institute for their keen interest in the work.

References

1 Agrawal M C & Upadhyay S K, *J sci ind Res*, 42 (1983) 508.
2 Sharma J P, Sing R N P, Sing A K & Singh Bharat, *Tetrahedron*, 42 (1986) 2739.
3 (a) Gupta Sushma, Ali Vazid & Upadhyay S K, *Int J chem Kinet*, 21 (1989) 315.
(b) Saxena Rashmi, Gupta Sushma & Upadhyay S K, *Indian J Chem*, 29A (1990) 847.
4 Ramakrishna S & Kandlikav S, *Indian J Chem*, 27A (1988) 23.
5 Cotton F A & Wilkinson G, *Advanced inorganic chemistry* (John Wiley, New York), 1967, p. 1026.
6 Bishop E & Jennings V J, *Talanta*, 1 (1958) 197.
7 Agrawal M C & Upadhyay S K, *J sci ind Res*, 49 (1990) 13.
8 Michaelis L & Menton M L, *Biochem Z*, 49 (1913) 333.
9 Mushran S P, Agrawal M C & Prasad B, *J chem Soc (B)*, (1971) 1712.

Indian Journal of Chemistry
Vol. 30A, February 1991, pp 158-161

Osmium(VIII) oxidation of chromium(III) in aqueous alkaline medium

S M Tuwar, S T Nandibewoor & J R Raju*
Department of Chemistry, Karnatak University, Dharwad 580 003

Received 4 June 1990; revised 27 August 1990; accepted 22 October 1990

Osmium(VIII) oxidation of Cr(III) in aq. alkaline medium ($[OH^-] \geq 0.20$ mol dm^{-3}) at 24°C is found to follow the rate law,

$-d[Os(VIII)]_T/dt = kK_2[Os(VIII)]_T [Cr(III)]_T/(1 + K_2[OH^-]_T)$

The constants K_2 and k respectively represent the equilibrium formation constant of the species $OsO_5(OH)^{3-}$ in the step $OsO_4(OH)_2^{2-} + OH^- \rightleftharpoons OsO_5(OH)^{3-} + H_2O$ and rate constant of $OsO_5(OH)^{3-} + Cr(OH)_4^-$ interaction ($Cr(OH)_4^-$ as Cr(III) species is known to occur predominantly in alkaline medium). The experimental values of K_2 and k are 7.5 ± 0.4 dm^3 mol^{-1} and 83.3 ± 2.0 dm^3 mol^{-1} s^{-1}, the main active species being $OsO_5(OH)^{3-}$ and $Cr(OH)_4^-$.

The amphoteric nature of Cr(III) in basic medium has recently been shown[1] to be due to the predominance of $Cr(OH)_4^-$ and not $Cr(OH)_6^{3-}$. The existence of $Cr(OH)_4^-$ was also supported by the kinetic evidence gathered during oxidation of Cr(III) by hexacyanoferrate(III) in alkaline medium[2]. The redox potentials of Os(VI)/Os(VIII) (−0.30V) and Cr(III)/Cr(VI) (+0.13V) couples in alkaline medium show that Os(VIII) should be able to oxidise Cr(III) in such a medium. Preliminary studies showed that such a reaction is amenable to kinetic investigation and hence the title study.

Materials and Methods

Reagent grade chemicals and doubly distilled water were used throughout. Osmium tetroxide (Johnson Mathey) was dissolved in 0.50 mol dm^{-3} sodium hydroxide and the solution standardised by adding excess standard hexacyanoferrate(II) in 1.0 mol dm^{-3} hydrochloric acid to it and, by titrating the unreacted hexacyanoferrate(II) after 1 hr, with Ce(IV) using ferroin as an indicator. The Cr(III) solution was obtained by dissolving the double salt, $Cr_2(SO_4)_3 \cdot K_2SO_4 \cdot 24H_2O$ (BDH) in water. The actual [Cr(III)] was estimated by oxidising it to Cr(VI) with persulphate in the presence of Ag(I), the Cr(VI) being titrated with iron(II). Chromium(VI) solution was made by dissolving potassium dichromate (BDH, AR) in water. Osmium(VI) solution was obtained by mixing equivalent concentrations of Cr(III) and Os(VIII) in 0.50 mol dm^{-3} sodium hydroxide. Sodium perchlorate and sodium hydroxide were used to adjust the ionic strength and alkalinity in reaction solutions respectively. All solutions were always prepared afresh for each kinetic run.

Kinetic run—The reaction was followed spectrophotometrically (Hitachi 150 spectrophotometer) under second order conditions at 24° ± 0.05°C by mixing the reactant solutions which also contained the required amounts of sodium hydroxide and sodium perchlorate. The absorbances of the aliquots of the reaction mixture were measured in matched quartz cells of 1 cm path length at regular time intervals at 280, 321 and 372 nm, as three of the four species, Os(VIII), Os(VI) and Cr(VI) (to the exclusion of Cr(III) which absorbs in the visible region) absorb practically in the entire UV/visible region; further no single λ_{max} is available for any one of these species. The absorption of Cr(III) at these three wavelengths was negligible. In view of the overlapping absorption regions, the reaction could be followed only by recording the absorbances at the three wavelengths mentioned above and solving[3] the sets of triple simultaneous equations with a prior knowledge of the relevant molar absorbancy indices (ε) at the respective wavelengths. The adherance of Os(VIII), Os(VI) and Cr(VI) to Beer's law had been individually tested at the above three wavelengths in the concentration range of 5.0×10^{-5} to 5.0×10^{-4} mol dm^{-3} in 0.20 mol dm^{-3} sodium hydroxide (Table 1). Initial rates were measured by the plane mirror method and were reproducible within 10%. In the case of Os(VIII) species, the absorbance depended on $[OH^-]$. Consequently, the molar absorbancy index (ε) had to be evaluated for each $[OH^-]$ in the reaction by a test of the application of Beer's law at the three wavelengths (Table 2). No such dependency on $[OH^-]$ was observed in the case of Os(VI) and Cr(VI).

Kinetic runs at $pH > 12$ gave satisfactory results.

Table 1—Molar absorbancy indices[a] for Os(VIII), Cr(VI) and Os(VI) at different wavelengths in 0.20 mol dm^{-3} NaOH

Species	280 nm	321 nm	372 nm
Os(VIII)	1550	2190	1270
Cr(VI)	3300	300	4670
Os(VI)	960	720	320

[a]Molar absorbancy indices (ε) agreed within ± 1.5%

Table 2—Molar absorbancy indices[a] for Os(VIII) at different wavelengths at different [OH$^-$]

[OH$^-$] mol dm^{-3}	0.02	0.04	0.08	0.10	0.20	0.30
372 nm	800	920	1050	1090	1270	1370
321 nm	1640	1930	2045	2060	2190	2190
280 nm	1550	1550	1550	1550	1550	1550

[a]Molar absorbancy indices (ε) agreed within ± 1.5%

However, when [OH$^-$] < 0.020 mol dm^{-3}, the reaction mixture tended to become turbid presumably due to precipitation of $Cr(OH)_3$; hence the study was restricted to runs under conditions of pH > 12. It was found that this reaction can be carried out in all glass vessels, quartz vessels or polyacrylate vessels with no significant variation in the results. The atmospheric oxygen also had no influence on the results.

Results

Stoichiometry—Reaction mixtures containing different [Os(VIII)] and [Cr(III)] and fixed [OH$^-$] of 0.20 mol dm^{-3} were kept aside for 8 hr at 24°C and then analysed as follows. Osmium(VIII) was extracted with chloroform and its concentration measured in the organic layer spectrophotometrically at 282 nm (ε_{282} = 1870). Chromium(VI) left behind after extraction of Os(VIII), was titrated with iron(II) solution after acidifying the reaction mixture. Chromium(III) could be measured at 590 nm (ε = 25 ± 1). The results support a 3:2 stoichiometry for the reaction: 3Os(VIII) + 2Cr(III) = 3Os(VI) + 2Cr(VI).

Reaction order—Orders in each reactant were found from log-log plots of initial rates against concentrations. Order in Os(VIII) was ~0.93 between 2.50×10^{-5} and 2.25×10^{-4} mol dm^{-3} of [Os(VIII)] at fixed [Cr(III)] and [OH$^-$] of 1.5×10^{-4} mol dm^{-3} and 0.20 mol dm^{-3} respectively (Table 3). Order in Cr(III) was around unity as studied between 0.50×10^{-4} and 5.0×10^{-4} mol dm^{-3} [Cr(III)] at fixed [Os(VIII)] of 2.25×10^{-4} mol dm^{-3} and [OH$^-$] of 0.20 mol dm^{-3}. The effect of [OH$^-$] on the reaction was studied from 0.020 to 0.30 mol dm^{-3} at fixed [Os(VIII)] and [Cr(III)] and I = 0.30 mol dm^{-3} (Table 3) and the order in [OH$^-$] was found to be ~ 0.60.

Table 3—Effect of [Os(VIII)], [Cr(III)] and [OH$^-$] on Os(VIII)-Cr(III) reaction at 24°C and I = 0.30 mol dm^{-3}

[Cr(III)] × 10^4 mol dm^{-3}	[Os(VIII)] × 10^4 mol dm^{-3}	[OH$^-$] mol dm^{-3}	(Initial rate) × 10^6 mol dm^{-3} s^{-1}	
			Expt.	Calc.[a]
0.50	2.25	0.20	0.55	0.56
0.80	2.25	0.20	0.86	0.89
1.00	2.25	0.20	1.20	1.15
1.50	2.25	0.20	1.66	1.68
3.00	2.25	0.20	3.10	3.37
5.00	2.25	0.20	5.35	5.62
1.50	0.25	0.20	0.24	0.19
1.50	0.50	0.20	0.44	0.38
1.50	0.65	0.20	0.53	0.49
1.50	0.70	0.20	0.59	0.53
1.50	0.90	0.20	0.74	0.67
1.50	1.60	0.20	1.33	1.20
1.50	2.25	0.20	1.66	1.68
1.50	2.25	0.02	0.36	0.37
1.50	2.25	0.04	0.60	0.64
1.50	2.25	0.08	1.00	1.05
1.50	2.25	0.10	1.26	1.21
1.50	2.25	0.20	1.66	1.68
1.50	2.25	0.30	2.10	1.96

[a]Initial rates were calculated from Eq. (3) using K_2 and k as 7.5 ± 0.4 dm^3 mol^{-1} and 83.3 ± 2.0 dm^3 mol^{-1} s^{-1} respectively.

Effect of added products and ionic strength—Initial addition of products, Cr(VI) and Os(VI) between 3.0×10^{-5} and 3.0×10^{-4} mol dm^{-3}, keeping [Os(VIII)] and [Cr(III)] and ionic strength fixed, did not have any significant effect on the reaction. The rate increased from 1.66×10^{-6} to 2.50×10^{-6} mol dm^{-3} s^{-1} with increase in ionic strength from 0.20 to 0.90 mol dm^{-3}, other conditions being constant.

As observed in an earlier study[1] increase in temperature favours the formation of dimeric, trimeric, etc. forms of Cr(III). Presumably, a part of Cr(III) which undergoes polymerisation is more difficult to oxidise and our attempts at finding the rates at higher temperatures actually resulted in marginal decreases in rates. Hence, temperature effect on the reaction could not be studied.

Discussion

The reaction is approximately first order in Cr(III) and fractional order each in [Os(VIII)] and [OH$^-$]. Osmium(VIII) is known to form different complexes with OH$^-$ in basic media as shown in

Eqs (1) and (2) with equilibrium constants of K_1 and K_2 having the values of (24 and 6.8 $dm^3\ mol^{-1}$ respectively[4].

$$OsO_3(OH)_3^- + OH^- \rightleftharpoons OsO_4(OH)_2^{2-} + H_2O\ K_1 \quad ...(1)$$

$$OsO_4(OH)_2^{2-} + OH^- \rightleftharpoons OsO_5(OH)^{3-} + H_2O\ K_2 \quad ...(2)$$

It is seen that a progressive increase in $[OsO_4(OH)_2^{2-}]$ and $[OsO_5(OH)^{3-}]$ occurs with increase in $[OH^-]$ and, at $[OH^-]$ of 0.20 mol dm^{-3}, used in this study, virtually all Os(VIII) is present as $OsO_4(OH)_2^{2-}$ and $OsO_5(OH)^{3-}$. Indeed, $[OsO_5(OH)^{3-}]$ may be calculated on the basis of K_1 and K_2 to be about 20% at an $[OH^-]$ of 0.020 mol dm^{-3} when total $[Os(VIII)] = 2.25 \times 10^{-4}$ mol dm^{-3}, and over 90% of the total [Os(VIII)] when $[OH^-]$ is 0.20 mol dm^{-3}. It is also found that the absorbance of Os(VIII) does become almost constant beyond an $[OH^-]$ of around 0.15 mol dm^{-3} indicating the predominance of one species, presumably $OsO_5(OH)^{3-}$. Because of this reason and the fact that the initial rate is a function of $[OH^-]$ with fractional order in $[OH^-]$, the main oxidant species is likely to be $OsO_5(OH)^{3-}$ and its formation in the equilibrium (2) is of importance in the reaction. As for the reductant, Cr(III), the forms $CrOH^{2+}$, $Cr(OH)_2^+$, $Cr(OH)_3$ and $Cr(OH)_4^-$ besides polymeric species are known in basic solutions[1]. In acid medium, $CrOH^{2+}$ and $Cr(OH)_2^+$ exist and, between *p*H 7 and 10, $Cr(OH)_3$ in colloidal form is known. The amphoterism of Cr(III) is due to formation of $Cr(OH)_4^-$ and this is the form in which almost the entire dissolved Cr(III) exists[1] above *p*H 12 under the conditions employed in this reaction. The absorption spectra of Cr(III) in the aqueous medium in the visible region in the presence and absence of OH^- were all similar except that some hyperchromicity is found in the spectrum in the presence of alkali. A mechanism in terms of $OsO_5(OH)^{3-}$ and $Cr(OH)_4^-$ can account for the experimental results as in Scheme 1 where Os(VIII) species, formed in a preequilibrium step (i), interacts with the Cr(III) species in a slow step (ii) (see Scheme 1). Scheme 1 leads to rate law (3) where K_2 and k represent the formation constant of $OsO_5(OH)^{3-}$ (step i) and the rate constant of

$$OsO_4(OH)_2^{2-} + OH^- \overset{K_2}{\rightleftharpoons} OsO_5(OH)^{3-} + H_2O \quad ... (i)$$

$$OsO_5(OH)^{3-} + Cr(OH)_4^- \xrightarrow{k} OsO_5(OH)^{4-} + Cr(OH)_4$$

$$(\text{or } Os(VII) + Cr(IV)) \quad ...(ii)$$

$$Os(VIII) + Cr(IV) \xrightarrow{\text{fast}} Os(VII) + Cr(V) \quad ... (iii)$$

$$Os(VIII) + Cr(V) \xrightarrow{\text{fast}} Os(VII) + Cr(VI) \quad ... (iv)$$

$$Os(VII) + Cr(OH)_4^- \xrightarrow{\text{fast}} Os(VI) + Cr(IV)\ \text{etc} \quad ... (v)$$

Scheme 1

the slow step (ii). In Eq. (3), the denominator must also contain the factor $(1 + K_2\ [Os(VIII)]_T]$ which is left out since

$$\frac{-d[Os(VIII)]_T}{dt} = \frac{kK_2[Os(VIII)]_T[Cr(III)]_T[OH^-]_T}{(1 + K_2[OH^-]_T)} \quad ... (3)$$

it approximates to unity. It may be noted that Os(VIII) oxidation of Cr(III) (Scheme 1) takes place in single equivalent steps giving rise to species such as Os(VII) and Cr(IV). The one equivalent steps written in Scheme 1 are in agreement with the fact that single electron transfer steps are more probable than others. Intervention of oxidation states of Os lower than Os(VI) in the mechanism is unlikely in view of the reasonable stability of the Os(VI) species in an alkaline medium.

Intervention by the free radicals in the reaction is expected, if Scheme 1 is found valid but radical scavenging tests using the monomers acrylamide and acrylonitrile failed as Os(VIII) was found to oxidise the monomers themselves. The mechanism shown in Scheme 1 and rate law (3) may be verified by a plot of $[Os(VIII)]_T[Cr(III)]_T$/rate versus $1/[OH^-]_T$ which should be linear (from Eq. 3) and the slope and intercept should lead to the values of K_2 and k.

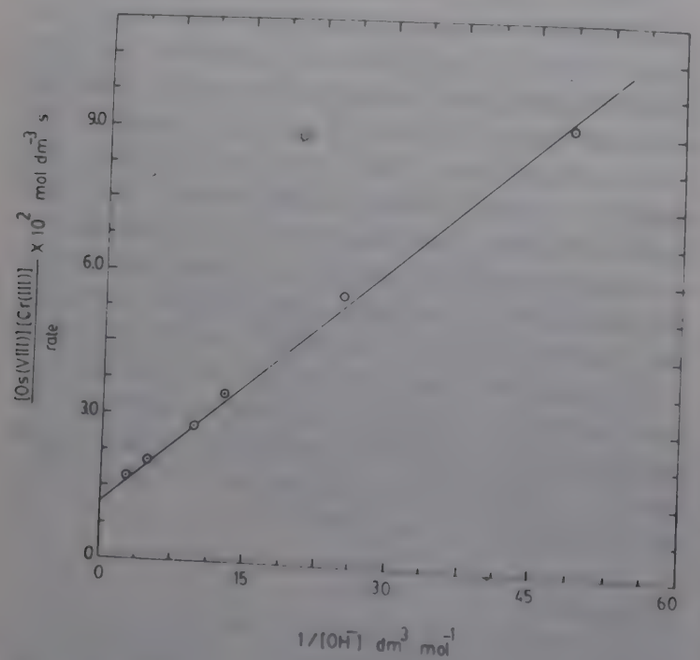

Fig. 1—Verification of rate law (3) ($[Cr(III)] = 1.50 \times 10^{-4}$, $[Os(VIII)] = 2.25 \times 10^{-4}$, $I = 0.30$ (mol dm^{-3}), temp. 24°C)

Such a plot is shown in Fig. 1 with $K_2 = 7.5 \pm 0.4$ $dm^3\ mol^{-1}$ ($K_2 = 6.8\ dm^3\ mol^{-1}$ at 50°C from earlier work[4]) and $k = 83.3 \pm 2.0\ dm^3\ mol^{-1}\ s^{-1}$. The values of K_2 and k were further used to calculate rates for several experimental situations. Rates calculated in this way have been found to be comparable with the experimentally measured rates. The marginal increase in rate with increase in ionic strength is as expected qualitatively from the mechanism of Scheme 1 where ions of like charge interact in the rate-determining steps.

It was also found that added ions like Li^+ and Cl^- had practically no effect on the reaction. These results and the fact that the species of Os(VIII) and Cr(III) in alkaline medium are $HOOsO_5^-$ and $Cr(OH)_4^-$ (coupled with the high value of k) indicate that the oxidation presumably occurs by an inner sphere mechanism. This conclusion is supported by the results of earlier work[5,6].

References

1 Dhanpat Rai, Saas B M & Moore D A, *Inorg Chem*, 26 (1987) 345.

2 Tuwar S M, Nandibewoor S T & Raju J R, *Trans met Chem*, 1990 (In press).

3 Vogel A I, *Textbook of quantitative inorganic analysis* (ELBS, Longman, New York) (1978) p. 763.

4 Bhatt L, Sharma P D & Gupta Y K, *Indian J Chem*, 23A (1984) 560.

5 Swinehart J H, *J inorg nucl Chem*, 27 (1967) 2313.

6 Lancaster J M & Murray R S, *J chem Soc* (*A*) (1971) 2755.

Indian Journal of Chemistry
Vol. 30A, February 1991, pp 162-165

Cationic diamine complexes of cyclopentadienylruthenium(II)

Rajendra Prasad, Lallan Mishra† & U C Agarwala*
Department of Chemistry, Indian Institute of Technology, Kanpur 208 016

Received 21 May 1990; accepted 22 August 1990

Purely σ donor bidentate chelate diamine complexes of the type $(RuCp(EPh_3)(N-N)]Y$ and $[RuCp(EPh_3)_2(N-N)]Y$, where $Cp = (\eta^5\text{-}C_5H_5^-)$; E = P, As, Sb; N – N = ethylenediamine, 1,2-diaminopropane, 1,3-diaminopropane, 1,6-diaminohexane, 1,2-phenylenediamine, and dimethylglyoxime; Y = BF_4^-, PF_6^-, BPh_4^- have been synthesised. These complexes have been characterised, using microanalytical data, conductance measurements and spectral (IR, NMR, and UV-Visible) methods.

The half sandwich complexes of the type $[RuCp(EPh_3)_2Cl]$ (where $Cp = (\eta^5 - C_5H_5^-)$, and E = P, As, Sb) are common precursors to synthesise their various substituted products[1]. Thus these complexes undergo a variety of interesting reactions, but most of the previous work includes the stabilization of the low oxidation state of ruthenium(II) by strong π-acid ligands[2-11].

The published literature lacks substitution reactions using bidentate chelating strong σ donor ligands having no π-acid capabilities. This observation has led us to probe into the substitution reactions of these complexes using α,ω-diamines as substituents. As a follow up of our previous work, We report herein the reactions of $[RuCp(EPh_3)_2Cl]$ with ethylenediamine (en), 1,2-diaminopropane(1,2-dap), 1,3-diaminopropane (1,3-dap), 1,6-diaminohexane(1,6-dah), *ortho*-phenylenediamine (1,2 dab) and dimethylglyoxime (dmg H_2).

Materials and Methods

Literature methods[10-12] were used to synthesize the complexes of the type $[RuCp(EPh_3)_2Cl]$. Liquid diamines were distilled before use. 1,6-Diaminohexane, 1,2-phenylenediamine and dimethylglyoxime were chemically pure. Various solvents were of AR grade and used as received.

The physicochemical measurements on the complexes (melting points, IR, electronic and PMR spectra were carried out as described elsewhere[13].

The typical procedures to isolate the complexes are as follows:

(A) *Preparation of chloride salts of* $[RuCp(EPh_3)(diamine)]^+$ *cation*

Diamine (0.4 to 0.8 mmole) was refluxed with a suspension of $[RuCp(EPh_3)_2Cl]$ (0.2 mmole) in methanol (25 ml) for one and a half hr. A yellow solution resulted which was concentrated to 2-3 ml under reduced pressure, filtered through neutral alumina (deactivated by methanol) column (1 cm in length)†. The eluate was collected, which was subsequently used to isolate the complexes (vide supra).

(B) *Preparation of chloride salts of* $[RuCp(EPh_3)_2(diamine)]^+$ *cations*

Diamine (0.4-0.8 mmole) was stirred with $[RuCp(EPh_3)_2Cl]$ (0.2 mmole) in methanol (25 ml) for 6-8 hr. Solvent was removed under suction from the reaction mixture and the reduced volume was filtered through neutral alumina (deactivated by methanol) column (1 cm in length). The salts of the complex were obtained from the filtrate.

The tetraphenylborate salts of the complexes were obtained by adding concentrated methanolic solution of $NaBPh_4$ to the concentrated solution of chloride complexes obtained from procedures A and B. Yellow precipitate was formed immediately which was separated by filtration, washed with methanol followed by ether and dried under reduced pressure over $CaCl_2$. It was recrystallized from CH_2Cl_2/petroleum ether.

PF_6^- and BF_4^- salts do not separate out easily. They were obtained by adding a few drops of methanolic solutions of their sodium salts to the solutions of cationic complexes and removing the solvent under reduced pressure to obtain dry residue. It was extracted with dichloromethane and recrystallized by adding excess of petroleum ether. Precipitate was filtered and dried *in vacuo* over $CaCl_2$.

†Present address: Department of Chemistry, Banaras Hindu University, Varanasi

†Filtration through methanol deactivated neutral almina was necessary to remove certain suspended white particles from the complex solution.

(C) *Preparation of* $[RuCp(EPh_3)(dmgH)$ *complexes*

$[RuCp(Eph_3)_2Cl]$ (0.1 mmole) and dimethylglyoxime (0.02 g; 0.2 mmole) in methanol (25 ml) was refluxed in the presence of sodium acetate (0.2 g). The reaction mixture was concentrated, cooled, the yellow solid filtered off, washed with methanol, followed by ether and dried *in vacuo* over $CaCl_2$.

Results and Discussion

Treatment of chlorocomplexes $[RuCp(EPh_3)_2Cl]$ with a very large excess of diamines in methanol, both at room temperature and under refluxing conditions resulted in the formation of yellow diamine cationic complexes by rapid displacement of one of the bulky EPh_3 groups and the chloride ion in more than 50% yield. Their microanalytical data, melting points and the empirical formulae are listed in Table 1. All the complexes are stable in air at room temperature in solid state and are highly soluble in organic polar solvents like, CH_2Cl_2, $CHCl_3$, acetone, DMF, etc. However, the tetraphenyl borate salts are only sparingly soluble in methanol and ethanol.

The molar conductivities (ΔM) of their hexafluorophosphate salts (1×10^{-4} molar solutions) were found to be in the range of $145 \pm 5\ \Omega^{-1}cm^2mol^{-1}$. This is well within the range for 1:1 electrolytes[14]. The complexes 55-57 shown in Table 1 have molar conductances of around $6\Omega^{-1}cm^2mol^{-1}$ under identical conditions, indicating their nonelectrolytic nature.

The reaction of ethylenediamine, 1,2-diaminopropane and 1,2-phenylenediamine were smooth. These behaved as bidentate chelating ligands replacing Cl and one EPh_3 from $[RuCp(EPh_3)_2Cl]$ in methanol by both the methods (A) and (B). 1,3-Diaminopropane behaved as a bidentate ligand under method (A) but under method (B) it gave a mixture of mono- and bidentate products. With the increase in stirring period, the monodentate products got gradually converted into bidentate ones. Thus their monodentate cations have not been isolated.

The products of the reactions of 1,6-diaminohexane under refluxing condition (method A) yielded a mixture of monodentate and bidentate diamine complexes. But seemingly the amino groups and the six-carbon alkyl chain underwent some sort of rearrangement under the reaction conditions (method A), because no proper PMR signals for $-NH_2$ and $-CH_2-$ protons were observed in the PMR spectra of the products (vide supra). Variation in the reaction period has no effect on the nature of the mixture-product. In case only one molar excess of 1,6-diaminohexane was stirred with $[RuCp(EPh_3)_2Cl]$ in methanol, the cation complex $[RuCp(EPh_3)_2(1,6\text{-}dah)]^+$ was formed as a result of the facile ionization of chloride ion with subsequent attachment of diamine molecule. 1,6-Diaminohexane did not serve as a bidentate ligand in its reactions with $[RuCp(EPh_3)_2Cl]$ even after stirring upto 16 hr (method B).

Formation of hydrido derivative, $[RuCp(EPh_3)_2H]$* has been frequently encountered as a parallel side reaction when the diamines and precursor complex are taken in 1:1 molar ratio. It is well documented[15] that when alcohols which contain α-hydrogen are used as reaction medium for $(RuCp(EPh_3)_2Cl)$, bases catalyse formation of hydride complexes. However, this side reaction is completely suppressed when the diamine is taken in excess amount, yielding exclusively diamine substitution products. Under these conditions amines directly displaces solvent (alcohol) molecule from the solvated cation of the precursor complex rather than abstracting proton and facilitating-hydrogen migration to give hydrides. Since the corresponding hydride complexes do not undergo substitution reaction by diamine, under similar conditions the possibility of the derivative as the intermediate is ruled out.

IR spectra

The IR and the PMR spectral data of the representative complexes are listed in Table 2. In their IR spectra all the complexes exhibited two absorption bands in the $\nu N-H$, viz $\nu_s(NH)$ and $\nu_{as}(NH)$ in the region of 3250-3350 cm^{-1}. The absorption bands characteristic of cyclopentadienyl, EPh_3 and counter anions dominate the rest of the IR spectrum.

^1H NMR spectra

As expected, all complexes contained only one signal corresponding to cyclopentadienyl protons. Coordinated NH_2 protons appeared deshielded[16] by nearly 1 ppm. The cyclopentadienyl proton signals in bidentate chelate complexes is invariably shifted low field than that in the corresponding monodentate cations (complexes 28-36). This downfield shift could tentatively be assigned to increased electron density on Ru atom[17].

Visible spectra

The lowest energy band in the diamine complexes assigned to Ru → Cp charge transfer (MLCT) appeared at 355-360 nm which is only little blue shifted compared to that in $[RuCp(PPh_3)_2Cl]$ (365 nm).

Complexes $[RuCp(EPh_3)_2L]^+$ where L is a non π-bonding ligand are well known to undergo solvo-

* The hydrides thus obtained have been characterised by comparing the reaction products with the authentic samples[15].

Table 1—Microanalytical data

Complex	m.p. °C	Found (calc), % C	H	N
1. $[RuCp(PPh_3)(en)](PF_6)$	160	52.41(52.17)	5.01(4.87)	5.10(4.87)
2. $[RuCp(PPh_3)(en)](PF_6)$	165	47.70(47.39)	4.66(4.42)	4.72(4.42)
3. $[RuCp(PPh_3)(en)](BPh_4)$	188	72.69(72.86)	5.87(5.95)	3.59(3.47)
4. $[RuCp(AsPh_3)(en)](BF_4)$	160	48.73(48.47)	4.71(4.52)	4.43(4.52)
5. $[RuCp(AsPh_3)(en)](PF_6)$	165	46.60(46.31)	4.08(4.14)	4.08(4.14)
6. $[RuCp(AsPh_3)(en)](BPh_4)$	187	69.31(69.10)	5.69(5.64)	3.22(3.29)
7. $[RuCp(SbPh_3)(en)](BF_4)$	162	44.87(45.05)	4.41(4.20)	4.32(4.20)
8. $[RuCp(SbPh_3)(en)](PF_6)$	166	41.71(41.44)	3.67(3.87)	3.84(3.87)
9. $[RuCp(SbPh_3)(en)](BPh_4)$	188	65.65(65.48)	5.44(5.35)	3.23(3.12)
10. $[RuCp(PPh_3)(1,2\text{-dap})](BF_4)$	161	53.23(52.97)	5.20(5.09)	4.64(4.75)
11. $[RuCp(PPh_3)(1,2\text{-dap})](PF_6)$	169	48.50(48.22)	4.47(4.64)	4.42(4.33)
12. $[RuCp(PPh_3)(1,2\text{-dap})](BPh_4)$	187	73.33(73.08)	6.23(6.09)	3.50(3.41)
13. $[RuCp(AsPh_3)(1,2\text{-dap})](BF_4)$	161	49.11(49.29)	4.87(4.74)	4.56(4.42)
14. $[RuCp(AsPh_3)(1,2\text{-dap})](PF_6)$	167	45.33(45.15)	4.47(4.34)	4.20(4.05)
15. $[RuCp(AsPh_3)(1,2\text{-dap})](BPh_4)$	187	69.21(69.36)	5.83(5.78)	3.29(3.24)
16. $[RuCp(SbPh_3)(1,2\text{-dap})](BF_4)$	160	45.97(45.88)	4.55(4.41)	4.19(4.12)
17. $[RuCp(SbPh_3)(1,2\text{-dap})](PF_6)$	168	42.43(42.28)	3.98(4.07)	3.82(3.79)
18. $[RuCp(SbPh_3)(1,2\text{-dap})](BPh_4)$	190	65.62(65.79)	5.62(5.48)	3.18(3.07)
19. $[RuCp(PPh_3)(1,3\text{-dap})](BF_4)$	162	53.16(52.97)	5.21(5.09)	4.61(4.75)
20. $[RuCp(PPh_3)(1,3\text{-dap})](PF_6)$	165	48.37(48.22)	4.54(4.64)	4.52(4.33)
21. $[RuCp(PPh_3)(1,3\text{-dap})](BPh_4)$	175	73.22(73.08)	6.00(6.09)	3.39(3.41)
22. $[RuCp(AsPh_3)(1,3\text{-dap})](BF_4)$	160	49.15(49.29)	4.89(4.74)	4.53(4.42)
23. $[RuCp(AsPh_3)(1,3\text{-dap})](PF_6)$	166	45.02(45.15)	4.21(4.34)	4.16(4.05)
24. $[RuCp(AsPh_3)(1,3\text{-dap})](BPh_4)$	186	69.48(69.36)	5.83(5.78)	3.20(3.24)
25. $[RuCp(SbPh_3)(1,3\text{-dap})](BF_4)$	162	45.97(45.88)	4.26(4.41)	4.02(4.12)
26. $[RuCp(SbPh_3)(1,3\text{-dap})](PF_6)$	168	42.41(42.28)	4.25(4.07)	3.92(3.79)
27. $[RuCp(SbPh_3)(1,3\text{-dap})](BPh_4)$	188	65.87(65.79)	5.59(5.48)	3.17(3.07)
28. $[RuCp(PPh_3)_2(1,6\text{-dah})](BF_4)$	120	63.29(63.16)	5.64(5.71)	3.09(3.14)
29. $[RuCp(PPh_3)_2(1,6\text{-dah})](PF_6)$	110	59.52(59.31)	5.42(5.36)	2.87(2.94)
30. $[RuCp(PPh_3)_2(1,6\text{-dah})](BPh_4)$	115	75.81(75.73)	6.41(6.31)	2.43(2.49)
31. $[RuCp(AsPh_3)_2(1,6\text{-dah})](BF_4)$	121	57.64(57.49)	5.33(5.20)	2.96(2.85)
32. $[RuCp(AsPh_3)_2(1,6\text{-dah})](PF_6)$	111	54.13(54.28)	4.87(4.91)	2.76(2.69)
33. $[RuCp(AsPh_3)_2(1,6\text{-dah})](BPh_4)$	117	70.30(70.24)	5.69(5.85)	2.25(2.31)
34. $[RuCp(SbPh_3)_2(1,6\text{-dah})](BF_4)$	122	52.37(52.49)	6.77(6.61)	2.69(2.61)
35. $[RuCp(SbPh_3)_2(1,6\text{-dah})](PF_6)$	111	49.89(49.80)	4.43(4.50)	2.43(2.47)
36. $[RuCp(SbPh_3)_2(1,6\text{-dah})](BPh_4)$	117	65.16(65.21)	5.64(5.43)	2.10(2.14)
37. $[RuCp(PPh_3)(1,2\text{-dab})](BF_4)$	125	55.80(55.86)	4.59(4.49)	4.37(4.49)
38. $[RuCp(PPh_3)(1,2\text{-dab})](PF_6)$	118	51.24(51.10)	4.04(4.11)	4.23(4.11)
39. $[RuCp(PPh_3)(1,2\text{-dab})](BPh_4)$	110	74.45(74.39)	5.56(5.61)	3.23(3.27)
40. $[RuCp(AsPh_3)(1,2\text{-dab})](BF_4)$	128	52.37(52.17)	4.14(4.20)	4.29(4.20)
41. $[RuCp(AsPh_3)(1,2\text{-dab})](PF_6)$	118	48.11(48.00)	3.77(3.86)	3.81(3.86)
42. $[RuCp(AsPh_3)(1,2\text{-dab})](BPh_4)$	112	70.83(70.75)	5.42(5.34)	3.10(3.11)
43. $[RuCp(SbPh_3)(1,2\text{-dab})](BF_4)$	128	48.59(48.76)	3.85(3.92)	3.97(3.92)
44. $[RuCp(SbPh_3)(1,2\text{-dab})](PF_6)$	118	45.26(45.09)	3.52(3.63)	3.68(3.63)
45. $[RuCp(SbPh_3)(1,2\text{-dab})](BPh_4)$	112	67.30(67.25)	5.15(5.08)	2.92(2.96)
46. $[RuCp(PPh_3)(dmgH_2)](BF_4)$	142	51.44(51.35)	4.60(4.44)	4.37(4.44)
47. $[RuCp(PPh_3)(dmgH_2)](PF_6)$	186	47.19(47.02)	4.01(4.06)	4.15(4.06)
48. $[RuCp(PPh_3)(dmgH_2)](BPh_4)$	180	70.83(70.92)	5.67(5.56)	3.20(3.24)
49. $[RuCp(AsPh_3)(dmgH_2)](BF_4)$	140	48.09(48.00)	4.26(4.15)	4.08(4.15)
50. $[RuCp(AsPh_3)(dmgH_2)](PF_6)$	185	44.33(44.20)	3.74(3.82)	3.90(3.82)

Contd

Table 1—Microanalytical data—*Contd.*

Complex	m.p. °C	Found (calc.), % C	H	N
51. $[RuCp(AsPh_3)(dmgH_2)](BPh_4)$	180	67.41(67.48)	5.23(5.29)	3.05(3.09)
52. $[RuCp(SbPh_3)(dmgH_2)](BF_4)$	143	44.75(44.89)	3.79(3.88)	3.81(3.88)
53. $[RuCp(SbPh_3)(dmgH_2)](PF_6)$	185	41.67(41.55)	3.63(3.59)	3.63(3.59)
54. $[RuCp(SbPh_3)(dmgH_2)](BPh_4)$	178	64.03(64.17)	5.11(5.03)	2.87(2.94)
55. $[RuCp(PPh_3)(dmgH)]$	210	59.83(59.67)	4.92(4.97)	5.20(5.16)
56. $[RuCp(AsPh_3)(dmgH)]$	211	55.12(55.20)	4.55(4.60)	4.76(4.77)
57. $[RbCp(SbPh_3)(dmgH)]$	213	51.08(51.12)	4.34(4.26)	4.57(4.42)

Colour of the compound No., 37-45 yellowish green, the rest, bright yellow

Table 2—IR and ^1H NMR spectral assignments of some selected complexes

Complex	IR ν_{N-H} cm^{-1}		^1H NMR (δ/PPM)		
	ν_{as}	ν_s	Hcp	H($-NH_2$)	H(diamine skelton)
$[RuCp(PPh_3)(en)](PF_6)$	3330	3280	4.35	2.1	2.8
$[RuCp(PPh_3)(1.2\ dap)](PF_6)$	3340	3285	4.35	2.1	1.1(CH_3) 2.4-2.8
$[RuCp(PPh_3)(1.3\ dap)](PF_6)$	3340	3290	4.4	2.1(8H, NH_2 and terminal CH_2)	2.8(2H, Middle-CH_2-)
$[RuCp(PPh_3)(1.6\ dah)](PF_6)$	3380, 3395	3320,3340,	4.2	1.9(2H)	1.4,1.55(8H) 2.5(4H-terminal CH_2)
$[RuCp(PPh_3)(O\text{-}Phda)](PF_6)$	3340	3280	4.4	3.9	
$[RuCp(PPh_3)(dmgH_2)](PF_6)$	OH	3450	5.0	—	2.1(CH_3)
$[RuCp(PPh_3)(dmgH)]$	OH	3400(broad)	4.70	—	2.1(CH_3)

lysis[18], hence the corresponding aliphatic diamine complexes especially bidentate chelate ones are expected to give solvated cations of the type

$$[Cp(EPh_3)Ru(N-N)]^+ \xrightarrow{Solvent} [Cp(EPh_3)(Sol)Ru^+-N-N]$$

These cations could lead to many interesting reactions which is our current interest of investigation.

Acknowledgement

We thank RSIC(CDRI), Lucknow for providing certain microanalytical data. One of the authors (RP) also thanks CSIR, New Delhi, for providing financial assistance during the period of this work.

References

1 a) Albers M O, Robinson D J & Singleton E, *Coord chem Rev*, 79 (1987) 1.
b) Bennet M A, Bruce M I & Matheson T W, *Comprehensive organometallic chemistry*, Vol 4 edited by G Wilkinson Pergamon, Oxford,. 783-793.
2 Gilbert J D & Wilkinson G, *J chem Soc (A)*, (1969) 1749.
3 Hains R J & Du-Preez A L, *J organometal Chem*, 84 (1975) 357.
4 a) Blackmore T, Bruce M I & Stone F G A, *J chem Soc Dalton Trans*, (1974) 106.
b) Ashby G S, Bruce M I, Tomkins I B & Wallis R, *Aust J Chem*, 32 (1979) 1003.
c) Wilczewski T, Bochenska M & Biernat J F, *J organometal Chem*, 215 (1981) 87.
5 (a) Bruce M I & Swincer A G, *Aust J Chem*, 33 (1980) 1471.
(b) Treichel P M, Komar D A & Vincenti P J, *Synth React Inorg Met Org Chem*, 14 (1984) 383.
(c) Wilczewski T & Dauter Z, *J organometal Chem*, 312 (1986) 349.
6 (a) Wilczewski T, *J organometal Chem*, 224 (1982) C-1.
(b) Uson R, Oro L A, Ciriano M A, Naval M M, Apreda M C, Foces-Foces C, Cano F H & Garcia-Blanco S, *J organometal Chem*, 256 (1983) 331.
(c) Rventos L B & Alonso A G, *J organometal Chem*, 309 (1986) 179.
7 Asok R F N, Gupta M, Arulsamy K S, Agarwala U C, *Inorg chim Acta*, 98 (1985) 161.
8 Rao K M, Mishra L & Agarwala U C, *Polyhedron*, 6 (1987) 1383.
9 Mishra A & Agarwala U C, *J chem Soc Dalton Trans*, (1988) 2897.
10 Rao K M, Mishra L & Agarwala U C, *Polyhedron*, 5 (1986) 1491.
11 Rao K M, Mishra L & Agarwala U C, *Indian J Chem*, 26A (1987) 755.
12 Bruce M I, Windsor N J, *Aust J Chem*, 30 (1977) 1601.
13 Prasad R, Mishra L, Agarwala U C, *Indian J Chem*, (communicated April 1990) (IC 6465).
14 Geary W J, *Coord chem Rev*, 7 (1971) 81.
15 Bruce M I, Hundsrey M G, Swincer A G, Wallis R C, *Aust J Chem*, 37 (1984) 1747 and reference therein
16 Ashahi Research Center, *Handbook of proton NMR spectra and data*, Vols 1 and 2 (Academic Press, NY), 1985, spectrum numbers 89, 227, 228, 356, 917, 1160
17 Bruce M I, Wong F S, Skelton B W & White A H, *J chem Soc Dalton Trans*, (1981) 1398.

Indian Journal of Chemistry
Vol. 30A, February 1991, pp 166-171

Mössbauer, infrared and thermal decomposition studies of Iron(III) complexes with substituted malonic acids

R B Lanjewar & A N Garg*

Department of Chemistry, Nagpur University, Nagpur 440 010

Received 20 March 1990; revised 19 June 1990; accepted 13 August 1990

Iron(III) complexes with alkyl (methyl, ethyl and dimethyl) and phenyl substituted malonic acids have been synthesized, Mössbauer spectra of all the complexes exhibit small quadrupole doublet with $\Delta E_Q = 0.43\text{-}0.84$ mm s^{-1}. Isomer shift (δ) values are in the range 0.62-0.76 mm s^{-1} (w.r. to SNP) indicating iron(III) to be in high spin state. This assertion is further supported by magnetic moment data. Nature of alkyl group does seem to affect the electron density at the iron nucleus. Infrared spectral studies indicate monodentate nature of the carboxylate group which leads to tris type chelate complexes in all cases except in the case of malonic acid where diaquobis (malonato)ferrate(III) is formed. Thermogravimetric (TGA) data show two-stage decomposition; first two ligand molecules are lost at 120°C and finally Fe_2O_3 is formed at 230°C. This is supported by Mössbauer spectral evidence.

Unique bonding characteristics of carboxylate ion

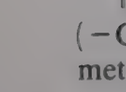

(−C−O)-depend primarily on the nature of the metal ion, alkyl group attached to the carboxylate ion and the reaction conditions[1-3]. Recent studies have indicated the formation of hexa-, tris- and bis-type of carboxylate complexes by mono-, di- and tricarboxylic acids respectively. Extensive Mössbauer and infrared spectroscopic studies and thermal decomposition behaviour of these complexes have been reported in the literature[4-10]. In a recent study Randhawa *et al.*[4] have studied thermal decomposition of magnesium tris(malonato)ferrate(III) decahydrate and identified $MgFe_2O_4$ as a product.

Amongst various carboxylate ligands, malonate seems to behave in a peculiar manner as it can form either a simple salt[7] or tris type of complexes[9] depending on whether iron powder or ferric nitrate is treated with the aqueous solution of the acid and its sodium salt respectively. In this paper we report synthesis of iron(III) complexes with alkyl (methyl, dimethyl and ethyl) and phenyl substituted malonic acids and their Mössbauer and infrared spectroscopic studies. We have also studied the thermal decomposition behaviour of the complexes.

Materials and Methods

All the chemicals used were of AR or GR grade (Aldrich USA or Fluka, Switzerland). The complexes were prepared by mixing 0.56 g of iron powder (electrolytic grade; S. Merck) in a warm aqueous solution of the carboxylic acid (0.03 *M*). Evolution of gas started which ceased at the end of the reaction. Later, the solution was digested on a water bath for about 2 hr so as to complete the reaction. After digestion, the solution was filtered and kept overnight when coloured crystals of the complexes were obtained. These were separated from the mother liquor and dried *in vacuo* over fused $CaCl_2$. Compositions of the complexes were determined from C, H and Fe analyses (Table 1). Fe was determined spectrophotometrically using 1,10-phenanthroline.

Mössbauer spectra were recorded using a constant acceleration transducer driven Mössbauer spectrometer in conjunction with a PC based 1K Multichannel Analyzer (Nucleonix, Hyderabad). A 5 mCi ^{57}Co(Rh) source (obtained from BARC, Bombay) was used. All the spectra were recorded at room temperature and were visually fitted with Lorentzian line shape. The spectrometer was calibrated using natural iron foil and recrystallised sodium pentacyanonitrosylferrate(II) dihydrate (SNP) as the standard. For recording Mössbauer spectra of thermal decomposition products, the compounds were heated at 150, 200 and 400°C for 4 hr in a muffle furnace and cooled at room temperature.

Reflectance spectra were recorded using a Shimadzu model UV-240 spectrophotometer employing MgO as the reference. Infrared spectra (4000-200 cm^{-1}) in KBr medium were recorded on a Pye-Unicam IR spectrophotometer. Differential thermal analysis (DTA) and thermogravimetric analysis (TGA) were carried out at heating rates of 20° and 10°C per min respectively employing a Perkin-Elmer Ther-

Table 1—Analytical data of the complexes of various substituted malonic acids

Complex	Colour	Found (calc.), %		
		Fe	C	H
1 $H\left[Fe(III)\left\{CH_2\begin{matrix}COO\\COO\end{matrix}\right\}_2\cdot 2H_2O\right]H_2O$	Light green	17.02 (17.78)	22.35 (22.85)	3.25 (3.17)
$H_2\left[Fe(II)\left\{CH_2\begin{matrix}COO\\COO\end{matrix}\right\}_2\cdot 2H_2O\right]\cdot H_2O$		(17.72)	(22.78)	(3.81)
2 $Na_3\left[Fe\left(CH_2\begin{matrix}COO\\COO\end{matrix}\right)_3\right]\cdot 3H_2O$	Light green	11.68 (11.54)	22.45 (22.27)	2.59 (2.47)
3 $H_3\left[Fe\left(CH_3CH\begin{matrix}COO\\COO\end{matrix}\right)_3\right]$	Grey	13.69 (13.75)	35.50 (35.38)	4.02 (3.68)
4 $H_3\left[Fe\left\{(CH_3)_2C\begin{matrix}COO\\COO\end{matrix}\right\}_3\right]$	Middle buff	12.47 (12.47)	40.43 (40.08)	5.01 (4.67)
5 $H_3\left[Fe\left(C_2H_5CH\begin{matrix}COO\\COO\end{matrix}\right)_3\right]$	Grey	12.85 (12.47)	40.65 (40.08)	4.95 (4.67)
6 $H_3\left[Fe\left(C_6H_5CH\begin{matrix}COO\\COO\end{matrix}\right)_3\right]\cdot H_2O$	Brown	9.29 (9.16)	53.35 (53.02)	4.13 (3.76)

mogravimetric Analyzer System Model TGS-2, Thermal Analysis Data Station TADS 3600 and Derivative Thermal Analysis System DTA-1700 through the courtesy of RSIC, Nagpur. Magnetic moments were determined from magnetic susceptibilities measured using Gouy's balance and $Hg[Co(SCN)_4]$ as the standard.

Results and Discussion

All the complexes were found to be coloured solids and stable under atmospheric conditions. Unlike earlier results from our laboratory on mono- and dicarboxylate complexes[5,9], our attempts to prepare tris type complexes from ferric nitrate and the sodium salt of the corresponding carboxylic acid failed. Jagannathan *et al.*[6,7], have reported the preparation of Fe(II) salts by mixing iron powder with hot aqueous solution of malonic or maleic acids. Therefore, we also attempted to follow this route. But instead of Fe(II) salts we got Fe(III) complexes in which three carboxylate ligands are bonded to form an octahedron except in the case of malonic acid where two distinct complexes $H_2[Fe(II)\{CH_2(COO)_2\}\cdot 2H_2O]\cdot H_2O$ and $H[Fe(III)\{CH_2(COO)_2\}_2.2H_2O]\cdot H_2O$ are formed. It seems that with alkyl substituted malonic acids, iron first gets oxidized to Fe(III) and then tris type complexes of general formula $H_3[Fe\{RCH(COO)_2\}_3]$ are formed.[8] However, in the case of malonic acid, a mixture of hydrogen diaquobis(malonato)ferrate(III) monohydrate, $H[Fe(III)\{CH_2(COO)_2\}_2.2H_2O].H_2O$ and hydrogen diaquobis(malonato) ferrate(II) monohydrate, $H_2[Fe(II)\{CH_2(COO)_2\}_2.2H_2O].H_2O$ are formed where unlike other cases, only two malonate ligands are coordinated and the other two positions, possibly trans, are occupied by two water molecules. This is evident from the complex nature of Mössbauer spectra.

In all cases, iron is surrounded by three alkyl substituted malonate ligands to form an octahedral complex. Obviously, it is likely to form a six-membered stable ring with the central iron atom acquiring the configuration $t_{2g}^3 e_g^2$. Reflectance spectra of all the complexes except complex 1 (see Table 1) exhibited two bands of low intensity at 18000 and 25000 cm^{-1} corresponding to $^6A_{1g} \rightarrow {}^4T_{1g}$ and $^6A_{1g} \rightarrow {}^4T_{2g}$ spin forbidden transitions[11] respectively. In the case of alkyl substituted malonic acids a further distortion in geometry is expected.

Typical Mössbauer spectra of malonato and substituted malonato complexes are shown in Fig. 1. All the complexes exhibited a well resolved quadrupole

Table 2—Mössbauer spectral and magnetic data for various carboxylato ferrate(III) complexes

Complex	Mössbauer parameters		μ_{eff} (B.M.)
	Isomer shift* (δ), mm s^{-1}	Quadrupole splitting** (ΔE_Q), mm s^{-1}	
1 a Hydrogen diaquobis(malonato) ferrate(III) monohydrate	0.62	0.83	5.40
1 b Hydrogen diaquobis(malonato) ferrate(II) monohydrate	1.58	2.76	
2 Sodium tris(malonato)ferrate(III) trihydrate	0.69	0.58	5.64
3 Hydrogen tris(methylmalonato) ferrate(III)	0.75	0.64	5.44
4 Hydrogen tris(dimethylmalonato) ferrate(III)	0.64	0.43	5.37
5 Hydrogen tris(ethylmalonato) ferrate(III)	0.76	0.62	5.35
6 Hydrogen tris(phenylmalonato) ferrate(III) monohydrate	0.66	0.63	5.65

*Relative to SNP as a standard.
**Error within ± 0.02 mm s^{-1}.

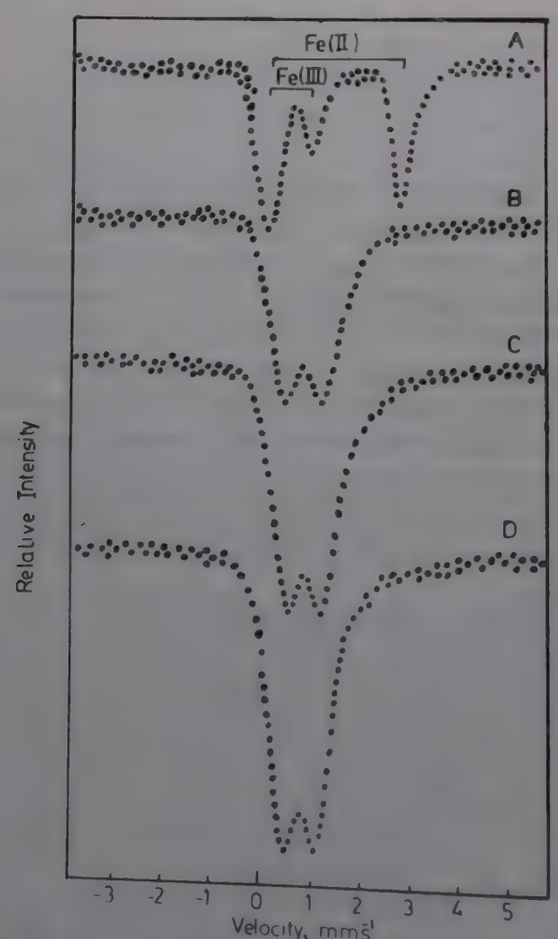

Fig. 1—Mössbauer spectra of (A) hydrogen diaquobis(malonato) ferrate(III) monohydrate, (B) hydrogen tris(methylmalonato)ferrate (III), (C) hydrogen tris(ethylmalonato)ferrate (III) and (D) hydrogen tris(phenylmalonato)ferrate (III) monohydrate at room temperature.

doublet except in the case of malonato complex, where a three line spectrum was observed. Possibly, Mössbauer spectrum of the complex 1 can be resolved into two sets of doublets, one corresponding to Fe(II) complex, $H_2[Fe(II)\{CH_2(COO)_2\}_2 \cdot 2H_2O] \cdot H_2O$ and the other, more intense to Fe(III) complex, $H[Fe(III)\{CH_2(COO)_2\}_2 \cdot 2H_2O] \cdot H_2O$. Mössbauer parameters, δ (w.r. to SNP as a standard) and ΔE_Q alongwith magnetic moment data are given in Table 2.

Magnetic moments

Magnetic moments of all the complexes showed the presence of five unpaired electrons (μ_{eff} = 5.35-5.65 B.M.) indicating high spin state of Fe(III). The μ_{eff} values are slightly lower than expected (5.9 B.M.) which may possibly be due to partial quenching.

Mössbauer parameters

Isomer shift (δ) values for all the complexes are in the range 0.62-0.76 mm s^{-1} indicating Fe(III) to be in high spin state[12]. The minimum value of 0.62 mm s^{-1} is observed for the bis(malonato)ferrate(III) and the maximum value of 0.76 mm s^{-1} is obtained for tris(methyl/ethyl malonato)ferrate(III) complexes. For phenyl substituted malonato complex, however, δ becomes 0.66 mm s^{-1} indicating that electron donor or withdrawal character does affect the *s*-electron density and hence the δ value. Similar type

of behaviour has been observed earlier for monocarboxylatoferrate(III) complexes[5]. Quadrupole splitting also varies in a large range (ΔE_Q = 0.43-0.83 mm s^{-1}) indicating varying distortion depending upon the nature of alkyl group[13]. Surprisingly hydrogen tris(dimethylmalonato)ferrate (III) complex exhibits the minimum ΔE_Q value of 0.43 mm s^{-1}; it also exhibits a lower δ value. ΔE_Q for this complex is lower than even that for sodium tris(malonato)ferrate(III) trihydrate complex. Presumably, in this case two methyl groups do not allow the chelate ring to oscillate like a swing but instead keep it tight enough so as to cause the minimum distortion. In other cases, however, distortion increases becoming maximum for diaquobis(malonato)ferrate(III) complex. For diaquobis(malonato)ferrate(II) complexes, high value of quadrupole splitting, (ΔE_Q = 2.76 mm s^{-1}) is due to high spin state of Fe(II) (electronic configuration, $t_{2g}^4 e_g^2$) which compares well with 2.68 mm s^{-1} observed by Ravi *et al.*[7] Probably malonic acids with more bulky groups as substituents need to be further investigated to understand this aspect.

Earlier we had observed a single broad line spectrum[9], resolved into a doublet, for the sodium tri(malonato)ferrate(III) trihydrate complex, $Na_3[Fe\{CH_2(COO)_2\}_3].3H_2O$ with ΔE_Q = 0.58 mm s^{-1}. Bassi *et al.*[14] had observed a single line spectrum with Γ = 1.08-1.39 mm s^{-1} for alkali metal tris(malonato)ferrate(III) complexes. However, Ravi *et al.*[7] have reported δ = 1.41 mm s^{-1} and ΔE_Q = 2.68 mm s^{-1} for ferrous malonate dihydrate salt, $Fe(CH_2C_2O_4)_4.2H_2O$. Therefore, in the Mössbauer spectrum of hydrogen diaquobis(malonato)ferrate(III) monohydrate complex the parameters, δ = 1.48 mm s^{-1} and ΔE_Q = 2.76 mm s^{-1} compare well with those for the Fe(II) malonate dihydrate. All the other complexes, however, gave well resolved doublet indicating the formation of a single complex.

Infrared spectra

The carboxylate group may act as a unidentate, bidentate or bridged ligand depending on the nature of metal ion and reaction conditions[15,16]. The most prominent vibrational bands affected by coordination are ν_{as}(OCO), ν_s(OCO) and δ(OCO). These intense and well defined bands are observed in the regions 1690-1590, 1430-1400 and 800-710 cm^{-1} respectively. Another important band observed in the region 580-515 cm^{-1} is due to Fe-O stretching vibrations[16]. It has been suggested that the magnitude of separation, $\Delta\nu = [\nu_{as}(OCO) - \nu_s(OCO)]$ should be higher for unidentate carboxylate ligand as compared to that for simple ionic carboxylates[17-20]. In all the dicarboxylate complexes studied here $\Delta\nu$ values (170-230 cm^{-1}) are higher than that for sodium acetate (164 cm^{-1}) which is purely ionic. This indicates unidentate nature of all the substituted malonate ligands.

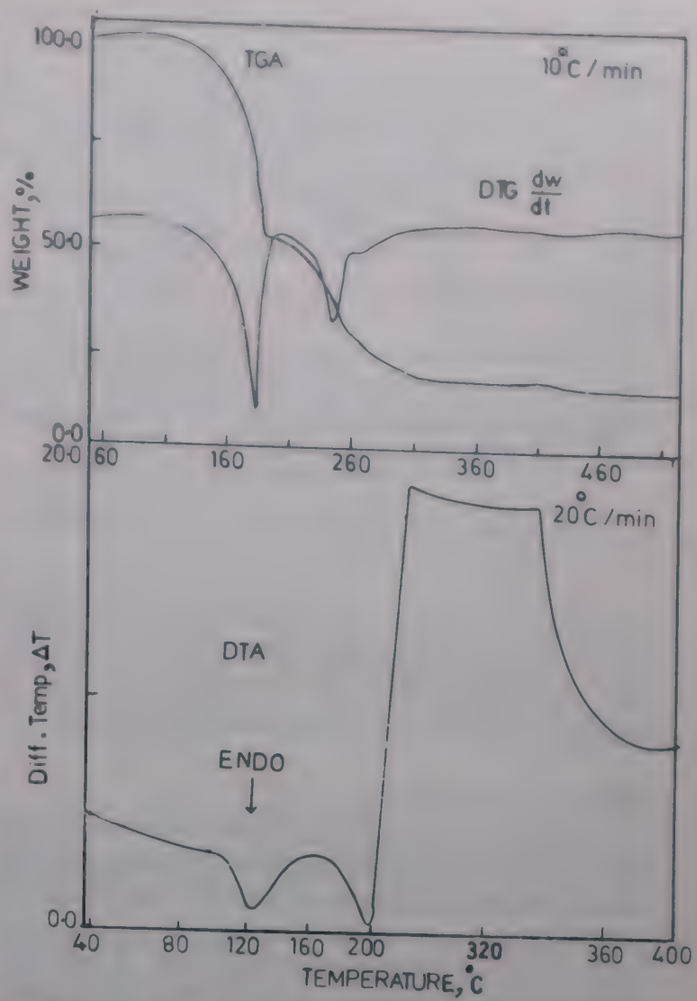

Fig. 2—TGA, DTG, and DTA plots of hydrogen tris(ethylmalonato)ferrate(III) complex.

It has also been suggested that the shift of ν_{as}(OCO) mode of coordinated unidentate carboxylate ligand should be higher as compared to the corresponding mode in simple ionic carboxylate[15,16]. In the present study, it is observed that ν_{as}(OCO) modes appear either at the same or higher wavenumber than in ionic salts. Similarly, ν_s(OCO) mode appears at the lower wavenumber with respect to that for sodium acetate. This further confirms the unidentate nature of the carboxylate ligand[16,20].

The νFe-O mode in the compounds studied here appears in the region 580-515 cm^{-1} in accordance with literature reports[17-20]. There is however, no regularity with respect to size of alkyl group except that νFe-O is lowest for tris(dimethylmalonato)ferrate(III) complex (i.e. 515 cm^{-1}) suggesting a possible change in the polarity of Fe-O bond. The

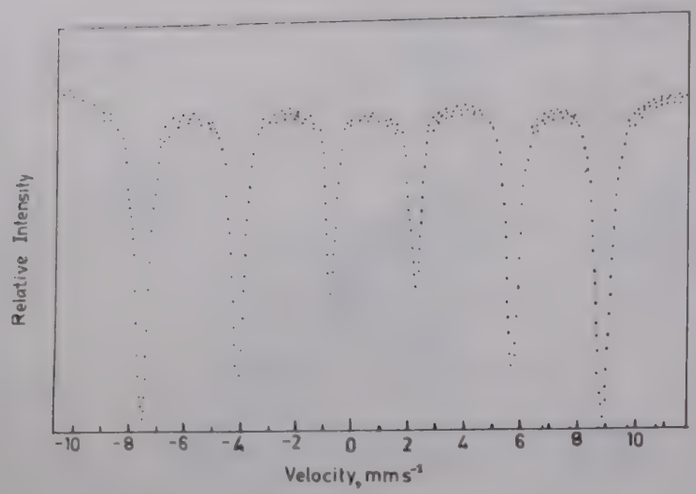

Fig. 3—Mössbauer spectrum of hydrogen tris(dimethylmalonato)ferrate(III) complex heated at 400°C for 4 hr.

νC−O), ν_{as}(C−C), ν_s(C−C) and ν(C−H) modes observed in the range 1090-1040, 1230-1170, 950-880 and 3000-2960 cm^{-1} respectively, are in agreement with those reported in the literature[23,24].

Thermal decomposition

Thermal decomposition of iron carboxylates has been of interest to many workers[25-28] because of the wide applicability of these carboxylates as medicinal agents, catalysts etc. In all the present cases, decomposition behaviour seems to be similar; all the complexes decompose in two stages. The TGA, DTG and DTA curves obtained for hydrogen tris(ethylmalonato)ferrate(III) complex are shown in Fig. 2 as a typical case. There are significant mass losses first at 180°C and then at 230°C. The mass loss at 230°C corresponds to the formation of Fe_2O_3 in all the cases and there is no further mass loss beyond this temperature. In order to confirm the formation of Fe_2O_3, complexes were heated at 400°C for 4 hr and their Mössbauer spectra were recorded. A typical six line spectrum obtained for the end product of hydrogen tris(dimethylmalonato)ferrate(III) is shown in Fig. 3. It gives an isomer shift of 0.67 mm s^{-1} which compares well with 0.63 mm s^{-1} for α-Fe_2O_3. However, first mass loss at 180°C corresponds to the loss of two carboxylate ligands in each case. Vithal and Jagannathan[6] have proposed loss of one ligand molecule in the thermal decomposition of maleato complex. Somewhat similar observation has been reported by Saha and Mitra[29] for several malonato complexes. Therefore, the possible mechanism of decomposition could be represented as follows:

$$H_3[Fe(RCH(COO)_2)_3] \xrightarrow{180°C} [Fe(COO)_2CHR\,OH] + 2RCH(COOH)_2$$

$$2[Fe(COO)_2CHR(OH)] \xrightarrow{230°C} Fe_2O_3 + CO_2 + ..$$

Abras *et al.*[29] have studied the thermal decomposition of potassium tris(malonato)ferrate(III) trihydrate and suggested the formation of α-Fe_2O_3 and K_2CO_3. When the corresponding sodium compound was heated at 200°C for 4 hr it still gave a two line spectrum with $\Delta E_Q = 0.77$ mm s^{-1}. On further heating at 400°C for 4 hr, it exhibited a six line spectrum with $\delta = 0.75$ mm s^{-1}. Thus, the formation of α-Fe_2O_3 in all the cases is confirmed. In the case of DTA, two peaks are observed, one endothermic at 150°C and another flat, broad exothermic peak at 230°C. At 150°C, it may possibly involve melting whence two carboxylate ligands escape and later it undergoes oxidative decomposition. Randhawa *et al.*[4] have also observed endothermic and exothermic peaks for magnesium tris(malonato)ferrate(III) decahydrate. Thus, basically there seems to be a two step decomposition ultimately yielding Fe_2O_3 as the final product.

Acknowledgement

Grateful thanks are due to the CSIR, New Delhi for financial assistance. Thanks are due to Prof S S Parmar, Guru Nanak Dev University, Amritsar for his help in recording IR spectra, and Regional Sophisticated Instrumentation Centres at Lucknow and Nagpur for elemental and thermal analyses respectively. We also thank one of the referees for constructive suggestions.

References

1 Oldham C, *Progress in inorganic chemistry* Vol. 10, edited by F A Cotton (Interscience Publishers, New York) 1968, 223.
2 Mehrotra R C & Bohra R, *Metal carboxylates* (Academic Press, London) 1983, 396.
3 Jorgenson C K, *Inorganic complexes* (Academic Press, London) 1963, 94.
4 Randhawa B S, Kaur S & Bassi P S, *Indian J Chem*, 28A (1989) 463.
5 Garg A N, Parwate D V & Raj D, *Indian J Chem*, 26A (1987) 304.
6 Vithal M & Jagannathan R, *Transit Met Chem*, 9 (1984) 73.
7 Ravi N, Jagannathan R, Rama Rao B & Hussain M R, *Inorg Chem*, 21 (1982) 1019.
8 Dziobkowski C T, Wrobleski J T & Brown D B, *Inorg Chem*, 20 (1981) 671.
9 Lanjewar R B, Waditwar A M & Garg A N, *J Radioanal nucl Chem Art*, 125 (1988) 75.
10 Brar A S & Randhawa B S, *J Physiq*, 44 (1983) 1345; *Polyhedron*, 3 (1984) 169.
11 Figgis B N, *Introduction to ligand fields* (Wiley Eastern Ltd, New Delhi) 1976, 226.
12 Bancroft G M, *Mössbauer spectroscopy: An introduction for inorganic chemists and geochemists* (McGraw Hill Book Co, London) (1973), 127.

13 Inoue H, Sasagawa S, Fluck E & Shirai T, *Bull chem Soc. Japan*, 56 (1983) 3434.
14 Bassi P S, Randhawa B S & Kaur S, *Hyperfine Interact*, 28 (1986) 745.
15 Alcock N W, Tracy V M & Wanddington T C, *J chem Soc.* (1976) 243.
16 Manhas B S & Trikha A K, *J Indian chem Soc*, 59 (1982) 315.
17 Ferraro J R, Driver R, Walker W R & Waznaik W, *Inorg Chem*, 6 (1967) 1586.
18 Baylis B R W & Bailar J C, *Inorg Chem*, 9 (1970) 641.
19 (a) Deacan G B & Philips R J, *Aust J Chem*, 31 (1978) 1709. (b) Deacon G B, Huber F & Philips R J, *Inorg chim Acta*, 104 (1984) 41.
20 Nakamoto K, Marimato Y & Martel A E, *J Am chem Soc*, 83 (1961) 4528.
21 Tyagi A S & Srivastava C P, *J Indian chem Soc*, 58 (1981) 284; **59** (1982) 823.
22 Schmelz M J, Nakagawa I, Mizushima S & Quagliano J V, *J Am chem Soc*, 81 (1959) 287.
23 Nakamoto K, *Infrared and Raman spectra of inorganic and coordination compounds*, 4th Edn, (Wiley-Interscience, New York) 1986, 231.
24 Rao C N R, *Chemical applications of infrared spectroscopy* (Academic Press, New York) 1963, 357.
25 Bassi P S, Randhawa A S & Bilaspuri G K, *J thermal Anal*, 121 (1988) 21.
26 Music S, Ristic M & Popovic S, *J Radioanal nucl Chem Art*, 121 (1988) 21.
27 Saha H L & Mitra S, *Thermochim Acta*, 116 (1987) 53.
28 (a) Ladriere J, *Hyperfine Interact*, 42 (1988) 993.
28 (b) Ladriere J & Apers D, *Hyperfine Interact*, 42 (1988) 1005.
29 Abras A, De Jesus Filho M F & Braga M M, *Thermochim Acta*, 101 (1986) 35.

Indian Journal of Chemistry
Vol. 30A, February 1991, pp 172-176

Low temperature fluorination of some non-metals and non-metal compounds with fluorine

D K Padma*, R G Kalbandkeri, B S Suresh & V Subrahmanya Bhat

Department of Inorganic and Physical Chemistry, Indian Institute of Science, Bangalore 560 012

Received 25 April 1990; accepted 1 October 1990

Low temperature fluorination with elemental fluorine of elemental phosphorus, sulphur, silicon, amorphous carbon and phosphorus trichloride, phosphorus pentoxide, triphenylphosphine, hexafluorodisilane, hexachlorodisilane, hexabromodisilane, tetrasulphur tetranitride, sulphur dioxide, thionyl chloride and sulphuryl chloride has been carried out in freon-11 medium. The corresponding fluoro compounds have been isolated in near quantitative yields, purified by low temperature fractional condensation and characterised by IR spectroscopy and elemental analysis.

Low temperature fluorination of non-metal leads to a variety of products with variable yields depending on the temperature of fluorination[1-4]. One mode of controlling the exothermicity of the reaction is by diluting fluorine with dry nitrogen and/or employing freon as a solvent. Such modes of fluorination have stabilised the lower valency states of the compounds, e.g., yield of sulphur tetrafluoride is maximised under such conditions[5]. It was, therefore, of interest to study the action of elemental fluorine on a few non-metals such as phosphorus, sulphur, silicon and amorphous carbon and non-metal compounds such as phosphorus trichloride, phosphorus pentoxide, triphenylphosphine, hexafluorodisilane, hexachlorodisilane, hexabromodisilane, tetrasulphur tetranitride, sulphur dioxide, thionyl chloride and sulphuryl chloride at low temperature in freon medium. Alternatively, sulphuryl chloride could be used as a solvent as it is found not to react with elemental fluorine at low temperature. The products, the corresponding fluorocompounds, have been isolated and characterised by IR spectroscopy and elemental analysis.

Materials and Methods

All the reagents were BDH samples except hexafluorodisilane[6], hexachlorodisilane[7], hexabromodisilane[8] tetrasulphur tetranitride[9] which were prepared by reported methods and their purity checked by spectral and elemental analyses. The solvent freon-11 was obtained from Mafron India Ltd., Bombay, India. Elemental fluorine was obtained from Messrs Kali Chemie, West Germany.

General procedure

The experimental set up is shown in Fig. 1. A small teflon covered magnetic follower was placed at the bottom of the tube, T_1. Freon (20-30 ml) is freshly distilled into the reaction tube and dry nitrogen is flushed. The outlet was connected to two empty traps followed by a tower of sodium chloride and a bubbler consisting of sodium hydroxide (4*N*) [These help to destroy unreacted fluorine]. When the outgoing gas showed the presence of fluorine (tested by moist KI paper), fresh tower and bubbler were introduced. The nitrogen stream was allowed for 15 minutes. The reactants (non-metal/non-metal compounds) were then introduced from the top opening and stopcocks fitted with G−G joints are well closed. The reaction trap (T_1) was now cooled to −80°C to −50°C as needed. The next trap (T_2) was cooled by liquid nitrogen and the temperature of the trap T_3 was maintained at −20°C. After cooling the set up for 30 min at desired temperatures; fluorine was slowly admixed with nitrogen in the ratio of 1:5 (F_2:N_2) and passed at a rate of 1.5 to 2.0 litres/hr. The mixture of gases was precooled in a coil which dipped in an alcohol slush bath maintained at −70°C. The cooled gas entered the reaction zone. The contact with fluorine initiated immediate reaction and the reaction tube had to be continuously cooled to overcome the heat generated due to reaction. The flow of fluorine was stopped at the end of 2/4 hr and nitrogen was flushed for another 2 hr to remove excess fluorine and also the dissolved products from the reaction vessel, which got condensed in trap 2. The tem-

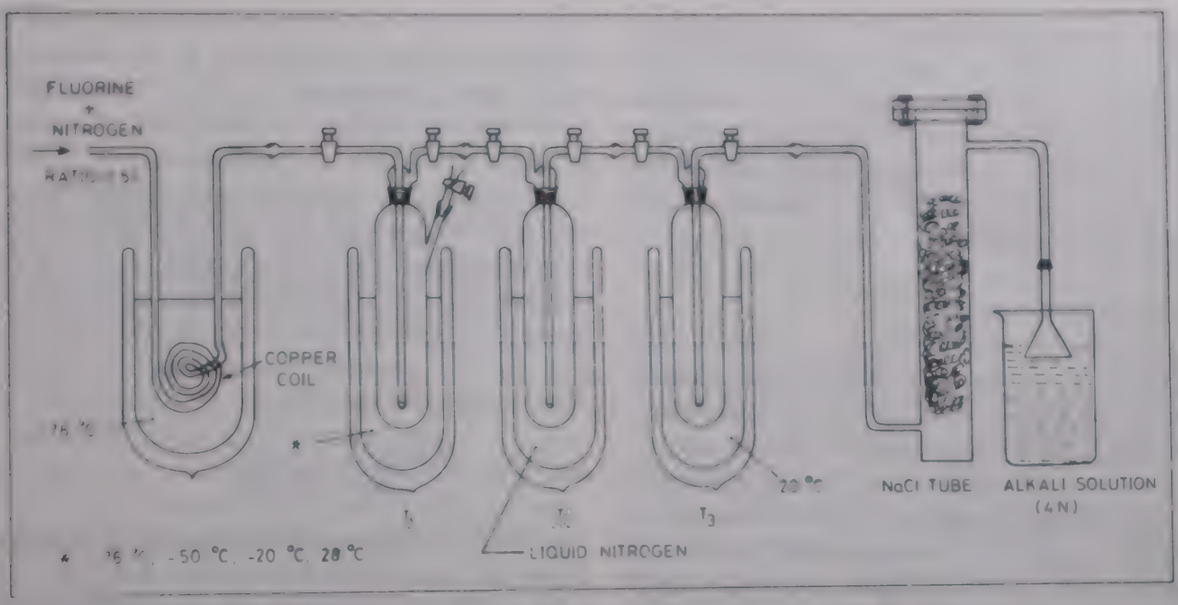

Fig. 1 – Experimental set up for fluorination using elemental fluorine

perature of the trap T_1 was slowly raised to room temperature as the nitrogen flow was maintained for another 30 min. With this operation all the gaseous products formed were driven off from the reaction trap T_1 and got collected in trap T_2. Trap T_2 held at liquid nitrogen temperature was disconnected and the uncondensable gases at this temperature were pumped out. The condensed product gases were then sublimed out into a dry glass globe (1 litre) fitted with GG joints by slowly raising the temperature of T_2 to ambient. The solvent vapours were removed from the product gases by dissolving the former in benzene. Solvent free gases were collected after freezing out benzene. The gaseous products were identified by IR spectroscopy (Perkin Elmer Model 599 spectrophotometer using 10 cm gas cell with KBr windows).

The same experimental set-up and procedure were used for experiments without solvent except that the last step of removing solvent vapours was not necessary.

The freon solvent in trap T_1 was evaporated and any solid or liquid remaining in T_1 was characterised by IR spectroscopy and chemical analyses.

Results and Discussion

Reaction of elemental fluorine on phosphorus, phosphorus trichloride, phosphorus pentoxide and triphenylphosphine at low temperature: (a) *phosphorus*

The IR spectrum of the fluorination product of red phosphorus (0.5 g) in freon-11 (20 ml) exhibits absorptions corresponding to phosphorus pentafluoride, PF_5, at 535, 575, 610, 950, 1025 cm^{-1}; reported[10] 534, 575, 640, 948, 1026 cm^{-1} and only very weak absorptions due to phosphoryl fluoride, POF_3, and silicon tetrafluoride, SiF_4. In the absence of the solvent, the IR spectrum showed absorption bands for the presence of phosphoryl fluoride, at 475, 485, 875, 990, 1415 cm^{-1}; reported[11] 473, 485, 873, 990, 1415 cm^{-1}, silicon tetrafluoride, at 780, 1030, 1060, 1190, 1295 cm^{-1}; reported[12] 780, 1031, 1065, 1191, 1295 cm^{-1} along with phosphorus pentafluoride. The reaction was smooth and no burning was noticed. In confirmation of the earlier reports[13] the reaction of fluorine with red phosphorus at room temperature proceeded vigorously with burning giving phosphorus pentafluoride and phosphoryl fluoride. The results of the present investigation showed that PF_5 can be generated in more than 90% yield by carrying the reaction at $-50°C$ in freon-11. The contaminants, POF_3 and SiF_4 were removed by fractional condensation and separation. The overall reaction is represented as:

$$P + F_2 \xrightarrow[-50°C]{\text{freon-11}} PF_5\,(90\%) + [POF_3 + SiF_4].$$

(b) *Phosphorus trichloride* (PCl_3)

Phosphorus trichloride (1 ml) directly or in freon-11 (20 ml) held at $-80°C$, reacted with elemental fluorine during 2 hr to form a variety of gaseous mixed halides such as PF_5 (ref. 10), PF_3Cl (ref. 14), PF_3Cl_2 (ref. 15), POF_3 (ref. 11) SiF_4 (ref. 12) (all of them identified from their reported infrared spectral data) as well as a white solid product left in the reaction tube consisting of $PCl_4^+F^-$ and $PCl_4^+PF_6^-$. These results are similar or one observed by Payne *et al.*[16] who carried out direct fluorination of PCl_3 at room temperature in va-

pour phase. It is thus evident that decreasing the temperature of reaction either with or without solvent has not drastically altered the oxidative fluorination that phosphorus trichloride[16] undergoes in the presence of fluorine. However, the ratio of the products formed are dependent on the temperature of fluorination.

(c) *Phosphorus pentoxide* (P_4O_{10})

Since phosphorus pentoxide is a solid it was well dispersed in freon-11 (−80°C) and treated with fluorine at a rate of 0.2-0.25 litres/hr for 2 hr. The solid, P_4O_{10}, was consumed in the course of the reaction and formed a gaseous product which was identified as phosphoryl fluoride along with a small amount of silicon tetrafluoride. A very small amount of unidentified polymeric solid remained in trap T_1. Moissan[17] has observed that reaction of phosphorus pentoxide with elemental fluorine at room temperature led to both phosphoryl fluoride and phosphorus pentafluoride. However, in the present investigation, formation of PF_5 was not observed. Therefore, it can be surmised that the mechanism of fluorination involves cleavage of P−O−P− bonds in P_4O_{10} and formation of POF_3 which further gets fluorinated at room temperature to PF_5. The other mode of POF_3 formation is by cleavage of all bonds in P_4O_{10} and PF_5 thus formed further reacting with generated O−F species (formed by the reaction of cleaved oxygen with fluorine) to form POF_3. This mode does not occur (as PF_5 was not observed) and the primary reaction is itself the cleavage of P−O P−bond such that the P−O bond undergoes fluorination to POF_3.

(d) *Triphenylphosphine* ϕ_3 P

Triphenylphosphine (0.5) was dispersed in freon-11 (20 ml) and cooled in trap T_1. Fluorine admixed with nitrogen was passed at a rate of 0.2 litre/hr for 2 hr while stirring the contents. After removal of residual fluorine, the gaseous component was separated. The IR spectrum of this sample indicated the presence of small amount of SiF_4 only. So, the freon-11 in T_1 was distilled out and the remaining solid was dried *in vacuo* at room temperature. The IR spectrum of the solid exhibited peaks at 3100, 1445, 755, 730 cm^{-1} which could be correlated with the reported[18] peaks of $(C_6H_5)_3PF_2$ (i.e. at 3000-3200, 1450, 760, 730 cm^{-1}). The melting point of the solid (134-137°C) as well as the elemental analyses (P = 10.75% and F = 12.71%) agreed well with those for difluorotriphenylphosphorane $(C_6H_5)_3PF_2$.

This result is very interesting in that at low temperature the cleavage of P−C bond does not occur and phosphorus is able to undergo oxidation with the addition of two more fluorine atoms to attain the stable +5 oxidation state. This result is similar to one reported with milder fluorinating reagents such as sulphur tetrafluoride[18] and tetrafluorohydrazine (N_2F_4)[19] thereby testifying that elemental fluorine functions like mild fluorinating reagent at low temperature, in low concentration and in the presence of a solvent. The overall equation for the reaction is

$$\phi_3P + F_2 \xrightarrow[-50°C]{\text{freon-11}} \phi_3PF_2$$

Reaction of elemental fluorine with hexahalodisilanes

(Si_2F_6, Si_2Cl_6, Si_2Br_6): (a) *Direct*−Hexahalodisilane, (1.0-1.5 mmoles), Si_2F_6, Si_2Cl_6, Si_2Br_6, was taken in the evacuated trap T_1 and frozen with the coolant liquid nitrogen. An even number of moles of elemental fluorine was condensed onto it and the two reactants slowly warmed during 2 hr to attain room temperature (~28°C). Reaction was over by this time as seen from the spectral data, absence of the IR absorption peaks of Si_2F_6 (ref. 20), Si_2Cl_6 (ref. 21) and Si_2Br_6.

(*b*) *With solvent*−About 3 g of the chloro and bromo analogue was dissolved/dispersed in dry freon-11 (20 ml) and treated with nitrogen diluted fluorine at −30°C and −60°C.

(*c*) *Without solvent*−About 3 g of the chloro and bromo analogue was spread out on the sides of the reaction tube by rolling the tube with the solid, and cooled to −30°C/−60°C and nitrogen diluted fluorine (1:5) was passed over it for 2 hr.

It is observed that in all the above experiment (a-c) the fluorination products for the hexahalodisilanes are the same and only the amount varies. The major produt is silicon tetrafluoride indicating that Si−Si bond undergoes easy cleavage even at low temperature. In the case of the chloro analogue, in addition, formation of mixed chlorofluoro silanes also occurs (IR, $SiClF_3$: obs. 1010, 880, 590; reported[22], 1010, 876, 590 $SiCl_2F_2$: obs. 990, 910, 660; reported[22] 990, 912, 656 $SiCl_3F$: obs. 940, 640, 460; reported[22], 942, 634, 464 cm^{-1}. Even with dibromohexafluorosilane, the first bond to undergo cleavage is the Si−Si bond as expected. Formation of mixed bromofluorides are also observed (peaks at 600, 830 and 910 cm^{-1}) along with the completely fluorinated product SiF_4. The other major products present are chlorine and bromine respectively. This indicates that fluorine attacks these halogens slowly at low

temperature. Even at −76°C the Si−Si bond cleavage occurs in the presence of elemental fluorine giving rise to silicon tetrafluoride as the major product.

Reaction of elemental fluorine on tetrasulphur tetranitride (S_4N_4), sulphur dioxide (SO_2), thionyl chloride ($SOCl_2$) sulphuryl chloride (SO_2Cl_2) elemental sulphur, silicon and amorphous carbon

(a) *Tetrasulphur tetranitride*

Direct fluorination of S_4N_4 by passing elemental fluorine on solid S_4N_4 results in the rupture of the ring and formation of sulphur fluorides and nitrogen[23]. Even fluorine diluted with nitrogen ruptures the ring at room temperature. However, at −78°C in the presence of helium-diluted fluorine, formation of trithiazyl trifluoride ($S_3N_3F_3$) is noted. Thiazyl fluoride and thiazyl trifluoride are also formed at low temperature[24]. In the present investigation it is found that S_4N_4 (0.5 g) suspended in freon-11 at −80°C gives rise to thiadithiazyl difluoride, $S_3N_2F_2$, as the major product of fluorination. The gaseous products are sulphur dioxide and silicon tetrafluoride indicating some reaction of the products with glass. The trap T_1 also contains a solution with some yellowish green suspension. The freon is distilled off in vacuo and the yellowish green solid left in the trap is found to be highly hygroscopic and soluble in carbon tetrachloride and chloroform giving a greenish red solution. The compound melts around 82°. The CCl_4 solution shows an intense absorption peak at 375 nm corresponding to that reported[25] for $S_3N_2F_2$. It is interesting to note that $S_4N_4F_4$, a direct fluorine addition product, is not formed at low temperature but cleavage results with ring contraction.

(b) *Sulphur dioxide (SO_2)*

Sulphur dioxide dissolved in freon (5 mg of SO_2 per ml of freon) at −60°C undergoes oxidative fluorine addition to form SO_2F_2 in quantitative yields; IR bands at 540, 545, 555, 850, 885, 1270 and 1505 cm^{-1} could be correlated with the reported peaks for sulphuryl fluoride[26] at 539, 553, 848, 885, 1269 and 1502 cm^{-1}. There is one report of the action of fluorine on sulphur dioxide at 650°C to form sulphur hexafluoride[27]. Thus, this low temperature fluorination preserves the S−O bond and the molecule undergoes oxidative fluorine addition to form SO_2F_2.

(c) *Thionyl chloride ($SOCl_2$)*

Fluorination of thionyl chloride (0.5 ml) in freon (50 ml) at −50°C yields thionyl fluoride (80% (IR: 530, 750, 810 and 1335 cm^{-1}. Reported[28] 530, 748, 806 and 1333 cm^{-1}). It is interesting to note that no mixed halide (chlorofluoride) is formed and no oxidation of sulphur in $SOCl_2$ (IV) to VI state occurs with fluorine addition i.e. formation of SO_2F_2 or SOF_4. There is only cleavage of the S−Cl bond to yield the S−F bond with the S−O bond intact as with other mild fluorinating reagents[29].

(d) *Sulphuryl chloride (SO_2Cl_2)*

Fluorination of neat liquid sulphuryl chloride, as well as in freon medium, has been tried at various temperatures ranging from −80°, −60°, −40°, −20° and 0°C. In both these modes and at different temperatures, sulphuryl chloride is not attacked by elemental fluorine. This indicates that S−O and S−Cl bonds in SO_2Cl_2 are very stable at low temperature. Thus, liquid SO_2Cl_2, is a good candidate as solvent for elemental fluorine reactions and as a replacement for freon.

(e) *Elemental sulphur*

Fluorination of elemental sulphur at 0°-5°C in freon solvent indicates a 90% conversion to SF_6 in contrast to 90% conversion to SF_4 (ref. 5) at −76°C. This differential reaction could be used to synthesise the respective pure gases. The gases can be purified by low temperature fractional condensation and identified by their IR spectra.

(f) *Elemental silicon*

Fluorination of elemental silicon at −70°C in freon medium yields only silicon tetrafluoride. The reaction is smooth and immediate. No lower silicon fluorides are identified in the IR spectrum of the product gas which exhibits bands of SiF_4 only.

(g) *Amorphous carbon*

The fluorination of amorphous carbon suspended in freon-11 at −76°C yields carbon tetrafluoride as identified by its IR spectrum. The reaction is smooth. It was interesting to note that solid carbon fluorides are not formed at this low temperature though at high temperature graphite fluoride results[30].

References

1 Cohen B, Hooper T R, Higill D & Peacock R D, *Nature*, 207 (1965) 748.

2 Peacock R D, *Proceedings of the Chemical Society*, (1957) 59.

3 Cohen B, Hooper T R, Peacock R D, *Chem Commun*, (1966) 32.

4 Lagow R J & Margrave J L, *Progress in inorganic chemistry* (John Wiley, New York) 26 (1979) 161.

5 Naumann D & Padma D K, *Z anorg allg chem*, 401 (1973) 53.
6 Suresh B S & Padma D K, *Bull chem Soc Japan*, 58 (1985) 1867.
7 Schumb W C & Gamble E L, *Inorg Synth*, 1 (1939) 42.
8 Schumb W C, *Inorg Synth*, 2 (1946) 98.
9 Padma D K, Subrahmanya Bhat V & Vasudeva Murthy A R, *Inorg chim Acta*, 20 (1976) L 53.
10 Pemsler J P & Planet W G, *J chem Phys*, 24 (1956) 920.
11 Gutowsky H S & Liehr A D, *J chem Phys*, 20 (1952) 1652.
12 Padma D K, Suresh B S & Vasudeva Murthy A R, *J Fluorine Chem*, 14 (1979) 327.
13 Moissan H, *Ann chim Phys*, 24 (1891) 224.
14 Carter R P & Homes R R, *Inorg Chem*, 4 (1965) 738.
15 Salthouse J A & Waddington T C, *Spectrochim Acta*, 23A (1967) 1069.
16 Kesavadas T & Payne D S, *J chem Soc (A)*, (1967) 1001.
17 Moissan H, *Ann chim Phys*, 6 (1885) 433.
18 Smith W C, *J Am chem Soc*, 82 (1960) 6176.
19 Ya Derkach N & Kirsanov A V, *Zh Obsch Khim*, 38 (1968) 331.
20 Timms P L, Kent R A, Ehlert T C & Margrave J L, *J Am chem Soc*, 87 (1965) 2824.
21 Morino Y, *J chem Phys*, 24 (1956) 164.
22 Hamada K, Ozin G A & Robinson E A, *Bull chem Soc, Japan*, 44 (1971) 2555.
23 Argo W L, Mathers F C, Humilton B & Anderson C O, *Trans electrochem Soc*, 35 (1919) 335.
24 Leech H R, *Quart Rev (London)*, 3 (1949) 22.
25 Rudge A J, *Chemy Ind (London)*, (1949) 427.
26 Rudge A J, in *Industrial electrochemical processes* edited by A T Kuhn (Elsevier, Amsterdam) 1971, 1-65.
27 Latimer W H & Hildebrand J H, *The reference book of inorganic chemistry*, (Macmillan, New York) 1940, p. 159.
28 Froning J F, Richards M K, Stricklin T W & Turnbull S G, *Ind eng Chem*, 39 (1947) 275.
29 Padma D K, Subrahmanya Bhat V & Vasudeva Murthy A R, *J inorg nucl Chem*, 43 (1981) 3009.
30 Watanabe N, Touhara H, Nakajima T, Bartlett N, Mallouk T & Selig H in *Inorganic solid fluorides*, edited by Paul Hagenmuller (Academic Press, New York) 1985, 331.

Indian Journal of Chemistry
Vol. 30A, February 1991, pp 177-180

Notes

Sustained oscillations in a simple reaction model

R P Rastogi* & G P Misra

Department of Chemistry, Banaras Hindu University, Varanasi 221 005, India

Received 4 June 1990; accepted 11 July 1990

It is shown that the reaction sequence comprising steps (i) and (ii) and undergoing in a continuous flow stirred tank reactor generates oscillations (A and B represent the concentration of reactant A and intermediate B)

$$A + B \rightarrow 2B \quad \ldots (i)$$

$$B \rightarrow C \quad \ldots (ii)$$

The reaction (i) is autocatalytic and reaction (ii) obeys half-order kinetics.

The need for 'a very simple example of a kinetic mechanism', through which oscillatory reactions can be understood, has been reemphasised recently[1-4]. Although, Lotka-Volterra scheme[5] first put forward in 1920, accounted for oscillatory behaviour, it did not provide stable limit cycle behaviour characteristic of self-oscillating systems. Versions of cubic autocatalator were later suggested by Sel'kov[6] and also by Lefever[7] involving the core

$$A + 2B \rightarrow 3B$$

$$B \rightarrow C$$

Prigogine and Lefever[8] while retaining the core, suggested a scheme known as Brusselator where a few steps were added. This has been extensively used to investigate temporal and spatio-temporal oscillations including dissipative structures in model systems[9,10].

A number of simple reaction schemes have been proposed in the literature[9-12], which show oscillatory behaviour under certain conditions. Very recently a two-step model[11], containing an autocatalytic step and a decay step, has been proposed which shows sustained oscillations in a continuous flow stirred tank reactor (CSTR). The model consists of the following steps:

$$A + B \rightarrow 2B \quad \ldots (i)$$

$$B \rightarrow C \quad \ldots (ii)$$

where A and B are the reactants and C is the product. Damped oscillations are obtained when linear decay of B is assumed. However sustained oscillations are obtained when Michaelis-Menten type of rate law (1) for step (ii) is assumed, i.e.

$$\text{Rate} = kB/(1 + rB) \quad \ldots (1)$$

where k is the rate constant and r is another constant, B denotes the concentration of the reactant B itself.

We propose to examine in this paper the consequences of assuming half order kinetics for step (ii), i.e.

$$\text{Rate} = k_2 B^{1/2} \quad \ldots (2)$$

Search for simple schemes is desirable for understanding the basic control of oscillatory behaviour and hence the present investigation was undertaken. It may be noted that fractional order kinetics is quite common in heterogeneous reactions and the rate can be expressed by the relation (3)

$$\text{Rate} = \bar{k}p^n \qquad (1 > n > 0) \quad \ldots (3)$$

where $\bar{k}$ is a constnat, p is the pressure and n denotes the order. Further, n = 1 when the surface is sparesely covered while n = 0 when the surface is completely covered. An illustrative example[13] is the decomposition of arsine on metallic arsenic for which n = 0.6.

Analysis of simple reaction model

According to the present model, the rates of step (i) and (ii) would be given by:

$$\text{Rate (i)} = k_1 AB \quad \ldots (4)$$

$$\text{Rate (ii)} = k_2 B^{1/2} \quad \ldots (5)$$

We can consider step (i) as simple A → B with the rate law given by Eq. (4) as pointed out by Cook *et al.*[4] Considering A and B as dynamic variables, for an open system (flow reactor) the kinetic equations can be expressed by Eqs (6) and (7)

$$\frac{dA}{dT} = -k_1 AB + k_f(A_0 - A) \quad \ldots (6)$$

$$\frac{dB}{dT} = k_1 AB - k_2 B^{1/2} + k_f(B_0 - B) \quad \ldots (7)$$

where k_f is the inverse of residence time and A_0 and B_0 are concentrations of reactant and radical re-

spectively. In dimensionless form, Eqs (6) and (7) may be written as:

$$\frac{dx}{dt} = -yx + (1-x)/t_{res} \quad \ldots (8)$$

$$\frac{dy}{dt} = xy - y^{1/2}/t_2 + (y_0 - y)/t_{res} \quad \ldots (9)$$

where $x = A/A_0$; $y = B/A_0$; $y_0 = B_0/A_0$; $t = k_1 A_0 T$; $t_{res} = k_1 A_0/k_f$ and $t_2 = k_1 A_0^{3/2}/k_2$ (where t_{res} is residence time).

Computer solution shows that when $t_{res} = \infty$ (batch reactor condition) or when $y_0 = 0$ oscillations are not obtained. However for CSTR under certain condition sustained oscillations are obtained.

From Eq. (8), we obtain for the steady state when

$$\frac{dx}{dt} = 0,$$

$$y = (1-x)/(Xt_{res}) \quad \ldots (10)$$

Now, combining Eq. (9) with Eq. (8) for the steady state situation when both $\frac{dx}{dt}$ and $\frac{dy}{dt}$ are zero, we get

$$x^4 t_{res}^2 t_2^2 - x^3 2(t_2^2 t_{res}^2 + t_{res} t_2^2 + y_0 t_2^2 t_{res}^2) + x^2(t_2^2 t_{res}^2 + 2y_0 t_{res} t_2^2 + 3y_0 t_2^2 t_{res}^2 + 4t_{res} t_2^2 + t_{res}^3 + t_2^2) - x(t_{res}^3 + 2t_2^2 + 2y_0 t_{res} t_2^2 + 2t_{res} t_2^2) + t_2^2 = 0. \quad \ldots (11)$$

Solution of equation (11) gives the steady state values of x and y at different values of t_{res} and t_2. Obviously Eq. (11) will give four roots indicating the possibility of multistability.

Normal mode analysis

Applying normal mode analysis[10] the secular equation (12) is obtained, when $y_0 = 0$ or $y_0 \neq 0$

$$\begin{vmatrix} (\omega + 1/t_{res} + y_s) & x_s \\ y_s & (x_s - 1/(2y_s^{1/2} t_2) - 1/t_{res} - \omega) \end{vmatrix} = 0$$

where ω is the frequency. $\quad \ldots (12)$

Equation (12) can be rewritten as

$$\omega^2 - \omega\{x_s - y_s - 2/t_{res} - 1/(2t_2 y_s^{1/2})\} + [\{1/t_{res}(-x_s + 1/t_{res} + y_s)\} + y_s^{1/2}/2t_2\{1 + 1/(t_{res} y_s)\}] = 0 \quad \ldots (13)$$

where x_s and y_s are steady state values of x and y respectively.

Or $\omega^2 - p\omega + q = 0$

where

$$p = x_s - y_s - 2/t_{res} - 1/(2t_2 y_s^{1/2})$$

and

$$q = [\{1/t_{res}(-x_s + 1/t_{res} + y_s)\} + y_s^{1/2}/2t_2\{1 + 1/(t_{res} y_s)\}]$$

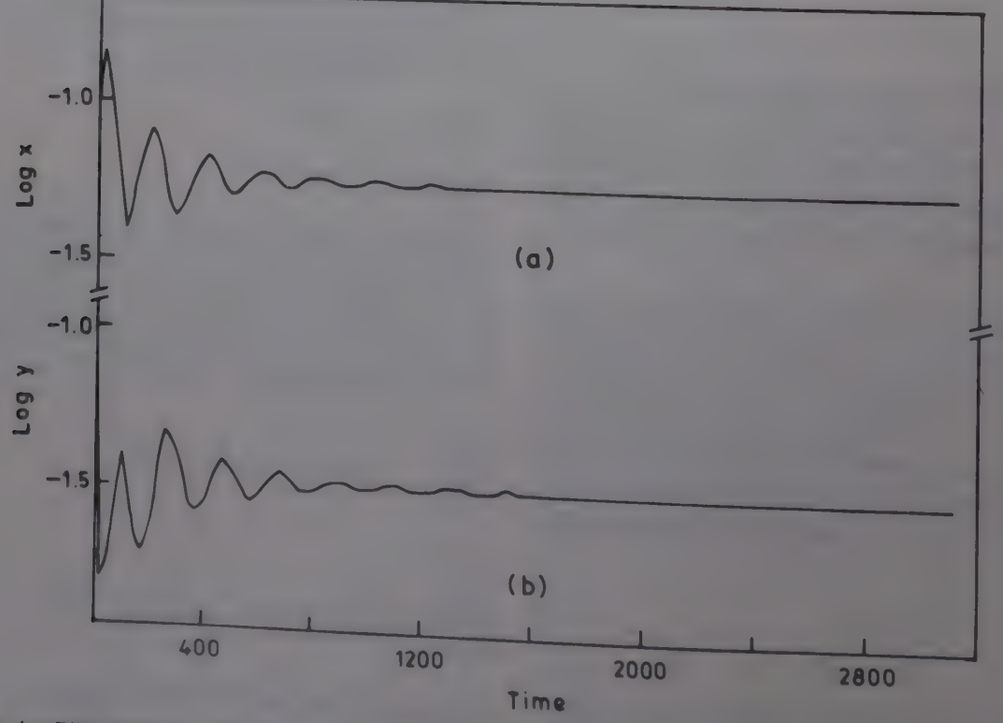

Fig. 1 — Plot of computed values of (a) log x and (b) log y versus time for $t_{res} = 500$, $t_2 = 100$ and $y_0 = 0.0$.

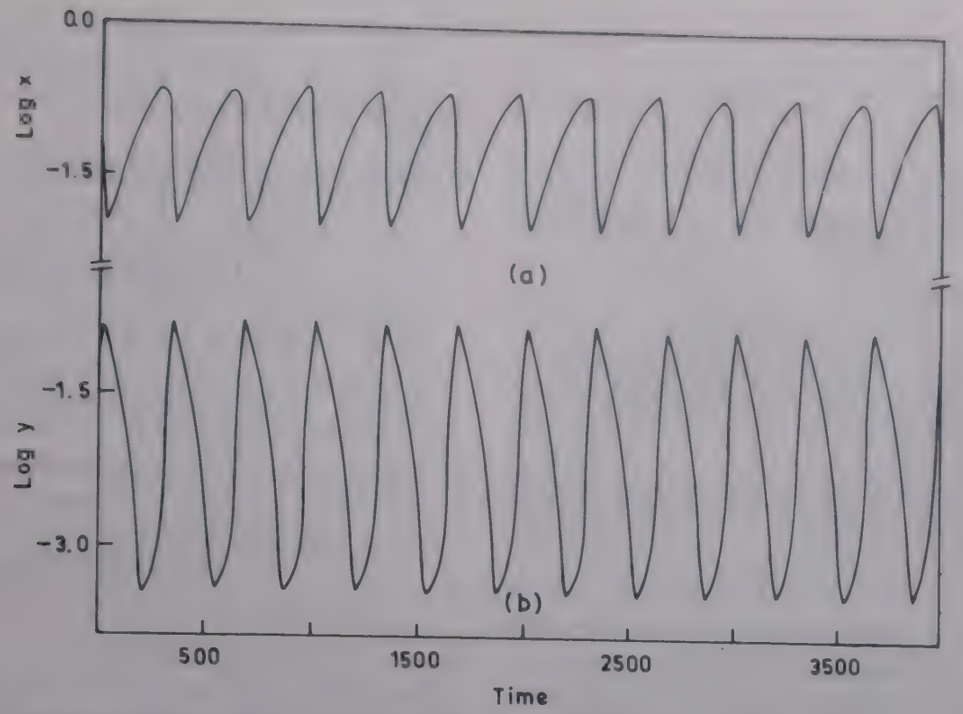

Fig. 2—Plot of computed values of (a) log x and (b) log y versus time for $t_{res} = 700$, $t_2 = 100$ and $y_0 = 0.1$.

Bifurcation would occur when $q > 0$ and $p = 0$ so that at the bifurcation point,

$$x_s - y_s - 2/t_{res} - 1/(2t_2 y_s^{1/2}) = 0 \quad \ldots (14)$$

Numerical solution

Numerical solution of Eqs (8) and (9) were obtained for different values of t_2 and t_{res} and typical results for $t_2 = 100$, $t_{res} = 500$ and $y_0 = 0$ are plotted in Fig. 1. In this situation damped oscillations are obtained. Now, if we consider the case when y_0 is finite, computer solution gives oscillatory behaviour as shown in Fig. 2, when $t_{res} = 700$, $t_2 = 100$ and $y_0 = 0.1$. In all the cases when $t_{res} \geqslant 700$ sustained oscillations are obtained. We also computed numerically the nature of stability/instability when $t_2 = 100$, $y_0 = 0.1$ and t_{res} is varying. The results are given in Table 1.

Table 1—Dependence of oscillatory nature on t_{res} ($t_2 = 100$, $y_0 = 0.1$)

t_{res}	Nature of oscillation
100	No oscillation
200	" "
.	" "
.	" "
500	Damped oscillation
600	" "
700	Sustained oscillation
800	" "
.	" "
.	" "

Equation (11) was also solved for $t_2 = 100$, $y_0 = 0.1$ and for varying values of t_{res} and accepted solutions of x and y i.e. $(0 < x < 1;\ 0 < y < 1)$ were obtained. These values were then substituted in Eq. (14) in order to find out when the left hand side of the Eq. (14) is negative, zero or positive in order to identify the bifurcation point for particular values of t_{res}. It is found that when $t_{res} \geqslant 723$, instability occurs.

The finding that an autocatalytic reaction followed by a reaction obeying half-order kinetics displays oscillatory behaviour in a CSTR may have some implication in oscillations in heterogeneous reaction system. Experimental observations reveal that under certain conditions, the rate of several oxidation reactions oscillate continuously and never attain a steady state[14]. Some of the examples are: (a) oxidation of hydrogen by oxygen on nickel[15]; (b) oxidation of hydrogen on supported Pt-catalyst[16a], and (c) oxidation of CO on supported catalyst[16b,16c].

Combustion instability in solid propellant rocket motors using ammonium perchlorate (AP) as an oxidizer can also be possibly understood on the basis of the above model since it is widely accepted that burning rate of composite propellants is primarily governed[17] by the autocatalytic production of $HClO_4$ by the decomposition of AP which is followed by heterogeneous decomposition of $HClO_4$.

Acknowledgement

Thanks are due to Council of Scientific & Industrial Research, New Delhi for the award of Senior Research Fellowship to one of us (GPM).

References

1 Scott S K, *Acc chem Res*, 20 (1987) 186.

2 Gray P, Scott S K & Merkin J H, *J chem Soc, Faraday Tran I*, 84 (1988) 993.

3 Lefever R, Nicolis G & Borckmans P, *J chem Soc, Faraday Tran I*, 84 (1988) 1015.

4 Cook G B, Gray P, Knapp D G & Scott S K, *J phys Chem*, 93 (1989) 2749.

5 Lotka A J, *J Am chem Soc*, 20 (1920) 1595.

6 Sel'kov E E, *Eur J Biochem*, 4 (1968) 79.

7 Lefever R, *Bull Acad R Belg Sci*, 54 (1968) 712.

8 Lefever R & Prigogine I, *J chem Phys*, 48 (1968) 1695.

9 Glansdorff P & Prigogine I, *Thermodynamic theory of structure, stability and fluctuations* (Wiley, Interscience, New York) 1971.

10 Nicolis G & Prigogine I, *Self-organization in non-equilibrium systems* (Wiley Interscience, New York) 1977.

11 Scott S K, *J chem Soc, Faraday Tran II*, 81 (1985) 789.

12 King G A H, *J chem Soc, Faraday Tran I*, 79 (1983) 75.

13 Moore Walter J, *Physical Chemistry*, (Longmans) 1960, p. 582.

14 Scheintuch M & Schnitz R A, *Cat Rev Sci and Eng*, 15 (1977) 107.

15 Kurtanjek Z, Scheintuch M & Luss D, *Discussion meeting-Bunsen gesselshaft für physikalische Chemie*, Aachen, September 1979, Vol. I, p. 191.

16 Eiswirth M, Möller P & Ertl G in *Symposium on spatial inhomogeneities and transient behaviour in chemical kinetics*, Brussels, Aug 1987, (a) p. 45, (b) p. 68, (c) Somorjai G A, *J phys Chem*, 94 (1990) 1013.

17 Rastogi R P, Rao R P & Syal V, *J non-equilib Thermodyn*, 10 (1985) 163.

Indian Journal of Chemistry
Vol. 30A, February 1991, pp 181-183

β-Cyclodextrin catalysed autooxidation of benzoin in alkaline medium

M M Maheswaran & S Divakar*
Organic Chemistry Section/Food Chemistry Discipline,
Central Food Technological Research Institute, Mysore 570 013

Received 5 June 1990; revised 26 July 1990;
accepted 7 September 1990

Autooxidation of benzoin is catalysed by β-cyclodextrin in the presence of a mild base with 3.7 fold enhancement in rate. A mechanism commensurate with the kinetic data has been proposed.

Cyclodextrins catalyse a wide variety of organic reactions[1] and one such reaction is autooxidation of α-hydroxy ketones like furoin and pyridoin to corresponding α-diketones[2-4]. In this paper we report the kinetics and mechanism of autooxidation of benzoin in the presence of an equimolar amount of mild base and catalytic amounts of β-cyclodextrin. Autooxidation of benzoin is very slow in the presence of alkali[5].

Experimental

Solution of freshly prepared benzoin (0.059 mol dm^{-3}) containing appropriate concentration of β-cyclodextrin (BCD, Aldrich) was taken in ethyl alcohol (15 ml) and $NaHCO_3$ buffer (5 ml, 0.24 mol dm^{-3}) of *p*H 11.15 ± 0.1 such that the final buffer concentration was 0.06 mol dm^{-3}. The reaction mixture was maintained at 77 ± 1°C. For buffer solutions above *p*H 8.5, $NaHCO_3$ was used and for those between *p*H 6.0 and 7.0 phosphate was used. Tris-HCl was used for buffer solutions between *p*H 7.0 and 8.5. A control dynamics *p*H meter fitted with an Ingold combination electrode was used for *p*H measurements. Buffer *p*H was adjusted with 0.1 mol dm^{-3} NaOH solution.

In the presence of BCD at benzoin: BCD ratio of 27: 1 under above mentioned conditions, the reaction with solution saturated with air was found to proceed to about 50% completion in about 9 hr. The reaction proceeded further only when the alkali concentration was increased alongwith increase in oxygen content. Although, the solubility of oxygen in water is very low (5.762 mm/litre at 25°C and 760 mm pressure) its solubility in an alcoholic solution is about 12 times greater than that in water and also the solubility in an alkaline solution is slightly greater than that in water. The product of the reaction, benzil, isolated from the reaction mixture by chromatography was found to be identical (spectral data) with an authentic sample.

Kinetic measurements were carried out by monitoring the decrease in [benzoin] with the help of ^1H NMR spectroscopy (^1H NMR spectra were recorded on a Varian EM 390 instrument operating on a continuous wave mode at 35 ± 1°C). Aliquots (0.5 ml) were withdrawn at regular intervals of time, the residue obtained after evaporation of alcohol was dissolved in CCl_4 (0.5 ml) and a drop of DMSO for recording the spectra. As benzoin was converted into benzil, the decrease in the area of CH (δ 6.08) or OH (δ 4.54) proton signal was measured and from the total area of aromatic protons observed between δ 7.33 and 8.1 ppm, the relative proportions of benzoin and benzil were estimated.

The results show that one mole of benzoin absorbs one mole of oxygen to form one mole each of benzil and hydrogen peroxide in a first order reaction. Small amount of H_2O_2 formed was found to have very little effect on the *p*H of the medium as the *p*H of the reaction mixture before and after the run was found to be the same. Pseudo-first-order rate constants were determined from a linear least square analysis of a plot of log (A_0/A) versus time (s), where A_0 and A represent [benzoin] at initial time and after a period *t* respectively. Each kinetic run was repeated at least twice to arrive at the k_{obs} values. Correlation coefficient values for the plots were invariably within 0.88-1.0. The rate constants determined for the catalysed (k_{obs}) and uncatalysed (k_{un}) reactions were reproducible within 10-15%. Such high percentage of error is probably expectged as it involves determination of concentrations from area measurements of NMR signals of such a slow reaction.

Results and discussion

A typical plot for the evaluation of rate constants (k_{obs}) is given in Fig. 1. The k_{obs} values were found to increase within increase in [BCD] in the range of 2.15×10^{-4}-2.2×10^{-2} mol dm^{-3} at *p*H 11.15 ± 0.1. A plot of k_{obs} versus [BCD] showed an asymptotic behaviour (not shown) above [BCD] of 0.003 mol dm^{-3}. This behaviour is similar to that observed for enzyme-substrate systems and the Michaelis-Menten type kinetics can be depicted by Eq. (1)[6]

$$C + S \underset{k_{-1}}{\overset{k_1}{\rightleftharpoons}} C.S \xrightarrow{k_{cat}} C + P$$

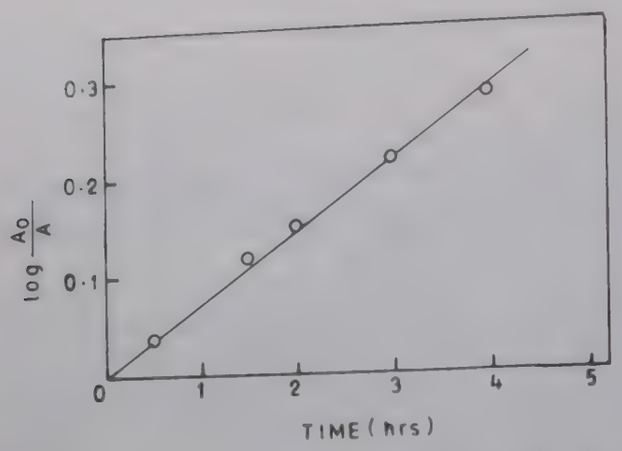

Fig. 1—A typical plot to evaluate pseudo-first-order rate constant (k_{obs}) values for the conversion of benzoin to benzil ([Benzoin] = 0.059 mol dm^{-3}; [BCD] = 0.0132 mol dm^{-3}; [$NaHCO_3$] = 0.0625 mol dm^{-3}; pH = 11.15 ± 0.1).

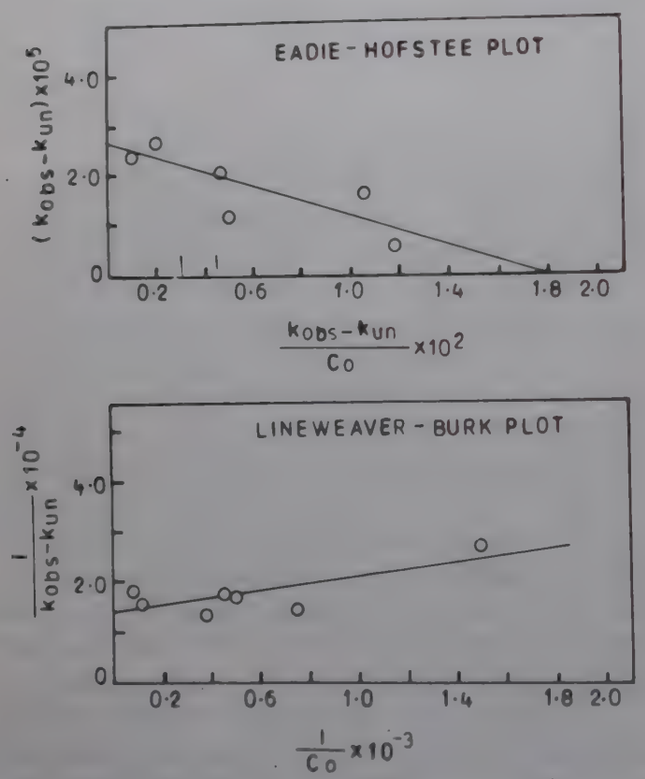

Fig. 2—Upper trace: Eadie-Hofstee plot. [Slope($-K_D$) = −0.00151 mol dm^{-3}; intercept (k_{cat}) = 2.64 × 10^{-5} s^{-1}].
Lower trace: Lineweaver-Burk plot. [Slope (K_D/k_{cat}) = 14.07 mol dm^{-3} s; intercept ($1/k_{cat}$) = 28029 s; K_D = 0.000515 mol dm^{-3} and k_{cat} = 3.569 × 10^{-5} s^{-1} respectively. Rate-constant values were: k_{un} = 8.298 × 10^{-6} s^{-1}; k_{obs} values for the catalysed reactions varied from 8.4 × 10^{-6} s^{-1} to 4.03 × 10^{-5} s^{-1} in the [BCD] range 2.15 × 10^{-4} − 2.2 × 10^{-2} mol dm^{-3}].

where C, S and P represent BCD, benzoin and product respectively.

A modified Lineweaver-Burk plot was constructed with the data, where a plot of $1/(k_{obs} - k_{un})$ versus 1/[BCD] was linear with intercept equal to $1/k_{cat}$ and slope to K_D/k_{cat} (Fig. 2). The data were also treated for an Eadie-Hofstee plot where the departure from linearity which might not be apparent in the above plot was magnified. The plot of $(k_{obs} - k_{un})$ against $(k_{obs} - k_{un})$/[BCD] was linear with slope equal to $-1/K_D$ and intercept equal to k_{cat} (Fig. 2). In both the treatments K_D refers to the dissociation constant of the benzoin-BCD complex and k_{cat} to the catalytic rate constant value. From both the plots an average value for k_{cat}/k_{un} was evaluated to be 3.7 along with a K_D value of 0.001013 mol dm^{-3}.

At fixed [base] (0.06 mol dm^{-3}), the rates for the catalysed and uncatalysed reactions increased with pH. However, the rates for the catalysed reactions were found to be slightly higher than those for the uncatalysed reactions in the pH range of 6.0-12.5 (Table 1). The ionisation of 2-OH and 3-OH of BCD ($pK \simeq 12.0$, ref. 1) in alkaline pH probably has very little effect on the catalysis.

Table 1—Kinetics of BCD catalysed autooxidation of benzoin [Benzoin] = 0.059 mol dm^{-3}; [$NaHCO_3$] = 0.06 mol dm^{-3}

[BCD] × 10^3 (mol dm^{-3})	pH	k_{obs} × 10^5 (s^{-1})	[p-Nitrophenol] × 10^4 (mol dm^{-3})
—	11.06	0.73	—
—	11.22	0.93 (Aver = 0.83)	—
0.895	11.18	0.909	18.71
1.126	11.06	0.767	27.19
—	6.52	0.496	—[a]
—	7.58	0.493	—
—	8.05	0.873	—
—	8.58	0.749	—
—	9.13	0.825	—
—	10.49	1.384	—
—	12.05	1.99	—
1.103	6.02	0.435	—
1.103	7.1	1.39	—
1.1	8.26	1.23	—
1.113	9.65	2.0	—
1.117	10.7	1.9	—
1.102	11.18	1.95	—
1.126	11.8	2.62	—
1.108	12.09	2.71	—
1.095	12.64	2.75	—
0.24	11.15	0.84	—
0.65	11.15	0.934	—
1.102	11.15	1.95	—
1.54	11.15	2.46	—
2.21	11.15	1.96	—
4.41	11.15	2.9	—
8.824	11.15	4.03	—
13.22	11.15	3.54	—

Percentage of error in k_{obs} values = ± 15%. Although a large number of kinetic run were performed, only values which gave best fit for the Lineweaver-Burk or Eadie-Hofstee were shown.
[a]no inhibitor was used.

The k_{obs} values for the BCD catalysed reactions at different [*p*-nitrophenol] were not significantly different from those of the uncatalysed reactions (Table 1) indicating that complexation of BCD with *p*-nitrophenol deprived benzoin of any catalytic effects by BCD since BCD formed a fairly stabler complex with *p*-nitrophenol ($K_D = 0.04 \times 10^{-2}$ mol dm^{-3}, ref. 1) than benzoin.

Benzoin was found to form a 1:1 inclusion complex with BCD (present work) when an equimolar solution of benzoin and BCD were examined in DMSO-d_6 by ^1H NMR. Chemical shift values of benzoin aromatic protons and BCD protons in DMSO-d_6 showed quite appreciable shifts on complexation, indicating that one of the phenyl ring is included within the cavity. Since benzil contains phenyl rings attached to carbonyl groups, its inclusion within BCD did not cause greater shifts in the aromatic protons of benzil, in comparison to those of benzoin, to distinguish the phenyl ring in benzoin that has been included within the cavity. However, the benzoin aromatic protons (especially those that belong to the phenyl ring next to CHOH) exhibited slightly greater shifts than the aromatic protons of benzil. This indicates that the phenyl ring next to CHOH in benzoin is included within the BCD cavity.

The CH and OH signals which appear as doublets ($J = 6.0$ Hz), show progressive broadening of the OH with CH signal losing its splitting character. After sometime, the OH signal disappears completely and the CH appears as a sharp singlet. Hence, the mechanism in the presence of BCD involves formation of $C_6H_5CHO^-COC_6H_5$ ion which is later converted into the dienolate anion by the loss of a proton. The dienolate anion undergoes oxidation by oxygen to form benzil (Scheme 1).

Since the rate-determining step is the enolisation of benzoin anion to the enol form, BCD enhances the shift of the keto-enol equilibria towards the more reactive enol form.

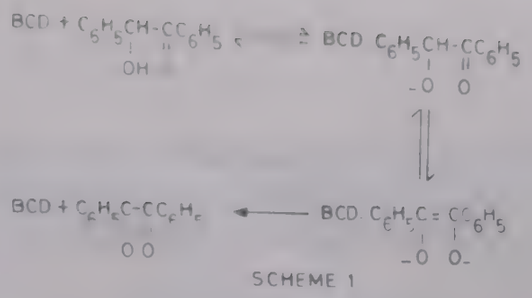

SCHEME 1

The rate of oxidation of furoin catalysed by a 2:1 complex of 6-β-aminoethylamino-6-deoxy-β-cyclodextrin-Cu^{2+}, was reported to be 20 times faster than that for the uncatalysed reaction[2]. In comparison, an enhancement of about 3.7 times observed for benzoin in the present work, although modest, involves a molecule like benzoin which does not possess an activating group in the vicinity of CHOH like furoin or pyridoin. The role of BCD here may be similar to that of a solvent mixture like propanol-water, in the decarboxylation of *p*-chlorophenylcyanoacetic acid anion catalysed by BCD[1]. By complexing with benzoin, BCD because of its microsolvent characteristics orients the latter for facile action by molecular oxygen.

Acknowledgement

The authors are grateful to the Director Dr B L Amla and Dr D Rajagopal Rao for facilities and encouragement. One of the authors (MMM) thanks the CSIR (New Delhi) for the award of a junior research fellowship. Thanks also to Mr A S Vittal Rao for valuable suggestions and fruitful discussions.

References

1 Bender M L & Komiyama M, *Cyclodextrin chemistry* (Springer, Berlin) 1978.
2 Matsui Y, Yokoi T & Mochida K, *Chem Letters*, (1976) 1037.
3 Cramer F, *Chem Ber*, 86 (1953) 1576.
4 Cramer F & Dietsche W, *Chem Ber*, 92 (1959) 1739.
5 Weissberger A, Mainz H & Strasser E, *Ber*, 62B (1929) 1942.
6 Van Etten R L, Sebastian J F, Clowes G A & Bender M L, *J Am chem Soc*, 89 (1967) 3242, 3253.

Indian Journal of Chemistry
Vol. 30A, February 1991, pp 184-186

Kinetics and mechanism of anation of *cis*-diaquo-bis(biguanide) chromium(III) ion by β-phenylalanine in aqueous medium

A K Gangopadhyay & G S De*

Department of Chemistry, University of Burdwan, Burdwan 713 104

Received 10 January 1990; revised 24 August 1990; accepted 15 October 1990

Substitution of aquo ligands from *cis*-diaquo-bis(biguanide)-chromium(III) ion by β-phenylalanine in aqueous medium has been studied spectrophotometrically. Activation parameters have been calculated. A mechanism involving the prior formation of ion pair followed by associative interchange (I_a) has been suggested for the anation of the Cr(III) complex.

Experimental evidences have been adduced in recent years that depending on the nature of the system inner or outer sphere mechanism may operate in ligand substitution reactions in both Co(III) and Cr(III). The present paper reports the results of one such study, i.e. reaction (1)

$$cis\text{-}[Cr(Bigh)_2(H_2O)_2]^{3+} + PhenylalaH \rightarrow [Cr(BigH)_2(Phenylala)]^{2+} + H_2O + H_3O^+ \quad \ldots(1)$$

where phenylalaH is the zwitterionic form of β-phenylalanine.

Experimental

cis-$[Cr(BigH)_2(H_2O)_2](ClO_4)_3$[complex-I] was prepared *in situ* by the literature method and the purity checked by UV spectra. The absorption spectra of 1:1, 1:2 and 1:3 mixtures of reactants preequilibrated at 45°C for 48 hr at *p*H 4.0 and containing fixed [complex-I] (0.005 mol dm^{-3}) exhibited λ_{max} at 490 nm. The product of the reaction between $[Cr(BigH)_2(H_2O)_2]^{3+}$ and β-phenylalanine was prepared by mixing these in 1:1 molar ratio and refluxing for 48 hr on a water bath. The reaction mixture was concentrated to yield a solid product which on analysis revealed the composition $[Cr(BigH)_2(Phenylala)]^{2+}$[complex-II]. Absorption spectrum of the isolated product exhibited λ_{max} at 490 nm.

Preequilibrated solutions of β-phenylalanine and complex-I were mixed under pseudo-first order conditions and the absorbances of aliquots from the reaction mixture withdrawn at regular intervals were measured at 460 nm where a substantial difference existed in the spectra of complex-I and complex-II. Pseudo-first order rate constant (k_{obs}) was evaluated graphically by plotting $\log(A_\alpha - A_0/A_\alpha - A_t)$ versus time *t*, where A_α, A_0 and A_t are the absorbances at infinite time, in the beginning and after time *t*, respectively.

Results and discussion

The values of k_{obs} ($\times 10^4$) were found to be 3.8, 4.0 and 4.1 s^{-1} at [complex-I] = 0.005, 0.006 and 0.0075 mol dm^{-3} respectively at fixed μ = 0.5 mol dm^{-3}, *p*H = 4.0, [phenylalaH] = 0.1 moldm^{-3} and temp. = 45°C. The k_{obs} values are in good agreement with the first order rate law (2)

$$\frac{d[\text{complex-II}]}{dt} = k_{obs}[\text{complex-I}] \quad \ldots(2)$$

Other conditions being the same, at fixed [complex-I] (0.005 mol dm^{-3}) and [phenylalaH] (0.075 mol dm^{-3}), k_{obs} ($\times 10^4$) values were 2.9, 3.0, 3.2, 3.3 and 3.6 s^{-1} at *p*H 3.5, 3.7, 4.0, 4.43 and 5.58 respectively. The *p*H of the medium was adjusted by adding $HClO_4$ and NaOH. The increase in rate with *p*H may be explained by considering Eq. (3).

$$cis\text{-}[Cr(BigH)_2(H_2O)_2]^{3+} \overset{K}{\rightleftharpoons} cis\text{-}[Cr(BigH)_2(H_2O)(OH)]^{2+} + H^+ \quad \ldots(3)$$

The *pK* of reaction (3) was determined *p*H-metrically as 8.0 at 25°C. This shows that the nature of the substrate complex changes with the change in *p*H. Now considering the above equilibrium effect of *p*H, k_{obs} can be expressed by Eq. (4)

$$k_{obs} = k_1 + k_2 K[H^+]^{-1} \quad \ldots(4)$$

where k_1 is the observed rate constant when reacting species is diaquo complex and k_2 is the observed rate constant for hydroxoaquo complex. It is seen from Eq. (4) that increase in *p*H increases the reaction rate. This may be due to the fact that at higher *p*H the percentage of hydroxoaquo species $[Cr(BigH)_2(H_2O)(OH)]^{2+}$ increases. Being a labile complex, it increases the rate of reaction in the higher *p*H range. The *pK* values of the ligand (pK_1 = 1.83, pK_2 = 9.13 at 25°C) indicate that in the experimental *p*H range the PhenylalaH form (i.e. zwitterionic form) is predominant. As the nature of ligand remains almost same, the effect of varying *p*H on rate is due to the change in species from hydroxo to diaquo.

At [complex-I] = 0.005 mol dm^{-3}, *p*H = 4.0 and

Table 1—Variation of pseudo-first order rate constant (k_{obs}) with [phenylalaH]

$[Cr(BigH)_2(H_2O)_2^{3+}] = 0.005$ mol dm^{-3}, $\mu = 0.5$ mol dm^{-3}, $pH = 4.0$

[PhenylalaH] (mol dm^{-3})	k_{obs} ($\times 10^4$) s^{-1}			
	30°	35°	40°	45°
0.050	0.93	1.33	2.17	2.60
0.075	1.30	1.84	2.80	3.20
0.100	1.70	2.27	3.32	3.80
0.125	1.90	2.66	3.70	4.20
0.150	2.05	2.80	4.20	4.70

$\mu = 0.5$ mol dm^{-3}, the rate of reaction increases with increase in [ligand] (Table 1) in the range 0.05 to 0.15 mol dm^{-3} but at a high [ligand] a limiting rate is reached. This may be due to completion of ion pair formation at higher [phenylalaH][1]. Based on the results the mechanism in Scheme 1 may be proposed to explain the variation of rate at varying concentrations of incoming ligand.

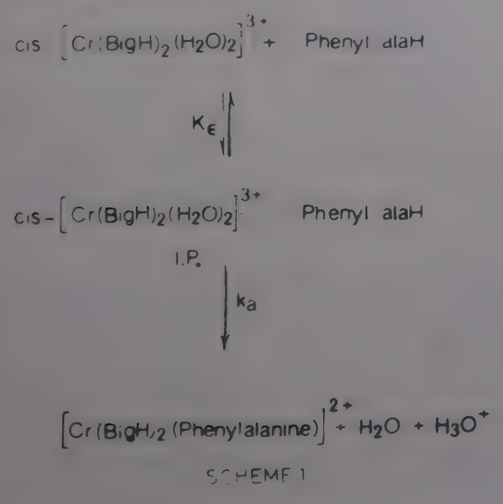

SCHEME 1

Scheme 1 leads to rate law (5)

$$\frac{d}{dt}[Cr(BigH)_2(phenylalanine)]^{2+} = \frac{k_a K_1 [Cr(BigH)_2(H_2O)_2^{3+}]_{total}[PhenylalaH]}{1 + K_1[phenylalaH]} \quad \ldots(5)$$

$$= k_{obs}[Cr(BigH)_2(H_2O)_2^{3+}]_{total} \quad \ldots(6)$$

Therefore,

$$k_{obs} = \frac{k_a K_1 [phenylalaH]}{1 + K_1[phenylalaH]} \quad \ldots(7)$$

$$\text{or, } 1/k_{obs} = 1/k_a + 1/k_a K_1 [phenylalaH] \quad \ldots(8)$$

According to Eq. (8) plot of $1/k_{obs}$ versus $1/[phenylalaH]$ should be linear. This is found to be so (Fig. 1). From such a linear plot k_a and K_1 values

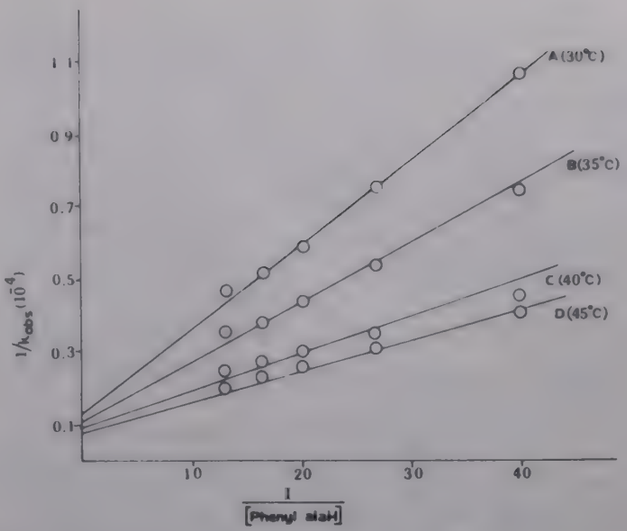

Fig. 1—Plot of $1/k_{obs}$ versus $1/[ligand]$ at different temperatures.

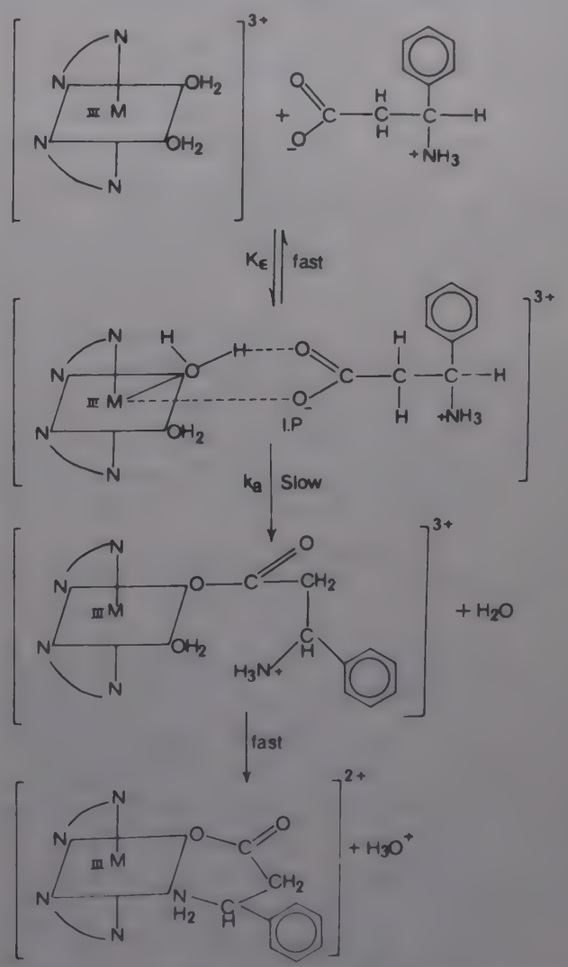

Scheme 2 – Probable Mechanism for the Anation Process

were obtained from the intercept ($1/k_a$) and slope ($1/k_a K_1$) respectively. The K_1 values are found to be almost constant (5.08 to 10.23) at 30°, 35°, 40° and 45°C and 10^4 k_a values are found to be 8.20, 9.52, 11.11 and 13.50 respectively.

Activation parameters, ($\Delta H^{\neq}$ and $\Delta S^{\neq}$) evaluated from the linear Eyring plot of log k_a/T versus

1/T, have been compared with those for the substitution of aquo ligands of the title complex by neutral ligands like 2,2′-dipyridyl[2] ($\Delta H^{\neq} = 85.83$ kJ mol^{-1}, $\Delta S^{\neq} = 2.92$ JK^{-1}mol^{-1}) and 1,10-phenanthroline[2] ($\Delta H^{\neq} = 43.30$ kJmol^{-1}, $\Delta S^{\neq} = -1.75$ JK^{-1}mol^{-1}). The authors observed high activation energy for such systems and suggested an I_d mechanism. But for our present system the $\Delta H^{\neq}$ value (27.21 ± 2.09 kJmol^{-1}) is quite low and a large negative $\Delta S^{\neq}$ (-214.79 ± 2.09 JK^{-1}mol^{-1}) value is obtained indicating a significant ligand participation in the transition state.

The results obtained in the present study suggest that the reaction between $[Cr(BigH)_2(H_2O)_2]^{3+}$ and β-phenylalanine involves outer sphere association between the two reacting species followed by an associative interchange process where both bond breaking and bond making occur concertedly. The energy of bond breaking is thus largely compensated by the energy released due to the bond formation by the incoming ligand in the transition state. In the present system such a mechanism is well reflected from the low $\Delta H^{\neq}$ value as compared to the other ligand substitution reaction involving Cr(III) centre. The probable reaction mechanism is shown in Scheme 2. A compact activated complex is formed via ion pair formation between complex-I and the ligand which is further stabilised by H-bonding. The negative $\Delta S^{\neq}$ value can also be accounted for by the formation of such a transition state.

References

1 Basolo F & Pearson R G, *Mechanism of inorganic reactions* (Wiely Eastern, New Delhi) 1977, 154.

2 Sengupta S & Banerjea D, *Z Anorg alleg Chem*, 93-96 (1976 424.

Indian Journal of Chemistry
Vol. 30A, February 1991, pp 187-189

Kinetics and mechanism of the oxidation of hyponitrous acid with chromium(VI) in acid perchlorate solutions

Pankaj Bhatnagar, R K Mittal & Y K Gupta*
Department of Chemistry, University of Rajasthan,
Jaipur 302 004

Received 4 April 1990; accepted 28 September 1990

Oxidation of hyponitrous acid with chromate in acid solutions occurs in accord with reaction,

$$3H_2N_2O_2 + 4Cr(VI) + 6H_2O \rightarrow 6HNO_2 + 4Cr(III) + 12H^+$$

with a rate law

$$-d[Cr(VI)]/dt = \frac{[Cr(VI)][H_2N_2O_2](k_1K_2[H^-] + k_2)}{(1 + K_2[H^-])}$$

where k_1 and k_2 are the rate constants for $(H_2CrO_4 + H_2N_2O_2)$ and $(HCrO_4^- + H_2N_2O_2)$ reactions respectively and $(1/k_2)$ is the first acid dissociation constant of H_2CrO_4. The values of k_1 ($dm^6mol^{-2}s^{-1}$) and k_2($dm^3mol^{-1}s^{-1}$) have been found to be 1.5 and 0.072 respectively at 40°. The known trioxodinitrate(II) is not an intermediate of the reaction.

Oxidation of hyponitrous acid with Tl(III)[1], Ce(IV)[2], hexacyanoferrate(III)[3] and chloramine-T[4] has already been reported from this laboratory. The end product in all these cases is nitrite or nitrate with or without evolution of N_2O and the results do not indicate the intermediacy of trioxodinitrate(II). The title investigation is one more support to this conclusion.

Experimental

Sodium hyponitrite (purity 65 to 96%) was prepared in 13% yield by electrolytic reduction[5] of nitrite[6]. The absorption coefficient in NaOH solutions of the samples (0.1 mol dm^{-3}) at 248 nm (λ_{max}) was found to be (6580 ± 300) $dm^3mol^{-1}cm^{-1}$. The literature values are (6550 ± 200)[6] and (6920 ± 140)[7] $dm^3mol^{-1}cm^{-1}$. Solutions of $H_2N_2O_2$ were prepared whenever required in aqueous $HClO_4$ (0.5 mol dm^{-3}) to which 0.1 mol% ethyl alcohol was added to prevent its decomposition. Sodium trioxodinitrate(II) was prepared by literature method[8] and the absorption coefficient of 0.1 mol dm^{-3} NaOH solution was found to be 8100 ± 200 $dm^3mol^{-1}cm^{-1}$ at 248 nm (literature value[9] is 8200 $dm^3mol^{-1}cm^{-1}$). The solid compound $Na_2N_2O_3$ after recrystallisation was kept under ethanol in a refrigerator. In aqueous solutions it decomposed slowly but in acidic solutions it decomposed readily.

All the chemicals were of either AR(BDH) or GR(E. Merck) quality. Doubly distilled water was used throughout.

Kinetic procedure—Thermally equilibrated (40 ± 0.1)° aqueous perchloric acid solution of hyponitrous acid was added to a mixture of potassium chromate and other required chemicals equilibrated at the same temperature. Aliquots (5 ml) were withdrawn at appropriate time intervals and added to a known excess of ferrous ammonium sulphate in 2.0 mol dm^{-3} H_2SO_4. The unreacted iron(II) was back titrated against a standard solution of Ce(IV) in aq. H_2SO_4 using N-phenylanthranilic acid as indicator.

The data were treated for initial rates (v_0) by the plane mirror method[10]. First and second order plots were also made wherever conditions permitted. The second order rate constants from the three plots were almost identical. The results were reproducible to ± 5%.

Results and discussion

Several determinations with different concentrations of hyponitrite, $HClO_4$ and excess concentration of chromate (estimated by the method described above) yielded $(\Delta[H_2CrO_4]/\Delta[H_2N_2O_2]) = (1.34 \pm 0.03)$ in accord with Eq. (1).

$$3H_2N_2O_2 + 4Cr(VI) + 6H_2O \rightarrow 6HNO_2 + 4Cr(III) + 12H^+ \quad \ldots(1)$$

No gas was evolved. This showed that the decomposition of $H_2N_2O_2$ is not significant in this reaction. Addition of methyl methacrylate tothe reaction mixture did not show polymerisation ruling out the possibility of involvement of stable free radicals. Some of the experiments were conducted in the presence of sulphamic acid and the stoichiometry was again 1.34. In our such experiments nitrogen evolved as per Eq. (2) and collected over water was (98.7 ± 0.4)% of the calculated value. The product nitrite is thus confirmed. Although a slow reaction between chromium VI and HNO_2 is reported[11], there does not seem to be any significant reaction in the present system.

$$HNO_2 + NH_2SO_3H \rightarrow N_2 + H_2SO_4 + H_2O \quad \ldots 2$$

The effect of varying [chromate] was studied in the range 2.0×10^{-4} mol dm^{-3} to 6.0×10^{-3}

Table 1—Second order rate constants of Cr(VI)-$H_2N_2O_2$ reaction from different type of plots at 40° and $[H^+]=1.1$ mol dm^{-3}; $k=v_0/[Cr(VI)][H_2N_2O_2]$ also equal to $k_0/[H_2N_2O_2]$ where k_0 and k are pseudo-first order and second order rate constants at constant $[HClO_4]=1.1$ mol dm^{-3}.

10^3[Cr(VI)] mol dm^{-3}	$10^3[H_2N_2O_2]$ mol dm^{-3}	10^7 (v_0) mol dm^{-3}s^{-1}	k from v_0 dm^{3}mol^{-1}s^{-1}	k from second order plots dm^{3}mol^{-1}s^{-1}	10^4k_0 from pseudo-first order plots s^{-1}	k from pseudo-first order plots dm^{3}mol^{-1}s^{-1}
0.2	2.5	1.08	0.216	—	4.61	0.184
0.4	2.5	1.92	0.192	—	4.28	0.171
0.6	2.5	2.67	0.178	—	4.61	0.184
0.8	2.5	3.67	0.184	0.185	—	—
1.0	2.5	4.92	0.197	0.184	—	—
1.2	2.5	5.92	0.197	0.184	—	—
1.6	2.5	7.17	0.179	0.183	—	—
2.0	2.5	9.67	0.193	0.182	—	—
3.0	2.5	15.0	0.200	0.184	—	—
4.0	2.5	19.2	0.192	0.177	—	—
5.0	2.5	24.2	0.193	0.166	—	—
6.0	2.5	28.3	0.189	0.177	—	—
0.99	0.5	1.08	0.218	0.184	—	—
0.99	0.75	1.50	0.202	0.188	—	—
0.99	1.0	1.67	0.170	0.196	—	—
0.99	1.5	2.50	0.170	0.183	—	—
0.99	2.0	3.83	0.193	0.183	—	—
0.99	4.0	7.00	0.177	—	—	—
0.99	6.0	10.8	0.182	—	10.3	0.172
0.99	8.0	14.7	0.185	—	16.1	0.201
		Average	0.190 ± 0.010	0.182 ± 0.012		0.182 ± 0.009

mol dm^{-3} at fixed $[Na_2N_2O_2]=2.5\times10^{-3}$ mol dm^{-3} and $[HClO_4]=1.1$ mol dm^{-3}. The plot of initial rate versus [chromate] was linear passing through the origin indicating first order in Cr(VI). The calculated second order rate constant was 0.19 dm^{3}mol^{-1}s^{-1} at 40°. The effect of varying [hyponitrite] was studied in the range 5.0×10^{-4} mol dm^{-3} to 8.0×10^{-3} mol dm^{-3} at fixed $[Cr(VI)]=1.0\times10^{-3}$ mol dm^{-3}. A similar treatment of the rate data showed first order in $[Na_2N_2O_2]$ and the second order rate constant was 0.18 dm^{3}mol^{-1}s^{-1} at the same temperature and $[H^+]$. These results are shown in Table 1.

Dependence of rate on $[H^+]$ was studied at fixed $I=2.5$ mol dm^{-3} adjusted with $LiClO_4$. The rate increases with the increase in $[H^+]$ (Table 2).

Ionic strength was varied from 1.1 mol dm^{-3} to 2.5 mol dm^{-3} by the addition of $LiClO_4$ at fixed $[Cr(VI)]=1.0\times10^{-3}$ mol dm^{-3}, $[Na_2N_2O_2]=2.5\times10^{-3}$ mol dm^{-3}, $[H^+]=1.1$ mol dm^{-3} at 40°. The rate slightly increases from a value of 4.8×10^{-7} to 6.0×10^{-7} mol dm^{-3}s^{-1}.

There was no change in the rate in the presence of added Cr(III) in the concentration range of $2.0\times10^{-4}-5.0\times10^{-3}$ mol dm^{-3}.

Table 2—Initial rates (v_0) at different $[H^+]$ at three temperatures $[Cr(VI)]=1.0\times10^{-3}$ mol dm^{-3}; $[H_2N_2O_2]=2.5\times10^{-3}$ mol dm^{-3}; $I=2.0$ mol dm^{-3}

$[H^+]$/ mol dm^{-3}	10^7 (v_0) mol dm^{-3}s^{-1} at		
	30°	40°	50°
0.20	—	—	6.0
0.50	1.67	4.17	9.66
0.70	2.00	4.83	11.3
0.90	2.66	5.00	13.3
1.10	3.00	5.83	15.3
1.30	3.33	6.67	17.3
1.50	3.66	8.17	19.7
1.70	4.66	8.83	20.7
2.00	5.00	9.67	24.0

Acid dissociation constants of $H_2N_2O_2$ are reported[12,13] to be small ($K_a^1\approx10^{-7}$ and $K_a^2\approx10^{-11}$) and hence it would predominantly be present as undissociated molecule. The $[H^+]$ dependence is not likely to be connected with it. Chromium(VI) in acid solutions employed is likely to be present as H_2CrO_4 and $HCrO_4^-$ as per equilibria[14] (3) and (4).

$$CrO_4^- + H^+ \rightleftharpoons HCrO_4^-$$

$$(K_1 = 1.2 \times 10^6 \text{ mol}^{-1}\text{dm}^3 \text{ at } 25°) \quad \ldots(3)$$

$$HCrO_4^- + H^+ \rightarrow H_2CrO_4$$

$$(K_2 = 0.21 \text{ mol}^{-1}\text{dm}^3 \text{ at } 25°) \quad \ldots(4)$$

Since a plot of rate versus $[HClO_4]$ is linear with an intercept, both the species of Cr(VI) appear to be reactive. Thus the two reactions are ($H_2CrO_4 + H_2N_2O_2 - k_1$ path) and ($HCrO_4^- + H_2N_2O_2 - k_2$ path) and the rate law (5) can be deduced.

$$-\frac{d[Cr(VI)]}{dt} = v_0 = \frac{[Cr(VI)]_T[H_2N_2O_2](k_1K_2[H^+] + k_2)}{(1 + K_2[H^+])} \quad \ldots(5)$$

or $$k = \frac{k_1K_2[H^+] + k_2}{1 + K_2[H^+]}$$

The plot of $v_0(1 + K_2[H^+])$ versus $[H^+]$ in the concentration range of 0.2 to 2.0 mol dm^{-3} was linear with an intercept. From K_2 values at 25° (0.21 dm^3mol^{-1}) and 4° (0.35 dm^3mol^{-1}), the values at 30°, 40° and 50°C were found to be 0.179, 0.143 and 0.115 respectively. With these values of K_2 and plots for $v_0(1 + K_2[H^+])$ versus $[H^+]$, k_1 ($dm^6mol^{-2}s^{-1}$) and k_2($dm^3mol^{-1}s^{-1}$) were found to be 0.60 and 0.024 at 30°, 1.5 and 0.072 at 40° and 4.4 and 0.14 at 50°C.

In view of apparent non-participation of free radicals, and stoichiometry ($\Delta[Cr(VI)]/\Delta[Na_2N_2O_2]$) of 4:3 in the present reaction, it appears that both Cr(V) and Cr(IV) are likely to participate in the reaction since a molecule of $H_2N_2O_2$ or its immediate oxidation product, $H_2N_2O_3$ has two nitrogen atoms and must involve atleast two electron change in one step. This implies the reduction of Cr(VI) to Cr(IV), but the latter being one electron oxidant is not likely to be involved in the oxidation of either $H_2N_2O_2$ or $H_2N_2O_3$. It appears that Cr(IV) reacts with Cr(VI) yielding two moles of Cr(V). This is possible since disproportionation of Cr(V) into Cr(VI) and Cr(IV) has been well recognised[15]. Thus Cr(V) can undergo two electron change and participate in the reaction.

A few kinetic runs with trioxodinitrate(II) and Cr(VI) show the reaction to be slow (pseudo-first order rate constant being $\sim 10^{-4}s^{-1}$ at 25° for $[H_2N_2O_2] = 2.0 \times 10^{-3}$ mol dm^{-3}). As a matter of fact oxidations of trioxodinitrate(II) so far studied and reported[16,17] are not fast. Also trioxodinitrate(II) is said to decompose[18-20] in a slow process. Hence trioxodinitrate(II) cannot be the intermediate in the Cr(VI)-$H_2N_2O_2$ reaction. On the basis of the results reported, the following mechanism may be suggested, where $H_2N_2O_3$

$$HCrO_4^- + H_2N_2O_2 \xrightarrow{\text{slow}} HCrO_3^- + H_2N_2O_3 \quad \ldots(6)$$

$$HCrO_4^- + H_2N_2O_3 \xrightarrow{\text{fast}} HCrO_3^- + 2HNO_2 \quad \ldots(7)$$

$$2HCrO_4^- + 2HCrO_3 + 4H^+ \xrightarrow{\text{rapid}} 4HCrO_3 + 2H_2O \quad \ldots(8)$$

$$(2Cr(VI) + 2Cr(IV) \xrightarrow{\text{rapid}} 2Cr(V))$$

$$4HCrO_3 + 2H_2N_2O_2 + 12H^+ \xrightarrow{\text{fast}}$$

$$4Cr(III) + 4HNO_2 + 8H_2O \quad \ldots(9)$$

is an unidentified product similar to trioxodinitrate(II).

References

1 Goyal M R, Mittal R K & Gupta Y K, *Indian J Chem*, 27A (1988) 487.

2 Goyal M R, Bhatnagar Pankaj, Mittal R K & Gupta Y K, *Indian J Chem*, 28A (1989) 382.

3 Goyal M R, Bhatnagar Pankaj, Mittal R K & Gupta Y K, *Indian J Chem*, 28A (1989) 280.

4 Goyal M R, Mittal R K & Gupta Y K, *Indian J Chem*, 27A (1988) 584.

5 Polydoropoulos C N, *Chem & Industry*, (1963) 1686.

6 Polydoropoulos C N & Voliotis S D, *Anal Chim Acta*, 40 (1968) 170.

7 Hughes M N & Donald C E, Ref. 5 in *J chem Soc, Dalton Trans*, (1989) 523 (Bonner F T, Donald C E & Hughes M N).

8 Addison C C, Gamlen G A & Thompson R, *J chem Soc*, (1952) 338.

9 Hughes M N & Wimbledon P E, *J chem Soc, Dalton Trans*, (1976) 703.

10 Latshaw M, *J Am chem Soc*, 47 (1925) 793.

11 Durham D A, Dozsa L & Beck M T, *J inorg nucl Chem*, 33 (1971) 2971.

12 Polydoropoulos C N & Pipinis M, *Zeit physik Chem*, 40 (1964) 322.

13 Hughes M N & Stedman G, *J chem Soc*, (1963) 1239.

14 Schwarzenback G & Meyer J, *J inorg Nucl Chem*, 8 (1958) 302; Haight (Jr) G P, Richardson D C & Coburn N H, *Inorg Chem*, 3 (1964) 1777; Tong J Y, *Inorg Chem*, 3 (1964) 1804; Tong J Y & Johnson R L, *Inorg Chem*, 5 (1966) 1902.

15 Espenson J H, *J Am chem Soc*, 86 (1964) 5101; Krumpole M & Rocek J, *J Am chem Soc*, 98 (1976) 872; Ip D & Rocek J, *J Am chem Soc*, 101 (1979) 6311.

16 Akhtar M J, Bonner F T, Hughes M N, Lu Chun-Su, Wallis H L & Wimbledon P E, *Inorg Chem*, 26 (1987) 2437.

17 Akhtar M J, Bonner F T, Hughes M N, Humphreys E J & Lu Chun-Su, *Inorg Chem*, 25 (1986) 4635.

18 Donald C E, Hughes M N, Thompson J M & Bonner F T, *Inorg Chem*, 25 (1986) 2676.

19 Bazylinski D A, Goretski J & Hollocher T C, *J Am chem Soc*, 107 (1985) 7986.

20 Bazylinski D A & Hollocher T C, *J Am chem Soc*, 107 (1985) 7982.

Indian Journal of Chemistry
Vol. 30A, February 1991, pp 190-192

Oxidation of thallium(I) by permanganate in aqueous perchloric acid

S A Chimatadar, S C Hiremath & J R Raju*

Department of Chemistry, Karnatak University, Dharwad 580 003

Received 20 March 1990; revised 13 July 1990; accepted 7 August 1990

Permanganate oxidation of thallium(I) in aqueous perchloric acid has 2:3 stoichiometry (oxidant: reductant) and manganese(IV) and thallium(III) are the products. A clean second order kinetics is followed by the reaction with fractional dependence on [acid]. The results are explained by a mechanism involving $HMnO_4$ as the active oxidant species.

Thallium(I) is a two-electron reductant and is easily oxidised by permanganate in acid medium but the mechanism is not known and hence the title investigation. Reduction of permanganate to either manganese(IV) or manganese(II) is possible, the former state being attained in reactions with two electron reductants[1].

Experimental

Reagent grade chemicals and doubly distilled water were used. Aqueous solutions of potassium permanganate (BDH, AR) and thallium(I) sulphate were standardised by titrating against oxalic acid and potassium bromate respectively. Thallium(III) solution was prepared by dissolving thallium(III) oxide (BDH) in 2.0 mol dm^{-3} perchloric acid and standardised against EDTA solution. Manganese(IV) solution was prepared in hot 1:1 perchloric acid and standardised as reported in literature. Manganese(IV) solution of concentration higher than around 1.0×10^{-3} mol dm^{-3} was unstable under the experimental conditions employed. Therefore, solutions of manganese(IV) with concentrations less than $\sim 7.0 \times 10^{-4}$ mol dm^{-3} which were stable over 5-6 hrs under the experimental conditions were used in the study.

Kinetic procedure

Thermally equilibrated solutions of MnO_4^- and Tl(I), which also contained the required quantities of perchloric acid and sodium perchlorate to give the required acidity and ionic strength, were mixed and the reaction was followed spectrophotometrically by measuring the absorbance of MnO_4^- in the reaction mixture at 526 nm on a Bausch and Lomb Spectronic 2000 instrument. The application of Beer's law under the reaction conditions had earlier been verified in the concentration range of 0.50×10^{-4} to 4.0×10^{-4} mol dm^{-3} of MnO_4^- in 1.0 mol dm^{-3} perchloric acid with $\varepsilon = 2400 \pm 25$. Initial rates were reproducible within $\pm 5\%$.

Stoichiometry

Different reaction mixtures containing different [reactants] in 1.0 mol dm^{-3} perchloric acid solution and sodium perchlorate ($I = 1.10$ mol dm^{-3}) were kept at 25° for over 4 hrs. The oxidant, MnO_4^-, was found by measuring its absorbance at 526 nm. Tl(III) formed was analysed as the Tl(III)-PAN complex[2] by extraction of the latter into chloroform at $pH = 2.4$-5 and measuring its absorbance at 570 nm. Manganese(IV) was found from the absorption spectrum of the reaction mixture in 9 M sulphuric acid[3].

Manganese(IV) formed in the reaction showed no insoluble form under the reaction conditions as observed by Nepheloturbidimeter. However, under the conditions of [Mn(VII)] greater than around 1.0×10^{-3} mol dm^{-3}, the product formed showed a precipitate of manganese dioxide. The results of the reaction showed that two moles of oxidant were required for the oxidation of three moles of thallium(I).

$$2Mn(VII) + 3Tl(I) = 2Mn(IV) + 3Tl(III) \quad \ldots(1)$$

Results

Under the conditions of [MnO_4^-] in the range of 0.25×10^{-4} to 2.5×10^{-4} mol dm^{-3}, [Tl(I)] = 3.0×10^{-4} mol dm^{-3}, acidity = 1.0 mol dm^{-3} and ionic strength = 1.10 mol dm^{-3}, log-log plots of initial rates versus [MnO_4^-] led to an order of approximately unity in [oxidant]. Under similar conditions, the order in [Tl(I)] in the concentration range of 0.50×10^{-4} to 6.0×10^{-4} mol dm^{-3}, at [Mn(VII)] = 2.0×10^{-4} mol dm^{-3}, was also found to be unity. Measurement of initial rates at different [acid] ranging from 0.25 to 1.25 mol dm^{-3} perchloric acid, other conditions being constant, led to an order of around 0.83 in [acid]. Initially added product, Tl(III), did not affect the reaction significantly; but, initial addition of varying amounts of [Mn(IV)] increased the rate leading to an order of around 0.40 in [Mn(IV)].

The Mn(VII)-Tl(I) reaction has a stoichiometry of 2:3 ([Mn(VII)]:[Tl(I)]) and intervention or forma-

tion of Mn(III) and Mn(II) may be regarded as unlikely. This conclusion was supported by the non-detection of both Mn(III) and Mn(II) at the end of the reaction. Manganese(VI), Mn(V) and Tl(II) might be involved in the reaction. However, while Mn(VI) and Mn(V) are known only in basic solution[4]. Tl(II) is rather shortlived[5]. Hence, no experimental tests could be carried out in these cases.

Variation of ionic strength between 1.1 and 2.0 mol dm^{-3} by addition of the requisite $[NaClO_4]$ reduced the rate. For example, under the conditions $3[MnO_4^-] = 2[Tl(I)] = 6.0 \times 10^{-4}$ mol dm^{-3}, $[HClO_4] = 1.0$ mol dm^{-3} at 24°C, an increase in ionic strength from 1.1 to 2.0 moldm^{-3} decreased the initial rate from 11.3×10^{-7} to 5.17×10^{-7} mol $dm^{-3}s^{-1}$. On the other hand, the initial rate increased with increase in dielectric constant (decrease in acetic acid content) of the medium . Under identical conditions as mentioned above, when the acetic acid content (%v/v) was increased from 0 to 50, the initial rate decreased from 11.3×10^{-7} to 2.77×10^{-7} mol$dm^{-3}s^{-1}$. Salt effects on the reaction were also studied and, while added sodium nitrate and sodium sulphate did not affect the reaction rate to any significant extent, added chloride influenced the reaction rate appreciably.

At constant acidity, ionic strength and other constant conditions, the effect of increasing temperature between 24° and 34°C was studied (values of k_2 at 24.0°, 29.0° and 34.0°C were 41.3, 47.2 and 55.6 $dm^3mol^{-1}s^{-1}$ respectively) and the activation parameters obtained are: $E_a = 22.6 \pm 3$ kJmol^{-1} and $\Delta S^{\neq} = -148.3 \pm 4$ $JK^{-1}mol^{-1}$.

Discussion

The Mn(VII)-Tl(I) reaction is a noncomplementary one with the oxidant undergoing a three equivalent reduction and Tl(I) undergoing a two equivalent change. No evidence for the lower oxidation states of manganese such as Mn(III) and Mn(II) was found. Again, Mn(VI) and Mn(V) are unstable in acid media[4] and could not be detected. The intervention of Tl(II) in many cases of oxidation reaction of Tl(I) in acid solutions is well established although its intervention is difficult to detect since it is very short-lived[5]. Manganese(IV) which is a product, catalyses the reaction and hence the second order plot of $1/(a-x)$ versus time deviates from linearity (Fig. 1). The other product, Tl(III), has no effect on the reaction. The reaction order of two (unity in each reactant) and fractional order in acid can be accommodated by a mechanism shown in Scheme 1. The active oxidant species is likely to be the monoprotonated species of Mn(VII)($HMnO_4$) as indicated by the

$$H^+ + MnO_4^- \overset{K}{\rightleftharpoons} HMnO_4 \qquad \ldots(I)$$

$$Mn(VII) \text{ or } HMnO_4 + Tl(I) \xrightarrow{k_1 \text{ slow}} Mn(VI) + Tl(II) \qquad \ldots(II)$$

$$Mn(VII) + Tl(II) \xrightarrow{\text{fast}} Mn(VI) + Tl(III) \qquad \ldots(III)$$

$$Mn(VI) + Tl(I) \xrightarrow{\text{fast}} Mn(IV) + Tl(III) \qquad \ldots(IV)$$

Scheme 1

effect of acidity on the reaction. Oxidation by unprotonated oxidant occurs to a negligible extent, around 0.4% of the total oxidation. That permanganic acid ($HMnO_4$) is a stronger oxidant than MnO_4^- has also been observed in other cases[6]. The steps beyond the slow step are all likely to be fast in view of the fact that short-lived intermediates of manganese or thallium are involved. Since none of the intermediates could be identified, Scheme 1 is only one of the different possible mechanisms for the reaction, steps beyond step(II) being uncertain. It may be noted that both Mn(V) and Mn(VI) are stable only in strongly basic media[4]. However, Tl(II) has been found to intervene[5] in oxidation of Tl(I) in acid solutions. Scheme 1 leads to rate law (2) which may be rearranged to the form (3) suitable for verification. A plot

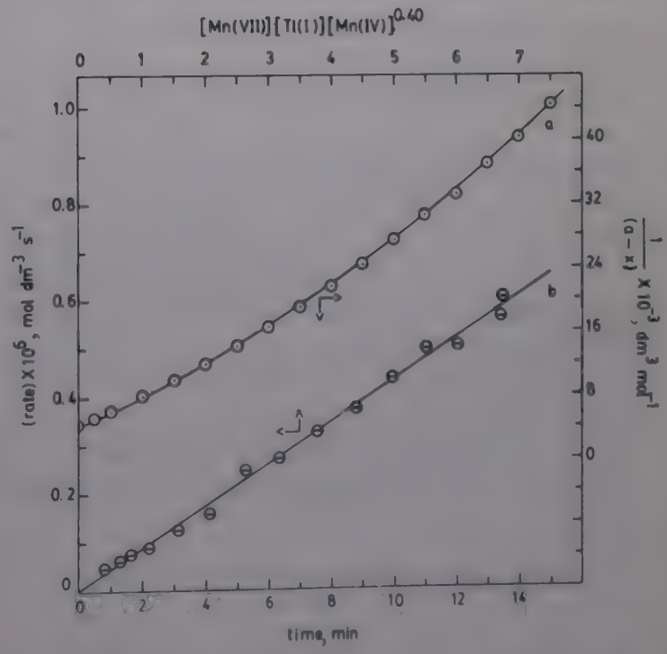

Fig. 1—Mn(VII)-Tl(I) reaction in aqueous perchloric acid at 24°C – (a) Plot of $1/(a-x)$ versus time; (b) Plot of rate versus $[Mn(VII)][Tl(I)][Mn(IV)]^{0.4}$ ($3[MnO_4^-] = 2[Tl(I)] = 6.0 \times 10^{-4}$ mol dm^{-3}; $[HClO_4] = 1.0$ mol dm^{-3}; $I = 1.3$ mol dm^{-3}).

$$-\frac{d[\mathrm{Mn(VII)}]}{dt}=\frac{Kk_1[\mathrm{Mn(VII)}]_T[\mathrm{Tl(I)}]_T[\mathrm{H^+}]_T}{(1+K[\mathrm{H^+}]_T)} \quad \ldots(2)$$

$$\frac{[\mathrm{Mn(VII)}]_T[\mathrm{Tl(I)}]_T}{(\text{Initial rate})}=\frac{1}{k_1K[\mathrm{H^+}]_T}+\frac{1}{k_1} \quad \ldots(3)$$

of the left hand side of Eq. (3) against $1/[H^+]_T$ must be linear with rate constant, k_1, and formation constant of $HMnO_4$, K, being obtainable from slope and intercept of such plot. The plot is linear and the values of k_1 and K are 50 $dm^3mol^{-1}s^{-1}$ and 0.61 dm^3mol^{-1} respectively. Using these values, initial rates for several situations as used in experiment were calculated and compared with experimental results. It is found that a fair agreement is obtained. The value of K of 0.61 dm^3mol^{-1} for the formation of $HMnO_4$ in the equilibrium step is much higher than may be expected on the basis of the reported pK_a values of permanganic acid of -2.25 in perchloric acid and -4.6 in sulphuric acid[7].

The role of Mn(IV), a product, is amply borne out by the linearity of the plot of rate versus $[Mn(VII)][Tl(I)][Mn(IV)]^{0.4}$. Soluble forms of Mn(IV) exist under certain conditions[8]. Thus, the catalysis by Mn(IV) (fractional order) of the reaction may be due to soluble species like $H_2MnO_4^{2-}$.

The effect of ionic strength and dielectric constant on the reaction may be understood in terms of their opposing effects on the first and second steps of Scheme 1. While step(I) is favoured by decreasing polarity of the solvent, the formation of the activated (charged) state (step (II)) may occur to a lesser extent[9]. The effect of ionic strength is that, while step(II) is favoured by the increase in ionic strength, step(I) is not. The rather small activation energy and the large entropy of activation indicate that the activated state is considerably ordered. The particular effect of chloride ions on the reaction is likely to be due to the fact that the product, Tl(III), forms highly stable chloride complexes[10] as compared to Tl(I), the product stabilisation accounting for the rate increase.

References

1 Wiberg K B in *Oxidation in organic chemistry* Part A, edited by K B Wiberg (Academic Press, New York) 1965, pp. 1-68.

2 Rakhmatullaev K & Tashmamatov Kh, *Analyt Abst*, 29 (1975) 4B82.

3 Mandal S K & Sant B R, *Talanta*, 23 (1976) 485.

4 Wiberg K B in *Oxidation in organic chemistry* Part A, edited by K B Wiberg (Academic Press, New York) 1965, pp. 2-6.

5 Lee A G, *The chemistry of thallium* (Elsevier, London). (1971) pp. 294-318.

6 Wiberg K B in *Oxidation in organic chemistry* Part A edited by K B Wiberg (Academic Press, New York) 1965, pp. 57-58.

7 Bailey N, Carrington A, Lott K A K & Symons M C R, *J chem Soc*, (1960) 290; Stewart R & Mocek M M, *Can J Chem*, 41 (1963) 1160.

8 Wiberg K B in *Oxidation in organic chemistry* Part A, edited by K B Wiberg (Academic Press, New York) 1965, p. 6.

9 Benson S W, *The foundations of chemical kinetics* (McGraw-Hill, New York) 1960, p. 536.

10 Wiberg K B in *Oxidation in organic chemistry* Part A, edited by K B Wiberg (Academic Press, New York) 1965, p. 47.

Indian Journal of Chemistry
Vol. 30A, February 1991, pp 193-195

Ternary complexes of copper(II) with L-histidine, aspartic acid and glutamic acid as primary ligands and substituted imidazoles as secondary ligands

Krishna B Pandeya* & Ram N Patel
Department of Chemistry, A.P.S. University,
Rewa (MP) 486 003
Received 16 January 1990; revised 25 June 1990; accepted 27 July 1990

Formation of ternary complexes of copper(II) with L-histidine, glutamic acid and aspartic acid as primary ligands and imidazole, 2-methylimidazole and 2-ethylimidazole as secondary ligands has been studied potentiometrically in aqueous medium. The stabilities of the ternary complexes follow the order aspA ≥ glutA > L-his with respect to amino acids and 2-methylimidazole ≥ 2-ethylimidazole > imidazole with respect to imidazoles. These orders have been explained in terms of electronic and molecular structures.

Ternary complexes play an important role in biological processes, as exemplified by many instances in which enzymes are known to be activated by metal ions[1,2] . Copper is an important trace element for plants and animals[3,4] and is involved in mixed ligand complex formation[6,7] in a number of biological processes[5,6]. In the present note we report the potentiometric studies of the formation constants of ternary complexes of Cu(II) with L-histidine, aspartic acid and glutamic acid as primary ligand and some imidazoles(I) as secondary ligands.

Experimental

The protonation constants of L-histidine, aspartic acid and glutamic acid and imidazoles and the formation constants of the binary complexes were determined by Calvin-Bjerrum's[7,8] technique as adopted by Irving and Rossotti[9]. The formation constants of the ternary complexes were evaluated using the method of Martell *et al.*[10,11] and Ozer[12]. *p*H-Measurements were made on a Control Dynamics *p*H-meter. The spectra were recorded on a Shimadzu UV-VIS recording spectrophotometer UV-160 with 1 cm quartz cell in aqueous solution at *p*H ~ 7.00. All the chemicals used were of AR grade and all solutions used were prepared in doubly distilled water. The titrations were carried out at 30°, 40° and 50°C. The temperature was maintained using a Yorko thermostat. Ionic strength of all the solutions was maintained at 0.1*M* ($NaClO_4$). For the ternary systems, following solutions were prepared (in total volume 25 ml) for titrations:

(i) 0.02*M* perchloric acid + 0.1*M* $NaClO_4$.
(ii) 0.02*M* perchloric acid + 0.1*M* $NaClO_4$.
(iii) 0.02*M* perchloric acid +0.002*M* secondary ligand + 0.1*M* $NaClO_4$.
(iv) 0.02*M* perchloric acid + 0.002M primary ligand + 0.002*M* $Cu(ClO_4)_2$ + 0.01*M* $NaClO_4$.
(v) 0.02*M* perchloric acid + 0.002*M* primary ligand + 0.002 secondary ligand + 0.002*M* $Cu(ClO_4)_2$ + 0.1*M* $NaClO_4$.

Each one of the above samples was titrated against 1.0*M* sodium hydroxide.

Results and discussion

Binary complexes

The values of $\log K^{Cu}_{CuA}$ for the binary complexes with amino acids are given in Table 1 along with earlier reported values. Our values are quite close to the literature values.

L-Histidine(II) binds to the metal ions through the nitrogen at position 3, amino nitrogen and the carboxylate group. Aspartic acid (III) and glutamic acid (IV), both have three potential coordinating sites, viz., the amino nitrogen and two carboxylate groups. There is some controversy regarding the coordination of the carboxylate. In most of the cases, aspartate is reported to act as tridentate ligand, whereas glutamate with the extended side chain has been reported to act as bidentate or tridentate ligand.

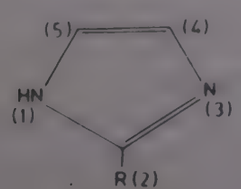

(a) R = H
(b) R = CH_3
(c) R = CH_2CH_3

I

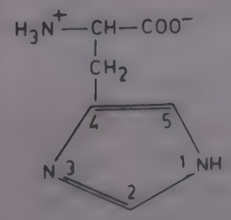

II

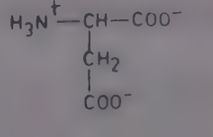

III

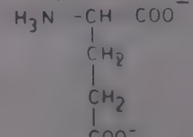

IV

Table 1—Protonation constants, formation constants and thermodynamic parameters for the binary complexes {[ligand] = [copper(II)] = $2.0 \times 10^{-3} M$ & $\mu = 0.1 M$ ($NaClO_4$)}

Ligand	Temp. (°C)	$\log K_1^H$	$\log K_2^H$	$\log K_{CuA}^{Cu}$	Thermodynamic Parameters		
					$-\Delta G^*$ (kcal mol^{-1})	$-\Delta H^*$ (kcal mol^{-1})	ΔS^* (cal mol^{-1} K^{-1})
L-Histidine	*25	9.15*	6.10*	10.1*			
	30	9.05	6.15	10.18	14.1	16.4	−7.7
		9.05*	6.23*	10.16*,9.79*			
	40	8.80	5.85	9.78			
	50	8.55	5.56	9.39			
Aspartic acid	*25	9.60*	3.70*	8.94*,8.08*			
	30	9.65	3.85	8.90	12.3	11.9	1.4
	40	9.50	3.70	8.62			
	50	9.40	3.55	8.35			
Glutamic acid	*25	9.50*	4.10*	8.39*,8.55*			
	30	9.58	3.67	8.55	11.8	10.5	4.4
	40	9.45	3.55	8.30			
	50	9.37	3.43	8.10			
Imidazole	*25	7.10*					
	30	7.10					
	40	6.80					
	50	6.60					
2-Methylimidazole	30	7.90					
	40	7.80					
	50	7.60					
2-Ethylimidazole	30	7.90					
	40	7.75					
	50	7.55					

*Literature values

The formation constants of the binary complexes with amino acids follow the order: L-his > aspA ≥ glutA. The log$K$ value for the L-histidine complex is highest owing to the NNO chelation. Also, the nitrogen at 3-position is a very strong donor. Aspartic acid and glutamic acid have ONO donor set. The log K value for glutamic acid complex is lower than that for aspartic acid complex which may be due to the difference in the size of chelate rings in the two cases; the former has a 5- and a 7-membered ring while the latter has a 5- and 6-membered ring.

Ternary complexes

Formation constants for the ternary complexes amino acid-Cu(II)-imidazole are given in the Table 2. The values decrease linearly with increase in temperature.

The order of log K with respect to amino acids is: aspA > glutA > L-his. The trends of formation constants for ternary complexes and binary complexes have been observed to be reverse to each other which has also been reported in the case of glycylglycine and glycylglycylglycine[13]. In fact, the log K values for the replacement of one water molecule from ligand-Cu(II)-OH_2 (where ligand is terdentate one) by imidazole follows the order: gg < glutA ≈ aspA > L-his, while the formation constant for the formation of the binary complex (ligand-Cu(II)-OH_2) follows exactly the reverse order, viz., L-his > aspA ≥ glutA > gg. This is also the order observed for the λ_{max} values (Table 2).

Formation constant values with respect to imidazoles

The order of log K values with respect to imidazoles is: 2-methylimidazole ≥ 2-ethylimidazole > imidazole. As we go from imidazole to 2-methylimidazole, an increase in log K values is observed, which is owing to the increase in basicity of ligands. From steric considerations the log K values in the case of complexes with substituted imidazoles should be smaller than that for imidazole complexes. The increase in basicity in substituted imidazoles, thus, compensates for the negative contribution of the steric effect and further enhances the value of log K by about ~ 0.35 in all the cases. Amongst the substituted imidazoles, there is not much difference

Table 2—Formation constants, thermodynamic parameters and visible band positions for ternary complexes {[ligand] = [copper (II)] = $2.0 \times 10^{-3} M$ & $\mu = 0.01 M$ ($NaClO_4$)}

System	Temp. (°C)	$\log K_{CuAL}^{CuA(*)}$	Thermodynamic parameters			λ_{max} (cm^{-1})
			$-\Delta G^\circ$ (kcal mol^{-1})	$-\Delta H^\circ$ (kcal mol^{-1})	ΔS° (cal mol^{-1} K^{-1})	
Cu(II)-L-His-imidazole (1:1:1)	30	3.36	4.6	13.0	−27.7	15750
	40	3.06				
	50	2.86				
Cu(II)-L-His-2-methyl-imidazole (1:1:1)	30	3.65	5.0	4.3	2.30	15500
	40	3.55				
	50	3.35				
Cu(II)-L-His-2-ethyl-imidazole (1:1:1)	30	3.65	5.0	6.9	−6.27	15360
	40	3.49				
	50	3.29				
Cu(II)-AspA-imidazole (1:1:1)	30	4.02,4.00*	5.6	10.4	−15.8	15600
	40	3.78				
	50	3.46				
Cu(II)-AspA-2-methyl-imidazole (1:1:1)	30	4.30	6.0	5.2	2.6	15000
	40	4.22				
	50	4.02				
Cu(II)-AspA-2-ethyl-imidazole (1:1:1)	30	4.34	6.0	7.4	−4.6	15330
	40	4.17				
	50	3.97				
Cu(II)-GlutA-imidazole (1:1:1)	30	3.90,3.93*	5.4	7.8	−7.9	15360
	40	3.72				
	50	3.42				
Cu(II)-GlutA-2-methyl-imidazole (1:1:1)	30	4.30	5.9	6.5	−1.9	15000
	40	4.15				
	50	3.93				
Cu(II)-GlutA-2-ethyl-imidazole (1:1:1)	30	4.30	5.9	6.9	−3.3	15300
	40	4.10				
	50	3.85				

*Literature values

either in the ligand basicities or in the steric effect, so that both, 2-methylimidazole and 2-ethylimidazole, give almost similar log K values. This is also the order of the λ_{max} values (Table 2).

The ΔH values for the binary (Table 1) and ternary (Table 2) complexes from the slopes of the Arrhenius plots (log K versus $1/T$) have been evaluated. The ΔS values have been obtained from Gibbs-Helmholtz relationship. The negative value of ΔG (in all the cases) suggests, spontaneous formation of the complexes. The ΔS values are, however, negative.

Acknowledgement

This work has been done with the financial assistance from the CSIR, New Delhi, Scheme No. (1046).

References

1 Helleman L & Stock C C, *J biol Chem*, 125 (1938) 771.
2 Valle B L & Coleman J E, *Compr Biochem*, 8 (1968) 1458.
3 Gaudin D & Fellman J H, *Biochem Biophys Acta*, 141 (1967) 64.
4 Sigel H, *Metal ions in biological systems*, Vol 3 (Marcel Dekker, New York) 1974.
5 Marcus Y & Eliezer I, *Coord Chem Rev*, 4 (1969) 273.
6 Calvin H & Wilson K W, *J Am chem Soc*, 67 (1945) 2003.
7 Bjerrum J, *Metal amine formation in aqueous solution* (P Haase & Sons, Copenhagen) 1941, 298.
9 Carey G H & Martell A E, *J Am chem Soc*, 89 (1967) 2859.
10 Carey G H, Bogucki R F & Martell A E, *Inorg Chem*, 3 (1964) 1288.
11 Ozer U Y, *J inorg nucl Chem*, 32 (1970) 1279.
12 Sunderberg R J & Martin R B, *Chem Rev*, 74 (1974) 471.
13 Pandeya K B & Patel R N, *Indian J Chem*, 29A (1990) 602.

Indian Journal of Chemistry
Vol. 30A, February 1991, pp 196-197

Separation of lanthanides and some associated elements by liquid-liquid extraction and reverse phase thin layer chromatography using high molecular weight amine-citrate system

Asha Jain, O V Singh & S N Tandon*
Department of Chemistry, University of Roorkee,
Roorkee 247 667
Received 5 February 1990; revised 25 July 1990;
accepted 20 August 1990

Primene JM-T has been used to study the extraction of Ce(III), Gd(III) and Yb(III) and other associated elements such as Y(III), Ti(IV), V(IV), Zr(IV), Th(IV) and U(VI) from citric acid medium. Based on distribution data it has been possible to achieve separation of lanthanides from titanium, zirconium, thorium and uranium with high separation factors. The amine-citrate system has also been used to study the reverse-phase TLC behaviour of Ce(III), Gd(III) and Yb(III) and of Y, Ti, V, Zr, Th and U. Binary separations involving lanthanides have also been achieved on amine impregnated layers.

The use of citrate buffers in ion exchange chromatography of lanthanides is well known. However, scanty information is available on the extraction of these metal ions from aqueous citrate medium[1,2]. The present communication reports the extraction behaviour of three representative lanthanides, namely Ce(III), Gd(III) and Yb(III) alongwith that of Y(III), Ti(IV), V(IV), Zr(IV), Th(IV) and U(VI) at different citric acid concentrations. Based on the distribution data optimum conditions for the separation of lanthanides from Ti(IV), Zr(IV), Th(IV) and U(VI) have been worked out. The feasibility of the separation procedure is checked by taking binary mixtures. A reverse-phase thin layer chromatographic (TLC) study investigating the effect of concentration of amine and citric acid on hR_f values of some lanthanides and other elements has also been carried out to provide some useful correlation between the thin layer and solvent extraction data and to find out optimum conditions for TLC separation.

Experimental

Equal volumes (10 ml) of the aqueous phase (1.0×10^{-3} *M* or any other concentration of metal ion) and organic phase (appropriate concentration of amine in chloroform) were shaken at room temperature for 5 min, the two phases separated and suitable aliquots of each were counted for gamma activity or employed for determination by ICP-AES (LABTAM, Australia).

The slurry of silica gel-G was prepared in chloroform solution containing high molecular weight amine of appropriate concentration. The plates of 0.5 mm layer thickness were used and the spots of metal ions (5 µl of 2.5% solution) were developed following the usual procedure.

Results and discussion

Liquid-liquid extraction studies

The extraction of Ce(III), Gd(III) and Yb(III) was studied using different diluents and it was observed that extent of extraction was much higher with chloroform and benzene but chloroform was preferred as a diluent because of lesser emulsification tendencies. All amines were converted into the citrate form by pretreatment with citric acid. It is found that the extraction of metal ions remains more or less invariable in the *p*H range of 3-4 and for all studies the equilibrium *p*H of the aqueous phase was maintained in the above range. The extraction was studied in Primene JM-T, Amberlite LA-2, Alamine-336 and Aliquat-336 and found to be the highest in Primene JM-T. Hence, Primene JM-T was used. The plots of log D versus log [amine] for Ce(III), Gd(III) and Yb(III) give slopes equal to three, suggesting extraction of these metal ions by anion exchange mechanism[2]. A concentration of 0.10 *M* of Primene JM-T has been chosen for other studies.

The effect of varying [citric acid] (1.0×10^{-3} to 5.0×10^{-3} *M*) on the extraction of Ce(III), Gd(III), Yb(III), Y(III), Ti(IV), V(IV), Zr(IV), Th(IV) and U(VI) was studied in chloroform solution of Primene JM-T. The extraction of Ce(III) and Gd(III) increases with increase in [citric acid] upto 5.0×10^{-3} *M* thereafter it remains more or less constant. But in case of Yb(III), the extraction is very poor and remains constant throughout the acid range. In case of Ti(IV), Zr(IV), Th(IV) and U(VI) extraction is very high (90-100%) in the range of [citric acid]. However, extraction of Y(III) and V(IV) is 60-75% under the above conditions. Based on these data, separation of lanthanides can be achieved from Ti(IV), Zr(IV), Th(IV) and U(VI).

Experiments for separations were conducted by taking binary mixtures of Ti(VI), Zr(IV), Th(IV), or

Table 1—Effect of varying [citric acid] on the hR_f values of various lanthanides and other associated metal ions at 3% Primene JM-T concentration

Metal ion	hR_f values at [citric acid]				
	0.01*M*	0.05*M*	0.1*M*	0.5*M*	1.0*M*
Ce(III)	52T	55T	60	80	75
Ce(IV)	68T	80T	60	80	76
Nd(III)	54T	60T	60	79	76
Eu(III)	55T	63T	62	80	75
Gd(III)	47T	55T	62	78	80
Tb(III)	48T	57T	65	80	75
Yb(III)	45	55	65	80	72
Y(III)	68	75	80	85	77
Ti(IV)	—	—	—	—	—
V(IV)	10	10	25	45	52
Zr(IV)	0	5	5	5	8
Th(IV)	5	15	15	25	28
U(VI)	7	10	20	15	16

T – Tailing

Table 2—Effect of varying [Primene JM-T] on the hR_f values of various lanthanides and other associated metal ions at 0.1 *M* citric acid concentration

Metal ion	hR_f values at [Primene JM-T]				
	0.030%	0.15%	0.30%	3.0%	5.0%
Ce(III)	90	90	90	60	45
Ce(IV)	90	90	85	60	58
Nd(III)	95	90	85	62	46
Eu(III)	95	90	85	61	48
Gd(III)	95	90	85	65	56
Tb(III)	95	90	85	63	59
Yb(III)	95	90	85	60	51
Y(III)	95	95	100	—	94
Ti(IV)	—	—	—	—	—
V(IV)	100	95	95	25	11
Zr(IV)	35	25	18	5	5
Th(IV)	80	75T	65T	15	10
U(VI)	90	85T	70	20	8

T – Tailing

U(VI) with Ce(III), Gd(III) or Yb(III) in varying concentration ratios. Titanium, zirconium, thorium and uranium could be recovered quantitatively from organic phase by washing with 6*M* HCl whereas thorium with 3*M* H_2SO_4. The results indicated that retention of lanthanides in aqueous phase was above 95% whereas Ti(VI), Zr(IV), Th(IV) and U(VI) could be recovered from organic phase to an extent of 90%.

TLC studies

To study the effect of citric acid on the hR_f values of the metal ions several plates impregnated with 3% ($\sim$ 0.1 *M*) Primene JM-T were run with varying [citric acid] (1.0×10^{-2} - 1.0 *M*). Results are given in Table 1. It is observed that the hR_f values increase with increase in [citrate] indicating an inverse relationship between the distribution coefficient and the hR_f values. Further, Ti(IV), V(IV), Zr(IV), Th(IV) and U(VI) ions are strongly retained and no significant movement is observed even on increasing [citric acid]. These metal ions show consistently high extraction in Primene JM-T at all [citric acid]. Apparently, the tailing seems to disappear at higher [eluant].

On development of chromatographic plates coated with varying concentrations of Primene JM-T it is observed that the hR_f values of the lanthanide ions decrease with the increase in [Primene JM-T] (Table 2). Here too, there is an inverse correlation between hR_f values and the %E of the metal ions. Testa[3] reported a similar trend on hR_f values of rare earths and some other metal ions using trioctylamine coated papers. The trends in hR_f values of metal ions are more or less similar on layers coated with different high molecular weight amines like Aliquat-336, Alamine-336 and Amberlite LA-2. As expected the hR_f values in Primene JM-T are the lowest.

Using Primene JM-T-citrate system the optimum conditions for binary separations of Ce(III), Gd(III) or Yb(III), from other associated metal ions [V(IV), Zr(IV), Th(IV) or U(VI)] are 3% impregnated and 0.10*M* eluant. Similar separations have also been achieved using other amines like Aliquat-336, Alamine-336 and Amberlite LA-2.

The above results establish the utility of amine - citrate system for separating lanthanides from some of the commonly associated elements by both liquid-liquid extraction and TLC.

Acknowledgement

The financial assistance of CSIR, New Delhi is gratefully acknowledged.

References

1 Moore F L, *Analyt Chem*, 37 (1965) 1235.
2 Jain A, Singh O V & Tandon S N, *Analyt Lett*, 21 (1988) 1927.
3 Testa C, *Analyt Chem*, 34 (1962) 1556

Indian Journal of Chemistry
Vol. 30A, February 1991, pp 198-199

Voltammetric estimation of Te(IV) in some natural samples

Mangla Dave & K S Pitre*
Department of Chemistry, Dr. Hari Singh Gour Vishwavidyalaya, Sagar (M.P.) 470 003

Received 5 February 1990; revised 14 May 1990; accepted 28 June 1990

A highly sensitive voltammetric method has been developed for the determination of tellurium. Tellurium(-IV) shows a single four electron cathodic reduction wave which is *p*H dependent and diffusion-controlled. Normal and differential pulse polarographic approaches for the determination of Te(IV) produced reliable results in ammonia-ammonium chloride as supporting electrolyte. Use of charging current compensated d.c. polarography improves the precision. The method has been used to determine Te(IV) content of some natural samples.

Increased awareness of the biological role[1,2] of tellurium has revived interest in methods for the trace determination of tellurium. Lingane and Niedrach[3] have shown that tellurium undergoes reduction at dropping mercury electrode in citrate buffer at *p*H = 0.4 to 6.9.

In the present investigation, polarographic and normal and differential pulse polarographic techniques have been employed to determine tellurium at trace levels in natural waters, some polluted samples and industrial wastes.

Experimental

The chemicals used were of AR grade. All the solutions were prepared in doubly distilled water. The metal ion solution was standardised by the reported method[4]. Solution of gelatin (0.1%) was used as the maximum suppressor and 1*M* ammonia-ammonium chloride as the supporting electrolyte.

Polarograms were recorded on an Elico pulse polarograph, model C-L 90 which was coupled with an X-Y polarocord model L-R 108. The electrochemical cell used, had a provision for inserting the dropping mercury electrode as a working electrode, a saturated calomel electrode as a reference electrode, Pt wire as an auxillary electrode and a bubbler for deaerating the solutions and for passing nitrogen. The d.m.e. used had the following characteristics: $m = 1.73 \times 10^{-3}$ g s^{-1} at t = 1.0 s in ammonia-ammonium chloride buffer at *p*H = 8.20 ± 0.02; capillary characteristics were: 1.441 $mg^{2/3}$ $sec^{-1/2}$ at 140 cm effective height of mercury reservoir; surface area of mercury drop = 0.0122 cm^2.

The *p*H measurements were made on an Elico digital *p*H meter model LI-120.

Results and discussion

The voltammogram of Te(IV) in ammonia buffer showed only a single well-defined wave with $E_{1/2} = -0.68$ V vs SCE. The wave height/peak height was found to be proportional to the tellurium taken. Current concentration relationship for charging current compensated d.c. polarography (CCCDCP), normal pulse polarography (NPP) and differential pulse polarography (DPP) were found to be linear. The results showed that the techniques were sufficiently sensitive for the determination of tellurium concentrations as low as 1.3 ng/L, 1.2 ng/L and 0.8 ng/L using calibration curves, and 1.25 ng/L, 1.00 ng/L and 0.75 ng/L using standard addition method by CCCDCP, NPP and DPP respectively.

Interference study

The method is fairly selective towards different ions, viz., Sb^{3+} (1:35), Cu^{2+} (1:22), Cd^{2+} (1:35), Bi^{3+} (1:10), Pb^{2+} (1:12), n^{2+} (1:33). However, even a trace of iron interfered seriously. Selenium did not interfere in any concentration. Se(IV) and Te(IV) could be determined simultaneously by DPP as the peak potential of Te(IV) is −0.735 V vs SCE while that of Se(IV) is −1.608 V vs SCE.

Determination of Te(IV) in natural water samples

The water samples were collected from upper, middle and lower layers of Sagar lake in Sagar town of Madhya Pradesh (India). Any suspended impurities were removed by filtration. Iron was removed by extraction with dithiozone, while digestion with conc. HNO_3 removed the last traces of organic matter. Suitable aliquots of water sample were taken in the cell containing ammonia buffer. The recovery experiments were performed with addition of known quantities of tellurium in the natural water samples. The concentration of Te(IV) was computed from calibration plots and was ascertained by standard addition method[4]. The recoveries were found to be 99.7%, 99.2% and 99.28% by CCCDCP method, 98.9%, 99.3% and 99.7% by NPP method and 99.2%, 99.24% and 99.9% by DPP method.

Table 1—Estimation of Te(IV) in natural waters
(From Sagar lake, Sagar, Madhya Pradesh)

S.No.	Sample location	Volume of aliquot (ml)	Te(IV) CCCDCP (μg)	NPP (μg)	DPP (μg)
1	Surface water	10.0	3.50	3.52	3.54
		20.0	7.10	7.08	7.04
		30.0	10.24	10.50	10.48
2	Middle level	10.0	4.10	4.09	4.06
		20.0	8.16	8.18	8.15
		30.0	12.24	12.20	12.22
3	Bottom level	10.0	5.22	5.20	5.24
		20.0	10.38	10.44	10.40
		30.0	15.60	15.66	15.70
	Standard deviation	—	±0.068	±0.032	±0.0092

The results show that the upper, middle and lower levels of Sagar city lake contain35.2 μg/100 ml, 40.8 μg/100 ml and 52.2 μg/100 ml respectively of tellurium (Table 1).

Determination of Te(IV) in rock phosphate

The sample was collected from Hirapur mine in Sagar district of Madhya Pradesh. The mineral (910.0 g) was washed with water and filtered. The filtrate was treated with HCl and with dithiozone to remove iron, and then treated with HNO_3 and evaporated to dryness. The residue was dissolved in distilled water. Suitable aliquots of this solution were taken in the polarographic cell containing appropriate volume of ammonia buffer for analysis by standard procedure, as mentioned above. The concentration of tellurium was ascertained by standard addition method. The values obtained by the calibration curve method were: CCCDCP:255.6; NPP: 255.5; DPP: 255.8. The corresponding values by standard addition method were 254.8, 254.6, and 254.3 μg of Te(IV) per kg respectively.

Analysis of rock phosphate obtained from Hirapur mines was found to contain 254.6 μg/kg Te(IV). The calculated standard deviation, i.e., 0.007 shows the accuracy of the method.

Determination of Te(IV) in industrial wastes water

The water samples were collected from Nepa Paper Mills, Nepanagar, Madhya Pradesh at different stages of forming rough paper. Any suspended impurities were removed by filtration and water was extracted with HNO_3. The precipitated impurities were filtered off and the filtrate was concentrated. An appropriate aliquot of the solution was taken for analysis of Te(IV) as described earlier. The results are given in Table 2.

Table 2—Determination of Te(IV) in industrial waste water samples
(From Nepa Paper Mill, Nepa Nagar, Madhya Pradesh, India)

Sample location		Wt. of Te(IV), μg/L CCCDCP	NPP	DPP
After crushing	A	—	0.482	0.492
bambooes	B	—	0.480	0.488
After third filtration of	A	—	1.060	1.0621
crushed material	B	—	1.010	1.0121
After last	A	149.20	148.90	148.586
stage	B	146.90	147.26	147.188

A: Calibration curve method; Standard deviation = ±0.008
B: Standard addition method: Standard deviation = ±0.009

Statistical analysis of the observed data showed that the methods are highly sensitive, accurate, precise and rapid with a minimum detection limit of 0.75 ng/L for Te(IV). The method is very useful for routine analysis of Te(IV) in industrial materials and naturally occurring substances.

Acknowledgement

The authors are highly thankful to Prof. S.P. Banerjee, Dean, Faculty of Science and Head, Department of Chemistry, for providing all necessary laboratory facilities. One of the authors (M.D.) is thankful to UGC, New Delhi for the award of Teacher Research Fellowship.

References

1 Underwood E J, *Trace elements in human and animal nutrition*, (Academic Press, New York) 1971.
2 Nazarnko I I & Ermakov A V, *Selenium and tellurium*, (Wiley, New York) 1972.
3 Lingane J J & Niedrach L N, *J Am chem Soc*, 71 (1949) 196.
4 Yogel A I, *Quantitative inorganic analysis*, 4th Ed, (ELBS Publication), 1962, pp 477.

Indian Journal of Chemistry
Vol. 30A, February 1991, pp 200-201

Extractive spectrophotometric determination of vanadium by complexation of V(III) with *o*-phenanthroline and salicylic acid

R S Chauhan & L R Kakkar*

Department of Chemistry, Kurukshetra University, Kurukshetra 132 119, Harayana, India

Received 7 February 1990; revised and accepted 11 July 1990

A simple spectrophotometric method for the determination of vanadium has been developed based on the reduction of pentavalent vanadium to V(III) and its complexation with *o*-phenanthroline and salicyclic acid. The coloured complex is extractable into dichloromethane. The method is free from the interference of a large number of metal ions, namely, Os(VIII), Re(VII), Mo(VI), Cr(VI), W(VI), U(VI), Ce(IV), Zr(IV), Cr(III), Al(III), Sb(III), Bi(III), Cu(II), Cd(II), Pb(II), Mg(II), Sr(II), Ca(II), Zn(II), Ba(II), and Ag(I).

Vanadium is known to form complexes[1-5] in its different oxidation states which differ in their stability and extraction behaviour towards different organic solvents. Vanadium (V) compounds are the most stable in acid as well as alkaline medium, whereas V(IV) compounds are stable only in acid solutions. Because of strongly reducing nature of V(III) and V(II) ions, earlier it was thought that they have hardly any meaningful role in the spectrophotometric determination of vanadium. Our studies on the analytical aspects of the complexation tendency of V(III) have led us to propose here an extractive spectrophotometric method for the determination of vanadium.

Experimental

Vanadium (V) solution containing 1 mg/ml was prepared by dissolving sodium metavanadate (Reachim) in distilled water.

Salicylic acid (2%) and *o*-phenanthroline (0.5%) solutions were prepared separately in ethanol. Sodium dithionite and dichloromethane used were of CP grade.

Procedure

The *p*H of an aliquot containing 200 µg vanadium (V) and/or other ions, 1.0 ml *o*-phenanthroline, 1.0 ml salicylic acid and 150 mg sodium dithionite was adjusted to 4.5. The contents were transferred to a 100 ml separatory funnel and the volume was finally made up to 20 ml. The solution was equilibrated with 10 ml dichloromethane gently for 30 s taking care to release the pressure occasionally through a stop cock. The aqueous phase was again equilibrated with another 10 ml portion of the solvent. The organic phases were combined and the coloured complex was filtered into a 25 ml volumetric flask using a Whatman filter paper No. 41 and the volume was made up to the mark with the pure solvent. Absorption of the complex was measured at 385 nm against the reagent blank using a UV-visible spectrophotometer (Shimadzu-UV-140-02). The amount of vanadium was determined from a standard curve drawn by plotting the absorbance values obtained corresponding to different concentrations of vanadium as described above in the procedure.

Results and discussion

Vanadium (III) obtained on reduction with sodium dithionite formed a yellowish brown complex with *o*-phenanthroline and salicylic acid at *p*H 4.3-4.6. The absorption spectrum of the complex showed λ_{max} at 385 nm, where the reagent blank prepared similarly had negligible absorption.

The formation and absorbance of the complex is influenced by various parameters. While making a study of these variables, the initial conditions maintained were: vanadium (V) = 200 µg, *o*-phenanthroline = 1 ml, salicylic acid = 1 ml, and sodium dithionite = 200 mg.

The absorbance of the vanadium complex was *p*H-dependent. At *p*H 4.0, it was 0.205 and reached a maximum 0.315 in the range *p*H 4.3-4.6. Further increase in *p*H lowered the absorbance. Therefore, *p*H 4.5 was considered suitable.

The effect of variation in the concentration of sodium dithionite as reductant for vanadium (V) was also studied. For [sodium dithionite] = 50 mg, the absorbance of the complex was 0.255. When the concentration of the reductant was increased to 100-300 mg, absorbance value was 0.315, and thereafter it decreased. Hence, for effecting quantitative reduction, 150 mg of dithionite was used.

In the absence of salicylic acid, the absorbance was nil. The absorbance was maximum (0.315) for 0.8-2.5 ml of 2% salicylic acid in ethanol. It was, therefore, sufficient to use 1 ml of salicylic acid to get optimum extraction.

The absorbance was only 0.045 if *o*-phenanthroline was not added to the aqueous solution. The absorbance was maximum (0.315) for 0.6-2.0 ml of *o*-phenanthroline. Therefore, 1 ml of *o*-phenanthroline was used in all subsequent estimations.

The absorbance also varied with vanadium concentration. It was found to rise with the increasing concentration of the metal ion. Aqueous solution containing 10, 50, 100, 400 and 800 μg vanadium (V) in 20 ml volume gave absorbance values of 0.02, 0.07, 0.15, 0.59 and 1.17, respectively, indicating increase in absorbance in a regular fashion. Thereafter, the absorbance increased but slowly.

On extraction, the equilibrium was achieved quite quickly. If the contact time was kept in the range 5-50 s, the absorbance was constant and continued to be maximum (0.315).

Extraction of the complex into different organic solvents was tried. The absorbance of the complex increased in the order: amyl alcohol (0.10), benzyl alcohol (0.11), butanol (0.20), butyl acetate (0.215), chloroform (0.24), tribenzylamine-chloroform (0.26) and dichloromethane (0.315). Isobutyl methyl ketone, ethyl methyl ketone and carbon tetrachloride did not extract the complex at all. Thus, dichloromethane was used as the extractant.

Effect of diverse ions

Under the chosen conditions, the effect of different ions, taken initially in 20 ml aqueous volume, was as follows:

Os(VIII), Cr(III) and Cu(II) (0.2 mg each); W(VI), Cd(II), Pb(II), Mg(II), Hg(II), Mn(II), Sr(II), Ca(II) and Ba(II) (10 mg each); U(VI), Ce(IV), Zr(IV), Al(III), Bi(III), Sb(III), Be(II), Zn(II) and Ag(I) (5 mg each); Cr(VI) (2.0 mg); Mo(VI) (0.1 mg); Se(IV) (0.5 mg); and Re(VII) (0.4 mg) had no adverse effect on the estimation. Ru(III), Pd(II) and Fe(III) (0.05 mg each); Pt(IV) and Fe(II) (0.2 mg each); and Sn(II) (0.5 mg) also had hardly any effect on absorbance. Co(II) and Ti(IV) (0.5 mg each) interfered in the estimation.

Chloride (1000 mg), sulphate (300 mg), nitrate (200 mg), thiocyanate (100 mg), ascorbic acid (80 mg) and thiourea (50 mg) did not change the absorbance of the complex either. However, acetate (50 mg), phosphate (50 mg), tartrate (50 mg); fluoride (50 mg), oxalate (50 mg), EDTA (50 mg), citrate (50 mg) and sulphosalicylic acid (50 mg) decreased it in the same order.

Stoichiometry of the complex, Beer's law obedience and Sandell's sensitivity

The ratio of V(III), *o*-phenanthroline and salicylic acid in the extracted species was found to be 1:1:2 by Job's method of continuous variations[6] as modified by Vosburgh and Cooper[7]. This composition was further supported by mole ratio method[8]. Beer's law was obeyed in the range 0-32 μg V/ml. The molar absorptivity was 2006.3694 1 $mol^{-1}cm^{-1}$, specific absorptivity 0.039386 mol g^{-1} cm^{-1}, and Sandell's sensitivity 0.0253 μg V/cm^2.

Applications

The proposed method for the determination of vanadium is quite sensitive and free from the interference of a large number of metal ions which seriously interfere in most of the methods employed for its determination. Micro amounts of the metal ion can be determined with greater accuracy with wider Beer's law range. The results obtained are highly reproducible with a standard deviation of 0.003. The applicability of the method was tested by the satisfactory analysis of a large variety of samples.

Acknowledgement

Our sincere thanks are due to the CSIR, New Delhi for financial support and the Chairman, Department of Chemistry, Kurukshetra University, Kurukshetra, for providing laboratory facilities.

References

1 Pandey L P, Singh B & Padhi K K, *J Indian chem Soc*, 65 (1988) 817.
2 Jimin Yu, Guanghui Wu, Xiangxi Fan & Huamin Hou, *Fenxi Huaxue*, 16 (1988) 1030.
3 Gordeeva M N & Antonova M S, *Vestn Leningr Univ Fiz Khim*, 3 (1981) 53.
4 Valero J, *An Quim Ser B*, 81 (1985) 372.
5 Bhadra A K, *Talanta*, 20 (1973) 13.
6 Job P, *Ann Chim*, 9 (1928) 113.
7 Vosburgh W C & Cooper G R, *J Am chem Soc*, 63 (1941) 437.
8 Yoe J H & Jones A L, *Ind Engng chem Anal, Anal Ed*, 16 (1944) 111.

Indian Journal of Chemistry
Vol. 30A, February 1991, p. 202

Corrigenda

1. Paper entitled, "Thermodynamic studies of ion-exchange equilibria of some bivalent metal ions with H^+ on stannic arsenate cation exchanger" [*Indian J Chem*, 28A (1989) 1090-92].

   (i) On page 1091, substitute,

   $$\ln K_a = Z_H - Z_M + \int_0^1 \ln K_c \, d\bar{X}_M \qquad \ldots (3)$$

   instead of $$\ln K_a = Z_M - Z_H + \int_0^1 \ln K_c \, d\bar{X}_M \qquad \ldots (3)$$

   (ii) On page 1092 (Ref. 14) substitute *J Am chem Soc*, 65 (1943) 1765, in place of *J Am chem Soc*, 65 (1943) 1978.

   (iii) On page 1091 (Table 1) the values of $\Delta G°$, $\Delta H°$ and $\Delta S°$ should be in kJ·equiv^{-1}, kJ equiv^{-1} and J deg^{-1} equiv^{-1} in place of kJ mol^{-1}, kJ mol^{-1} and J deg^{-1} mol^{-1}, respectively.

2. Paper entitled, "Deprotonation and transfer energetics of diglycine and triglycine in aqueous mixtures of urea and glycerol from emf measurements at different temperatures" [*Indian J Chem*, 29A (1990) 945-952].

   (i) On page 945, the superscript mark † in the fourth line from top in the right hand side column refers to the following footnote:
   †H Talukdar, Ph.D. Thesis, Jadavpur University, Calcutta, 1989.

   (ii) On page 947, column headings A to T $\delta(\Delta S°)$ in Table 2 should each be shifted by one position to the right hand side.

3. Paper entitled, "α-Benzildioxime as a reagent for microdetermination and separation of palladium from other platinum metals" [*Indian J Chem*, 29A (1990) 1034-1036].

   On page 1035, headings for columns 3 and 4 in Table 2 should read "Pd added (μg)" and "Pd found (μg)" respectively.

ISBN 81-85038-90-2

PP 157 + xii; Price: Rs 125.00; $ 45.00; £ 30.00

RECENT ADVANCES IN MAN-MADE FIBRES

Special Issue of

Indian Journal of Fibre & Textile Research

The March 1991 issue of the ***Indian Journal of Fibre & Textile Research*** is being brought out as a special issue on "*RECENT ADVANCES IN MAN-MADE FIBRES*".

Guest edited by Prof. V B Gupta of IIT-Delhi, the special issue will contain invited papers from internationally known experts. Among the authors are Prof. J W S Hearle, Dr.R Huisman, Dr. H M Heuvel, Dr T Manabe, Dr.A S Abhiraman, Dr. Satish Kumar, Prof. V B Gupta, Dr. K V Datye, Prof. A K Sengupta, Prof. Pushpa Bajaj, Prof. N V Bhat, Dr. B N Bandyopadhyay, Prof. A K Mukherjee, Prof. V K Kothari & Prof. B L Deopura.

The topics covered include: Unsolved problems in the science of nylon & polyester fibres; Advances in high performance and other man-made fibres; Fibres from polymer blends; Crystals: their nature & influence on fibre properties; Ceramic fibre precursors; Science & technology of man-made fibres: the Indian R & D scenario; Utilization of polyester waste; Recycling processes and products in nylon-6 fibre industry; Melt flow behaviour of poly(ethylene terephthalate); High-speed spinning of PET yarns; Nylon-6 tyre yarns; and Air-jet texturing.

The contents of this special issue are bound to be of immense use to researchers, technologists, managers and industrialists and would serve as a valuable reference.

Price	Rs 60.00	£ 16.00	$ 30.00

Orders accompanied by Bank Drafts/Cheques drawn in favour of PUBLICATIONS & INFORMATION DIRECTORATE, NEW DELHI 110 012 may be sent to the Senior Sales & Distribution Officer, Publications & Information Directorate (CSIR), Hillside Road, New Delhi-110 012 .

Printed & Published by Dr. G. P. Phondke, Director, Publications & Information Directorate (PID)
Hillside Road, New Delhi 110 012, at PID Photocomposition Unit

D(W) 103

RN 7090/63